CORRECTED VERSION*

PCT

INTERNATIONAL APPLICATION PUBLISHED UNDER THE PATENT COOPERATION TREATY (PCT)

(51) International Patent Classification [6] : G06F 17/50, C07K 1/00, 14/475, G01N 33/68	A3	(11) International Publication Number: WO 98/06048
		(43) International Publication Date: 12 February 1998 (12.02.98)

(21) International Application Number: PCT/CA97/00539

(22) International Filing Date: 31 July 1997 (31.07.97)

(30) Priority Data:
9616105.4   31 July 1996 (31.07.96)   GB

(71) Applicant *(for all designated States except US)*: QUEEN'S UNIVERSITY AT KINGSTON [CA/CA]; Kingston, Ontario K7L 3N6 (CA).

(72) Inventors; and
(75) Inventors/Applicants *(for US only)*: SHAMOVSKY, Igor, L. [RU/CA]; 6-202, 17 Van Order Drive, Kingston, Ontario K7M 1B5 (CA). ROSS, Gregory, M. [CA/CA]; 1090 Caitlin Crescent, Kingston, Ontario K7P 2S4 (CA). RIOPELLE, Richard, J. [CA/CA]; 32 Lakeshore Boulevard, Kingston, Ontario K7M 4J6 (CA). WEAVER, Donald, F. [CA/CA]; 27 Collegeview Crescent, Kingston, Ontario K7M 7J8 (CA).

(74) Agents: SCHUMACHER, Lynn, C. et al.; Hill & Schumacher, Suite 802, 335 Bay Street, Toronto, Ontario M5H 2R3 (CA).

(81) Designated States: AL, AM, AT, AU, AZ, BA, BB, BG, BR, BY, CA, CH, CN, CU, CZ, DE, DK, EE, ES, FI, GB, GE, GH, HU, IL, IS, JP, KE, KG, KP, KR, KZ, LC, LK, LR, LS, LT, LU, LV, MD, MG, MK, MN, MW, MX, NO, NZ, PL, PT, RO, RU, SD, SE, SG, SI, SK, SL, TJ, TM, TR, TT, UA, UG, US, UZ, VN, YU, ZW, ARIPO patent (GH, KE, LS, MW, SD, SZ, UG, ZW), Eurasian patent (AM, AZ, BY, KG, KZ, MD, RU, TJ, TM), European patent (AT, BE, CH, DE, DK, ES, FI, FR, GB, GR, IE, IT, LU, MC, NL, PT, SE), OAPI patent (BF, BJ, CF, CG, CI, CM, GA, GN, ML, MR, NE, SN, TD, TG).

Published
With international search report.

(88) Date of publication of the international search report:
6 August 1998 (06.08.98)

(54) Title: MOLECULAR MODELLING OF NEUROTROPHIN-RECEPTOR BINDING

(57) Abstract

The present invention relates to a computational method for identifying the bioactive conformations of peptide domains, in particular, the geometries of complexes of neurotrophins and their receptors. The bioactive conformation of the Nerve Growth Factor (NGF) amino and carboxyl termini (Trk binding domain) was determined. The complex of the NGF termini splits into two distinct regions: a rigid region (residues 9-11 and 112'-118') and a flexible loop (residues 1-8). The geometry of the rigid region, which is maintained by electrostatic interaction between Glu^{11} and $Arg^{118'}$, is conserved in active molecules only. The separation of the flexible loop from the rigid region is necessary in order to eliminate an influence of the loop on the biologically active conformation of the rigid region. The present invention also relates to a method for identifying and theoretically modelling specific receptor binding sites for Nerve Growth Factor (NGF) and Brain-Derived Neurotrophic Factor (BDNF) on their receptors, TrkA and TrkB, respectively. The present invention also relates to a method for identifying and theoretically modelling a receptor binding site for neurotrophins, such as NGF, BDNF, NT-3, and NT-4/5, of the common neurotrophin receptor $p75^{NTR}$.

FOR THE PURPOSES OF INFORMATION ONLY

Codes used to identify States party to the PCT on the front pages of pamphlets publishing international applications under the PCT.

AL	Albania	ES	Spain	LS	Lesotho	SI	Slovenia
AM	Armenia	FI	Finland	LT	Lithuania	SK	Slovakia
AT	Austria	FR	France	LU	Luxembourg	SN	Senegal
AU	Australia	GA	Gabon	LV	Latvia	SZ	Swaziland
AZ	Azerbaijan	GB	United Kingdom	MC	Monaco	TD	Chad
BA	Bosnia and Herzegovina	GE	Georgia	MD	Republic of Moldova	TG	Togo
BB	Barbados	GH	Ghana	MG	Madagascar	TJ	Tajikistan
BE	Belgium	GN	Guinea	MK	The former Yugoslav	TM	Turkmenistan
BF	Burkina Faso	GR	Greece		Republic of Macedonia	TR	Turkey
BG	Bulgaria	HU	Hungary	ML	Mali	TT	Trinidad and Tobago
BJ	Benin	IE	Ireland	MN	Mongolia	UA	Ukraine
BR	Brazil	IL	Israel	MR	Mauritania	UG	Uganda
BY	Belarus	IS	Iceland	MW	Malawi	US	United States of America
CA	Canada	IT	Italy	MX	Mexico	UZ	Uzbekistan
CF	Central African Republic	JP	Japan	NE	Niger	VN	Viet Nam
CG	Congo	KE	Kenya	NL	Netherlands	YU	Yugoslavia
CH	Switzerland	KG	Kyrgyzstan	NO	Norway	ZW	Zimbabwe
CI	Côte d'Ivoire	KP	Democratic People's	NZ	New Zealand		
CM	Cameroon		Republic of Korea	PL	Poland		
CN	China	KR	Republic of Korea	PT	Portugal		
CU	Cuba	KZ	Kazakstan	RO	Romania		
CZ	Czech Republic	LC	Saint Lucia	RU	Russian Federation		
DE	Germany	LI	Liechtenstein	SD	Sudan		
DK	Denmark	LK	Sri Lanka	SE	Sweden		
EE	Estonia	LR	Liberia	SG	Singapore		

PCT

INTERNATIONAL APPLICATION PUBLISHED UNDER THE PATENT COOPERATION TREATY (PCT)

(51) International Patent Classification 6 : G06F 17/50	A2	(11) International Publication Number: **WO 98/06048** (43) International Publication Date: 12 February 1998 (12.02.98)

(21) International Application Number: PCT/CA97/00539

(22) International Filing Date: 31 July 1997 (31.07.97)

(30) Priority Data:
9616105.4   31 July 1996 (31.07.96)   GB

(71) Applicant (for all designated States except US): QUEEN'S UNIVERSITY AT KINGSTON [CA/CA]; Kingston, Ontario K7L 3N6 (CA).

(72) Inventors; and
(75) Inventors/Applicants (for US only): SHAMOVSKY, Igor, L. [RU/CA]; 6-202, 17 Van Order Drive, Kingston, Ontario K7M 1B5 (CA). ROSS, Gregory, M. [CA/CA]; 1090 Caitlin Crescent, Kingston, Ontario K7P 2S4 (CA). RIOPELLE, Richard, J. [CA/CA]; 32 Lakeshore Boulevard, Kingston, Ontario K7M 4J6 (CA). WEAVER, Donald, F. [CA/CA]; 27 Collegeview Crescent, Kingston, Ontario K7M 7J8 (CA).

(74) Agents: SCHUMACHER, Lynn, C. et al.; Hill & Schumacher, Suite 802, 335 Bay Street, Toronto, Ontario M5H 2R3 (CA).

(81) Designated States: AL, AM, AT, AU, AZ, BA, BB, BG, BR, BY, CA, CH, CN, CU, CZ, DE, DK, EE, ES, FI, GB, GE, GH, HU, IL, IS, JP, KE, KG, KP, KR, KZ, LC, LK, LR, LS, LT, LU, LV, MD, MG, MK, MN, MW, MX, NO, NZ, PL, PT, RO, RU, SD, SE, SG, SI, SK, SL, TJ, TM, TR, TT, UA, UG, US, UZ, VN, YU, ZW, ARIPO patent (GH, KE, LS, MW, SD, SZ, UG, ZW), Eurasian patent (AM, AZ, BY, KG, KZ, MD, RU, TJ, TM), European patent (AT, BE, CH, DE, DK, ES, FI, FR, GB, GR, IE, IT, LU, MC, NL, PT, SE), OAPI patent (BF, BJ, CF, CG, CI, CM, GA, GN, ML, MR, NE, SN, TD, TG).

Published
Without international search report and to be republished upon receipt of that report.

(54) Title: MOLECULAR MODELLING OF NEUROTROPHIN-RECEPTOR BINDING

(57) Abstract

The present invention relates to a computational method for identifying the bioactive conformations of peptide domains, in particular, the geometries of complexes of neurotrophins and their receptors. The bioactive conformation of the Nerve Growth Factor (NGF) amino and carboxyl termini (Trk binding domain) was determined. The complex of the NGF termini splits into two distinct regions: a rigid region (residues 9-11 and 112'-118') and a flexible loop (residues 1-8), the geometry of the rigid region, which is maintained by electrostatic interaction between Glu^{11} and $Arg^{118'}$, is conserved in active molecules only. The separation of the flexible loop from the rigid region is necessary in order to eliminate an influence of the loop on the biologically active conformation of the rigid region. The present invention also relates to a method for identifying and theoretically modelling specific receptor binding sites for Nerve Growth Factor (NGF) and Brain-Derived Neurotrophic Factor (BDNF) on their receptors, TrkA and TrkB, respectively. The present invention also relates to a method for identifying and theoretically modelling a receptor binding site for neurotrophins, such as NGF, BDNF, NT-3, and NT-4/5, of the common neurotrophin receptor $p75^{NTR}$.

MOLECULAR MODELLING OF NEUROTROPHIN-RECEPTOR BINDING

FIELD OF THE INVENTION

5   The present invention relates to a computational method for identifying minimum-energy structures in molecular systems, and more particularly for determining the bioactive conformations of peptide domains. The invention relates to determination of the bioactive conformations of the amino and carboxyl termini of Nerve Growth Factor (NGF) and analogues thereof, and the 3-dimensional structures of their complexes with the 24-amino

10   acid second leucine-rich motif (LRM) of TrkA which represents the binding site for NGF. The invention further relates to the theoretically identified geometries of the TrkB and the $p75^{NTR}$ receptor binding sites and to the mechanisms of neurotrophin binding.

BACKGROUND OF THE INVENTION

15

The neurotrophins are a family of structurally and functionally related proteins, including Nerve Growth Factor (NGF), Brain-Derived Neurotrophic Factor (BDNF), Neurotrophin-3 (NT-3), Neurotrophin-4/5 (NT-4/5) and Neurotrophin-6 (NT-6). These proteins promote the survival and differentiation of diverse neuronal populations in both the peripheral

20   and central nervous systems (Hefti, 1986; Hefti and Weiner, 1986; Levi-Montalcini, 1987; Barde, 1989; Leibrock et al., 1989; Maisonpierre et al., 1990; Rosenthal et al., 1990; Hohn et al., 1990; Gotz et al., 1994; Maness et al., 1994) and are involved in the pathogenesis of diverse neurological disorders. Neurotrophins exert certain of their biological effects through specific interactions with a class of transmembrane receptor tyrosine kinases (TrkA, TrkB and

25   TrkC) (Kaplan et al., 1991; Klein et al., 1991, 1992; Soppet et al., 1991; Squinto et al., 1991; Berkemeier et al., 1991; Escandon et al., 1993; Lamballe et al., 1991). Specificity of neurotrophin action results from their selective interactions with Trk. That is, TrkA only binds NGF (Kaplan et al., 1991; Klein et al., 1991); TrkB binds BDNF, NT-3 and NT-4/5 (Soppet et al., 1991; Squinto et al., 1991; Berkemeier et al., 1991; Escandon et al., 1993; Lamballe et

30   al., 1991; Klein et al., 1992; Vale and Shooter, 1985; Barbacid, 1993); and TrkC exclusively binds NT-3 (Lamballe et al., 1991; Vale and Shooter, 1985). This is particularly evident when the Trk receptors are coexpressed with the common neurotrophin receptor $p75^{NTR}$ (For review see Meakin and Shooter, 1992; Barbacid, 1993; Chao, 1994; Bradshaw et al., 1994; Ibáñez, 1995).

35   The common neurotrophin receptor $p75^{NTR}$ is a transmembrane glycoprotein structurally related to the tumor necrosis factor and CD-40 receptors (Meakin and Shooter,

1

1992; Rydén and Ibáñez, 1996). As all neurotrophins bind to p75[NTR] with similar affinity
(Rodriguez-Tébar et al., 1990; Hallböök et al., 1991; Rodriguez-Tébar et al., 1992; Ibáñez,
1995), neurotrophin specificity is conventionally thought to be caused by the binding
selectivity for Trk receptors which are differentially expressed in different neuronal populations

5   (Ibáñez, 1995). However, accumulated experimental data on neurotrophin activity reveal
important functional aspects of p75[NTR] (Heldin et al., 1989; Jing et al., 1992; Herrmann, 1993;
Barker and Shooter, 1994; Dobrowsky et al., 1994, Matsumoto et al., 1995; Marchetti et al.,
1996; Washiyama et al., 1996). The common neurotrophin receptor enhances functions and
increases binding specificity of Trk receptors (Barker and Shooter, 1994; Mahadeo et al.,

10   1994; Chao and Hempstead, 1995; Rydén and Ibáñez, 1996). In addition, p75[NTR] possesses
unique, Trk-independent signalling properties which involve ceramide production through
activation of the sphingomyelin cycle (Dobrowsky et al., 1994), apoptosis (cell death) (Van der
Zee et al., 1996; Cassacia-Bonnefil et al., 1996; Frade et al., 1996), and activation of the
transcription factor NFκB (Carter et al., 1996). Recently, p75[NTR] has been demonstrated to

15   participate in human melanoma progression (Herrmann et al., 1993; Marchetti et al., 1996).
Furthermore, NGF and NT-3 increase the production of heparin by 70W melanoma cells,
which is associated with their metastatic potential (Marchetti et al., 1996). Although this
effect has been shown to be mediated by the common neurotrophin receptor, neither BDNF
nor NT-4/5 appeared to be active. Explicit modelling of the various neurotrophin receptors

20   will be critical to the rational design of neurotrophin-based drugs.

NGF displays high and low affinity binding sites in sensory and sympathetic neurons
and in pheochromocytoma PC12 cells (Sutter et al., 1979; Landreth and Shooter, 1980;
Schechter and Bothwell, 1981). The coexpression of the common neurotrophin p75[NTR]
receptor with TrkA is required to form the high affinity binding site (Hempstead et al., 1991;

25   Barker and Shooter, 1994; Mahadeo et al., 1994; Chao and Hempstead, 1995). Several
models of the TrkA-p75[NTR] interaction have been proposed to explain high affinity NGF
binding (Bothwell, 1991; Chao, 1992b; Chao and Hempstead, 1995; Wolf et al., 1995; Ross et
al., 1996; Ross et al., 1997). These models differ with respect to direct (conformational
model) or indirect (ligand-presentation model) interaction of p75[NTR] with TrkA. Direct TrkA-

30   p75[NTR] interaction is consistent with much of the existing experimental data.

NGF, a 118 amino acid protein, is an extremely important neurotrophin, being
implicated in the pathogenesis of Alzheimer's disease, epilepsy and pain (Ben and Represa,
1990; McKee et al., 1991; Leven and Mendel, 1993; Woolf and Doubell, 1994; Rashid et al.,
1995; McMahon et al., 1995). The binding of NGF to its receptors is determined by distinct

35   sequences within its primary amino acid structure. While several regions of NGF participate
in the NGF/TrkA interaction, mutation studies suggest that relatively few key residues, namely

2

those located in the NGF amino and carboxyl termini, are required for high affinity binding.

The hairpin loop at residues 29-35 is responsible for recognition by p75[NTR] (Ibáñez et al., 1992; Radziejewski et al., 1992), while the amino and carboxyl termini are important binding determinants for recognition by the TrkA receptor (Shih et al., 1994; Moore and
5   Shooter, 1975; Suter et al., 1992; Burton et al., 1992, 1995; Kahle et al., 1992; Luo and Neet, 1992; Drinkwater et al., 1993; Treanor et al., 1995; Taylor et al., 1991). Truncation of either the amino or carboxyl terminus of NGF produces less active NGF analogues; similarly most deletion or point mutations of the amino terminus also lead to NGF analogues with diminished activity (Shih et al., 1994; Burton et al., 1992, 1995; Kahle et al., 1992; Drinkwater et al.,
10   1993; Treanor et al., 1995; Taylor et al., 1991). On the other hand, the NGFΔ2-8 (NGF with residues 2-8 removed) and NGFΔ3-9 deletion mutants are almost as active as wild type NGF (Drinkwater et al., 1993). These NGF structure-activity relationships in combination with the considerable species variability (mouse, human, guinea pig and snake) of the amino acid sequence of the NGF termini (McDonald et al., 1991) are of potential value in understanding
15   the NGF/TrkA interaction.

NGF exerts its biological activity as a non-covalent dimer (Treanor et al., 1995; Burton et al., 1995; McDonald et al., 1991; Ibáñez et al., 1993; Bothwell and Shooter, 1977). Two 118 residue NGF monomers are dimerized by hydrophobic and van der Waals interactions between their three anti-parallel pairs of β-strands; consequently, the amino terminus of one
20   NGF monomer and the carboxyl terminus of the other are spatially juxtaposed (McDonald et al., 1991). Furthermore, although a dimer has 2 pairs of termini, only one pair of termini is required for TrkA receptor recognition (Treanor et al., 1995; Burton et al., 1995). Accordingly, solving the conformation of the complex formed by the amino terminus of one monomer and the carboxyl terminus of the other in dimeric NGF is of fundamental relevance to
25   understanding the interaction of NGF with TrkA.

The X-ray crystallographic 3-dimensional structure of a dimeric mouse NGF (mNGF) has been reported recently (McDonald et al., 1991). However, within this structure, the amino terminus (residues 1-11) and the carboxyl terminus (residues 112-118) remain unresolved for both pairs of termini. High flexibility of the NGF termini makes it difficult to experimentally
30   determine their bioactive conformations, particularly since transition metal ions commonly used in X-ray crystallography (McDonald et al., 1991) have high affinity for His residues (Gregory et al., 1993) which are present in the NGF amino terminus (Bradshaw et al., 1994). Indeed, conformational alterations in the receptor binding domains of NGF caused by Zn^{2+} cations leading to its inactivation have been described recently (Ross et al., 1997). Since the
35   amino and carboxyl termini are crucial for NGF bioactivity as mediated via TrkA and because of the significance of NGF in multiple neurologic disease processes, the determination of the

3

biologically active conformation of these termini is an important and challenging problem for computational chemistry.

In contrast with NGF, little is known about the BDNF binding determinant for TrkB activation. Although there were several attempts to identify structural elements of BDNF that determine its receptor specificity (Ibáñez et al., 1991, 1993, 1995; Suter et al., 1992; Ilag et al., 1994; Kullander and Ebendal, 1994; Urfer et al., 1994; Lai et al., 1996), the results of mutational experiments are still controversial. Thus, the reported importance of residues 40-49 (variable loop region II) for TrkB related activity of BDNF (Ibáñez et al., 1991; Ilag et al., 1994) has not been confirmed by recent studies (Lai et al., 1996), in which it has also been shown that the key residues of the TrkB receptor binding domain of BDNF are situated between residues 80 and 109. The latter result is consistent with earlier observations that the BDNF termini are not involved in TrkB binding and that the key residues of the BDNF binding epitope are Arg^{81} and Gln^{84} (Ibáñez et al., 1993). In addition, it has been found that receptor binding domains of BDNF and NT-3 are located in the same regions of the molecules, i.e. in their "waist" parts (Ibáñez et al., 1993; Urfer et al., 1994). As far as the NT-3 receptor binding domain is concerned, detailed mutational studies carried out by Urfer et al. (1994) revealed that it comprises a surface that includes major parts of the central β-strand stem, with the most important residues being Arg^{103}, Thr^{22}, Glu^{54}, Arg^{56}, Lys^{80} and Gln^{83}. These residues correspond to Arg^{104}, Thr^{21}, Glu^{55}, Lys^{57}, Arg^{81} and Gln^{84} of BDNF, respectively (McDonald et al., 1991).

The location of the neurotrophin binding sites within the Trk receptors is the subject of debate (MacDonald and Meakin, 1996). Published data indicate the existence of two putative neurotrophin binding sites of Trk proteins: the "second immunoglobulin-like domain" (residues Trp^{299t}-Asn^{365t}, denoted IgC2) and the "second leucine-rich motif" (LRM-2A and LRM-2B, residues Thr^{97}-Leu^{120} of TrkA and TrkB, respectively) (Schneider and Schweiger, 1991; Kullander and Ebendal, 1994; Pérez et al., 1995; Urfer et al., 1995; Windisch et al., 1995a, 1995b, 1995c; MacDonald and Meakin, 1996; Rydén and Ibáñez, 1996).

$p75^{NTR}$ belongs to a family of cell surface proteins that share a common pattern of four repeated cysteine-rich domains (CRDs) in the extracellular portion (Yan and Chao, 1991; Baldwin and Shooter, 1994). X-ray crystallographic studies on the extracellular portion of the related protein $p55^{TNFR}$ revealed that CRDs fold independently of each other, and three conserved disulfide bonds maintain a specific geometry of each CRD which consists of two loops (Banner et al., 1993) (loops A and B, Fig. 1a). Very little is known about the $p75^{NTR}$ receptor functional epitope and, particularly, about residues directly participating in molecular recognition processes. All four CRD repeats of $p75^{NTR}$ are found to be required for binding, with the second CRD being most important (Baldwin and Shooter, 1995). Residue Ser^{50} of

4

p75^{NTR} seems to be essential for NGF binding (Baldwin and Shooter, 1995).

The results of site-directed mutagenesis suggest that the p75^{NTR} receptor binding domains within neurotrophins are juxtaposed positively charged residues located in two adjacent hairpin loops which represent variable region I (residues 23-35) and V (residues 93-98) (Ibáñez et al., 1992; Rydén et al., 1995; Ibáñez, 1994; Ibáñez, 1995; Rydén and Ibáñez, 1996) (Fig. 1c). In NGF, residues Lys^{32}, Lys^{34}, and Lys^{95} have been found to be involved in p75^{NTR} receptor binding, with Lys^{32} making the strongest contact, followed by Lys^{34} and Lys^{95}. In addition, some role of Asp^{30}, Glu^{35}, Arg^{103}, Arg^{100}, Lys^{88}, and Ile^{31} in p75^{NTR} binding and biological activity has been demonstrated (Ibáñez et al., 1992; Ibáñez, 1994). Two residues of variable region I, namely Arg^{31} and His^{33}, have been demonstrated to be essential for binding of NT-3 to p75^{NTR}, whereas similarly located Arg^{34} and Arg^{36} mediate binding of NT-4/5 (Rydén et al., 1995). In contrast to NGF, a positively charged residue in variable region V is not critical for binding of NT-3 or NT-4/5 to p75^{NTR} (Rydén et al., 1995). In BDNF, however, only residues of variable region V, Lys^{95}, Lys^{96} and Arg^{97}, bind to p75^{NTR} and compensate for the lack of positively charged residues in variable loop region I (Rydén et al., 1995).

Therefore, it is an object of the invention to establish explicit atom-level models of the Trk and p75^{NTR} recognition sites for neurotrophins.

It is a further object of the invention to provide atom-level models of the mechanism of interaction of neurotrophins and their receptors.

SUMMARY OF THE INVENTION

The inventors describe a method of characterizing the interaction between non-contiguous domains of a ligand and its receptor. The specific examples of the method described in detail below concern the interaction of nerve growth factor (NGF) with its TrkA receptor binding site, brain-derived neurotrophic factor (BDNF) with its TrkB receptor binding site, and the interaction of the neurotrophins (e.g., NGF, BDNF, NT-3, and NT-4/5) with the neurotrophin binding site of the common neurotrophin receptor p75^{NTR}.

In one aspect of the invention there is provided a variable basis Monte-Carlo (VBMC) simulated annealing method for identifying an optimal structure in a molecular system. The method comprises:

(a)   providing a Markov chain with an initial basis set of N configurational variables which define a structure for said molecular system;

(b)   translating the N configurational variables simultaneously along a basis vector to produce a new structure for the molecular system, wherein magnitude of translation is chosen randomly within a preselected range;

5

(c)   calculating potential energy of the new state of the molecular system;

(d)   deciding whether to accept or reject the new structure using an effective temperature dependent transition function, and if the new structure is accepted, replacing the current structure with the accepted structure;

(e)   repeating steps (b) to (d), each repetition having a new basis vector, for a preselected first number of repetitions at a preselected upper temperature; then

(f)   decreasing temperature according to a preselected cooling schedule;

(g)   repeating steps (b) to (d) and (f), each repetition having a new basis vector, for a preselected second number of repetitions; then

(h)   storing current structure of the molecular system;

(I)   repeating steps (g) and (h) until a preselected number of stored structures have been accumulated; then

(j)   rotating the basis set of configurational variables according to an effective distribution of the accumulated structures so that basis vectors are directed along low-energy valleys of a potential energy hypersurface thereby accelerating conformational motions and structural transitions of the molecular system, and erasing accumulated structures from steps (h) and (I);

(k)   repeating steps (I) and (j) until, after an effective third number of repetitions, a preselected lower temperature limit is reached, thereby producing an unrefined global minimum structure; and

(l)   refining the global energy minimum structure so that at least one local minimum on the potential energy hypersurface is identified.

The present invention also provides a method of identifying structures of a peptide domain of a neurotrophin to bind with a binding site of a receptor. The method comprises providing a plurality of neurotrophin analogues wherein at least one of neurotrophin analogue binds the receptor, identifying an optimal or near-optimal structure for respective peptide domains of the neurotrophin analogues that bind the receptor by applying a preselected number of the variable basis Monte-Carlo (VBMC) annealing simulations described above to each of the respective peptide domains to identify minimum or near-minimum energy structures for the peptide domains, and comparing said minimum or near-minimum energy structures to identify common structural features shared by neurotrophin analogues exhibiting receptor mediated activity.

The step of providing neurotrophin analogues may include providing wild-type neurotrophin analogues or mutants thereof.

The present invention also provides a method of identifying structures of a domain of a ligand to bind with a binding site of a receptor, comprising providing a plurality of ligand

6

analogues wherein at least one ligand analogue binds the receptor, identifying an optimal or near-optimal structure for respective domains of the ligand analogues that bind the receptor by applying a preselected number of the variable basis Monte-Carlo (VBMC) annealing simulations described above to each of the respective domains to identify minimum or near-

5   minimum energy structures for the domains; and comparing said minimum or near-minimum energy structures to identify common structural features shared by ligands exhibiting receptor mediated activity.

As would be apparent to a person skilled in the art, methods of the present invention are not limited to neurotrophin-receptor interactions, but are applicable to the characterization

10   of other ligand-receptor interactions. That is, an array of ligands that are either known to interact with a specific receptor or are candidate ligands that may potentially interact with this receptor may be computationally analyzed to identify optimal or near-optimal structures that provide the desired interaction. In some embodiments of the invention, the ligand may have a peptide domain, e.g., the ligand may be a peptide hormone, such as insulin, prolactin, or

15   growth hormone. In some embodiments, the ligands or candidate ligands under study may be native ligands, mutants of native ligands, or isosteres of native ligands. They may be structurally different but have similar binding activity or functional effect(s). The optimal or near-optimal structure identified may act as an agonist or antagonist. "Isosteric" is an art-recognized term and, for purposes of this disclosure, a first moiety is "isosteric" to a

20   second when they have similar molecular topography and functionality. This term should not, therefore, be restricted to mere similarity in chemical bond configuration. Two compounds may have different chemical bond configurations but nonetheless be isosteric due their 3-dimensional similarity of form and chemical nature, e.g. relevant centers such as heteroatoms are located in the same position, charges and/or dipoles are comparable, and

25   the like.

The present invention provides a ligand for binding with TrkA, wherein TrkA comprises a leucine rich motif (LRM) comprising amino acid residues 93 to 117, the coordinates of the residues of said LRM given in Appendix 1, said LRM motif having five binding areas, area A comprising amino acid residue Phe^{105tA} capable of hydrophobic bonding, area B comprising

30   residues Phe^{111tA}, Phe^{113tA}, and Thr^{114tA} capable of hydrophobic bonding, area C comprising residues Asp^{109tA} and His^{112tA} capable of ionic interaction, area D comprising residue Lys^{100tA} capable of ionic interaction, and area E comprising residues Asn^{95tA} to Ile^{88tA} capable of multiple parallel β-strand type hydrogen bonding. The ligand includes at least three moieties each comprising effective atomic elements having spatial occupancy, relative atomic position,

35   bond type and charge to define a three dimensional conformation of said ligand so that a first moiety can bind with a first binding area, a second moiety can bind with a second binding

7

area, and a third moiety can bind with a third binding area.

Put another way, the ligand comprises at least three moieties effectively spaced relative to each other so that a first moiety can bind with a first binding area, a second moiety can bind with a second binding area, and a third moiety can bind with a third binding

5   area. More specifically, the ligand comprises at least one moiety being capable of hydrophobic bonding and being present in an effective position in the ligand to hydrophobically bind to area A, at least one positively charged moiety being present in an effective position in said ligand to ionically bind to area C, and at least one negatively charged moiety being present in an effective position in said ligand to ionically bind to area D.

10   The present invention also provides a method of designing a ligand to bind with an LRM of TrkA. The method comprises providing a template of said LRM of TrkA, said LRM comprising amino acid residue sequence 93 to 117 inclusive, said amino acid residues having spatial Cartesian coordinates given in Appendix 1 wherein binding area A in the sequence comprises residue Phe^{105tA} capable of hydrophobic bonding, binding area B comprises

15   residues Phe^{111tA}, Phe^{113tA}, Thr^{114tA} capable of hydrophobic bonding, binding area C comprises residues Asp^{109tA} and His^{112tA} capable of ionic interaction, binding area D comprises Lys^{100tA} capable of ionic interactions, and binding area E comprises residues Asn^{95tA} to Ile^{98tA} capable of multiple parallel β-strand type hydrogen bonding and computationally evolving a chemical ligand using any effective algorithm with preselected spatial constraints so that said evolved

20   ligand comprises at least three effective moieties of suitable identity and spatially located relative to each other in the ligand so that a first of the moieties hydrophobically interacts with binding area A, a second of the moieties ionically interacts with binding area C, and a third of the moieties ionically interacts with binding area D of the LRM of TrkA. The algorithm may be a genetic algorithm and the LRM may be the second LRM of a plurality of LRMs.

25   The invention further provides a method of designing a ligand to bind with an LRM of TrkA, comprising providing a template of said LRM of TrkA, said LRM comprising amino acid residue sequence 93 to 117 inclusive, the amino acid residues having spatial Cartesian coordinates given in Appendix 1 wherein binding area A comprises Phe^{105tA} capable of hydrophobic bonding, binding area B comprises Phe^{111tA}, Phe^{113tA}, Thr^{114tA} capable of

30   hydrophobic bonding, binding area C comprises Asp^{109tA} and His^{112tA} capable of ionic interaction, binding area D comprises Lys^{100tA} capable of ionic interaction, and binding area E comprises Asn^{95tA} to Ile^{98tA} capable of hydrogen bonding. The method comprises computationally evolving a ligand using an effective algorithm so that said evolved ligand comprises at least three effective moieties located relative to each other in the ligand so that

35   a first moiety can bind with a first of the five binding areas, a second moiety can bind with a second of the five binding areas, and a third moiety can bind with a third of the binding areas.

8

In another aspect the invention provides a ligand for binding with TrkB, wherein TrkB comprises a leucine-rich motif (LRM) comprising amino acid residues 93 to 117, the coordinates of the residues of said LRM given in Appendix 2, said LRM having five binding areas, binding area F comprising amino acid residue Asp^{100tB} capable of ionic interaction,

5   binding area G comprising amino acid residue Lys^{109tB} capable of ionic interaction, binding area H comprising amino acid residues Lys^{113tB} capable of ionic interaction, binding area I comprising amino acid residue Arg^{94tB} capable of ionic interaction, and binding area K comprising amino acid residue Lys^{104tB} capable of hydrogen bonding or ionic interaction. The ligand comprises at least three moieties effectively spaced relative to each other so that a

10 first moiety can bind with a first binding area, a second moiety can bind with a second binding area, and a third moiety can bind with a third binding area.

The present invention provides a method of designing a ligand to bind with TrkB, wherein TrkB comprises a leucine-rich motif (LRM) comprising amino acid residues 93 to 117, the coordinates of the residues of said LRM given in Appendix 2, said LRM having five

15 binding areas, binding area F comprising amino acid residue Asp^{100tB} capable of ionic interaction, binding area G comprising amino acid residue Lys^{109tB} capable of ionic interaction, binding area H comprising amino acid residue Lys^{113tB} capable of ionic interaction, binding area I comprising amino acid residue Arg^{94tB} capable of ionic interaction, and binding area K comprising amino acid residue Lys^{104tB} capable of hydrogen bonding or ionic interaction. The

20 method comprises computationally evolving a ligand using an effective algorithm so that the evolved ligand comprises at least three effective moieties located relative to each other in the ligand so that a first moiety can bind with a first of said five binding areas, a second moiety can bind with a second of said five binding areas, and a third moiety can bind with a third of the binding areas. The algorithm may be a genetic algorithm.

25 The invention also provides a ligand for binding with the common neurotrophin receptor p75^{NTR}, wherein p75^{NTR} comprises a binding site including amino acid residues Cys^{39p} to Cys^{94p} inclusive, said residues of said binding site having spatial coordinates given in Appendix 3, said binding site having three binding areas including binding loop 2A comprising region Cys^{39p} to Cys^{58p} capable of attractive electrostatic interactions, binding loop 2B

30 comprising region Cys^{58p} to Cys^{79p} capable of attractive electrostatic interactions, and binding loop 3A comprising region Cys^{79p} to Cys^{94p} capable of attractive electrostatic interactions. The ligand comprises at least two moieties effectively spaced relative to each other so that a first moiety can bind to a first loop and a second moiety can bind to a second loop.

The present invention also provides a method of designing a ligand for binding with

35 the common neurotrophin receptor p75^{NTR}, wherein p75^{NTR} comprises a binding site including amino acid residues Cys^{39p} to Cys^{94p} inclusive. The residues of the binding site have spatial

9

coordinates given in Appendix 3. The binding site has three binding areas including binding loop 2A comprising region Cys^{39p} to Cys^{58p} capable of attractive electrostatic interaction, binding loop 2B comprising region Cys^{58p} to Cys^{79p} capable of attractive electrostatic interaction, and binding loop 3A comprising region Cys^{79p} to Cys^{94p} capable of attractive

5   electrostatic interaction. The method comprises computationally evolving a ligand using an effective algorithm so that the evolved ligand comprises at least two effective moieties located relative to each other in the ligand so that a first moiety can bind to a first of the three loops and a second moiety can bind to a second loop of the three loops.

The invention provides a method of identifying a ligand to bind with a leucine rich motif

10   (LRM) of TrkA. The method comprises providing a three dimensional conformation for the LRM. The LRM comprises amino acid residue sequence 93 to 117 inclusive, the amino acid residues having spatial Cartesian coordinates given in Appendix 1. The LRM has five binding areas, area A comprising amino acid residue Phe^{105A} capable of hydrophobic interaction, area B comprising amino acid residues Phe^{111A}, Phe^{113A}, and Thr^{114A} capable of hydrophobic

15   interaction, area C comprising amino acid residues Asp^{109A} and His^{112A} capable of ionic interaction, area D comprising amino acid residue Lys^{100A} capable of ionic interaction, and area E comprising Asn^{95A} to Ile^{98A} capable of multiple parallel β-strand type hydrogen bonding. The method includes providing a data base containing molecules coded for spatial occupancy, relative atomic position, bond type and/or charge; and screening the data base to

20   select those molecules comprising moieties having a three dimensional conformation and effective charge that can bind with at least three of the five binding areas.

The invention provides a method of identifying a ligand to bind with a leucine rich motif (LRM) of TrkB. The method comprises providing a three dimensional conformation for the LRM. The LRM comprises amino acid residues 93 to 117, the coordinates of the residues of

25   the LRM are given in Appendix 2, the LRM having five binding areas, binding area F comprising amino acid residue Asp^{100B} capable of ionic interaction, binding area G comprising amino acid residue Lys^{109B} capable of ionic interaction, binding area H comprising amino acid residue Lys^{113B} capable of ionic interaction, binding area I comprising amino acid residue Arg^{94B} capable of ionic interaction, and binding area K comprising amino acid residue Lys^{104B}

30   capable of hydrogen bonding or ionic interaction. The method includes providing a data base containing molecules coded for spatial occupancy, relative atomic position, bond type and/or charge; and screening the data base to select those molecules comprising moieties having a three dimensional conformation and effective charge that can bind with at least three of the five binding areas.

35   The present invention also provides a method of identifying a ligand to bind with common neurotrophin receptor $p75^{NTR}$. The method comprises providing a three dimensional

conformation for the common neurotrophin receptor p75^{NTR}, wherein p75^{NTR} comprises a binding site including amino acid residues Cys^{39p} to Cys^{94p} inclusive. The residues of the binding site have spatial coordinates given in Appendix 3, the binding site having three binding areas including binding loop 2A comprising region Cys^{39p} to Cys^{58p} capable of
5   attractive electrostatic interaction, binding loop 2B comprising region Cys^{58p} to Cys^{79p} capable of attractive electrostatic interaction, and binding loop 3A comprising region Cys^{79p} to Cys^{94p} capable of attractive electrostatic interaction. The method includes providing a data base containing molecules coded for spatial occupancy, relative atomic position, bond type and/or charge; and screening the data base to select those molecules comprising moieties that can
10   bind with at least two of the three binding loops.

In one aspect of the invention, a ligand (e.g., small molecule) designed to interact with a receptor such as Trk or p75NTR may be bifunctional, such that a first portion of the ligand binds to one receptor monomer and a second portion of the ligand binds to a second receptor monomer. Thus, a receptor dimer is effectively cross-linked by the interaction of ligand with
15   both receptor monomers.

According to the invention, detailed information is provided regarding those amino acid residues of neurotrophins and of neutrophin receptors which are involved in neurotrophin-receptor binding. Such information includes the bioactive conformations of the respective peptide domains of the neurotrophins and receptors. This in turn permits the
20   design of small molecules which interact with said amino acid residues or domains. Where such interaction block the residues or changes the conformation of the domain, the small molecule can inhibit neurotrophin-receptor binding, in certain cases abolishing it completely. As would be appreciated by a person skilled in the art, small molecule design according to this aspect of the invention is applicable to other ligand-receptor interactions in addition to
25   neurotrophins, according to the methods disclosed herein.

As a person skilled in the art would appreciate, the invention not only provides molecules (ligands) that interact with receptors, but also molecules which, in their mimicry of a receptor's bioactive conformation, can bind to the receptor binding site of a ligand such as, for example, a neurotrophin. Such molecules, whether they interact with ligand or with
30   receptor, can block native ligand-receptor interaction. In some embodiments of the invention, a small molecule which binds to a receptor may even trigger signal transduction similar to that of the native ligand, i.e., act as an agonist.

35

BRIEF DESCRIPTION OF THE DRAWINGS

The invention will be described, by example only, reference being had to the accompanying drawings, in which:

5 Figure 1 shows the amino acid sequences of the conformationally variable termini of the dimeric NGF analogues under study. The residues are numbered from 1 to 118 for the first monomer, and from 1' to 118' for the second monomer. The fixed parts of the proteins simulated by the X-ray geometry of mouse NGF (McDonald et al., 1991) are underlined.

10 Figure 2 shows the structure of the complex of the amino and carboxyl termini of (1-118)hNGF homodimer. The carboxyl terminus is shown in grey, the amino terminus in white, and the interacting conservative region $His^{75'}$-$Asn^{77'}$ of the "south" part of the NGF dimer, in black.

Figure 3 shows the structure of the complex of the amino and carboxyl termini of (1-118)mNGF homodimer.

15 Figure 4 shows the structure of the complex of the amino and carboxyl termini of dimeric $mNGF\Delta3$-9 molecule.

Figure 5 shows the structure of the complex of the amino and carboxyl termini of dimeric hNGF-H4D molecule.

Figure 6 shows the structure of the complex of the amino and carboxyl termini of
20 dimeric $mNGF\Delta1$-8 molecule.

Figure 7 shows the structure of the complex of the amino and carboxyl termini of BDNF homodimer.

Figure 8 illustrates the TrkA leucine-rich motifs. Locations of parallel β-strands are illustrated by the shaded areas designated by symbol β. Fragments B1-B4 demonstrate NGF
25 binding affinity, while N1-N4 do not (Windisch et al., 1995a, 1995b).

Figure 9 shows sequences of the amino and carboxyl termini of fully active NGF analogues. Regions with rigid structures are underlined.

Figure 10 shows the predicted bioactive conformation of the NGF binding domain (a) and the structures of the NGF/LRM-2A complexes of hNGF (b), mNGF (c), $mNGF\Delta3$-9 (d),
30 and hNGF:NT-4/5 (e). Only residues essential for discussion are designated. A, B, C, D and E represent specific NGF/LRM-2A binding areas. The LRM-2A is illustrated in grey, NGF in white.

Figure 11 shows the TrkB receptor binding site of BDNF (a), predicted features of the BDNF/LRM-2B complex (b), and geometry of the "improper" NGF/LRM-2B complex (c). Only
35 residues essential for discussion are designated. F, G, H, I and K represent specific BDNF/LRM-2B binding areas. The LRM-2B is illustrated in grey, BDNF and NGF in white.

Figure 12 is a detail of the LRM-2A conformation when bound to hNGF. The three groups of the β-strand involved in H-bonding with the parallel β-strand motif of the NGF analogues are designated by NH or CO. Hydrophobic residues are illustrated as light, polar uncharged as dark, charged as black.

5   Figure 13 presents principal residues of the NGF binding domain essential for TrkA receptor recognition. Conserved residues of NGF molecules among all characterized species (McDonald et al., 1991) are designated by $\underline{X}$, whereas those which are substituted in NGF molecules derived from different species by similar amino acids and NGF residues maintaining the bioactive conformation or interacting with specific binding areas A-E of the
10   LRM-2A are indicated by X.

Figure 14 presents principal residues of the LRM-2A. The residues which are specific for TrkA (Windisch et al., 1995a, 1995b) and critical for the present model are designated by X and $\underline{X}$, respectively.

Figure 15 is a schematic representation of the second leucine-rich motif of TrkA
15   (residues 93tA to 116tA) (a) and TrkB (residues 93tB to 116tB) (b) as specific binding sites for NGF and BDNF, respectively. General consensus residues are shaded. Arrows designate distinct positions essential for molecular recognition processes.

Figure 16 represents the X-ray crystallography-derived geometry of the α-carbon trace of the two loops (2A and 2B) of the second cysteine-rich domain (white bonds) and the first
20   loop (3A) of the third cysteine-rich domain (grey bonds) of p55^{TNFR} (Banner et al., 1993) (a), the preferred geometry of the α-carbon trace of the corresponding fragment of p75^{NTR} (b), and the predicted bioactive conformation of mouse NGF (McDonald et al., 1991); (c). White and grey bonds in panel (c) illustrate different protomers. The p75^{NTR} binding determinant of NGF (loops I and V) is denoted. Disulfide bonds are shown in black.

25   Figure 17 shows the sequence of a putative binding site for neurotrophins within p75^{NTR} aligned with the corresponding sequence of homologous p55^{TNFR}. Conserved pattern of disulfide bonds is illustrated. Abbreviation (h) stands for human (Johnson et al., 1986), (r) for rat (Radeke et al., 1987), and (c) for chicken (Large et al., 1989) p75^{NTR}.

Figure 18 illustrates the most stable geometries of the complexes of the neurotrophins
30   with the common neurotrophin receptor p75^{NTR}: with NGF (a); with BDNF (b); with NT-3 (c); with NT-4/5 (d). The α-carbon traces of the neurotrophins are shown in white, while that of the p75^{NTR} binding site is shown in grey. Disulfide bonds are illustrated in black. Only residues mentioned in the text are denoted.

Figure 19 demonstrates geometric compatibility of the van der Waals surfaces of
35   BDNF (light) and the p75^{NTR} binding site (dark).

Figure 20 illustrates conformational changes of the p75^{NTR} binding site upon BDNF

13

binding. Conformation of the p75[NTR] receptor binding site before binding is illustrated in white, after binding in grey. The two conformations have been superimposed using the equilibrium positions of the reference α-carbon atoms located in loops 2A and 3A. Straight lines denote linear approximations of the conformations of the α-carbon traces of loop 2B in both
5   structures.

DETAILED DESCRIPTION OF THE INVENTION

PART A

10   THEORETICAL STUDIES OF THE BIOACTIVE CONFORMATION OF NERVE GROWTH FACTOR USING VBMC - A NOVEL VARIABLE BASIS MONTE-CARLO SIMULATED ANNEALING ALGORITHM FOR PEPTIDES

BACKGROUND TO THE VBMC ALGORITHM

15   The structural optimization of the peptide domains under study required a rigorous search of conformational space. As with other theoretical peptide studies, such calculations are plagued by a multiple-minima problem (Gibson and Scheraga, 1988) which traditionally is addressed using either molecular dynamics, Monte Carlo approaches or other algorithms. The Monte Carlo method, although exceedingly powerful, is limited by the excessive CPU
20   time requirements on existing computers. To remedy this problem, we have devised a novel Variable Basis Monte Carlo simulated annealing algorithm for peptides (VBMC).

         The potential energy hypersurface of a peptide has an enormous number of local minima (Gibson and Scheraga, 1988; Piela et al., 1989, 1994), but usually only the global energy minimum structure is required. Despite efforts to elaborate an efficient method of
25   global energy minimization (Gibson and Scheraga, 1988; Judson et al., 1994), the multiple-minima problem is far from being solved. Although simulated annealing (Kirkpatrick et al., 1983; Vanderbilt et al., 1984) is mathematically correct and guarantees convergence to the global minimum in principle, the suggested "cooling" schedule appears to be far too slow for practical purposes, and faster "cooling" has to be used (Gidas, 1985; Kushner, 1987).
30   Within the simulated annealing approach, thermal molecular motion can be simulated either by Monte Carlo (Kirkpatrick et al., 1983; Nayeem et al., 1991; Wilson et al., 1988; Snow, 1992; Shamovsky et al., 1992) or molecular dynamics (Lelj et al., 1991; Villani and Tamburro, 1994) methods.

         The major problem of the Monte Carlo technique is that motion of a molecular system
35   along a Markov chain is very slow (Piela et al., 1994; Scheraga, 1989; Nayeem et al., 1991). On the other hand, the Monte Carlo technique has several considerable advantages over

14

molecular dynamics. First, it does not require calculating forces. Second, potential energy functions do not have to be continuous. Third, much larger steps in conformational space can be utilized (Li and Scheraga, 1988; Kincaid and Scheraga, 1982). Fourth, the additional iterative self-consistent SHAKE routine (Ryckaert et al., 1977), which is used in molecular

5   dynamics simulations to deal with holonomic constraints (Brooks III and Case, 1993), is not required in the Monte Carlo method. This has led to efforts to accelerate configurational motion within the Monte Carlo approach (Raj et al., 1994; Snow, 1992; Kincaid and Scheraga, 1982; Rao et al., 1979; Rossky et al., 1978). The main reason for inefficiency with the conventional Monte Carlo method (Metropolis et al., 1953) is a slow and cumbersome

10   sequential change of configurational variables.

To overcome these problems, lessons can be learned from molecular dynamics. In molecular dynamics (Allen and Tildesley, 1987) configurational variables move simultaneously, and the soft modes of the system explicitly direct these motions. Soft modes are defined as low-energy valleys on the potential energy hypersurface. Although there have

15   been attempts to direct Monte Carlo configurational motion along the soft modes (Raj et al., 1994; Rao et al., 1979; Rossky et al., 1978), these improvements require calculating forces and, consequently, result in losing the main advantages of the Monte Carlo approach. An algorithm which would retain the advantages of the Monte Carlo method and direct configurational changes along the soft modes is thus required. One possible solution has

20   recently been suggested (Szentpaly et al., 1994).

The classical Monte Carlo-Metropolis method (Metropolis et al., 1953) consists of modelling a Markov chain containing subsequent conformations of the molecule under study: x_0, x_1, x_2,..., x_i,..., where x ($x_i = \{x_i^1 ... x_i^m ... x_i^N\}$) is the vector of independent structural parameters. Each vector x_{i+1} is derived from the preceding one, x_i, by means of a random

25   change of one randomly chosen variable:

$$x_{i+1}^m = x_i^m + \lambda_m \cdot \xi \qquad\qquad (1)$$

where ξ is a random quantity from the interval $(-1,1)$ and λ_m is a maximal allowed increment of

30   the given variable. N moves of the Markov chain (where N is the number of independent parameters) represent a Monte Carlo step. Whether the new state x_{i+1} is accepted or rejected is decided according to a transition probability function. The following functional form of transition probability is used in the present expression (2) (Gunningham and Meijer, 1976):

35   $$W(x_i \Rightarrow x_{i+1}) = 1/[1 + \exp(\Delta E_i /kT)] \qquad\qquad (2)$$

15

where ΔE_i is the difference between conformational energies of the states x_{i+1} and x_i, k is the Boltzmann constant and T is absolute temperature.

Those skilled in the art will appreciate that other functional forms of transition functions may be used to screen state a new state x_{i+1}. For example, another effective
5   temperature dependent transition function for screening a new state x_{i+1} derived from a previous state x_i is given by:

$$W(x_i \Rightarrow x_{i+1}) = 1, \qquad\qquad \text{if } E(x_{i+1}) \le E(W(x_i))$$

$$= \exp(-\Delta E_i /kT), \qquad \text{if } E(x_{i+1}) \ge E(W(x_i))$$

where ΔE_i is the difference between conformational energies of the states x_{i+1} and x_i, k is the
10 Boltzmann constant and T is absolute temperature.

The direct application of this conventional Monte Carlo technique to the conformational space study of protein structure is not efficient because the conformational variables of peptide chains appear to be mutually dependent, i.e., low-energy conformational motions involve several conformational variables. When applied to molecular systems such
15 as protein secondary, tertiary or quaternary structure, equation (1), in which structural parameters are sequentially changed one after another, results in very small values of ξ and, consequently, in a very slow conformational motion (Piela *et al.*, 1994; Scheraga, 1989; Nayeem *et al.*, 1991). In order to model a *simultaneous* change of the structural parameters, we have used Eq.(3) (instead of the conventional (1)),

20

$$x_{i+1} = x_i + \lambda_m \cdot \xi \cdot g^m \qquad\qquad\qquad (3)$$

where g^m is a randomly or sequentially chosen *basis vector* from a basis $G=\{g^m\}$, ξ is a random quantity from an interval (-1,1) and λ_m is a maximal acceptable move in direction g^m.
25 In this study λ_m was constant and equal to $10°$.

A basis G is formed from linear combinations of independent conformational parameters x for their change to be realized *along the soft modes* of the molecule. These modes are revealed by dispersion analysis of the distribution of the sequential configurational points of the Markov chain. The soft modes of the molecular system are to be directed along
30 the axes of the dispersion ellipsoid because they should correspond to the directions of maximal deviations made by the independent variables during a certain period of simulation. Initially, basis G coincides with a unit matrix, i.e., G = I, and Eq.(3) is equivalent to (1). The rotation of basis G is carried out after every 150 Monte Carlo steps based on the particular scattering of the previous 150 configurations x. Basis vectors g^m are made equal to the
35 eigenvectors of the covariant matrix D which has the following elements:

16

$$d_{ij} = (1/M) \cdot \sum_{n=1}^{M} (x_n' - (1/M) \cdot \sum_{n=1}^{M} x_n') \cdot (x_n' - (1/M) \cdot \sum_{n=1}^{M} x_n') \qquad (4)$$

where M is the number of points in the distribution (M=150), and x_n' is the i-th structural parameter at the n-th Monte Carlo step. Vectors g^m form the orthonormalized basis and are used in the Markov chain instead of independent conformational parameters. Periodic rotations of basis G in Monte Carlo simulations result in a simultaneous change of all the conformational variables along the valleys of a potential energy surface, which considerably accelerates conformational motions and transitions (Szentpaly et al., 1994).

The method disclosed herein is highly advantageous over known processes for several reasons. In the present process the preselected range from which the magnitude of translation is chosen is constant and does not depend on the basis set. Thus the present method is much more efficient than previous methods in part because the magnitude of translation along the basis vector is limited by a preselected range. The present method is also more efficient because rotation of the basis set of configurational variables is avoided at the upper temperatures and is implemented only at the lower temperatures.

IMPLEMENTATION OF THE VBMC ALGORITHM

VBMC was written in Fortran-77. The algorithm was then interfaced with the CHARMM force field (Brooks et al., 1983; The force field parameters are extracted from CHARMM release 23.1, Molecular Simulations, Inc., Waltham, MA). Torsional distortion, van der Waals and electrostatic interactions, and hydrogen bonding were thus explicitly considered. The united atom approach was used for all carbons with non-polar hydrogens. Point atomic charges of Weiner et al. (Weiner et al., 1984) were used. A dielectric constant equal to the interatomic separation in angstroms was utilized to implicitly simulate solvation effects (Weiner et al., 1984). All calculations were performed on an 8-node IBM Scalable POWERparallel 2 [SP2] high performance computer at Queen's University, Kingston, Canada. Each Monte Carlo simulated annealing computation required up to 120 hours of CPU time.

Appendix 4 is attached. Appendix 4 is a computer program written in Fortran-77 and is a non-limiting example of a program used to perform the VBMC simulated annealing method in accordance with the present invention.

Each run of the VBMC algorithm provides a unique final structure which would represent the global energy minimum structure, regardless of the initial geometry, if the "cooling" was performed infinitely slowly. However, since this is impossible, several Monte Carlo simulated annealing computations must be performed from different starting points x_0, using different initial temperatures T_0, "cooling" schedules and random sequences. An initial temperature of 1000° K is sufficient. The Markov chain is kept at a constant temperature T_0

17

for 10^4 Monte Carlo steps before the initiation of "cooling". The temperature T is then decreased at every Monte Carlo move (3) by a small increment such that after $2 \cdot 10^4$ Monte Carlo steps it reaches 120° K producing an unrefined global energy minimum structure.

5   The global energy minimum structure is then refined to identify the nearest local minimum or stationary point on the potential energy hypersurface. Refinement may be accomplished using any one of several non-linear minimization routines to identify the local minimum on the potential energy hypersurface. For example, gradient descent minimization and conjugate gradient minimization may be used. Quasi-Newton minimization methods such as the Newton-Raphson method may also be used. Other non-linear methods include the

10 Marquardt method, the Powell method and a variable metric method. Those skilled in the art will be aware of the various non-linear routines which may be used for refinement and those mentioned herein are more fully described in *Nonlinear Programming: Theory, Algorithms, and Applications.* 1983. New York: John Wiley & Sons.

APPLYING VBMC TO NGF

15   The aim of this computational study was to ascertain the biologically active conformation of the TrkA receptor binding determinant of NGF. A comprehensive review of the literature identified an initial study set of 17 proteins which have been assessed for TrkA mediated activity using comparable experimental methods. From these 17 analogues, a subset of six (three active and three inactive) which reflects the range of structural diversity

20 was selected for preliminary study. Accordingly, in the present invention the low-energy conformations of the amino and carboxyl termini of six NGF analogues were obtained by means of Monte Carlo simulated annealing calculations. Three of these analogues retain full TrkA mediated activity: human NGF (hNGF; Shih *et al.*, 1994; Burton *et al.*, 1992), mouse NGF (mNGF; Burton *et al.*, 1992; Drinkwater *et al.*, 1993), and mNGFΔ3-9 (deletion 3-9 of

25 mNGF; Drinkwater *et al.*, 1993). The other three analogues are biologically inactive: hNGF-H4D (a point mutation of hNGF in which His [H] in position 4 is replaced by Asp [D]; Shih *et al.*, 1994), mNGFΔ1-8 (Burton *et al.*, 1992; Drinkwater *et al.*, 1993; Taylor *et al.*, 1991) and BDNF (Suter *et al.*, 1992). The results and conclusions obtained from these six analogues were then validated by being applied to the remaining 11 analogues of the initial

30 study set.

      The amino acid sequences of the termini of the neurotrophin molecules under study are presented in Figure 1. Residues are numbered from 1 to 118 for the first monomer, and from 1' to 118' for the second monomer. The mutual orientation of the termini of the different monomers is determined by the disulfide bonds Cys^{15} - Cys^{80} and $Cys^{68'}$ - Cys^{110} and

35 hydrophobic interactions Val^{14} :$Val^{14'}$ and Val^{109} :$Val^{109'}$, which are absolutely conserved in all neurotrophins (McDonald *et al.*, 1991). The conformational space of the peptide molecules

18

consists of flexible torsional angles determining geometry of the amino terminus of one monomer and the carboxyl terminus of the other, while keeping the rest of the dimer fixed in the known geometry of mNGF (McDonald *et al.*, 1991). Covalent bond lengths and bond angles of the termini are kept fixed. The geometry of each residue is determined only by

5   flexible torsional angles of the peptide backbone (ϕ and ψ) and the side chain (χ_1, χ_2,...). All torsional angles of amino acid Pro except for ψ are fixed. Torsional angles describing structural motifs with the essentially planar geometry (such as peptide bonds or conjugated regions in side chains) are kept fixed. Likewise, the configurations of the sp^3-carbons are fixed. With these constraints, the total conformational space of the flexible termini of hNGF,

10   mNGF and BDNF consists of 74, 73 and 67 variables, respectively.

RESULTS AND DISCUSSION

By diagonalizing the covariant matrix in the framework of the VBMC algorithm, rigid modes of a molecular system, which should slow down conformational changes, are supposed to be revealed simultaneously with soft modes of the system. To test the efficiency

15   of the VBMC algorithm, its performance was compared with the conventional Monte-Carlo method at the equilibrium parts of the Markov chains generated at different constant temperatures. These comparisons showed that at high temperatures (700^0-1000^0K) the basis variability results in decreasing acceptance rates. On the other hand, the temperature decrease reinforces the advantage of the VBMC approach, and at temperatures below 600^0

20   acceptance rates of the VBMC Markov chains were significantly higher. Thus, at T=300^0 K the acceptance rate of the conventional Markov chain was found to be 0.22, which is very close to that recommended by Kincaid and Scheraga (1982) as optimal (0.20). The acceptance rate of the VBMC algorithm obtained at the same conditions was 0.26, i.e. 18% higher. These evaluations are in agreement with what one would expect. Indeed, at low

25   temperatures only soft modes of molecules are involved in thermal motions, hence, they are especially populated in corresponding Monte-Carlo generated conformational ensembles and can be revealed from them. Higher acceptance rates of the low temperature VBMC Markov chains over conventional Markov chains mean that the average increase of the sizes of the Monte-Carlo moves along soft modes of the system are higher than their decrease along the

30   rigid modes. Thus, the VBMC disclosed herein for evaluating peptide conformations not only changes directions of the Monte-Carlo moves, but also accelerates conformational changes by directing them along the soft modes of the molecule. Consequently, the present VBMC algorithm is more efficient than conventional Monte-Carlo method only at moderate and low temperatures, when thermal motions tend to take place along the valleys of the potential

35   energy surface. This particular temperature region causes serious problems in known simulated annealing algorithms, and the VBMC method disclosed herein provides a solution

19

to these problems.

Seven independent VBMC simulations for each of the six molecular systems under study were performed. Simultaneously, local energy refinements were periodically carried out from a number of points generated during the "slow cooling" stage. All local minimizations

5   resulted in higher energy stationary points on the potential energy surface than those produced by VBMC computations. This means that the VBMC technique as an approach to global minimization cannot be replaced by relatively inexpensive periodic energy refinements from the high-temperature conformational space; at high temperatures only high-energy conformers are sufficiently populated. Although VBMC runs did not converge to the same

10 conformation, the final structures differed insignificantly; i.e., the peptide backbone conformation remained unchanged but there were limited differences in the side chain torsional angles. Multiple VBMC simulations identified rigid and flexible parts of the molecules. Minimum energy structures of all molecules are displayed in Figures 2-7 while Table 1 presents optimized conformational parameters of the amino and carboxyl termini of

15 the considered NGF analogues.

GEOMETRIC SIMILARITY OF BIOACTIVE NGF CONFORMERS

Rigid regions of hNGF and mNGF which maintain the same conformation in all independent VBMC simulations are formed by residues 9-11 and 112'-118', creating a richly hydrogen bonded (H-bonded) 3-dimensional complex. Conformational variability within this

20 rigid zone is primarily restricted to side chains and does not affect the geometry of the backbone. An interesting example of such side chain mobility occurs with $Arg^{114'}$, which is H-bonded to the carbonyl oxygen of the ninth amino acid of the amino terminus and which is therefore expected to have a fixed conformation. Nevertheless, $Arg^{114'}$ has two distinct conformers in which the H-bonding is realized by the hydrogen atoms attached to the different

25 NH_2 groups, with the energy difference being about 1 kcal/mol. In addition to local conformational variability, hNGF and mNGF have a region of "cooperative" flexibility which is made up of residues 1-8. Several distinct conformations exist within this region, with its conformational variability being caused by a number of possibilities for the H-bond network formed by residues 1-3.

30 Comparison of the most stable conformers of hNGF (Figure 2) and mNGF (Figure 3) reveals striking conformational similarity between their rigid regions in spite of several differences in the primary structure of the amino and carboxyl termini (Figure 1). As shown in Table 1, both termini have the same conformation, except for the variable region consisting of residues 1-3. The most stable H-bond networks in this area differ considerably because of

35 the mT3hS substitution.

The essential difference between the amino acid sequences of the termini of hNGF

20

and mNGF is the mM9hR substitution, which does not change the geometry of the rigid region. Residues Met and Arg have different side chain types, i.e., the former is non-polar while the latter is polar and positively charged under physiological conditions. It is surprising that this substitution does not affect geometry since it introduces the positive charge of Arg^9

5   which is located in an electrostatic field created by at least five neighbouring charged functional groups. Conformational stability of the rigid region of hNGF is maintained by the exact fit of the Arg^9 side chain into a "hollow" in the rigid region, which is occupied by the Met^9 side chain in mNGF. Furthermore, the Arg^9 side chain, being in this "hollow", forms two additional interchain H-bonds with carbonyl oxygens of residues $Val^{117'}$ and $Arg^{118'}$. This

10   further stabilizes the rigid region of hNGF.

The physical reason for the geometric similarity of the rigid regions of hNGF and mNGF is that the structural features of these two complexes are determined by similar H-bonding and electrostatic interactions. The major stabilizing factor is the H-bonding and electrostatic interaction of charged side chains of residues Glu^{11} and $Arg^{118'}$. In addition,

15   these side chains are involved in other H-bonding: the carboxyl oxygens of Glu^{11} are bonded to the δ-NH group of His^8 , the hydroxyl group of $Ser^{113'}$ and the backbone NH group of $Lys^{115'}$; the side chain NH and NH_2 groups of $Arg^{118'}$ are bonded to the backbone Phe^7 and $Lys^{115'}$ carbonyl groups. There are some other common interchain H-bonds in hNGF and mNGF. The ε-amino group of the $Lys^{115'}$ side chain forms a H-bond with the δ-carbonyl oxygen of the

20     $Asn^{77'}$ residue, situated at the "south" part of NGF structure (McDonald et al., 1991).

In addition to H-bonding, the particular geometry of the rigid region in both molecules is also maintained by electrostatic interactions of positively charged residues, specifically His^4, His^8, $Arg^{114'}$, $Arg^{118'}$ and $His^{75'}$. An electrostatic repulsion between His^4 and boundary residues His^8 and $Arg^{118'}$ of the rigid region forces His^4 to be located as far as possible from

25   the rigid region, separating the 1-8 loop from the rest of the structure. This tendency is further reinforced in hNGF by the presence of a third positively charged boundary residue Arg^9. The $His^{75'}$ amino acid located in the "south" part of NGF also participates in maintaining the structure of the rigid region. An electrostatic repulsion between $His^{75'}$ and $Arg^{114'}$ prevents H-bonding of the amino group of $Arg^{114'}$ with the $Asn^{77'}$ side chain and the $Ser^{113'}$ backbone:

30   indeed, removing the ε-proton from $His^{75'}$ results in two H-bond contacts which change the global energy minimum structure of the complex.

The separation of flexible loop 1-8 from the rigid region is also determined by residue Pro^5. This amino acid imposes restrictions on conformational motion of the loop, making it "bent" at this particular point, and thereby defining the location of the adjacent His^4 residue at

35   the most distant point from the rigid region. Thus, residues His^4 and Pro^5 are primarily responsible for the separation of the flexible loop from the rigid region.

21

Although mNGFΔ3-9 does not have the flexible loop, the energy optimized geometric features of its termini are very similar to those of the hNGF and mNGF rigid regions (Table 1, Figures 2-4). There are only two structural elements which are specific for the rigid region of mNGFΔ3-9. First, although Arg[118'] has a different conformation, the result is functionally the same, namely both NH_2 groups of the Arg[118'] side chain are H-bonded to the Glu[11] side chain. In addition, the ε-NH group of Arg[118'], which is H-bonded to the Phe[7] carbonyl group of the flexible loop in both hNGF and mNGF, faces the carbonyl terminus in mNGFΔ3-9. Second, the "hollow", which is occupied by the ninth amino acid side chain in hNGF and mNGF, is now filled with the protein backbone of the remainder of the loop, i.e., residues 1-2. Functionally, the structure of the rigid region of mNGFΔ3-9 resembles that of hNGF because of the stabilizing interchain H-bond contacts of the moieties located in the "hollow".

GEOMETRIC DISTINCTION OF NGF ANALOGUES INACTIVE FOR TrkA BINDING

The energy minimum structures of the complexes formed by the amino and carboxyl termini of molecules, hNGF-H4D, mNGFΔ1-8 and BDNF, which are inactive with respect to TrkA binding, do not possess the common structural features found in active molecules. Point mutation H4D in hNGF incorporates negative instead of positive charge into the 1-8 loop. As a result of this mutation, the loop is no longer separated from the rigid region, forming a united complex instead (Figure 5). In this complex the negatively charged carboxyl group of Asp[4] is surrounded by four positively charged NH_2 groups of Arg[9] and Arg[114'], and residue His[8] is not H-bonded to the Glu[11] carboxyl group. Thus, because of the H4D point mutation, the common structural features inherent in hNGF and mNGF are lost from hNGF-H4D.

Deletion 1-8 also changes dramatically the most stable structure of the rigid region of mNGF (Figure 6). The newly created positively charged amino terminus is located between negatively charged carboxyl groups of Glu[11] and Arg[118'], with charged side chains of Arg[114'], Lys[115'] and Arg[118'] being substantially shifted from their preferred positions in active molecules. Thus, the electrostatic field caused by the positive charge of the new amino terminus in mNGFΔ1-8, located in the vicinity of the carboxyl group of Glu[11], is responsible for the destruction of the geometry of the rigid region inherent in the active molecules.

The complex formed by the amino and carboxyl termini of BDNF is also significantly different from those formed by the molecules active for TrkA binding (Figure 7, Table 1). There are several reasons for the considerable conformational changes in BDNF. First, negatively charged residue Asp[5] eliminates the separation of the flexible loop from the rigid region, and interacts with the positively charged His[3], Arg[9] and amino terminus. Second, because of its long tail, Arg[8] is unable to form the H-bond contact with the Glu[11] side chain and forms bifurcated H-bonds with the carbonyl group of Gly[10]. Third, Arg[116'] is H-bonded to

Glu[66'] located in the "south" part of the molecule, which imposes a specific restriction on conformational possibilities of the carboxyl terminus of BDNF.

EXPLANATION FOR THE OBSERVED STRUCTURE-ACTIVITY RELATIONSHIPS

5

10

15

The principal result of the molecular simulations presented is that the NGF molecules with full TrkA mediated activity considered in this study have regions with similar 3-dimensional structure, whereas in all inactive analogues, the geometry of this region is altered, mainly by novel electrostatic interactions. It is therefore reasonable to attribute the TrkA mediated activity to a specific conformation of this particular region. The amino and carboxyl terminal regions therefore represent a "functional epitope" which contains relatively few contact residues mediating high affinity binding. The ability of a small number of residues to cause high affinity binding has previously been demonstrated in other systems and may represent a general property of protein-protein interfaces. Some experimental data consistent with this concept are presented below.

The VBMC computations show that the following amino acids are critical in determining the structure of the complex in wild type NGF dimers: His^4, Pro^5, His^6, Arg^9, Glu^{11}, His^{75}, $Asn^{77'}$, $Lys^{115'}$ and $Arg^{118'}$. This is significant since residues His^4, Pro^5, Glu^{11}, His^{75}, $Asn^{77'}$ and $Lys^{115'}$ are conserved in NGF molecules across all species (McDonald et al., 1991). The overlap between these two sets reflects a tendency to maintain the particular geometry of the complex in natural NGF molecules. In addition, as demonstrated, the substitution of the important residue Arg^9 by the essentially different Met^9 does not result in geometric changes of the complex, which is consistent with equivalent bioactivity of hNGF and mNGF (Burton et al., 1992). Thus, because of multiple physical factors maintaining the geometry of the complex, some species variability observed in NGF termini (McDonald et al., 1991) is acceptable and does not cause geometric changes in the rigid region.

20

25

It is shown that each NGF terminus has several important residues, which determine the particular structure of the complex. This is consistent with high sensitivity of biological activity of NGF to the primary structure of both the amino and carboxyl termini (Klein et al., 1991; Shih et al., 1994; Burton et al., 1992, 1995; Kahle et al., 1992; Drinkwater et al., 1993; Treanor et al., 1995; Taylor et al., 1991). The lack of the TrkA mediated activity of the mNGFΔ3-11, mNGFΔ3-12, mNGFΔ3-13, mNGFΔ3-14, mNGFΔ9-14 and mNGFΔ112-118 deletion mutants (Drinkwater et al., 1993) is thus explained by the absence of the key residues Glu^{11} and $Arg^{118'}$.

30

The separation of the flexible loop from the rest of the complex is crucial in permitting the rigid region to exist with definite geometric features. Residues His^4 and Pro^5 which cause this separation are absolutely conserved elements of the wild type NGF molecules derived from different species (McDonald et al., 1991), and their compulsory location in the middle of

35

23

the flexible loop is well suited for facilitating the maximal separation. Point mutation P5A or H4D weakens or destroys the tendency of the loop to separate from the rigid region; accordingly, these mutations result in dramatic loss of TrkA related activity (Shih et al., 1994).

5   The flexible loop is not an essential structural element for TrkA activation since the mNGFΔ3-9 deletion mutant, which does not contain the loop (Figure 4), is as active as wild type mNGF (Drinkwater et al., 1993). However, complete elimination of all loop residues results in almost inactive mutants mNGFΔ1-8 (Burton et al., 1992; Drinkwater et al., 1993; Taylor et al., 1991) and hNGFΔ1-9 (Shih et al., 1994; Burton et al., 1992, 1995; Kahle et al., 1992; Luo and Neet, 1992). Our molecular simulation studies enable the explanation for this

10   apparent contradiction. It is demonstrated that the backbone of residues Ser^8 -Ser^9 in the mNGFΔ3-9 mutant is naturally incorporated into the structure of the rigid region because it matches the geometry of the "hollow" occupied by either Met^9 or Arg^9 side chain in wild type NGF dimers. On the contrary, total truncation of the flexible loop in the mNGFΔ1-8 deletion mutant results in placing the positively charged amino end in the vicinity of the key H-bonded

15   Glu^{11} and Arg^{118} charged side chains (Figure 3), which abolishes the desired geometry of the rigid region (Figure 6). The same applies to the hNGFΔ1-9 deletion mutant which has neither the 1-8 loop nor the stabilizing Arg^9 residue (Figure 2). This being the case, biological activity of amino terminus deletions of NGF should be determined by the length of the remainder of the terminus rather than its particular sequence. Indeed, available experimental data confirm

20   this point. Deletion mutant mNGFΔ2-8 which has exactly the same number of residues in the amino terminus as the highly active mNGFΔ3-9 mutant is also very active (Drinkwater et al., 1993). Some decrease in biological activity of mNGFΔ2-8 is likely to be caused by unfavorable directing of the Met^9 hydrophobic side chain away from the complex whereas in the mNGFΔ3-9 deletion mutant this side chain is replaced by the hydrophilic hydroxyl group

25   (Figure 4). Deletion mutants mNGFΔ3-8 (Drinkwater et al., 1993) and hNGFΔ1-5 (Shih et al., 1994), which contain a greater number of amino terminus residues, are remarkably less active than wild type NGF because the remainder of the loop is too long to occupy the "hollow" but too short to separate from the rigid region. The present explanations for the observed structure-activity relationships enable the prediction that, for example, a S2G

30   mutation in the mNGFΔ3-9 deletion mutant would retain high biological activity.

Although the bioactive conformation of the NGF binding determinant has been disclosed above, the question of which NGF residues are involved in NGF/TrkA recognition was not yet addressed. One would reason, most probably, those residues which are primarily responsible for maintaining the particular structure of the NGF termini do not directly interact

35   with the receptor. Thus, side chains of His^4, Pro^5, His^8, Met^9, Arg^9, Glu^{11} and Arg^{118} are not expected to play a crucial role in molecular recognition. On the other hand, charged residues

24

Arg[114'] and Lys[115'] which are conserved in NGF molecules across all species (McDonald *et al.*, 1991) but not involved in principal intramolecular electrostatic interactions are candidates for the centres of intramolecular electrostatic recognition. Although both Arg[114'] and Lys[115'] participate in stabilizing intramolecular H-bonding within the bioactive conformations of the

5   NGF termini, their electrostatic properties as charged residues are not utilized for this purpose.

The other structural element of the termini with potential for stereochemical fit to the TrkA receptor is a short exposed β-sheet motif located between the α-carbons of residues 7 and 9 (Figures 2,3). On the one hand, H-bonding between β-pleated sheets is rather

10   common for protein-protein interactions (Kobe and Deisenhofer, 1993, 1994, 1995; Yoder *et al.*, 1993; Baumann *et al.*, 1993). On the other hand, a short exposed β-sheet motif is generally inherent in the structure of a leucine-rich repeat (Kobe and Deisenhofer, 1993, 1994, 1995) which has been recently identified as the TrkA recognition site for NGF (Windisch *et al.*, 1995a, 1995b). Other regions of NGF might also be involved in the

15   NGF/TrkA recognition (Shih *et al.*, 1994; Ibáñez *et al.*, 1993). This will be discussed in depth below.

CONCLUSIONS

The Variable Basis Monte Carlo simulated annealing technique disclosed herein enables analysis of the low-energy conformational space of peptide molecules. Although

20   multiple VBMC calculations do not consistently converge to the global energy minimum structure, they do permit the biologically active conformation to be evaluated. Definite physical factors maintain and distinguish the bioactive conformation of a molecule, and these factors can be understood by analyzing the low-energy conformational space. The precisely defined global energy minimum structure is unnecessary, especially considering that any

25   empirical force field functions are not ideal. In biologically relevant molecular modelling, exploring the bioactive conformation is more important than determining the global energy minimum. VBMC is a useful tool for facilitating this exploration.

The present VBMC simulations predict that the amino (1-11) and carboxyl (112'-118') termini of dimeric (1-118)NGF form a complex comprised of a rigid region and a

30   conformationally variable loop. The rigid region is formed by residues 9-11 and 112'-118' while the variable loop is formed by residues 1-8. The major stabilizing factor of the rigid region is the ionic contact of the Glu[11] and Arg[118'] side chains. The separation of the loop from the rigid region arises from the electrostatic repulsion between His[4] and boundary residues of the rigid region His[8], Arg[9] (in hNGF) and Arg[118']. The geometry of the complex

35   explains observed structure-activity relationships. Accordingly, it is the conformation of the rigid region which is recognized by the TrkA receptor, defining the biologically active

conformation of NGF for TrkA activation.

The split of the complex of the NGF termini into two distinct moieties could have important biological implications. Although only the structure of the rigid region is recognized by the TrkA receptor, the flexible loop is able to control conformational stability of the

5   biologically active conformation of the rigid region and, consequently, NGF-induced TrkA phosphorylation.

PART B

THEORETICAL MODELLING OF Trk-RECEPTOR RECOGNITION SITES FOR NGF AND

10   BDNF

INTRODUCTION

As mentioned above, the location of the neurotrophin binding sites within the Trk receptors is the subject of debate (MacDonald and Meakin, 1996). Based upon published data, there is reason to believe that Trk proteins have two putative neurotrophin binding sites:

15   the "second immunoglobulin-like domain" (IgC2, residues Trp^{299}-Asn^{365}) and the "second leucine-rich motif" (LRM-2A and LRM-2B, residues Thr^{97}-Leu^{120} of TrkA and TrkB, respectively) (Schneider and Schweiger, 1991; Kullander and Ebendal, 1994; Pérez et al., 1995; Urfer et al., 1995; Windisch et al., 1995a, 1995b, 1995c; MacDonald and Meakin, 1996; Rydén and Ibáñez, 1996). LRM containing proteins are a diverse group with different

20   functions and cellular locations, and are known to mediate strong and selective protein-protein interactions (Kobe and Deisenhofer, 1993, 1994, 1995). The amino acid sequence of an LRM is characterized by conserved hydrophobic consensus residues (Schneider et al., 1988; Schneider and Schweiger, 1991; Kobe and Deisenhofer, 1993, 1994, 1995). Typically, LRMs exist as repetitive cassettes, with an individual LRM representing a

25   right-handed β-α hairpin unit (Kobe and Deisenhofer, 1993, 1994, 1995). Recent crystallographic studies on porcine ribonuclease inhibitor indicate that the side chains of the consensus residues form the hydrophobic core of the LRM modules, thereby determining their geometric features (Kobe and Deisenhofer, 1993).

According to the invention, the inventors report explicit atom-level models of the

30   receptor sites for NGF and BDNF based on the structures of the second LRMs of TrkA (LRM-2A) and of TrkB (LRM-2B), respectively. To deduce these models, we have investigated the interaction of the bioactive conformation of the NGF amino and carboxyl termini region with the LRM-2A and of the "waist" region of BDNF with the LRM-2B. A series of four active NGF analogues, namely human NGF (hNGF) (Burton et al., 1992; Shih et al., 1994), mouse NGF

35   (mNGF) (Burton et al., 1992; Drinkwater et al., 1993), the 3-9 deletion of mNGF (mNGFΔ3-9) (Drinkwater et al., 1993) and the hNGF:NT-4/5 heterodimer (Treanor et al., 1995), have been

26

docked to the LRM-2A of rat TrkA. For all four NGF molecules studied, a stereochemical fit of
the LRM-2A to the amino and carboxyl region was achieved. These results indicate that the
bioactive conformation of the NGF termini is a functional epitope which mediates high affinity
binding via an interaction with the LRM-2A. This approach has also been applied to

5   BDNF/LRM-2B docking, and their stereochemical fit, based mainly on electrostatic
complementarity, has been identified and is described below.

METHODS

A sequence of three logical steps has been used to deduce the models of the
interactions of NGF and BDNF with their respective Trk receptor binding sites: *Step 1:* The

10   bioactive conformations of the amino and carboxyl termini of NGF analogues were
determined. *Step 2:* The residues of the Trk proteins which form potential binding sites for
NGF and BDNF were identified. *Step 3:* The interaction of the bioactive conformation of the
NGF amino and carboxyl termini with the TrkA binding site and the BDNF β-strand stem
region with the TrkB binding site were modeled computationally. Finally, the predicted

15   features of the NGF/TrkA and BDNF/TrkB interaction models were validated against available
experimental data. Residues of the first monomer of a neurotrophin are designated 1 to 118,
those of the second monomer are designated 1' to 118'. Residues of the TrkA LRM-2A and
the TrkB LRM-2B binding sites are designated by abbreviations tA and tB, respectively.
Residues of the BDNF monomer are designated 1 to 119.

20   *Step 1:* REVEALING THE BIOACTIVE CONFORMATION OF THE NGF TERMINI

The most energetically favored conformations of the amino and carboxyl termini of
NGF analogues have been obtained by VBMC computations and are described above. Since
the 3-dimensional structures of the termini of fully active NGF molecules were found to be
different from those of TrkA-inactive analogues, the former conformations were predicted to

25   be "bioactive" for TrkA-mediated activity of NGF. That is, those geometric features that are
exclusively inherent to active NGF molecules are expected to be compatible with the structure
of the TrkA binding site for NGF. Since the geometry of the central β-strand stem of BDNF is
rigid and has been established by X-ray crystallography (Radziejewski and Robinson, 1993),
this logical step is bypassed for BDNF. Instead, it is assumed that the X-ray crystallography

30   deduced conformation of the amino acid backbone of the TrkB binding determinant of BDNF
represents its "bioactive" conformation.

Step 2: SELECTION OF THE LRM-2 BOUNDARIES WITHIN THE TRK RECEPTORS

Since there is controversy in the literature regarding the actual boundaries of LRMs
(Schneider *et al.*, 1988; Schneider and Schweiger, 1991; Kobe and Deisenhofer, 1993, 1994,

35   1995; Windisch *et al.*, 1995a, 1995b), the following experimental background (Figure 8) was
used to define boundaries for this computational study. According to Schneider and

27

colleagues (1988, 1991), the LRM domains of TrkA begin with Leu^{68lA}, Leu^{93lA} and Leu^{117lA}, whereas those boundaries are slightly shifted in the crystallographic studies of Kobe and Deisenhofer (1993). Furthermore, the boundaries of the "minimal" LRM module of TrkA (designated B4 in Figure 8), which demonstrates the same NGF binding affinity as wild type

5   TrkA, are substantially shifted towards the carboxyl terminus (Windisch et al., 1995a, 1995b) with respect to those suggested by Schneider and colleagues (1988, 1991). The same boundary shift has been suggested for the LRM-2B module (Windisch et al., 1995a, 1995b, 1995c). However, a comparison of active (B1 and B4) and inactive (N4) LRM domains indicates that the presence of the "minimal" amino acid sequence (B4) does not ensure NGF

10   binding. Understanding those factors which maintain the essential features of the LRM geometry in segments B1 and B4, and those factors which destroy them in N4, is of fundamental relevance to the correct assignment of the LRM boundaries.

β-Strand motifs exist in proteins only if hydrogen bonded (H-bonded) to other β-strands; otherwise their structure is unstable (Kobe and Deisenhofer, 1994). Tandem

15   repeats of LRMs represent a prominent example of H-bonded parallel β-strand motifs. The general location of the β-strand motifs in the LRM, according to X-ray data, is illustrated in Figure 8; however, in a single LRM their particular geometry is destroyed (Kobe and Deisenhofer, 1993, 1994, 1995). Consequently, the only possibe way to exclude dramatic conformational changes in a protein domain upon disruption of the inter-strand H-bonding

20   between β-strand motifs is to avoid those motifs. Accordingly, both boundaries of segment B4 are located in the middle of the β-strand regions of the adjacent LRMs such that this segment appears to be free of any β-strand. Nevertheless, the β-strand motif is a characteristic structural unit of LRMs, and thus it is likely that this unit is involved in the NGF/TrkA recognition process. Additionally, a short exposed β-strand motif has been

25   detected in the bioactive conformation of the NGF termini, as described above. The incorporation of the β-strand regions at both sides of the B4 segment (as in N4) results in cooperative H-bonding between these β-strands and a complete loss of NGF binding, which indicates that accessibility of the β-strand motif for intermolecular contacts is essential. On the other hand, the separation of the entire LRM segment from the adjacent LRMs within the

30   B1 molecule as a result of conformational kinking is likely to be energetically more favorable, since the entire LRM module has the internal stabilizing factors. Moreover, kinking between adjacent LRMs does not disrupt the structure of their β-strand motifs (since they remain H-bonded with their opposite sides), but makes them accessible for molecular recognition processes.

35   Accordingly, in the modelling of the present invention we used the conventional boundaries of the LRMs of TrkA and TrkB (Schneider et al., 1988; Schneider and Schweiger,

28

1991), which keep the β-strand motif in the LRM, and we explicitly arranged H-bonding of this unit with the parallel β-strand motif of the NGF amino terminus to preserve it from conformational reorganizations. Thus, the segments between residues Leu^{93tA} and Leu^{117tA} in TrkA, and Leu^{93tB} and Leu^{117tB} in TrkB, were respectively designated the LRM-2A and the

5   LRM-2B.

Step 3: COMPUTATIONAL SIMULATION OF THE NEUROTROPHIN/RECEPTOR INTERACTIONS

Docking interactions NGF/LRM-2A and BDNF/LRM-2B were simulated using a combined VBMC/CHARMM approach. As described above, the VBMC algorithm permits

10   conformational space search; CHARMM (Brooks *et al.*, 1983) is a force field which defines conformational energy. The same approach was also used to study improper docking interactions of the central β-strand stem region of NGF with the LRM-2B, as a negative control.

The VBMC algorithm performs conformational and orientational space searches of a

15   complicated molecular system with the aim of finding the structure which corresponds to the global minimum on the potential energy E_{tot} surface.

$$E_{tot} = E_t + E_w + E_e + E_{hb} + E_{qq} + E_{hy} + E_c \qquad (4)$$

The following potential energy terms have been considered in the framework of the united atom CHARMM force field (Brooks *et al.*, 1983; The force field parameters are

20   extracted from CHARMM version 23.1, Molecular Simulations, Inc., Waltham, MA): torsional distortion E_t, van der Waals interactions E_w, electrostatic interactions E_e, and hydrogen bonding E_{hb}. Since the united atom approach is not appropriate to treat rigorously the quadrupole-quadrupole interactions of benzene rings (which are important for determining their mutual orientations in proteins (Hunter and Sanders, 1990; Hunter *et al.*, 1991), single

25   quadrupoles have been placed at the centers of the benzene rings of phenylalanine, tryptophan and tyrosine, and the energy of the quadrupole-quadrupole interactions, E_{qq}, has been calculated as suggested by Schauer and Bernstein (1985). (The potential energy function of two interacting benzene molecules, comprising E_{qq} and E_w terms, has stationary points corresponding to both known electrostatically favorable "edge-to-face" and "offset

30   stacked" orientations, with the dimerization energy of 1.94 kcal/mol agreeing well with *ab initio* quantum mechanical calculations (Hobza *et al.*, 1994).) In addition, the conformationally dependent free energy of hydration, E_{hy}, has been calculated according to the hydration shell model including both nonspecific and specific hydration terms (Hopfinger, 1973; Hodes *et al.*, 1979). Point atomic charges of Weiner and colleagues (1984) have been used. A dielectric

35   constant equal to the interatomic separation in angstroms has been used to implicitly simulate solvation effects (Weiner *et al.*, 1984).

29

The E_c term is used only for the NGF/LRM-2A complex and represents the distance constraints which restrain the H-bonding of residues Glu[11] and Arg[118'] within the bioactive conformation of the NGF termini, as described above. In addition, two intermolecular H-bonds, arising from the alignment of complementary parallel β-strand motifs of NGF and

5   LRM-2A, are also constrained and contribute to E_c. In the Monte Carlo conformational space search, E_c is defined as follows:

$$E_c = 10 \times \sum \left(d_{AB} - 1.8 \right)^2, \qquad\qquad (5)$$

where d_{AB} is the distance in angstroms between atoms A and B which are to be H-bonded. The E_c term is neglected when performing final energy minimization following the VBMC

10   simulated annealing. In addition, this term has not been utilized when studying the mNGFΔ3-9/LRM-2A complex. Since, as described above, the mNGFΔ3-9 deletion mutant does not have a β-strand region, the geometry of its LRM-2A counterpart, namely Leu[93'A]-Ile[98'A], has been kept fixed in the crystallographic conformation (Kobe and Deisenhofer, 1993) during Monte Carlo simulations. The E_c term, being "soft", does not

15   preclude conformational and orientational changes to occur during Monte Carlo simulations. This term increases rigidity of the bioactive conformation of the ligand, which allows us to utilize the knowledge obtained at *Step 1*, instead of explicit considerations of inactive NGF analogues, in *Step 3*. In addition, this term keeps conformations of the β-strands of both ligand and binding site from destruction, and thereby allows us to avoid an explicit

20   consideration of the adjacent first LRM of TrkA. Furthermore, this term maintains the known orientation of the parallel β-strand motifs in the NGF/LRM-2A complex.

The amino acid sequences of the binding determinants of the NGF molecules studied are presented in Figure 9. The conformational space of the NGF analogues consists of torsional angles determining geometry of the amino terminus of one monomer (residues 1-11)

25   and the carboxyl terminus of the other (residues 112'-118'), while keeping the rest of the dimer in the experimental geometry of mNGF (McDonald *et al.*, 1991). The conformational spaces of the LRM domains of TrkA and TrkB consist of torsional angles representing fragments Arg[94'A]-Leu[117'A] and Arg[94'B]-Leu[117'B], respectively. Covalent bond lengths and bond angles have been kept fixed. The geometry of each i-th residue is determined only by flexible

30   torsional angles of the backbone (ϕ_i and ψ_i) and the side chain ($\chi_i 1, \chi_i 2,...$). All torsional angles for prolines, except ψ, have been fixed. Torsional angles describing structural motifs with planar geometries (such as peptide bonds or conjugated regions in side chains) were fixed. Likewise, the configurations of the sp[3]-carbons were fixed. The conformational space of BDNF consists only of torsional angles determining side-chain geometries of those

35   residues which are located in the vicinity of its central β-strand stem and define a molecular surface (Table 2). In addition to the conformational variables of each complex, the six

30

orientational variables (three Euler angles and three translations along the coordinate axes) were used to describe the ligand-receptor orientations.

In accordance generally with the simulated annealing approach (Kirkpatrick et al., 1983; Vanderbilt and Louie, 1984; Brünger, 1998; Nilges et al., 1988; Wilson et al., 1988; Wilson and Doniach, 1989), the molecular systems were kept at a constant temperature of $800°K$ for 2×10^6 Monte Carlo moves before the initiation of "cooling". The temperature was then decreased at every Monte Carlo move by a small increment such that after 2×10^6 Monte Carlo moves it reached $120°K$. At this time, a local energy refinement was performed to identify the nearest stationary point on the potential energy surface. According to the VBMC algorithm described above, the basis of independent structural parameters was recalculated after every 7×10^4 Monte Carlo moves to direct them along the valleys of the potential energy surface, thereby accelerating conformational and orientational changes.

All calculations were performed on an Indigo-2 Silicon Graphics Workstation and an 8-node IBM Scalable POWER parallel 2 [SP2] high performance computer.

RESULTS AND DISCUSSION

CONFORMATIONAL FLEXIBILITY WITHIN RECEPTOR ENVIRONMENTS

Five independent VBMC simulations from different initial configurations were performed for each of the six molecular complexes under study. The elimination of the distance constraints E_c in the complexes with the LRM-2A did not result in any noticeable conformational changes within the complexes. Although independent VBMC simulations did not always converge to the same geometry for the same molecule, the final structures differed insignificantly; i.e., the conformations of the peptide backbones remained unchanged with the exception of residues 1-3 of the NGF amino terminus and the terminal residue Leu^{117tA} of the LRM-2A. The differences between the VBMC generated structures were located in side-chain conformations of a limited number of residues, specifically Ser^1, $Val^{117'}$ ($Thr^{117'}$ in mNGF), Thr^{97tA} and Ser^{101tA}. These residues are not involved in intermolecular or intramolecular interactions, and do not affect the overall structures of the complexes. No considerable differences were identified in the independent VBMC-generated conformations of the BDNF/LRM-2B and the NGF/LRM-2B complexes.

A grid search of the internal space of the complexes using the water molecule radius 1.4 Å as a probe (Ponnuswamy and Manavalan, 1976) (as incorporated into the QUANTA program, Version 4.1, Molecular Simulations, Inc., Waltham, MA) showed that there is no internal cavity available for a solvent molecule in the hNGF/LRM-2A complex. This explains the rigidity of the complex and demonstrates the "perfect" stereochemical fit of the hNGF amino-carboxyl termini complex to the LRM-2A. Other complexes have some internal cavities, especially with the LRM-2B binding site.

31

SPECIFIC BINDING AREAS WITHIN RECEPTOR ENVIRONMENTS

The TrkA Receptor Binding Site

Comparison of the most stable structures of the different complexes with the LRM-2A binding site (Figure 10) shows their striking conformational similarity. In all molecules, ligand-receptor binding is caused by similar hydrophobic, ionic, H-bonding and van der Waals interactions. There are five distinct areas (A-E) within the NGF/LRM-2A fit: areas A and B have hydrophobic interactions, areas C and D have ionic H-bonding, and area E has cooperative H-bonding between parallel β-strand motifs.

Area A represents the hydrophobic region at which residue Phe^{105tA} interacts with $Trp^{76'}$, which in turn forms hydrophobic contacts with Phe^{12} and $Leu^{112'}$. The aromatic rings of Phe^{12}, $Trp^{76'}$ and Phe^{105tA} are approximately perpendicular to each other, which is energetically favorable (Hunter and Sanders, 1990; Hunter et al., 1991; Hobza et al., 1994). This particular geometry would create a hole within the complex, if it was not filled by hydrophobic residue $Leu^{112'}$.

In area B, Phe^7 of NGF is placed within the hydrophobic core of the LRM-2A created by the consensus residues (Schneider et al., 1988; Schneider and Schweiger, 1991; Kobe and Deisenhofer, 1993, 1994, 1995). Similar to the favorable orientation of the aromatic residues in area A, the aromatic rings of Phe^{111tA} and Phe^{113tA} are perpendicular to that of Phe^7. On the other hand, residues Phe^{111tA} and Phe^{113tA} are not perpendicular to each other; their orientation instead resembles the favorable "offset stacked" geometry described by Hunter and others (Hunter and Sanders, 1990; Hunter et al., 1991; Hobza et al., 1994). As in area A, a hole created by the three neighboring favorably oriented aromatic rings is filled by a fourth residue, Thr^{114tA}. Interactions between aromatic rings in proteins is very common and represent an important conformational driving force (Warme and Morgan, 1978; Hunter et al., 1991). Consequently, the fact that all three phenylalanine residues of the LRM-2A find their counterparts within the NGF binding domain supports the calculated structure of the NGF/LRM-2A complex.

In ionic binding area C, the negatively charged residue Asp^{109tA} exerts a central role. It is surrounded by the three positively charged amino acids His^{112tA}, $Arg^{114'}$ and $Lys^{115'}$ in hNGF, mNGF and mNGFΔ3-9, and by His^{112tA}, $Arg^{115'}$ and Arg^9 in hNGF:NT-4/5. Residue His^{112tA} plays a secondary role: it creates the electrostatic dipole $Asp^{109tA} \rightarrow His^{112tA}$ in the LRM-2A, which imposes constraints on the spatial positions of the recognized positively charged residues of NGF, thereby reinforcing geometric selectivity in this area. Although the hNGF:NT-4/5 heterodimer has two substitutions in the C-area segment of the NT-4/5 carboxyl terminus, namely R114S and K115R, the geometry of the C area remains qualitatively the same, since residues Arg^9 and $Arg^{115'}$ of hNGF:NT-4/5 functionally replace the absent $Lys^{115'}$

32

and Arg[114'] amino acids, respectively. Although Arg[9] also exists in the hNGF homodimer, it is not involved in the ionic binding in this molecule, since it is separated from area C due to electrostatic repulsions. Similarly, the charged amino end of mNGFΔ3-9, which functionally replaces Arg[9], is also separated from area C. There is no place for the fourth positively charged residue in area C. Thus, in all molecules studied, the two positively charged amino acids of the ligand saturate the coordination possibilities of the receptor residue Asp[109tA].

Area C is partially isolated from its surrounding environment by flanking hydrophobic residues Val[106tA] and Pro[115tA]. Similarly, the principal charged residues of NGF, namely His[8], Glu[11] and Arg[118'], are located between hydrophobic residues Ile[6] (Val[6] in mNGF), Val[111'] (Leu[113] in hNGF:NT-4/5) and Val[99tA] within the complexes. Thus, residues Val[99tA], Val[106tA] and Pro[115tA] of the LRM-2A participate in "compartmentalization" of the principal ionic interactions of the complexes, thereby shielding them from the conformation destructive influence of solvation. .

The organization of ionic binding area D is similar to that of area C. Positively charged residues Arg[59] and Arg[69] are located in the vicinity of negatively charged Asp[16] within the NGF structure (McDonald et al., 1991; Bradshaw et al., 1994), such that the coordination of the latter is not full. The third positively charged residue, Lys[100tA], comes from the LRM-2A to complete the Asp[16] coordination. In addition to the ionic binding, residue Lys[100tA] forms an H-bond with the Ser[13] side chain.

Area E consists of the H-bonded parallel β-strand motifs of the LRM-2A and NGF (Figure 10b, 10c and 10e), each of the β-strands having three peptide bonds. The LRM-2A β-strand motif is located between the α-carbon atoms of Asn[95tA] and Ile[98tA], whereas the NGF β-strand is located between the α-carbons of the sixth and ninth residues. The locations of the β-strand regions in the uncomplexed LRM (Kobe and Deisenhofer, 1993) and NGF (see above) resemble those in the complexes considered. In the complexed LRM-2A, the β-strand motif is shortened by one peptide bond at its amino end to accommodate the His[4] side chain of NGF. On the other hand, the two peptide bond β-strand of the uncomplexed NGF is lengthened by one peptide bond at its amino end in the complexes.

The TrkB Receptor Binding Site

Figure 11a illustrates the central β-strand stem region of BDNF, and Figure 11b presents the VBMC-generated structure of the BDNF/LRM-2B complex. In this complex, ligand-receptor binding is based mainly on intermolecular electrostatic interactions of either ionic or hydrogen bonding origin. There are five distinct binding areas (F-K) within the TrkB receptor environment: four salt bridges (areas F, G, H and I) and one H-bonding area K. In contrast with the NGF/LRM-2A binding pattern, there is no participation of the LRM-2B β-strand motif in cooperative H-bonding with the BDNF binding epitope.

In area F, the primary positively charged residue (Ibáñez et al., 1993) of the BDNF

33

binding domain, Arg[81], is bound to Asp[100tB], the only negatively charged residue of the LRM-2B. It should be noted that Arg[81] is exclusively inherent in BDNF molecules while being substituted by electrostatically neutral Thr in NGF or by Lys in NT-3 or NT-4/5 molecules (Bradshaw et al., 1994), which indicates the importance of this area in neurotrophin

5   recognition processes (see also Urfer et al., 1994). On the contrary, residue Gln[84], identified by Ibáñez and co-workers (1993) as important, is not directly involved in specific intermolecular interactions within the LRM-2B domain.

In binding area G, the negatively charged residue Glu[55], which is absolutely conserved in all neurotrophins (Bradshaw et al., 1994), exerts a central role. It is surrounded by the

10   three positively charged amino acids, Lys[25], Lys[57] and Lys[109tB]. Two of them, belonging to the neurotrophin, are also highly conserved (Bradshaw et al., 1994). The third one, Lys[109tB], is specific for the TrkB receptor site (Windisch et al., 1995a, 1995b, 1995c). All BDNF residues of the G binding area, namely Lys[25], Lys[57] and Glu[55], have been shown to be essential in NT-3 structure for TrkC receptor activation (Urfer et al., 1994), which is in agreement with

15   observations that the TrkB and TrkC binding domains are located in the same region of these neurotrophins. This particular arrangement of the three positively charged residues around one with a negative charge seems to be very common in neurotrophin-receptor recognition processes, since the NGF/LRM-2A interaction also includes two binding areas of this type (C and D). Existence of the absolutely conserved negatively charged residue Asp[106] in direct

20   proximity to area G increases binding affinity of Lys[109tB], thereby highlighting some importance of this area in the BDNF/TrkB recognition processes. Although detailed mutational experiments did not demonstrate importance of the equivalent residue Asp[105] in NT-3 for TrkC related activities (Urfer et al., 1994), its direct involvement in the Zn^{2+} mediated regulation of neurotrophin bioactivities has been recently proven by multidisciplinary studies (Ross et al.,

25   1997), and, therefore, its location within the binding determinants of BDNF and NT-3 is consistent with these observations.

In area H, conserved residue Asp[24] of BDNF forms a salt bridge with specific TrkB residue Lys[113tB]. Although Asp[24] has not been demonstrated to be involved in direct neurotrophin-receptor interactions, either for TrkB or TrkC related activities, it is highly

30   conserved in neurotrophins (Bradshaw et al., 1994) and located in direct proximity to Thr[22] in NT-3, which has been shown to be included in the TrkC receptor binding domain (Urfer et al., 1994). These observations are consistent with the present model of BDNF/TrkB binding, since substitution of the equivalent residue of BDNF, Thr[21], by bulky Gln (Urfer et al., 1994) would sterically hinder proper location of the LRM-2B domain (Figure 11b), whereas mutation

35   D24A, although lacking one specific ligand-receptor interaction, would not significantly alter the BDNF/LRM-2B orientation resulting from multiple-point electrostatic complementarity. In

34

addition, the absence of negatively charged residue Asp^{24} is shown to induce salt bridge interaction of Lys^{113tB} with neighboring Glu^{18}, with only minor conformational alterations of the LRM-2B.

In area I, Glu^{18}, a specific residue of BDNF (Bradshaw *et al.*, 1994), forms a salt bridge with the LRM-2B amino acid Arg^{94tB}. Residue Glu^{18} is also involved in intramolecular electrostatic interactions with Lys^{57}.

Area K is the only region of the distinct BDNF/LRM-2B interactions which is not of ionic nature. The positively charged residue Lys^{104tB} forms multiple H-bond contacts with the BDNF loop I backbone carbonyl groups and the neutral Thr^{35} side chain. The energy of such H-bonding is much lower than that of salt bridge contact, and, therefore, a substitution of the uncharged amino acid Thr^{35} by a negatively charged residue would stabilize the particular structure of the BDNF/LRM-2B complex. In accordance with the present model, the experimental substitution of BDNF residues 34-41 by the corresponding segment of NGF, which includes the substitution of negatively charged residue Glu^{35} for Thr^{35}, resulted in a significant increase in bioactivity of the resulting chimeric molecule relative to wild type BDNF in TrkB mediated survival (Lai *et al.*, 1996).

In addition to these five distinct binding areas of the BDNF/LRM-2B complex, there is one more area which reinforce binding specificity. The side chain of Pro^{60}, a specific residue of BDNF (Bradshaw *et al.*, 1994), demonstrates a perfect geometric fit into the hollow in the "zigzag"-shaped β-strand region of the LRM-2B (Figure 11b). This geometric complementarity indicates that Pro^{60} "recognizes" the β-strand motif of the receptor binding site. This interaction, obviously, does not significantly contribute to the total energy of the complex in the case of a perfect fit, but does represent a steric hindrance when this fit cannot be readily achieved. Accordingly, BDNF is very selective and does not bind non-cognate Trk receptors.

Figure 11c illustrates the VBMC-generated geometry of the "improper" NGF/LRM-2B complex. In this complex, specific binding areas F and I are absent due to lack of properly charged residues at positions 20 and 81, which would correspond to BDNF residues Glu^{18} and Arg^{81}, respectively. In addition, residue Pro^{60}, determining the proper BDNF/LRM-2B orientation, is substituted in NGF molecules (Bradshaw *et al.*, 1994). These substitutions cause dramatic conformational and orientational alterations in the complexed LRM-2B domain (compare Figure 11b and 11c). Predicted Cartesian 3-dimensional coordinates of atoms of the TrkB LRM-2B binding site in the complex with BDNF are presented in Appendix 2.

LIGAND-RECEPTOR INTERACTION ENERGY

NGF/TrkA Interactions

Table 3 presents the components of the intermolecular energies of the NGF/TrkA

35

complexes. Stability of the NGF/LRM-2A complexes results primarily from attractive electrostatic and van der Waals interactions, with intermolecular H-bonding playing a secondary role. It should be noted, however, that in the framework of the molecular mechanical approach, the H-bonding energy is partially incorporated into the electrostatic

5   interaction energy term, so the tabulated E_{hb} values reflect only part of the H-bonding energy. Accordingly, intermolecular H-bonding is more important for the NGF/LRM-2A interaction than it appears in Table 3. On the other hand, the intermolecular component of the E_{qq} term seems to be insignificant. The reason for the latter is that the aromatic moieties of Phe[7], Trp[76'], Phe[105'A], Phe[111'A] and Phe[113'A] are "preorganized" for intermolecular contacts with their

10   counterparts in the complexes in electrostatically attractive geometry in which the quadrupole-quadrupole interaction energy term is not significant. In addition, hydrophobic ligand-receptor interaction energy is presumably extremely important for NGF/LRM-2A complex formation, but rigorous quantitative evaluation is currently not possible.

Since neither electrostatic interactions nor hydrogen bonding can significantly stabilize

15   a ligand-receptor complex in a water environment, the stability of the complex generally results from van der Waals and hydrophobic interactions (Clackson and Wells, 1995). Considerable contribution of intermolecular van der Waals interaction energy E_w (Table 3) arises from the geometric complementarity of the NGF binding domain and the TrkA recognition site, such that the high value of the E_w term is due to a large number of

20   intermolecular van der Waals contacts. This complementarity is a consequence of the right-handed twists of both the NGF amino-carboxyl termini complex and the LRM-2A, this geometric feature being characteristic of each of these domains in both uncomplexed (Kobe and Deisenhofer, 1993; Shamovsky et al., 1996) and complexed conformations. Thus, purely geometric ligand-receptor compatibility together with distinct hydrophobic contacts play a

25   crucial role in NGF/TrkA recognition, while attractive electrostatic interactions and H-bonding further reinforce specificity of binding, which is in agreement with generalizations made by Clackson and Wells (1995).

BDNF/TrkB and NGF/TrkB Interactions

Table 4 presents the components of the potential energies of the complexes of BDNF and NGF with the LRM-2B in their minimum-energy conformations. Data presented in section

30   A of Table 4 indicate that the difference in total energies (92.0 kcal/mol) is almost exclusively a consequence of more favorable electrostatic interactions in the BDNF/LRM-2B complex than in the NGF/LRM-2B complex (negative control). Section B of Table 4 illustrates that the BDNF complex is also more favorable in terms of intermolecular electrostatic energy by 77.2

35   kcal/mol (85% of the difference in total electrostatic energies). On the contrary, intermolecular van der Waals interactions are more favorable in the "improper" NGF/LRM-2B complex.

36

Furthermore, the value of intermolecular van der Waals energy is significantly lower for NGF/LRM-2B than for the NGF/LRM-2A complex, whereas electrostatic contribution is more than twice as high. Consequently, in contrast to the NGF/TrkA binding pattern, molecular recognition of BDNF by the TrkB receptor binding site is almost exclusively based on

5   electrostatic complementarity, whereas the roles of van der Waals and hydrophobic interactions are insignificant. At the same time, such a perfect electrostatic fit could not be achieved without a purely geometric compatibility of the BDNF and the LRM-2B binding domains in size and shape (Figure 11b).

INDUCED CONFORMATIONAL CHANGES

10   **The NGF Amino and Carboxyl Termini**

Conformations of the NGF amino and carboxyl termini remain almost the same after complexation with the LRM-2A (Table 5; compare Figure 10a with 10b, 10c, 10d and 10e). A few local conformational changes occur in the $Arg^{114'}$ and the $Lys^{115'}$ side chains, and in the backbones of residues Ser^2 and Phe^7. As predicted above, conserved charged residues

15   $Arg^{114'}$ and $Lys^{115'}$ do not participate in principal intermolecular interactions within the NGF termini but are expected to form ionic intermolecular contacts with the TrkA binding site. Indeed, these are the intermolecular ionic NGF/LRM-2A interactions in area C, which change considerably the side-chain conformations of $Arg^{114'}$ and $Lys^{115'}$ while keeping their backbone geometry intact. The LRM-2A-induced conformational changes in residue Phe^7 are caused

20   by the intermolecular H-bonding in area E while the geometry of Ser^2 is slightly changed to accommodate the LRM-2A residue Thr^{114tA}. The rest of the structure of the LRM-2A-complexed NGF termini retains the energy minimum conformation of the uncomplexed molecules because it is controlled by multiple intramolecular H-bonds. Consequently, the geometry of the NGF termini is "preorganized" for complexation with the LRM-2A, and only

25   local conformational changes, primarily in residues $Arg^{114'}$ and $Lys^{115'}$, occur upon complexation. Geometric "preorganization" of the NGF termini as a ligand for binding to a leucine-rich motif is consistent with X-ray studies of Kobe and Deisenhofer (1995), who have demonstrated that ribonuclease A maintains a fixed geometry upon binding to the LRMs of ribonuclease inhibitor.

30   **The LRM-2A Domain**

Figure 12 illustrates the isolated structure of the LRM-2A from the hNGF/LRM-2A complex. Table 6 presents the equilibrium torsional angles of the hNGF-bound LRM-2A. As seen, the side chains of the general consensus residues, Leu^{93tA}, Leu^{96tA}, Ile^{98tA}, Leu^{103tA} and Phe^{111tA} (Schneider et al., 1988; Schneider and Schweiger, 1991), form the hydrophobic core,

35   similarly to their conformations in intact leucine-rich repeats (Kobe and Deisenhofer, 1993). Terminal consensus residue Leu^{117tA} is solvent-exposed due to a boundary effect. Amino

37

acids Ala^{107tA}, Pro^{108tA}, Ala^{110tA} and Phe^{113tA} are also incorporated into the LRM-2A hydrophobic

core. On the other hand, residues Val^{99tA}, Phe^{105tA}, Val^{106tA} and Pro^{115tA} are not involved in

hydrophobic interaction within the core, and apparently have specific roles in the recognition

site of TrkA. The most hydrophilic residues of the LRM-2A, namely Arg^{94tA}, Lys^{100tA}, Arg^{104tA},

5   Asp^{109tA}, His^{112tA} and Arg^{116tA} are exposed from the hydrophobic core in the complexes. Amino

acids Lys^{100tA}, Asp^{109tA} and His^{112tA} participate in specific intermolecular interactions, while the

other three are solvent-exposed. The reasonable locations of the hydrophobic and

hydrophilic residues of the LRM-2A within the NGF/LRM-2A complexes with respect to water

environment supports the calculated structures.

10   NGF/LRM-2A binding spans almost the whole LRM-2A domain, i.e., an interval

between residues Leu^{93tA} and Pro^{115tA} comprising three distinct regions: β-strand, α-helix, and

loop connecting the carboxyl terminus of the β-strand and the amino terminus of the α-helix.

This is in agreement with recent crystallographic studies on the ribonuclease A - porcine

ribonuclease inhibitor complex (Kobe and Deisenhofer, 1995), in which these particular

15   regions of leucine-rich repeats of ribonuclease inhibitor are also involved in the molecular

recognition process. While the β-strand structure exists in the complexed LRM-2A, the

α-helix motif is destroyed by intermolecular interactions with NGF. Accordingly, the LRM-2A

β-strand determines the proper orientation of the ligand with respect to the recognition site of

TrkA, but does not undergo noticeable conformational changes. Consequently, the

20   cooperative ligand-receptor H-bonding in area E cannot directly mediate those changes in

receptor conformation which trigger receptor phosphorylation processes. Available

experimental data confirm this point. First, the mNGFΔ3-9 deletion mutant, which does not

have the β-strand motif and, consequently, cannot specifically bind area E, is as active as

wild type mNGF (Drinkwater et al., 1993). Second, the 24-residue LRM fragment

25   Thr^{97tA}-Leu^{120tA} lacking the β-strand region (Kobe and Deisenhofer, 1993), demonstrates the

same kinetics of binding to NGF as wild type TrkA (Windisch et al., 1995a, 1995b).

The LRM-2B Domain

Table 7 presents the equilibrium torsional angles of the LRM-2B in the complex with

BDNF. Side chains of all general consensus residues of the LRM-2B, except for Phe^{111tB} and

30   terminal amino acid Leu^{117tB}, form the hydrophobic core and thereby stabilize the

characteristic hairpin shape of the LRM (Figure 11b). In contrast with the LRM-2A, aromatic

residues of the LRM-2B, namely Phe^{105tB}, Tyr^{108tB} and Phe^{111tB}, do not seem to have any

specific roles in BDNF/LRM-2B molecular recognition. They form a cluster in which their

aromatic rings interact with each other and are about mutually perpendicular (Figure 11b). On

35   the contrary, all charged residues of the LRM-2B, namely Arg^{94tB}, Asp^{100tB}, Lys^{104tB}, Lys^{109tB} and

Lys^{113tB}, are involved in specific electrostatic interactions with BDNF.

Similar to the NGF/LRM-2A complex, almost the whole LRM-2B domain, from $Leu^{93\iota B}$ to $Lys^{113\iota B}$, fits to the BDNF binding determinant (Figure 11b). On the other hand, there are significant differences of the neurotrophin-induced conformational alterations in the two LRM domains. First, since the BDNF binding domain does not have a β-strand motif which would

5   fit to the β-strand of the LRM-2B, the characteristic geometric features of the latter are lost. Second, region $Tyr^{108\iota B}$ to $Asn^{116\iota B}$ retains its α-helical structure in the BDNF-bound LRM-2B domain. The reason of this conformational stability is that the spacer between the two BDNF-bound residues, $Lys^{109\iota B}$ and $Lys^{113\iota B}$ (3 residues), is consistent with the period of an α-helix (3.5 residues).

10   **PRINCIPAL AMINO ACIDS INVOLVED IN MOLECULAR RECOGNITION**

Principal NGF Residues

The amino acids of NGF which are primarily responsible for maintaining bioactive conformations (McDonald et al., 1991; Shamovsky et al., 1996) or which directly participate in NGF/TrkA recognition are specified in Figure 13. Almost all residues of the amino and

15   carboxyl termini of NGF as well as the His^{75}-Asn^{77} region are involved in specific intra- or intermolecular interactions. Only five amino acids of the 30-residue binding domain of NGF do not seem to be essential for either maintaining its bioactive conformation or binding to the recognition site of TrkA. These include Ser^1, Ser^2, Ser^3, Ala^{116} and Val^{117}.

The observation that the important amino acids of the NGF binding domain are

20   conserved across all species while the apparently unimportant five residues are variable (Figure 13) (McDonald et al., 1991) supports the particular structural features of the NGF/LRM-2A complexes calculated herein. There are, however, exceptions which require explanation. In most cases, principal amino acids of NGF molecules derived from different species appear to be substituted by similar residues, e.g. I6V, F7L, L112I, S113T or R114K.

25   In some special cases, the substituted amino acid is quite different but the particular substitution is still consistent with the present model, e.g. R9M, R9L or R118Q (McDonald et al., 1991; Shamovsky et al., 1996); in the case of the H8N substitution (McDonald et al., 1991), histidine and asparagine have the same topology with respect to H-bonding to the Glu^{11} carboxyl oxygen. The structure of snake NGF (sNGF) requires special consideration.

30   Principal hydrophobic residues Phe^7 and Phe^{12} are replaced by histidine residues in sNGF. Although these mutations could be accompanied by structural differences in snake TrkA, they are consistent with the present model. According to the survey of Warme and Morgan (1978), side-chain interactions of histidine with tryptophan or threonine are very common in natural proteins, which implies the existence of specific inter-residue affinities. This being the

35   case, attractive interactions His^7...$Thr^{114\iota A}$ and His^{12}...Trp^{76} in areas B and A, respectively, may replace corresponding hydrophobic interactions with Phe^7 and Phe^{12}.

Principal LRM-2A Residues

The principal residues of the LRM-2A are shown in Figure 14. The general consensus residues (Schneider et al., 1988; Schneider and Schweiger, 1991) maintain the specific geometry of the LRM (Kobe and Deisenhofer, 1993, 1994, 1995). The amino acids which

5   form the distinct binding areas are involved in specific intermolecular interactions with the NGF binding domain. Since NGF does not activate the TrkB receptor, those residues which are specific for the TrkA receptor have been postulated to be directly involved in NGF/LRM-2A recognition (Windisch et al., 1995a, 1995b). As shown, the LRM-2A segment has nine specific residues, seven of them directly participating in NGF/LRM-2A recognition in the

10   framework of the present model. Thus, Lys^{100tA} binds Asp^{16} in area D, Pro^{108tA} is completely buried inside the NGF/LRM-2A complex, residues Asp^{109tA}, His^{112tA} and Pro^{115tA} form binding area C, and residues Phe^{113tA} and Thr^{114tA} are involved in forming area B. The other specific residues, Arg^{104tA} and Arg^{116tA}, do not seem to be required for specific NGF/LRM-2A interactions. It is seen, furthermore, that binding areas A and E are not specific for the

15   recognition site of TrkA, indicating that binding specificity of the LRM-2A is determined by Lys^{100tA}, Asp^{109tA} and Phe^{113tA}. The fact that these particular amino acids are replaced in the recognition site of TrkB by residues of a different chemical nature, namely Asp^{100tA}, Lys^{109tA} and Lys^{113tA}, respectively (Windisch et al., 1995a, 1995b), making NGF/TrkB binding impossible, supports the herein predicted details of NGF/LRM-2A recognition. Principal

20   residue Phe^{105tA}, although common to both the TrkA and TrkB recognition sites (Windisch et al., 1995a, 1995b), is also important for the NGF/TrkA recognition process, since oxidation of its counterpart, Trp^{76}, results in a complete loss of receptor binding (Merrell et al., 1975).

Principal BDNF residues

Since BDNF/TrkB molecular recognition is predicted to be primarily based on

25   electrostatic complementarity, principal BDNF and LRM-2B residues are identified by analysing their contribution to the intermolecular electrostatic energy. Table 8 presents a comparison of individual contributions of residues of BDNF, NGF and the LRM-2B to the intermolecular electrostatic energy for the BDNF/LRM-2B and the NGF/LRM-2B complexes, with cutoff being ±10 kcal/mol. BDNF/TrkB molecular recognition is achieved by those

30   residues that make significantly more favourable contacts with their counterparts than do corresponding residues in the "improper" NGF/LRM-2B interaction. Accordingly, in section A of Table 8, residues of BDNF that make more favourable contacts with the LRM-2B than do those of NGF by at least 10 kcal/mol, are highlighted. They are: Glu^{18}, Asp^{24}, Glu^{55}, Arg^{61} and Gln^{84}. These residues make up the BDNF binding epitope for TrkB activation. Only two of

35   them, Arg^{61} and Gln^{84}, have been previously identified (Ibáñez et al., 1993). The most unusual case is residue Gln^{84}, which does not markedly participate in electrostatic interactions

40

with the LRM-2B; however, its substitution by His[84] results in considerable repulsive interactions with positively charged residues of the receptor site. Therefore, Gln[84] cannot be referred to as a principal residue by itself in terms of the TrkB receptor binding, and its apparent importance (Ibáñez *et al.*, 1993) comes from unfavorable substitution by a positively

5   charged His[84]. The only residue of NGF which binds to the TrkB receptor site significantly more strongly than does the corresponding residue of BDNF is Glu[35], in agreement with observations (Lai *et al.*, 1996).

Principal LRM-2B residues

Section B of Table 8 identifies the LRM-2B residues which significantly contribute to

10   specificity of binding. Amino acids Arg[94tB], Asp[100tB], Ser[101tB], Lys[109tB] and Lys[113tB] make significantly more favorable contacts with their counterparts in BDNF than with those in NGF. Additionally, these residues are responsible for specific binding in areas F-K. The only residue of the LRM-2B that favours the NGF counterpart is Lys[104tB], which is caused by the abovementioned effect of Glu[35].

15   Figure 15 illustrates schematically the geometry of the LRM-2A and the LRM-2B receptor sites. Those residues which are predicted to form specific bonds with their preferred ligand are shown by arrows. The similarity of the binding patterns of the two LRMs is striking, especially bearing in mind the differences pointed out in the nature of the intermolecular interactions, and that the binding patterns were identified in independent computations.

20   Thus, binding specificity of TrkA and TrkB is determined by the residues located in distinct positions of their second LRMs, with their respective binding patterns being incompatible with each other.

It is shown that van der Waals and hydrophobic interactions play a more important role in TrkA than in TrkB recognition. As a part of this phenomenon, we have demonstrated

25   that NGF/LRM-2A binding is characterized by greater geometric complementarity, such that the ligand-receptor complex does not contain marked internal cavities. A plausible explanation for these particular features of Trk receptor recognition is that the NGF binding determinant is flexible and, because of that, more is required to stabilize its bioactive conformation in solution. Accordingly, TrkA receptor binding involves physical factors that are

30   more effective in an aqueous environment, namely van der Waals and hydrophobic interactions.

EXPLANATION FOR STRUCTURE-ACTIVITY RELATIONSHIPS

TrkA mediated activity has been evaluated for 27 point and deletion mutants of the TrkA binding domain of NGF: hNGF (Burton *et al.*, 1992; Shih *et al.*, 1994), mNGF (Burton *et*

35   *al.*, 1992; Drinkwater *et al.*, 1993), mNGFΔ3-9 (Drinkwater *et al.*, 1993), (1-120)hNGF (Schmelzer *et al.*, 1992), (1-120)mNGF (Luo and Neet, 1992), (1-117)hNGF (Schmelzer *et al.*,

41

1992) and hNGF:NT-4/5 (Treanor et al., 1995) retain full activity; mNGFΔ2-8, mNGFΔ61-66 (Drinkwater et al., 1993), hNGF-R9A, hNGFΔ1-5 and hNGF-P5A (Shih et al., 1994) demonstrate intermediate potency; hNGFΔ1-9 (Burton et al., 1992; Kahle et al., 1992; Luo and Neet, 1992; Drinkwater et al., 1993; Shih et al., 1994; Burton et al., 1995), mNGFΔ1-8

5   (Taylor et al., 1991; Burton et al., 1992), mNGFΔ1-9, mNGFΔ9-13 (Woo et al., 1995), mNGFΔ3-8, mNGFΔ3-11, mNGFΔ3-12, mNGFΔ3-13, mNGFΔ3-14, mNGFΔ9-14, mNGFΔ112-118 (Drinkwater et al., 1993), hNGF-H4A, hNGF-H4D (Shih et al., 1994), BDNF (Suter et al., 1992), and NT-4/5 (Treanor et al., 1995) are almost or completely inactive. The present model of NGF/LRM-2A recognition enables a comprehensive explanation for the

10   structure-activity relationships.

As demonstrated, fully active hNGF, mNGF and hNGF:NT-4/5 fit to the five binding areas A-E of the recognition site of TrkA, while the mNGFΔ3-9 deletion mutant fits only to A, C and D, without any specific binding taking place in areas B or E. Therefore, there are three common geometric features of the four fully active molecules which distinguish them from the

15   less active analogues. First, conformations of the amino and carboxyl termini of these NGF analogues are "preorganized" for binding to the principal LRM-2A binding areas A, C and D. Second, there is no stereochemical incompatibility in the binding areas B and E. Third, there is no hole inside the NGF/LRM-2A complexes.

The structures of the other three fully active NGF analogues, (1-120)hNGF,

20   (1-120)mNGF and (1-117)hNGF, are consistent with the above criteria. Indeed, since the NGF carboxyl end is located on the surface of the NGF/LRM-2A complexes (Figure 10) and does not directly participate in principal intermolecular interactions, the lengthening of the NGF carboxyl terminus by two amino acids does not explicitly affect NGF/LRM-2A compatibility. As far as the (1-117)hNGF molecule is concerned, terminal residue Arg^{118} of

25   NGF has been shown to form inter-chain ionic H-bonds with Glu^{11} (see above) and, hence, seems to be important in maintaining the structure of the NGF bioactive conformation. On the other hand, there is a second factor stabilizing the bioactive conformation of the hNGF termini, namely inter-chain H-bonding of residue Arg^9. Because of the latter binding, the above criteria are still fulfilled for (1-117)hNGF.

30   The deletion of principal residue Phe^{12}, which participates in hydrophobic interactions in area A, results in a substantial loss of TrkA mediated activity of the mNGFΔ3-12, mNGFΔ3-13, mNGFΔ3-14 and mNGFΔ9-14 deletion mutants (Drinkwater et al., 1993). Likewise, the absence of principal residues Arg^{114} and Lys^{115}, essential for the ionic binding in area C, results in dramatic loss of bioactivity of mNGFΔ112-118 (Drinkwater et al., 1993).

35   Similarly, geometric perturbations of the essential residues Arg^{59} and Arg^{69} in the mNGFΔ61-66 deletion mutant result in incomplete NGF/LRM-2A compatibility in area D and,

42

accordingly, a considerable loss of activity.

The specific location of the NGF ninth amino acid side chain in the "hollow" existing on the surface of the NGF rigid region has been predicted herein to be critical for high TrkA mediated activity. The present invention provides a detailed explanation for this prediction.

5   That is, the "hollow" is buried inside the NGF/LRM-2A complex, and a moiety located in this "hollow" fills the cavity which otherwise would exist inside the complex and destroy NGF/LRM-2A compatibility. Since this moiety is located in the internal cavity of the complex (Figure 10), severe limitations are imposed on its size. A short side chain does not fill this cavity; therefore, the hNGF-R9A mutant demonstrates noticeably diminished activity (Shih et al.,

10   1994). The cavity preferably is filled either by a bulky amino acid side chain, such as arginine (e.g. hNGF), methionine (e.g. mNGF) or leucine (sNGF), or by the two residue peptide backbone (mNGFΔ3-9 or mNGFΔ2-8). A longer amino terminus tail (e.g. in mNGFΔ3-8, mNGFΔ9-13 or mNGFΔ1-5) cannot be accommodated in the internal cavity of the NGF/LRM-2A complex and, hence, interferes with binding areas B and E.

15   Most deletion or point mutations of the NGF amino terminus destroy the exposed β-strand motif Phe^7-Arg^9 and change the proper orientation of the Phe^7 side chain, thereby affecting NGF/LRM-2A compatibility in areas B and E. Thus, incorporation of a negatively charged residue into the relatively long NGF amino terminus, as in hNGF-H4D, BDNF, NT-3 and NT-4/5, or substitution H8R, which is characteristic for BDNF and NT-4/5, has each been

20   demonstrated to cause dramatic conformational changes in the complex of the neurotrophin amino-carboxyl termini, making it incompatible with the LRM-2A. This stereochemical incompatibility of the geometry of the NGF amino terminus with binding areas B and E of the LRM-2A is the reason for the partial or complete loss of TrkA-related activity of mNGFΔ3-8, mNGFΔ1-5, hNGF-P5A, hNGF-H4A, hNGF-H4D, mNGFΔ1-8, hNGFΔ1-9, mNGFΔ1-9,

25   mNGFΔ9-13, mNGFΔ3-11, BDNF and NT-4/5.

As demonstrated, both NGF monomers are directly involved in specific ligand-receptor interactions, i.e., the first monomer binds areas B, D and E, whereas the second one binds areas A and C. Consequently, the dimeric structure of NGF is necessary to retain high biological activity, which is also consistent with experimental data (Maness et al., 1994). On

30   the contrary, only one BDNF protomer is essential for TrkB binding (Figure 11a, 11b).

In addition, recent reports of experiments have demonstrated the importance of residues Phe^7 (Kullander and Ebendal, 1996), Leu^{112}, Arg^{114} and Lys^{115} (Krüttgen et al., 1996) for TrkA mediated activity of NGF. This is consistent with their participation in the specific NGF/LRM-2A binding in the framework of the present model.

35   CONCLUSIONS

The complexes of the amino and carboxyl termini of the four fully active NGF

43

analogues with the second leucine-rich motif of TrkA were obtained using Variable Basis Monte Carlo simulated annealing calculations. The same methodology was utilized to define the structure of the complex of the second leucine-rich motif of TrkB with the BDNF receptor binding determinant. The structural features of the resulting NGF/TrkA and BDNF/TrkB

5   binding predictions are supported by the following: (i) geometric and electrostatic complementarity of the binding domains of NGF and BDNF to binding sites of TrkA and TrkB, respectively, without considerable conformational changes of the ligands; (ii) appropriate environments for hydrophobic and hydrophilic residues within the complexes; (iii) analysis of structural variability of both binding domains; and (iv) comprehensive explanation of currently

10   published structure-activity relationships. Within these complexes, NGF/TrkA molecular recognition is based upon multiple-point intermolecular interactions of hydrophobic, van der Waals, ionic and hydrogen bonding type. Extensive intermolecular van der Waals contacts arise from complementarity of the NGF binding domain and the TrkA recognition site in size and shape. In addition, there are five specific binding areas within the receptor model:

15   hydrophobic A and B, ionic C and D and cooperative hydrogen bonding E. The NGF/TrkA stereochemical compatibility in areas A, C and D is required for TrkA receptor activation, whereas areas B and E reinforce binding specificity, making the NGF molecule a very sophisticated key triggering the chain of biological events following receptor phosphorylation. The 3-dimensional structures of the binding domains of the fully active NGF analogues are

20   "preorganized" for stereochemical fit to the second leucine-rich motif of TrkA. Five distinct binding areas F-K were also identified in the BDNF/TrkB complex, although, in contrast with NGF/TrkA binding, BDNF/TrkB recognition is based primarily on ionic and hydrogen bonding interactions. In spite of significant differences in the nature of ligand-receptor interactions involved in TrkA and TrkB recognition processes, binding patterns of their receptor binding

25   sites for NGF and BDNF are almost identical. The predicted mechanism of high affinity NGF/TrkA and BDNF/TrkB binding is consistent with the conformational model of TrkA-p75^{NTR} interactions (Chao and Hempstead, 1995).

PART C

30   ## THEORETICAL MODELLING OF THE P75^{NTR} RECEPTOR RECOGNITION SITE FOR NEUROTROPHINS

INTRODUCTION

As summarized above, the neurotrophins represent a family of structurally and
35   functionally related proteins which play a crucial role in the development, survival and maintenance of the sympathetic and sensory neurons (Purves, 1988; Snider and Johnson,

44

1989; Barde, 1989; Thoenen, 1991; Korsching, 1993; Persson and Ibáñez, 1993; Davies, 1994; Ibáñez, 1995). The neurotrophin family consists of nerve growth factor (NGF), brain-derived neurotrophic factor (BDNF), neurotrophin-3 (NT-3), neurotrophin-4/5 (NT-4/5), and more recently discovered neurotrophin-6 (NT-6) (Berkmeier et al., 1991; Barde, 1991;

5   Barbacid, 1993; Bradshaw et al., 1994; Chao, 1994; Gotz et al., 1994). Each neurotrophin is capable of binding independently with the common neurotrophin receptor $p75^{NTR}$, as opposed to specific Trk receptor interactions.

METHODS

The geometric features of complexes of monomeric neurotrophins with the $p75^{NTR}$

10   receptor binding site have been obtained by multiple molecular dynamics runs of 200-300 ps at constant temperatures between 300 and 400°K, followed by local energy refinements. The QUANTA V4.1 molecular modelling program (Molecular Simulations Inc., Waltham, MA) with the united atom CHARMM potential energy terms (Brooks et al., 1983) has been used. Residues of $p75^{NTR}$ are designated by abbreviation p.

15   According to the invention, we superimposed the binding domains of NGF, BDNF, NT-3 and NT-4/5 with a putative binding site of $p75^{NTR}$ and carried out multiple molecular dynamics computations of the ligand-receptor complexes. These calculations revealed the 3-dimensional structures of the binding domains of the neurotrophins and $p75^{NTR}$, demonstrated their geometric and electrostatic complementarity, and identified principal residues involved in

20   receptor recognition. All neurotrophins are believed to induce similar conformational changes in the $p75^{NTR}$ binding site, generally located in the orientation of the sequential loops within the cysteine-rich repeats.

Initial geometries of individual components of the complexes were based upon the X-ray crystallographic coordinates of neurotrophins NGF (McDonald et al., 1991), BDNF and

25   NT-3 (Robinson et al., 1995) and the $p55^{TNFR}$ receptor extracellular domain (Banner et al., 1993) which is homologous to $p75^{NTR}$. Geometry of the NT-4/5 monomer was constructed from the X-ray derived structure of NT-3 (Robinson et al., 1995). Since NGF and other neurotrophins fold in similar rigid conformations, their molecular motions were restricted by imposing the following atom constraints. First, peptide backbones of the neurotrophins were

30   fixed at their crystallographic coordinates. Further, conformations of the amino acid side chains of the neurotrophins were also fixed except for those located within and in the vicinity of the variable loop regions I and V (the $p75^{NTR}$ binding determinant). Thus, amino acid side-chain motions were allowed for residues 23-35 and 93-98 (NGF numbering) as well as for eight additional neighboring residues, namely His^{84} (Gln in other neurotrophins), Phe^{85} (Tyr in

35   other neurotrophins), Lys^{88} (Arg in other neurotrophins), Trp^{99}, Arg^{100}, Phe^{101} (Trp in NT-3 and NT-4/5), Arg^{103}, and Asp^{105}. The flexible amino and carboxyl termini of the neurotrophins were

45

excluded to avoid artefactual spacial hindrances for the receptor binding.

Fig. 16a represents a fragment of the crystallographically resolved structure of the p55[TNFR] extracellular domain (Banner et al., 1993), corresponding to the second CRD (loops 2A and 2B) and the first loop of the third CRD (loop 3A). Fig. 17 illustrates the sequence of
5   this fragment and its alignment with the three known p75[NTR] peptides (Johnson et al., 1986; Radeke et al., 1987; Large et al., 1989). Fig. 16b presents the minimum energy conformation of the corresponding fragment of human p75[NTR]. As is apparent, its size and shape are complementary to the exposed p75[NTR] binding determinant of NGF (Fig. 16c). Accordingly, this 58-amino acid fragment of p75[NTR], including the second and the beginning of the third
10   CRDs (Fig. 17), has been considered as a putative binding site for neurotrophins. The artefactual charges on the terminal amino and carboxyl groups of the peptide representing the p75[NTR] binding site were neglected.

Once the most stable equilibrium 3-dimensional structures of the complexes being studied were obtained, the residues contributing the most to the energy of intermolecular
15   interactions were identified. Point atomic charges of Weiner et al. (1984) and a dielectric constant equal to the interatomic separation in angstroms (to implicitly simulate solvation effects) (Weiner et al., 1984) were utilized to calculate the electrostatic intermolecular terms. The van der Waals intermolecular terms were evaluated by the united atom CHARMM force field (Brooks et al., 1983). The calculations were performed on a 200 MHz Indigo-2
20   SiliconGraphics Workstation.

RESULTS AND DISCUSSION

The most stable structures of the complexes of the neurotrophins with the putative p75[NTR] receptor binding site obtained by the molecular dynamics computations described herein are illustrated in Fig. 18. Table 9 presents net values of the electrostatic and van der
25   Waals terms of the ligand-receptor interaction energy. Tables 9 and 10 list individual residues of the neurotrophins and the p75[NTR] receptor which significantly contribute to the intermolecular electrostatic interaction energy. The highlighted residues represent the functional epitopes of the ligands (Table 9) and the receptor (Table 10), whereas the other listed residues, although being located within the binding interfaces, apparently do not
30   participate in major ligand-receptor electrostatic interactions in the particular complex. Predicted Cartesian 3-dimensional coordinates of atoms of the p75[NTR] binding sites in the complexes with NGF and BDNF are presented in Appendix 3.

Significant contributions of electrostatic interactions to the ligand-receptor interaction energy (Table 9) result from opposite net charges of the binding domains of neurotrophins
35   (positively charged) and the common neurotrophin receptor (negatively charged), which effect is consistent with published predictions (Rydén et al., 1995). Data presented in Tables 9 and

46

10 demonstrate that, on the average, the interaction between the functional epitopes is responsible for 94% of intermolecular electrostatic energy, but only 43% of van der Waals interaction energy. Consequently, residues participating in strong and specific ligand-receptor interactions represent only a part of a bigger binding interface in which significant van der

5   Waals contribution is accumulated from a large number of weak contacts, which is possible only as a consequence of geometric complementarity of the binding domains. Fig. 19 presents the structure of the BDNF/p75^{NTR} complex as atomic van der Waals spheres and demonstrates the geometric fit of the binding domains. The van der Waals energy and, therefore, geometric complementarity of the binding interfaces in the NGF/p75^{NTR} complex is

10 significantly lower than in the other neurotrophin/p75^{NTR} complexes (Table 9), which is consistent with its fastest rate of dissociation (Ibáñez, 1995). However, the pure geometric factor cannot explain the slowest rate of dissociation observed for the BDNF/p75^{NTR} complex (Ibáñez, 1995). Thus, stability of the complex arises from a combination of geometric and electrostatic complementarities of the binding interfaces, consistent with the generalizations

15 of Clackson and Wells (1995). A specific feature of the neurotrophin/p75^{NTR} binding interfaces is that they do not include substantially hydrophobic residues, so they do not have a hydrophobic core, which has been found in many other protein-protein complexes (Clackson and Wells, 1995; Livnah et al., 1996). The predominant interactions within the binding domains of the complexes under study are of the salt-bridge type.

20   Specificity of binding of the neurotrophins to the p75^{NTR} receptor is determined by charged residues within the binding domains (Rydén et al., 1995). As seen in Fig. 18, they create 3-dimensional networks in which most of them are in contact with more than one residue of the opposite charge. Therefore, any missing charge would destroy more than just one bond, but a significant portion of, if not the whole, network. That is, the electrostatic

25 complementarity of the binding interfaces would be altered, which is consistent with the experimentally observed sensitivity of binding to mutations of charged residues (Ibáñez et al., 1992; Rydén et al., 1995; Rydén and Ibáñez, 1996). Both ligand and receptor provide the network with positive and negative charges (Table 9 and 10, Fig. 18), even though negative charges dominate in the receptor, and positive in the ligands. This particular spatial

30 arrangement of the charges increases specificity of binding and prevents electrostatic repulsions within the same binding domains. For example, in all the complexes, positively charged residue Lys^{56p} of the receptor forms salt-bridges with negatively charged residues Asp^{75p} and Asp^{76p} of the receptor, thereby occupying one site of their coordination, such that only the opposite sides of the latter residues remain available for intermolecular ionic

.35 interactions (Fig. 18). Negatively charged residue Asp^{93} of BDNF holds together positively charged residues Arg^{97} and Arg^{101} of BDNF, such that they are both able to interact with

47

juxtaposed amino acids Asp^{75p} and Asp^{76p} of the receptor (Fig. 18b). Similarly, negatively charged residue Asp^{30} of the neurotrophins forms a salt-bridge interaction with Arg^{100}, which directly interacts with $p75^{NTR}$.

In spite of the differences in the binding interfaces of the respective complexes, binding patterns of the $p75^{NTR}$ receptor are similar. All three loops of the receptor binding site (2A, 2B and 3A) are involved in binding (Fig. 18). The principal residues of loop 2A are Asp^{47p} and Lys^{56p}; those of loop 2B are Asp^{75p} and Asp^{76p}; and those of loop 3A are Asp^{88p} and Glu^{89p}. As is seen in Table 10, loop 2B forms the strongest contacts. In addition to the principal binding pattern, the $p75^{NTR}$ binding domain comprises specific residues for ionic interactions with particular neurotrophins (Table 10, Fig. 18). Thus, Arg^{80p} interacts only with Glu^{35} of NGF; residue Glu^{53p} interacts only with Lys^{96} of BDNF, and Glu^{60p} and Glu^{73p} interact only with residues of NT-3 and NT-4/5.

Site-directed mutagenesis studies of the $p75^{NTR}$ binding site have suggested that mutation of any one of the residues Asp^{75p}, Asp^{76p} or Glu^{89p} to Ala does not affect NGF binding, whereas mutation of Ser^{50p}, which does not participate in major ionic interactions, results in the complete abolishment of binding (Baldwin and Shooter, 1995). The apparent discrepancy with the present theoretical studies can be explained, since the cited experimental observations are still controversial. Indeed, although both Asp^{75p} and Asp^{76p} are involved in ionic interactions in the loop 2B region with positively charged residues of neurotrophins, one of them might be enough to maintain binding to NGF. Likewise, the functional role of the missing residue Glu^{89p} in loop 3A might be fulfilled by adjacent Asp^{88p}. Residue Ser^{50p} of $p75^{NTR}$ is predicted to be hydrogen bonded to Gln^{96} of NGF (Fig. 18a), and its mutation to Asn, Ala or Thr, which abolishes receptor binding (Baldwin and Shooter, 1995), may create steric hindrances in the NGF/$p75^{NTR}$ interface. The present molecular modelling studies suggest that Ser^{50p} is not important for binding of any other neurotrophin (Fig. 18, b-d).

In contrast to the $p75^{NTR}$ receptor binding pattern, there are only two common residues of the binding interfaces of neurotrophins which directly interact with the receptor site, Arg^{100} and Arg^{103}. Contribution of Arg^{103} is significant in all the complexes, while Arg^{100} seems to be less important for the NGF/$p75^{NTR}$ binding.

As is seen in Table 9, most important residues of the NGF binding domain are (in order of decreasing significance) Lys^{32}, Lys^{34}, Arg^{103}, Lys^{95}, and His^{84}, all of them forming specific ionic contacts with negatively charged residues of $p75^{NTR}$ (Fig. 18a). Involvement of Lys^{32}, Lys^{34}, and Lys^{95} in $p75^{NTR}$ binding has been very well established experimentally, with the same order of significance being observed (Ibáñez, 1994). The most important residues of NGF, Lys^{32} and Lys^{34}, bind to the loop 2B residues of $p75^{NTR}$ (Fig. 18a). Here we

48

demonstrate that residue Lys[88] is not critical for p75[NTR] binding, whereas residues Arg[103] and His[84] make direct ionic contacts with the receptor binding site. Importance of the latter residue has not been previously reported in the context of p75[NTR] binding. The roles of Asp[30], Glu[35] and Arg[100] seem to be secondary, since their contributions are relatively small.

5   Hydrophobic residue Ile[31] is not directly involved in ligand-receptor interactions.

In BDNF, all three positively charged residues of variable region V, Lys[95], Lys[96] and Arg[97] (Rydén et al., 1995), bind to negatively charged residues of the p75[NTR] binding site, namely Asp[47p], Glu[53p] and Asp[75p], respectively (Fig. 18b). In addition, the residues Arg[88] and Arg[101] play a more important role than in the NGF case (Table 9); they bind to the loop 2B

10   residues Asp[75p] and Asp[76p] of p75[NTR], thereby fulfilling the function of missing positively charged residues of loop I. The increased importance of residue Arg[88] in BDNF and other neurotrophins relative to that of Lys[88] in NGF (Table 9) is permitted by a longer side chain of Arg, which results in a decrease of the separation between opposite charges (Fig. 18). Because of missing residue His[84], only the positively charged residue Arg[104] binds to the loop

15   3A residues Asp[88p] and Glu[89p] of p75[NTR].

In NT-3, the loop 2B residues of the receptor Glu[73p], Asp[75p], and Asp[76p] bind to Arg[31], His[33], Arg[100], and Arg[87]. Residue Asp[47p] of loop 2A of the receptor also binds to Arg[100]. Residue Lys[95] of variable region V does not form any salt-bridge contact with the receptor, consistent with its reported insignificance for NT-3 binding (Rydén et al., 1995). Thus, the

20   present results agree well with the established roles of Arg[31] and His[33] of NT-3 (Rydén et al., 1995; Rydén and Ibáñez, 1996) and predict the increased importance of residue Arg[100] in NT-3 for p75[NTR] binding (Table 9). The binding pattern of NT-4/5 is similar to that of NT-3 (Fig. 18, c,d). The increased electrostatic contribution of Arg[36] with respect to corresponding NT-3 residue His[33] (Table 9) is caused by the longer side chain of the former, which results in

25   formation of a salt-bridge contact with residue Glu[60p] of the receptor (Fig. 18d).

Binding of a neurotrophin induces conformational changes in the p75[NTR] binding site. The conformational space of the three loops (2A, 2B and 3A) is limited by eight disulfide bonds; therefore, the most significant changes occur in the junction areas of those loops. Fig. 20 illustrates the superimposed equilibrium geometries of the free and the BDNF-

30   complexed p75[NTR] binding site. The superimposition is performed by a least-square minimization technique using the α-carbon reference atoms of loops 2A and 3A. As is apparent, the orientation of loop 2B with respect to the two flanking loops is considerably changed upon binding. Because of striking similarities between the binding patterns of the p75[NTR] receptor with the different neurotrophins, a similar conformational change takes place

35   in all four complexes under investigation. The driving force behind this particular conformational transition is ionic interactions of the principal residues of loop 2B, Asp[75p] and

49

Asp^{76p}, with positively charged residues of the neurotrophins, taking into account that spacial positions of the flanking loops 2A and 3A are fixed by ionic interactions of residues Asp^{47p}, Lys^{56p}, Asp^{88p}, and Glu^{89p} with corresponding residues of the neurotrophins (Fig. 18). Thus,

5   structural variability between the neurotrophins does not preclude them from inducing similar conformational change in the common neurotrophin receptor.

The binding pattern of neurotrophins to the p75^{NTR} receptor predicted by the present molecular modelling studies can be additionally verified by checking conservation of the identified principal residues. The sequences of the binding site of the p75^{NTR} receptor from different species (Fig. 17) demonstrate that principal residues forming its common binding

10   pattern, namely Asp^{47p}, Lys^{56p}, Asp^{75p}, Asp^{76p}, Asp^{88p}, and Glu^{89p}, are conserved in p75^{NTR}. The known variability of regions I and V among neurotrophins (Rydén et al., 1995) implies that conservation of the principal residues of the p75^{NTR} binding determinants may be checked only within the same neurotrophin derived from different species. Study of a recent sequence alignment of neurotrophins (Bradshaw et al., 1994) allowed us to conclude that the functional

15   epitope of the neurotrophins (Table 9) is generally conserved within the same neurotrophin even though there are some exceptions, often represented by the substitution by a similar amino acid. Arg^{100} and Arg^{103} are the only two residues of the binding epitopes which are conserved throughout all neurotrophins (Bradshaw et al., 1994). Other residues within the functional epitopes maintain specificity of binding of different neurotrophins.

20   The present model also represents a key to understanding the conservation of residues which do not directly participate in receptor binding. For example, Gly^{33} is absolutely conserved in all neurotrophins, yet is not involved in any specific interactions with the receptor binding site. However, within the present model, its conservation can be understood, since it is located very close to loop 3A of the receptor and forms van der Waals contacts with it (Fig.

25   18), such that any other residue would impose steric hindrance which would alter or destroy the ligand-receptor geometric complementarity.

The principal NGF/TrkA binding areas necessary to trigger TrkA phosphorylation and subsequent biological events have been discovered by the inventors. Specifically, the inventors have discovered that essentially the full binding site of the second leucine rich motif

30   (LRM) of TrkA, amino acid residues 93 to 117, forms the binding site for NGF, and comprises five distinct binding areas, A, B, C, D and E. Appendix 1 provides the Cartesian coordinates of the LRM-2A residues defining the areas A to E in PDB format. Binding areas A and B bind hydrophobically to ligands, areas C and D form ionic bonds with charged portions on ligands and area E forms hydrogen bonds with ligands.

35   The stereochemical fit to at least three of these binding sites, A, C and D by a ligand is necessary to activate TrkA receptor. Binding areas B and E reinforce stereoselectivity of

50

the TrkA binding site by selecting an NGF analogue with a stereochemically compatible amino terminus.

Binding area A of the second LRM comprises hydrophobic interaction of residue Phe^{105IA}. Binding area B comprises hydrophobic interaction of residues Phe^{111IA}, Phe^{113IA} and Thr^{114IA}. Binding area C comprises attractive ionic interaction between a suitable portion on the ligand and Asp^{109IA}. Binding area D comprises attractive ionic interaction between a suitable portion on the ligand and residue Lys^{100IA}. Binding area E comprises multiple parallel β-strand type hydrogen bonding with region Asn^{95IA}-Ile^{98IA}.

Main structural features of the bioactive conformation of NGF include: 1) ionic hydrogen bonding between Glu^{11} in the amino terminus and Arg$^{118'}$ in the carboxyl terminus; 2) separation of the flexible loop 1-8 from the rigid region (9-11 and 112' to 118') because of electrostatic repulsions caused by His^{4} and conformational restrictions imposed by Pro^{5}; 3) packing the side chain of Arg^{9} or Met^{9} in the "hollow" of the rigid region, this "hollow" being an indentation in the protein structure by residues Lys$^{115'}$-Arg$^{118'}$; and 4) an embryonic β-sheet structure present between the α-carbons of the 7th and 9th residues.

Within NGF, residues Trp$^{76'}$, Arg$^{114'}$, Lys$^{115'}$ and Asp^{16} comprise the pharmacophore which binds TrkA. Any synthetic molecule, whether peptide or non-peptide, which fits into binding areas A, C and D is contemplated to elicit a biological response (agonist) or block biological response (antagonist).

The present invention provides a ligand for binding with TrkA, wherein TrkA comprises a second leucine rich motif (LRM) region comprising amino acid residues 93 to 117, the coordinates of the residues of said LRM given in Appendix 1, said LRM motif having five binding areas, area A comprising hydrophobic interaction of amino acid residue Phe^{105IA}, area B comprising hydrophobic interaction of amino acid residues Phe^{111IA}, Phe^{113IA}, and Thr^{114IA}, area C comprising ionic interaction of amino acid residues Asp^{109IA} and His^{112IA}, area D comprising ionic interaction of amino acid residue Lys^{100IA}, and area E comprising multiple parallel β-strand type hydrogen bonding of region Asn^{95IA} to Ile^{98IA}. The ligand comprises at least one functional group being capable of hydrophobic bonding and being present in an effective position in the ligand to hydrophobically bind to area A, at least one positively charged functional group being present in an effective position in the ligand to ionically bind to area C, and at least one negatively charged functional group being present in an effective position in the ligand to ionically bind to area D.

Secondary features of the ligand include at least one effective functional group present in a position in the ligand to hydrophobically bind to area B of TrkA, and a functional group present in an effective position in the ligand to hydrogen bind to area E of TrkA.

The invention further provides the ligand comprising amino acid residues, at least one

51

of the residues being capable of hydrophobic bonding and being present in an effective
position in the ligand to hydrophobically bind to Phe^{105tA} in area A on the TrkA receptor, at
least one of the residues being a positively charged residue present in an effective position in
the ligand to ionically interact with Asp^{109tA} and His^{112tA} forming area C on the TrkA receptor,

5   and one of the residues being a negatively charged residue present in an effective position in
the ligand to ionically bind to Lys^{100tA} in area D on the TrkA receptor.

The present invention also provides a method of designing a ligand to bind with an
LRM binding site on TrkA. The method includes computationally evolving a chemical ligand
using an effective genetic algorithm with preselected spatial constraints so that the evolved

10   ligand comprises at least three effective functional groups of suitable identity and spatially
located relative to each other in the ligand so that a first of the functional groups
hydrophobically interacts with binding area A, a second of the functional groups ionically
interacts with binding area C, and a third one of the functional groups ionically interacts with
binding area D of the second LRM of TrkA. Those skilled in the art will be aware of the

15   various techniques which may be used for de novo ligand design. For example, packages
such as Quanta, Discover and Insight provide computational methodologies for generating
ligands.

Some ligands according to the present invention may be peptides or peptidomimetics.
Morgan and co-workers (Morgan et al., 1989) define peptide mimetics as "structures which

20   serve as appropriate substitutes for peptides in interactions with receptors and enzymes".
The mimetic must possess not only affinity but also efficacy and substrate function. For
purposes of this disclosure, the terms "peptide mimetic" and "peptidomimetic" are used
interchangeably according to the above excerpted definition. That is, a peptidomimetic
exhibits function(s) of a particular peptide, without restriction of structure. Peptidomimetics of

25   the invention, e.g., analogues of the neurotrophin and receptor binding sites described herein,
may include amino acid residues or other chemical moieties which provide functional
characteristics described herein.

Known compounds may also be screened to determine if they satisfy the spatial and
functional requirements for binding with the second LRM of TrkA. The molecules in the data

30   bases are screened to determine if they contain effective moieties spaced relative to each
other so that a first moiety hydrophobically interacts with binding area A, a second of moiety
ionically interacts with binding area C, and a third moiety ionically interacts with binding area
D of the second LRM of TrkA.

The contents of all references and appendices (see Appendices 1, 2, 3, and 4) cited

35   throughout this application are hereby expressly incorporated by reference.

52

EQUIVALENTS

Those skilled in the art will recognize, or be able to ascertain using no more than routine experimentation, many equivalents to the specific embodiments of the invention described herein. Such equivalents are intended to be encompassed by the following claims.

Table 1. Equilibrium variable torsional angles (in degrees) of the amino and carboxyl termini of the most stable conformations of the NGF dimers and analogues.*

No.		Active structures				Inactive structures				
		hNGF		mNGF		mNGFD3-9		hNGF-H4D	mNGFD1-8	BDNF
					Amino terminus					
11	ψ	E	82.9	E	85.9	E 89.2	E 80.9	E 63.7	E 68.2
	φ		55.7		56.3	57.8	57.2	47.9	56.3
	χ1		-69.8		-72.0	-72.1	-75.0	-66.2	-76.9
	χ2		72.7		71.7	66.0	72.6	71.2	70.1
	χ3		-120.4		-111.7	-107.0	-104.8	-102.8	-97.7
10	ψ	G	-89.1	G	-95.1	G -88.0	G -129.5	G -81.6	G -134.1
	φ		-172.5		-178.6	-177.5	104.7	-80.8	155.0
9	ψ	R	-36.1	M	-21.1	S 146.5	R -46.5	M -66.6	R 71.4
	φ		-92.8		-91.4	-103.6	-80.9	157.5	-128.5
	χ1		-77.2		-75.2	-66.7	-115.0	-142.4	-73.5
	χ2		-173.9		-179.7	64.0	69.5	-69.7	-179.8
	χ3		-175.5		179.9	-	-141.9	178.3	-71.4
	χ4		134.3		-	-	98.1	-	-109.8
8	ψ	H	118.6	H	110.4	S 106.1	H 151.6	-	R 105.2
	φ		-116.5		-110.4	52.8	-53.7	-	-100.1
	χ1		-89.7		-90.9	-45.9	-62.0	-	179.6
	χ2		-73.8		-71.5	-172.3	-72.5	-	-105.5
	χ3		-		-	-	-	-	162.1
	χ4		-		-	-	-	-	133.7
7	ψ	F	135.7	F	129.4	-	F 142.3	-	A 161.6
	φ		-68.8		-89.0	-	-114.8	-	-166.6
	χ1		-171.6		-163.9	-	-170.7	-	-
	χ2		-96.3		-91.5	-	-100.2	-	-
6	ψ	I	40.3	V	61.7	-	I 40.0	-	P 114.4
	φ		40.4		47.7	-	39.9	-	-
	χ1		-159.7		-177.3	-	-159.7	-	-
	χ2		87.1		-	-	88.6	-	-

	5	ψ	P	156.0	P	149.8	-	P	105.5	-	D	82.8
		φ		-		-	-		-	-		56.5
		χ1		-		-	-		-	-		-176.9
		χ2		-		-	-		-	-		-112.8
5	4	ψ	H	121.4	H	122.1	-	D	117.9	-	S	136.2
		φ		-129.2		-129.8	-		-102.8	-		-53.4
		χ1		-162.5		-163.3	-		-66.4	-		-172.9
		χ2		-69.1		-69.2	-		-97.5	-		-178.3
	3	ψ	S	2.1	T	-1.9	-	S	-25.0	-	H	153.8
10		φ		-91.9		-84.5	-		-68.2	-		48.2
		χ1		-171.8		-174.9	-		39.3	-		82.1
		χ2		-53.2		-51.2	-		-120.5	-		69.8
	2	ψ	S	138.5	S	139.4	-	S	38.5	-		-
		φ		-128.9		-114.1	-		50.8	-		-
15		χ1		173.3		169.7	-		-173.2	-		-
		χ2		-141.9		-139.8	-		-120.6	-		-
	1	ψ	S	133.0	S	127.9	-	S	131.9	-		-
		φ		48.6		49.4	-		-133.8	-		-
		χ1		-43.2		-44.1	-		-43.5	-		-
20		χ2		-171.5		-172.4	-		-173.6	-		-

Carboxyl terminus

	112'	φ	L	-113.3	L	-113.0	L	-112.4	L	-112.0	L	-111.5	L	-110.6
25		ψ		98.8		98.7		99.2		97.7		89.9		100.1
		χ1		-72.3		-71.6		-71.6		-71.7		-71.8		-72.1
		χ2		163.7		163.0		162.6		162.2		161.9		161.1
	113'	φ	S	-83.4	S	-77.2	S	-77.4	S	-76.8	S	-91.9	T	-89.5
		ψ		136.1		146.0		143.5		141.7		149.4		134.0
30		χ1		177.0		179.4		176.3		175.6		169.6		57.4
		χ2		65.2		60.6		59.0		57.5		73.2		-179.7
	114'	φ	R	-66.7	R	-71.5	R	-78.0	R	-75.1	R	-117.0	I	-57.9
		ψ		-47.0		-53.7		-59.3		-57.1		-31.9		-32.2
		χ1		-99.1		-145.6		-93.4		177.5		-168.1		-162.1
35		χ2		-173.1		-179.8		-171.5		-159.7		86.5		87.9
		χ3		170.4		-173.6		-172.9		58.1		-73.8		-

55

Residue	Angle						
	χ4	138.4	140.3	141.5	124.7	173.4	-
115'	φ	K -163.2	K -162.1	K -167.1	K -163.0	K -133.4	K -167.7
	ψ	110.6	132.0	153.3	157.6	141.7	126.1
	χ1	-139.8	-143.3	-140.1	-137.8	-164.0	-142.2
	χ2	78.7	81.7	85.0	79.3	172.4	83.5
	χ3	-96.4	-97.9	-95.8	-97.4	133.9	-100.4
	χ4	129.5	120.9	131.0	133.6	-73.6	109.2
	χ5	-39.1	-35.6	-47.7	-44.1	9.6	-9.5
116'	φ	A -60.5	A -69.6	A -58.2	A -63.9	A -51.6	R -61.4
	ψ	-47.5	-40.7	-47.5	-42.4	-45.3	-39.3
	χ1	-	-	-	-	-	-80.9
	χ2	-	-	-	-	-	-173.4
	χ3	-	-	-	-	-	174.3
	χ4	-	-	-	-	-	129.6
117'	φ	V -71.8	T -85.5	T -64.6	V -41.0	T -114.6	G -73.3
	ψ	112.0	116.4	108.2	130.2	168.4	77.3
	χ1	-74.3	53.4	50.9	-66.2	57.2	-
	χ2	-	60.5	58.0	-	-170.5	-
118'	φ	R -93.8	R -118.2	R -58.5	R -125.2	R -51.5	R -49.0
	ψ	-57.9	-48.4	-37.6	141.3	-56.3	-40.3
	χ1	-104.3	-80.9	-109.5	-126.2	-153.8	-125.9
	χ2	79.1	109.1	73.3	106.7	88.0	98.0
	χ3	147.7	116.1	-76.3	-78.8	-74.9	-76.6
	χ4	147.0	116.1	-87.2	-98.5	-125.9	-111.5

*Torsional angles are designated according to the IUPAC-IUB rules (1970).

Table 2. Residues of BDNF and NGF defining the surfaces of their central β-strand stems, the side-chain thermal motion of which is taken into account when optimizing the structures of the complexes with the LRM-2B.

BDNF		NGF	
Ile[16]	Lys[57]	-	Lys[57]
Glu[18]	Asn[59]	Val[18]	Arg[59]
Val[20]	Met[61]	Val[20]	Ser[61]
Thr[21]	Lys[65]	Val[22]	-
Asp[24]	Gln[79]	Asp[24]	Tyr[79]
Lys[25]	Arg[81]	Lys[25]	Thr[81]
Lys[26]	Thr[82]	Thr[26]	Thr[82]
Thr[27]	Gln[84]	Thr[27]	His[84]
Val[29]	Tyr[86]	Thr[29]	Phe[86]
Thr[35]	Arg[104]	Glu[35]	Arg[103]
Glu[55]	Asp[106]	Glu[55]	Asp[105]

Table 3. Components of the molecular mechanical potential energy of the intermolecular NGF/LRM-2A interactions (in kcal/mol)

Term	hNGF	mNGF		mNGFΔ3-9	hNGF:NT-4/5
E_w	-61.2	-57.9		-39.3	-65.1
E_e	-96.2	-87.9		-99.0	-65.2
E_{hb}	-7.4	-5.9	-3.1	-4.6	
E_{qq}	-0.3	-0.3	-0.1	-0.1	
Total	-165.1	-152.0		-141.5	-135.1

Table 4.   Components of the molecular mechanical potential energy of the BDNF/LRM-2B
and the NGF/LRM-2B complexes (in kcal/mol)

A. Components of the potential energy

	BDNF/LRM-2B	NGF/LRM-2B	Difference*
E_w	89.3	82.3	-7.0
E_{el}	-183.8	-93.1	**90.7**
E_{hb}	-31.0	-21.5	9.5
Et	114.9	114.0	-0.9
E_{qq}	0.4	0.0	-0.4
Total	-10.2	81.8	**92.0**

B. Components of the intermolecular interactions energy

	BDNF/LRM-2B	NGF/LRM-2B	Difference*
E_w	-48.0	-64.9	-16.9
E_{el}	-221.4	-144.2	**77.2**
E_{hb}	-5.6	-4.3	1.3
Total	-275.0	-213.5	61.5

*Difference of the energy terms within the minimum-energy structures of the NGF/LRM-2B
and the BDNF/LRM-2B complexes. Underlined values demonstrate that the difference in
intermolecular electrostatic interactions dominates in the differences in potential energies of
the complexes.

Table 5. Equilibrium variable torsional angles (in degrees) of the amino and carboxyl termini of the most stable conformations of the uncomplexed (UC) and complexed (C) NGF analogues.*

No.			hNGF UC	C		mNGF UC	C		mNGFΔ3-9 UC	C
						Amino terminus				
11	ψ	E	82.9	78.2	E	85.9	85.4	E	89.2	96.6
	ϕ		55.7	60.3		56.3	56.3		57.8	60.3
	χ_1		-69.8	-69.3		-72.0	-69.4		-72.1	-73.7
	χ_2		72.7	70.2		71.7	71.3		66.0	67.0
	χ_3		-120.4	-117.6		-111.7	-117.1		-107.0	-109.2
10	ψ	G	-89.1	-122.1	G	-95.1	-103.2	G	-88.0	-94.8
	ϕ		-172.5	-166.5		-178.6	174.1		-177.5	168.7
9	ψ	R	-36.1	-25.7	M	-21.1	-14.3	S	146.5	166.1
	ϕ		-92.8	-84.2		-91.4	-77.3		-103.6	-132.1
	χ_1		-77.2	-92.9		-75.2	-84.9		**-66.7**	**-179.1**
	χ_2		-173.9	-174.1		-179.7	179.0		**64.0**	**122.2**
	χ_3		-175.5	158.1		179.9	171.5		-	-
	χ_4		134.3	136.4		-	-		-	-
8	ψ	H	118.6	98.3	H	110.4	96.1	S	106.1	**156.1**
	ϕ		-116.5	-127.3		-110.4	-121.8		52.8	46.0
	χ_1		-89.7	-108.0		-90.9	-104.1		-45.9	-35.5
	χ_2		-73.8	-87.9		-71.5	-65.8		-172.3	-174.1
7	ψ	F	135.7	113.6	F	129.4	106.7		-	-
	ϕ		**-68.8**	**-122.4**		**-89.0**	**-130.8**		-	-
	χ_1		-171.6	-147.2		-163.9	-143.9		-	-
	χ_2		-96.3	-85.8		-91.5	-87.5		-	-
6	ψ	I	40.3	57.9	V	61.7	67.9		-	-
	ϕ		40.4	38.5		47.7	48.3		-	-
	χ_1		-159.7	-165.7		-177.3	-177.3		-	-
	χ_2		87.1	88.3		-	-		-	-
5	ψ	P	156.0	164.8	P	149.8	153.3		-	-

59

4		ψ	H	121.4	125.4	H	122.1	122.9	-	-	
		φ		-129.2	-133.8		-129.8	-125.9	-	-	
		χ1		-162.5	-163.2		-163.3	-161.8	-	-	
		χ2		-69.1	-71.9		-69.2	-69.9	-	-	
5	3	ψ	S	2.1	-4.9	T	-1.9	-5.1	-	-	
		φ		-91.9	-78.9		-84.5	-82.3	-	-	
		χ1		-171.8	-172.3		-174.9	-171.4	-	-	
		χ2		-53.2	-51.2		-51.2	-52.3	-	-	
	2	ψ	S	138.5	135.7	S	139.4	139.4	-	-	
10		φ		**-128.9**	**-157.5**		**-114.1**	**-160.3**	-	-	
		χ1		173.3	173.4		169.7	170.3	-	-	
		χ2		-141.9	-133.0		-139.8	-134.5	-	-	
	1	ψ	S	133.0	129.5	S	127.9	128.6	-	-	
		φ		48.6	46.6		49.4	53.8	-	-	
15		χ1		-43.2	-41.9		-44.1	-44.0	-	-	
		χ2		-171.5	-171.0		-172.4	-170.9	-	-	

Carboxyl terminus

20	112'	φ	L	-113.3	-113.1	L	-113.0	-114.1	L	-112.4	-113.7
		ψ		98.8	95.5		98.7	99.3		99.2	103.9
		χ1		-72.3	-72.1		-71.6	-72.1		-71.6	-72.1
		χ2		163.7	163.2		163.0	164.1		162.6	163.8
	113'	φ	S	-83.4	-72.5	S	-77.2	-70.5	S	-77.4	-63.0
25		ψ		136.1	147.9		146.0	148.6		143.5	145.8
		χ1		177.0	179.1		179.4	-177.9		176.3	-177.0
		χ2		65.2	56.0		60.6	56.3		59.0	52.4
	114'	φ	R	-66.7	-101.6	R	-71.5	-92.5	R	-78.0	-92.3
		ψ		-47.0	-41.9		-53.7	-43.8		-59.3	-50.4
30		χ1		**-99.1**	**-175.3**		**-145.6**	**-173.2**		**-93.4**	**-167.4**
		χ2		**-173.1**	**-130.0**		**-179.8**	**-114.8**		**-171.5**	**-101.4**
		χ3		170.4	159.9		-173.6	151.4		-172.9	172.3
		χ4		138.4	-117.4		140.3	-139.0		141.5	-130.9
	115'	φ	K	-163.2	-155.3	K	-162.1	-152.2	K	-167.1	-161.4
35		ψ		110.6	111.2		132.0	111.0		153.3	132.6

60

		$\chi 1$		-139.8	-150.7		-143.3	-156.2		-140.1	-144.6
		$\chi 2$		**78.7**	**-170.9**		**81.7**	**-170.0**		**85.0**	**-177.7**
		$\chi 3$		**-96.4**	**177.2**		**-97.9**	**-174.3**		**-95.8**	**-169.3**
		$\chi 4$		**129.5**	**-165.4**		120.9	**-173.7**		131.0	175.4
5		$\chi 5$		-39.1	-63.2		-35.6	-61.4		-47.7	-53.3
	116'	ϕ	A	-60.5	-62.3	A	-69.6	-61.7	A	-58.2	-67.9
		ψ		-47.5	-43.9		-40.7	-47.8		-47.5	-40.4
	117'	ϕ	V	-71.8	-106.1	T	-85.5	-106.0	T	-64.6	-74.3
		ψ		112.0	107.0		116.4	98.5		108.2	107.7
10		$\chi 1$		-74.3	-75.0		53.4	55.1		50.9	56.6
		$\chi 2$		-	-		60.5	63.2		58.0	54.0
	118'	ϕ	R	-93.8	-58.0	R	**-118.2**	**-58.4**	R	-58.5	-79.4
		ψ		-57.9	-53.7		-48.4	-59.7		-37.6	-49.6
		$\chi 1$		-104.3	-88.5		-80.9	-84.7		-109.5	-135.3
15		$\chi 2$		79.1	74.4		109.1	79.7		73.3	108.0
		$\chi 3$		147.7	161.4		116.1	147.5		-76.3	-70.1
		$\chi 4$		147.0	119.7		116.1	118.7		-87.2	-135.3

20   *Torsional angles are designated according to the IUPAC-IUB rules (1970). Torsional angles undergoing considerable changes upon LRM-2A binding are shown in bold.

61

Table 6. Optimized conformational variables (in degrees) of hNGF-complexed LRM-2A.*

	No.	Type	ϕ	ψ	χ^1	χ^2	χ^3	χ^4	χ^5
5	94tA	Arg	-161.6	-62.5	-169.2	-164.9	66.8	172.2	
	95tA	Asn	-114.1	132.0	33.0	-111.6			
	96tA	Leu	-131.9	114.2	-161.2	141.1			
	97tA	Thr	-145.0	125.0	-179.9	-176.6			
	98tA	Ile	-123.1	21.6	61.3	105.7			
10	99tA	Val	-61.2	107.3	175.7				
	100tA	Lys	54.4	40.8	-75.6	161.7	-174.8	166.2	-41.3
	101tA	Ser	-97.4	-40.0	-176.4	167.7			
	102tA	Gly	144.4	46.5					
	103tA	Leu	-135.6	155.5	-85.0	90.0			
15	104tA	Arg	-81.7	179.3	-33.6	165.0	-52.8	-144.7	
	105tA	Phe	-68.6	-40.8	-159.4	93.3			
	106tA	Val	-106.1	94.3	176.1				
	107tA	Ala	-173.5	-54.8					
	108tA	Pro		-26.2					
20	109tA	Asp	-85.5	64.7	-116.1	102.8			
	110tA	Ala	-117.5	-57.2					
	111tA	Phe	-79.4	135.3	38.4	89.8			
	112tA	His	-132.1	78.5	-67.1	89.9			
	113tA	Phe	-120.8	-29.0	54.6	95.4			
25	114tA	Thr	-59.9	-56.0	-23.4	-176.5			
	115tA	Pro		-47.9					
	116tA	Arg	-150.8	142.7	46.8	98.5	-100.4	155.7	
	117tA	Leu	-76.3	-39.4	57.0	117.9			

30 *Torsional angles are designated according to the IUPAC-IUB rules (1970).

62

Table 7. Optimized conformational variables (in degrees) of BDNF-complexed LRM-2B.*

No.	Type	ϕ	ψ	χ^1	χ^2	χ^3	χ^4	χ^5
94tB	Arg	-109.3	-54.2	-69.7	169.4	-171.6	119.4	
95tB	Asn	-163.6	141.0	-129.4	-109.4			
96tB	Leu	-81.9	86.5	-92.9	-58.2			
97tB	Thr	-138.3	143.5	-177.9	169.6			
98tB	Ile	-136.4	136.6	-164.6	86.9			
99tB	Val	-107.6	151.8	-70.1				
100tB	Asp	-68.8	-72.8	23.6	95.2			
101tB	Ser	36.4	36.0	-156.1	157.6			
102tB	Gly	42.0	44.4					
103tB	Leu	-118.2	149.0	49.9	87.1			
104tB	Lys	-92.9	68.5	-147.2	173.5	91.3	-169.5	45.1
105tB	Phe	73.7	-78.5	-160.5	-111.0			
106tB	Val	52.6	19.9	-174.2				
107tB	Ala	-113.9	26.4					
108tB	Tyr	-58.7	-20.3	-46.5	102.7	-74.2		
109tB	Lys	-71.4	-27.6	62.1	-113.2	176.6	176.6	-55.9
110tB	Ala	-91.7	-32.6					
111tB	Phe	-63.5	-37.4	-168.3	83.6			
112tB	Leu	-60.3	-43.2	-169.7	91.0			
113tB	Lys	-61.5	-48.0	-78.9	152.7	-167.9	63.2	22.9
114tB	Asn	-59.4	-36.6	-70.9	-107.4			
115tB	Ser	-68.6	-32.9	-60.0	68.6			
116tB	Asn	-80.7	-45.4	-83.4	-96.8			
117tB	Leu	-127.8	-58.8	-75.6	105.5			

*Torsional angles are designated according to the IUPAC-IUB rules (1970).

Table 8.   Contributions of individual residues to intermolecular electrostatic interaction energies of the complexes BDNF/LRM-2B and NGF/LRM-2B (in kcal/mol)*.

A. Binding epitopes of neurotrophins

	BDNF/LRM-2B		NGF/LRM-2B		Difference‡
5	Glu^{18}	-61.6	Val^{18}	0.3	61.9
	Asp^{24}	-65.1	Asp^{24}	-44.9	20.2
	Lys^{25}	25.3	Lys25	15.5	-9.8
	Gly^{33}	-11.9	Gly^{33}	-13.4	-1.5
	Thr^{35}	-11.4	Glu^{35}	-50.5	-39.1
10	Glu^{55}	-50.2	Glu^{55}	-18.9	31.3
	Lys^{57}	27.1	Lys^{57}	22.5	-4.6
	Arg^{81}	-32.2	Thr^{81}	0.1	32.3
	Gln^{84}	1.2	His^{84}	11.5	10.3
	Arg^{104}	-14.3	Arg^{103}	-9.5	4.8
15	Asp^{106}	-39.7	Asp^{105}	-46.4	-6.7
	Total	-232.8		-133.7	99.1

B. Binding epitopes of the LRM-2B

	BDNF/LRM-2B		NGF/LRM-2B	Difference‡
20	Arg^{94tB}	-40.9	4.2	45.1
	Asn^{95tB}	0.2	-12.8	-13.0
	Asp^{100tB}	-42.1	-9.3	32.8
	Ser^{101tB}	-17.9	-0.1	17.8
25	Gly^{102tB}	-1.3	-12.0	-10.7
	Lys^{104tB}	-18.5	-48.1	-29.6
	Lys^{109tB}	-46.4	-21.5	24.9
	Lys^{113tB}	-54.6	-37.2	17.4
30	Total	-221.5	-136.8	84.7

*The ±10 kcal/mol cutoff of intermolecular electrostatic interaction energy has been used to identify binding epitopes within the complexes. ‡Difference of the intermolecular electrostatic interaction energies of the given residue within the minimum-energy structures of the NGF/LRM-2B and the BDNF/LRM-2B complexes. Residues within the binding epitopes of BDNF and the LRM-2B which cause their binding specificity are bolded.

Table 9. Contributions of individual residues of the neurotrophins to the intermolecular interaction energy of their complexes with the common neurotrophin receptor p75[NTR] (kcal/mol)*

NGF			BDNF			NT-3			NT-4/5		
Res.	EL	VDW	Res.	EL	VDW	Res.	EL	VDW	Res.	EL	VDW
D-30	17.9	-0.9	**D-30**	25.0	-1.8	**D-29**	24.6	-2.6	**D-32**	19.8	-1.8
K-32	-94.9	-6.0	S-32	0.5	-4.5	**R-31**	-48.2	-8.0	**R-34**	-42.6	-9.3
K-34	-88.8	-3.3	G-34	-1.8	-3.1	**H-33**	-35.0	-7.1	**R-36**	-57.2	-7.7
E-35	-10.0	-2.2	T-35	1.7	-1.4	Q-34	0.5	-2.3	D-37	-0.8	-1.7
H-84	-30.9	-1.0	Q-84	1.19	-2.4	Q-83	0.8	-0.7	Q-83	0.6	-1.0
F-86	-0.2	-0.3	Y-86	-0.5	-0.5	**Y-85**	-13.4	0.3	Y-96	-9.2	-0.3
K-88	-8.5	-0.1	**R-88**	-12.7	-0.2	**R-87**	-20.0	-0.3	**R-98**	-16.2	-0.2
D-93	-9.0	-1.3	**D-93**	13.7	-2.2	**E-92**	24.1	-2.8	D-103	9.0	-2.1
K-95	-63.7	-5.6	**K-95**	-82.9	-7.6	N-94	-0.1	-0.2	Q-105	-0.3	-0.2
Q-96	-0.3	-3.7	**K-96**	-58.2	2.0	**K-95**	-49.6	-2.6	G-106	-0.6	-0.6
A-97	0.2	-0.2	**R-97**	-79.3	-5.7	L-96	-0.5	-6.7	**R-107**	-28.0	-11.2
R-100	-11.8	-0.7	**R-101**	-59.2	-1.1	**R-100**	-79.3	1.7	**R-111**	-57.8	-1.9
R-103	-64.5	0.0	**R-104**	-64.2	-1.6	**R-103**	-51.5	0.6	**R-114**	-55.3	-2.9
D-105	10.6	-0.2	D-106	8.3	-0.2	D-105	5.5	-0.1	D-116	4.8	-0.1
Total	-336.1	-15.6		-317.8	-18.2		-248.3	-15.6		-237.3	-35.0
	100%	55%		99%	39%		97%	32%		102%	61%
Net	-337.3	-32.3		-321.4	-46.7		-254.8	-48.9		-233.0	-57.5

*EL and VDW denote electrostatic and van der Waals terms of the ligand-receptor interaction energy, respectively. The ±10 kcal/mol cutoff of the intermolecular electrostatic interaction energy has been used to identify the functional epitopes (bolded). "Total" electrostatic and van der Waals contributions of the functional epitopes to the "net" values of the intermolecular interaction energy calculated over the whole binding interface are presented. Residue numbering corresponds to the general alignment of neurotrophins (Bradshaw et al., 1994).

Table 10. Contributions of individual residues of p75[NTR] to the intermolecular interaction energy of their complexes with neurotrophins (kcal/mol)*.

NGF			BDNF			NT-3			NT-4/5		
Res.	EL	VDW	Res.	EL	VDW	Res.	EL	VDW	Res.	EL	VDW
D-47	-46.0	0.2	D-47	-67.1	0.1	D-47	-50.5	-0.3	D-47	-26.7	-4.1
E-53	-2.6	-0.2	E-53	-55.4	1.6	E-53	-6.6	-0.2	E-53	-3.6	-0.1
P-54	-12.4	-2.8	P-54	-13.5	-2.5	P-54	-15.1	0.2	P-54	-5.3	-0.8
C-55	-1.4	-0.9	C-55	-8.4	-1.3	C-55	-14.9	-1.0	C-55	-3.0	-1.2
K-56	21.8	-4.5	K-56	13.2	-4.8	K-56	32.9	-5.0	K-56	14.8	-5.8
E-60	-6.2	-0.3	E-60	-3.0	-0.1	E-60	-10.0	-0.2	E-60	-10.4	-0.4
E-73	-4.2	0.0	E-73	-9.7	-0.2	E-73	-12.5	-0.3	E-73	-11.2	-0.3
D-75	-56.5	0.6	D-75	-77.1	0.4	D-75	-65.5	-1.1	D-75	-59.4	-2.7
D-76	-91.6	-2.0	D-76	-22.3	-8.4	D-76	-39.9	-3.7	D-76	-39.3	-5.1
R-80	-18.5	-3.9	R-80	2.9	-2.1	R-80	5.3	-4.0	R-80	3.1	-4.3
D-88	-49.1	0.4	D-88	-39.8	-0.4	D-88	-34.4	0.4	D-88	-33.1	-1.2
E-89	-32.5	-1.6	E-89	-25.2	-6.2	E-89	-33.8	-3.8	E-89	-33.0	-5.9
Total	-285.4	-13.6		-287.2	-20.2		-243.7	-14.8		-198.3	-25.5
	84%	42%		89%	43%		96%	30%		85%	44%

*See footnote to Table 9.

Appendix 1. Geometry of the LRM-2A in PDB format.*

REMARK   1 The bioactive conformation of the second LRM of TrkA.

REMARK   2   HSC stands for charged HIS

5   REMARK   3

ATOM	1 N	LEU S 93	19.399 -23.034 -15.306 1.00 -0.45
ATOM	2 CA	LEU S 93	18.757 -22.140 -14.332 1.00 -0.07
ATOM	3 C	LEU S 93	19.555 -20.869 -14.130 1.00 0.53
ATOM	4 O	LEU S 93	20.777 -20.864 -14.044 1.00 -0.50
ATOM	5 CB	LEU S 93	18.635 -22.886 -13.002 1.00 0.02
ATOM	6 CG	LEU S 93	17.661 -22.206 -12.037 1.00 0.05
ATOM	7 CD1	LEU S 93	16.251 -22.083 -12.617 1.00 -0.01
ATOM	8 CD2	LEU S 93	17.517 -22.968 -10.718 1.00 -0.01
ATOM	9 1H	LEU S 93	19.651 -23.930 -14.841 1.00 0.15
ATOM	10 2H	LEU S 93	18.742 -23.223 -16.089 1.00 0.15
ATOM	11 3H	LEU S 93	20.260 -22.582 -15.677 1.00 0.15
ATOM	12 N	ARG S 94	18.551 -20.159 -13.624 1.00 -0.52
ATOM	13 CA	ARG S 94	18.777 -19.044 -12.708 1.00 0.24
ATOM	14 C	ARG S 94	17.460 -18.800 -12.010 1.00 0.53
ATOM	15 O	ARG S 94	17.364 -18.941 -10.781 1.00 -0.50
ATOM	16 CB	ARG S 94	19.316 -17.812 -13.451 1.00 0.05
ATOM	17 CG	ARG S 94	19.818 -16.700 -12.515 1.00 0.06
ATOM	18 CD	ARG S 94	20.009 -15.345 -13.215 1.00 0.11
ATOM	19 NE	ARG S 94	18.720 -14.803 -13.642 1.00 -0.49
ATOM	20 CZ	ARG S 94	18.631 -13.550 -14.138 1.00 0.81
ATOM	21 NH1	ARG S 94	19.703 -12.767 -14.256 1.00 -0.63
ATOM	22 NH2	ARG S 94	17.444 -13.087 -14.518 1.00 -0.63
ATOM	23 H	ARG S 94	17.611 -20.389 -13.873 1.00 0.25
ATOM	24 HE	ARG S 94	17.892 -15.358 -13.571 1.00 0.29
ATOM	25 1HH1	ARG S 94	19.604 -11.843 -14.627 1.00 0.36
ATOM	26 2HH1	ARG S 94	20.606 -13.094 -13.977 1.00 0.36
ATOM	27 1HH2	ARG S 94	17.363 -12.161 -14.887 1.00 0.36
ATOM	28 2HH2	ARG S 94	16.633 -13.666 -14.434 1.00 0.36
ATOM	29 N	ASN S 95	16.446 -18.435 -12.789 1.00 -0.52
ATOM	30 CA	ASN S 95	15.116 -18.165 -12.251 1.00 0.22
ATOM	31 C	ASN S 95	14.111 -19.178 -12.745 1.00 0.53

	ATOM	32	O	ASN S 95	14.047	-19.466	-13.950	1.00	-0.50
	ATOM	33	CB	ASN S 95	14.629	-16.742	-12.566	1.00	0.00
	ATOM	34	CG	ASN S 95	15.171	-16.300	-13.911	1.00	0.68
	ATOM	35	OD1	ASN S 95	16.007	-15.410	-13.997	1.00	-0.47
5	ATOM	36	ND2	ASN S 95	14.657	-16.965	-14.959	1.00	-0.87
	ATOM	37	H	ASN S 95	16.591	-18.340	-13.774	1.00	0.25
	ATOM	38	1HD2	ASN S 95	14.948	-16.750	-15.892	1.00	0.34
	ATOM	39	2HD2	ASN S 95	13.976	-17.684	-14.820	1.00	0.34
	ATOM	**40**	**N**	**LEU S 96**	**13.325**	**-19.720**	**-11.819**	**1.00**	**-0.52**
10	ATOM	41	CA	LEU S 96	12.308	-20.713	-12.151	1.00	0.20
	ATOM	**42**	**C**	**LEU S 96**	**11.023**	**-20.296**	**-11.479**	**1.00**	**0.53**
	ATOM	**43**	**O**	**LEU S 96**	**10.934**	**-20.287**	**-10.242**	**1.00**	**-0.50**
	ATOM	44	CB	LEU S 96	12.767	-22.109	-11.701	1.00	0.02
	ATOM	45	CG	LEU S 96	12.022	-23.268	-12.383	1.00	0.05
15	ATOM	46	CD1	LEU S 96	12.921	-24.464	-12.732	1.00	-0.01
	ATOM	47	CD2	LEU S 96	10.797	-23.704	-11.562	1.00	-0.01
	ATOM	**48**	**H**	**LEU S 96**	**13.428**	**-19.444**	**-10.863**	**1.00**	**0.25**
	ATOM	49	N	THR S 97	10.026	-19.951	-12.289	1.00	-0.52
	ATOM	50	CA	THR S 97	8.726	-19.526	-11.778	1.00	0.27
20	ATOM	51	C	THR S 97	7.604	-19.988	-12.678	1.00	0.53
	ATOM	52	O	THR S 97	7.607	-19.702	-13.884	1.00	-0.50
	ATOM	53	CB	THR S 97	8.692	-18.000	-11.598	1.00	0.21
	ATOM	54	OG1	THR S 97	7.420	-17.594	-11.097	1.00	-0.55
	ATOM	55	CG2	THR S 97	9.014	-17.248	-12.899	1.00	0.01
25	ATOM	56	H	THR S 97	10.163	-19.980	-13.279	1.00	0.25
	ATOM	57	HG1	THR S 97	7.431	-16.635	-11.053	1.00	0.31
	ATOM	**58**	**N**	**ILE S 98**	**6.645**	**-20.701**	**-12.095**	**1.00**	**-0.52**
	ATOM	59	CA	ILE S 98	5.499	-21.213	-12.841	1.00	0.20
	ATOM	60	C	ILE S 98	4.166	-20.765	-12.292	1.00	0.53
30	ATOM	61	O	ILE S 98	3.134	-21.406	-12.544	1.00	-0.50
	ATOM	62	CB	ILE S 98	5.633	-22.735	-13.006	1.00	0.03
	ATOM	63	CG1	ILE S 98	5.655	-23.480	-11.662	1.00	0.02
	ATOM	64	CG2	ILE S 98	6.841	-23.109	-13.880	1.00	0.00
	ATOM	65	CD1	ILE S 98	4.338	-24.216	-11.369	1.00	0.00
35	**ATOM**	**66**	**H**	**ILE S 98**	**6.703**	**-20.897**	**-11.116**	**1.00**	**0.25**
	ATOM	67	N	VAL S 99	4.183	-19.667	-11.541	1.00	-0.52

68

	ATOM	68	CA	VAL	S 99	2.969	-19.119	-10.945	1.00	0.20
	ATOM	69	C	VAL	S 99	1.976	-18.727	-12.013	1.00	0.53
	ATOM	70	O	VAL	S 99	2.172	-17.725	-12.717	1.00	-0.50
	ATOM	71	CB	VAL	S 99	3.389	-17.945	-10.045	1.00	0.03
5	ATOM	72	CG1	VAL	S 99	2.188	-17.207	-9.432	1.00	0.01
	ATOM	73	CG2	VAL	S 99	4.444	-18.324	-8.993	1.00	0.01
	ATOM	74	H	VAL	S 99	5.050	-19.197	-11.376	1.00	0.25
	ATOM	75	N	LYS	S 100	0.911	-19.514	-12.136	1.00	-0.52
	ATOM	76	CA	LYS	S 100	-0.131	-19.257	-13.126	1.00	0.23
10	ATOM	77	C	LYS	S 100	0.517	-19.154	-14.486	1.00	0.53
	ATOM	78	O	LYS	S 100	0.146	-18.291	-15.296	1.00	-0.50
	ATOM	79	CB	LYS	S 100	-0.916	-17.989	-12.753	1.00	0.04
	ATOM	80	CG	LYS	S 100	-1.911	-18.178	-11.597	1.00	0.05
	ATOM	81	CD	LYS	S 100	-2.337	-16.845	-10.961	1.00	0.05
15	ATOM	82	CE	LYS	S 100	-3.230	-17.043	-9.726	1.00	0.22
	ATOM	83	NZ	LYS	S 100	-3.328	-15.780	-8.983	1.00	-0.27
	ATOM	84	H	LYS	S 100	0.814	-20.308	-11.536	1.00	0.25
	ATOM	85	1HZ	LYS	S 100	-2.395	-15.321	-8.953	1.00	0.31
	ATOM	86	2HZ	LYS	S 100	-3.649	-15.972	-8.012	1.00	0.31
20	ATOM	87	3HZ	LYS	S 100	-4.008	-15.150	-9.454	1.00	0.31
	ATOM	88	N	SER	S 101	1.485	-20.030	-14.739	1.00	-0.52
	ATOM	89	CA	SER	S 101	2.199	-20.048	-16.012	1.00	0.36
	ATOM	90	C	SER	S 101	1.652	-21.075	-16.974	1.00	0.53
	ATOM	91	O	SER	S 101	1.546	-20.813	-18.182	1.00	-0.50
25	ATOM	92	CB	SER	S 101	3.695	-20.297	-15.758	1.00	0.19
	ATOM	93	OG	SER	S 101	4.426	-20.237	-16.981	1.00	-0.55
	ATOM	94	H	SER	S 101	1.736	-20.701	-14.041	1.00	0.25
	ATOM	95	HG	SER	S 101	5.354	-20.203	-16.738	1.00	0.31
	ATOM	96	N	GLY	S 102	1.302	-22.243	-16.444	1.00	-0.52
30	ATOM	97	CA	GLY	S 102	0.758	-23.329	-17.254	1.00	0.25
	ATOM	98	C	GLY	S 102	1.148	-24.732	-16.854	1.00	0.53
	ATOM	99	O	GLY	S 102	1.526	-25.548	-17.708	1.00	-0.50
	ATOM	100	H	GLY	S 102	1.413	-22.390	-15.461	1.00	0.25
	ATOM	101	N	LEU	S 103	1.058	-25.015	-15.558	1.00	-0.52
35	ATOM	102	CA	LEU	S 103	1.402	-26.331	-15.027	1.00	0.20
	ATOM	103	C	LEU	S 103	0.326	-26.726	-14.045	1.00	0.53

69

	ATOM	104	O	LEU S 103	-0.356 -25.860 -13.476 1.00 -0.50
	ATOM	105	CB	LEU S 103	2.792 -26.289 -14.372 1.00 0.02
	ATOM	106	CG	LEU S 103	3.957 -26.492 -15.354 1.00 0.05
	ATOM	107	CD1	LEU S 103	4.502 -25.183 -15.949 1.00 -0.01
5	ATOM	108	CD2	LEU S 103	5.078 -27.333 -14.723 1.00 -0.01
	ATOM	109	H	LEU S 103	0.745 -24.311 -14.920 1.00 0.25
	ATOM	110	N	ARG S 104	0.170 -28.031 -13.843 1.00 -0.52
	ATOM	111	CA	ARG S 104	-0.832 -28.558 -12.921 1.00 0.24
	ATOM	112	C	ARG S 104	-0.225 -28.464 -11.541 1.00 0.53
10	ATOM	113	O	ARG S 104	0.920 -28.016 -11.387 1.00 -0.50
	ATOM	114	CB	ARG S 104	-1.253 -29.984 -13.311 1.00 0.05
	ATOM	115	CG	ARG S 104	-1.250 -30.233 -14.827 1.00 0.06
	ATOM	116	CD	ARG S 104	-1.308 -31.721 -15.207 1.00 0.11
	ATOM	117	NE	ARG S 104	-0.254 -32.467 -14.521 1.00 -0.49
15	ATOM	118	CZ	ARG S 104	0.365 -33.502 -15.129 1.00 0.81
	ATOM	119	NH1	ARG S 104	0.042 -33.880 -16.366 1.00 -0.63
	ATOM	120	NH2	ARG S 104	1.319 -34.159 -14.478 1.00 -0.63
	ATOM	121	H	ARG S 104	0.754 -28.678 -14.334 1.00 0.25
	ATOM	122	HE	ARG S 104	0.018 -32.215 -13.592 1.00 0.29
20	ATOM	123	1HH1	ARG S 104	0.519 -34.651 -16.789 1.00 0.36
	ATOM	124	2HH1	ARG S 104	-0.672 -33.401 -16.875 1.00 0.36
	ATOM	125	1HH2	ARG S 104	1.786 -34.927 -14.915 1.00 0.36
	ATOM	126	2HH2	ARG S 104	1.569 -33.884 -13.549 1.00 0.36
	ATOM	127	N	PHE S 105	-0.990 -28.886 -10.538 1.00 -0.52
25	ATOM	128	CA	PHE S 105	-0.535 -28.854 -9.152 1.00 0.21
	ATOM	129	C	PHE S 105	0.558 -29.894 -9.090 1.00 0.53
	ATOM	130	O	PHE S 105	1.596 -29.679 -8.447 1.00 -0.50
	ATOM	131	CB	PHE S 105	-1.656 -29.230 -8.170 1.00 0.04
	ATOM	132	CG	PHE S 105	-1.354 -28.726 -6.778 1.00 0.01
30	ATOM	133	CD1	PHE S 105	-1.851 -27.471 -6.366 1.00 -0.01
	ATOM	134	CD2	PHE S 105	-0.575 -29.526 -5.913 1.00 -0.01
	ATOM	135	CE1	PHE S 105	-1.566 -27.007 -5.067 1.00 0.00
	ATOM	136	CE2	PHE S 105	-0.290 -29.063 -4.616 1.00 0.00
	ATOM	137	CZ	PHE S 105	-0.788 -27.809 -4.206 1.00 0.00
35	ATOM	138	H	PHE S 105	-1.906 -29.236 -10.732 1.00 0.25
	ATOM	139	N	VAL S 106	0.329 -31.021 -9.758 1.00 -0.52

70

	ATOM	140	CA	VAL S 106	1.297	-32.114	-9.787	1.00	0.20
	ATOM	141	C	VAL S 106	1.984	-32.186	-11.130	1.00	0.53
	ATOM	142	O	VAL S 106	1.469	-32.815	-12.067	1.00	-0.50
	ATOM	143	CB	VAL S 106	0.545	-33.403	-9.418	1.00	0.03
5	ATOM	144	CG1	VAL S 106	1.433	-34.654	-9.506	1.00	0.01
	ATOM	145	CG2	VAL S 106	-0.212	-33.313	-8.084	1.00	0.01
	ATOM	146	H	VAL S 106	-0.530	-31.131	-10.258	1.00	0.25
	ATOM	147	N	ALA S 107	3.145	-31.545	-11.226	1.00	-0.52
	ATOM	148	CA	ALA S 107	3.920	-31.529	-12.463	1.00	0.22
10	ATOM	149	C	ALA S 107	5.237	-30.854	-12.163	1.00	0.53
	ATOM	150	O	ALA S 107	6.308	-31.425	-12.415	1.00	-0.50
	ATOM	151	CB	ALA S 107	3.199	-30.751	-13.576	1.00	0.03
	ATOM	152	H	ALA S 107	3.504	-31.056	-10.432	1.00	0.25
	ATOM	153	N	PRO S 108	5.161	-29.640	-11.625	1.00	-0.26
15	ATOM	154	CA	PRO S 108	6.351	-28.871	-11.283	1.00	0.11
	ATOM	155	C	PRO S 108	7.264	-29.638	-10.357	1.00	0.53
	ATOM	156	O	PRO S 108	8.481	-29.403	-10.336	1.00	-0.50
	ATOM	157	CB	PRO S 108	5.782	-27.574	-10.686	1.00	0.00
	ATOM	158	CG	PRO S 108	4.356	-27.900	-10.256	1.00	0.04
20	ATOM	159	CD	PRO S 108	3.932	-28.917	-11.305	1.00	0.08
	ATOM	160	N	ASP S 109	6.680	-30.556	-9.591	1.00	-0.52
	ATOM	161	CA	ASP S 109	7.439	-31.374	-8.649	1.00	0.25
	ATOM	162	C	ASP S 109	7.956	-32.544	-9.451	1.00	0.53
	ATOM	163	O	ASP S 109	7.574	-33.697	-9.200	1.00	-0.50
25	ATOM	164	CB	ASP S 109	6.510	-31.884	-7.536	1.00	-0.21
	ATOM	165	CG	ASP S 109	6.933	-31.318	-6.195	1.00	0.62
	ATOM	166	OD1	ASP S 109	6.290	-30.391	-5.711	1.00	-0.71
	ATOM	167	OD2	ASP S 109	7.907	-31.800	-5.626	1.00	-0.71
	ATOM	168	H	ASP S 109	5.692	-30.697	-9.657	1.00	0.25
30	ATOM	169	N	ALA S 110	8.824	-32.252	-10.416	1.00	-0.52
	ATOM	170	CA	ALA S 110	9.406	-33.282	-11.270	1.00	0.22
	ATOM	171	C	ALA S 110	10.898	-33.275	-11.034	1.00	0.53
	ATOM	172	O	ALA S 110	11.481	-34.304	-10.662	1.00	-0.50
	ATOM	173	CB	ALA S 110	9.132	-33.009	-12.758	1.00	0.03
35	ATOM	174	H	ALA S 110	9.090	-31.300	-10.566	1.00	0.25
	ATOM	175	N	PHE S 111	11.517	-32.118	-11.249	1.00	-0.52

71

	ATOM	176	CA	PHE S 111	12.956	-31.964	-11.061	1.00	0.21
	ATOM	177	C	PHE S 111	13.127	-31.810	-9.568	1.00	0.53
	ATOM	178	O	PHE S 111	12.376	-31.064	-8.923	1.00	-0.50
	ATOM	179	CB	PHE S 111	13.497	-30.712	-11.770	1.00	0.04
5	ATOM	180	CG	PHE S 111	12.526	-29.559	-11.656	1.00	0.01
	ATOM	181	CD1	PHE S 111	12.618	-28.673	-10.561	1.00	-0.01
	ATOM	182	CD2	PHE S 111	11.542	-29.391	-12.654	1.00	-0.01
	ATOM	183	CE1	PHE S 111	11.710	-27.601	-10.462	1.00	0.00
	ATOM	184	CE2	PHE S 111	10.634	-28.321	-12.556	1.00	0.00
10	ATOM	185	CZ	PHE S 111	10.727	-27.436	-11.461	1.00	0.00
	ATOM	186	H	PHE S 111	10.987	-31.324	-11.549	1.00	0.25
	ATOM	187	N	HSC S 112	14.112	-32.515	-9.019	1.00	-0.52
	ATOM	188	H	HSC S 112	14.681	-33.099	-9.597	1.00	0.25
	ATOM	189	CA	HSC S 112	14.393	-32.465	-7.587	1.00	0.19
15	ATOM	190	CB	HSC S 112	13.775	-33.685	-6.885	1.00	0.21
	ATOM	191	CG	HSC S 112	12.263	-33.637	-6.920	1.00	0.10
	ATOM	192	CD2	HSC S 112	11.396	-33.062	-5.986	1.00	0.35
	ATOM	193	ND1	HSC S 112	11.533	-34.176	-7.915	1.00	-0.61
	ATOM	194	HD1	HSC S 112	11.881	-34.643	-8.703	1.00	0.48
20	ATOM	195	CE1	HSC S 112	10.215	-33.947	-7.619	1.00	0.72
	ATOM	196	NE2	HSC S 112	10.132	-33.262	-6.434	1.00	-0.69
	ATOM	197	HE2	HSC S 112	9.308	-32.971	-5.991	1.00	0.49
	ATOM	198	C	HSC S 112	15.841	-32.262	-7.208	1.00	0.53
	ATOM	199	O	HSC S 112	16.534	-33.221	-6.836	1.00	-0.50
25	ATOM	200	N	PHE S 113	16.299	-31.017	-7.301	1.00	-0.52
	ATOM	201	CA	PHE S 113	17.678	-30.673	-6.967	1.00	0.21
	ATOM	202	C	PHE S 113	17.554	-29.654	-5.860	1.00	0.53
	ATOM	203	O	PHE S 113	18.444	-29.545	-5.003	1.00	-0.50
	ATOM	204	CB	PHE S 113	18.418	-30.047	-8.160	1.00	0.04
30	ATOM	205	CG	PHE S 113	17.666	-28.854	-8.702	1.00	0.01
	ATOM	206	CD1	PHE S 113	18.011	-27.554	-8.270	1.00	-0.01
	ATOM	207	CD2	PHE S 113	16.627	-29.064	-9.635	1.00	-0.01
	ATOM	208	CE1	PHE S 113	17.306	-26.447	-8.780	1.00	0.00
	ATOM	209	CE2	PHE S 113	15.922	-27.959	-10.145	1.00	0.00
35	ATOM	210	CZ	PHE S 113	16.268	-26.661	-9.712	1.00	0.00

72

	ATOM	211 H	PHE S 113	15.686 -30.289 -7.608 1.00 0.25
	ATOM	212 N	THR S 114	16.454 -28.908 -5.874 1.00 -0.52
	ATOM	213 CA	THR S 114	16.200 -27.883 -4.866 1.00 0.27
	ATOM	214 C	THR S 114	16.150 -28.477 -3.478 1.00 0.53
5	ATOM	215 O	THR S 114	16.898 -28.053 -2.585 1.00 -0.50
	ATOM	216 CB	THR S 114	14.903 -27.124 -5.185 1.00 0.21
	ATOM	217 OG1	THR S 114	14.606 -27.224 -6.576 1.00 -0.55
	ATOM	218 CG2	THR S 114	14.967 -25.648 -4.762 1.00 0.01
	ATOM	219 H	THR S 114	15.774 -29.046 -6.595 1.00 0.25
10	ATOM	220 HG1	THR S 114	13.824 -26.691 -6.734 1.00 0.31
	ATOM	221 N	PRO S 115	15.270 -29.457 -3.296 1.00 -0.26
	ATOM	222 CA	PRO S 115	15.113 -30.124 -2.008 1.00 0.11
	ATOM	223 C	PRO S 115	16.420 -30.691 -1.510 1.00 0.53
	ATOM	224 O	PRO S 115	16.789 -30.490 -0.343 1.00 -0.50
15	ATOM	225 CB	PRO S 115	14.024 -31.174 -2.277 1.00 0.00
	ATOM	226 CG	PRO S 115	14.008 -31.384 -3.788 1.00 0.04
	ATOM	227 CD	PRO S 115	14.364 -29.999 -4.305 1.00 0.08
	ATOM	228 N	ARG S 116	17.122 -31.399 -2.390 1.00 -0.52
	ATOM	229 CA	ARG S 116	18.405 -32.006 -2.048 1.00 0.24
20	ATOM	230 C	ARG S 116	19.201 -32.059 -3.330 1.00 0.53
	ATOM	231 O	ARG S 116	18.642 -32.307 -4.408 1.00 -0.50
	ATOM	232 CB	ARG S 116	18.212 -33.381 -1.388 1.00 0.05
	ATOM	233 CG	ARG S 116	17.213 -34.284 -2.128 1.00 0.06
	ATOM	234 CD	ARG S 116	17.881 -35.312 -3.055 1.00 0.11
25	ATOM	235 NE	ARG S 116	17.832 -34.856 -4.444 1.00 -0.49
	ATOM	236 CZ	ARG S 116	18.735 -35.300 -5.346 1.00 0.81
	ATOM	237 NH1	ARG S 116	19.694 -36.161 -5.009 1.00 -0.63
	ATOM	238 NH2	ARG S 116	18.663 -34.866 -6.600 1.00 -0.63
	ATOM	239 H	ARG S 116	16.767 -31.523 -3.317 1.00 0.25
30	ATOM	240 HE	ARG S 116	17.128 -34.209 -4.737 1.00 0.29
	ATOM	241 1HH1	ARG S 116	20.347 -36.471 -5.701 1.00 0.36
	ATOM	242 2HH1	ARG S 116	19.767 -36.501 -4.072 1.00 0.36
	ATOM	243 1HH2	ARG S 116	19.324 -35.186 -7.279 1.00 0.36
	ATOM	244 2HH2	ARG S 116	17.947 -34.219 -6.864 1.00 0.36
35	ATOM	245 N	LEU S 117	20.506 -31.828 -3.216 1.00 -0.52
	ATOM	246 CA	LEU S 117	21.399 -31.846 -4.370 1.00 0.23

73

```
     ATOM   247 C   LEU S 117      21.643 -33.299 -4.741  1.00  0.50
     ATOM   248 O   LEU S 117      21.687 -33.594 -5.933  1.00 -0.25
     ATOM   249 CB  LEU S 117      22.706 -31.110 -4.038  1.00  0.02
     ATOM   250 CG  LEU S 117      23.454 -31.672 -2.818  1.00  0.05
5    ATOM   251 CD1 LEU S 117      24.851 -32.222 -3.147  1.00 -0.01
     ATOM   252 CD2 LEU S 117      23.506 -30.647 -1.674  1.00 -0.01
     ATOM   253 OXT LEU S 117      21.785 -34.114 -3.834  1.00 -0.25
     ATOM   254 H   LEU S 117      20.894 -31.634 -2.315  1.00  0.25
     END
10   _____
```

*Principal residues are bolded.

SUBSTITUTE SHEET (RULE 26)

Appendix 2. Geometry of the LRM-2B in PDB format.*

REMARK   1 The bioactive conformation of the second LRM of TrkB.

REMARK   2

	ATOM	1	N	LEU S 93	-32.287	14.723	17.944	1.00 -0.45
5	ATOM	2	CA	LEU S 93	-33.186	15.831	17.679	1.00 -0.07
	ATOM	3	C	LEU S 93	-32.411	17.027	17.215	1.00 0.53
	ATOM	4	O	LEU S 93	-31.203	17.150	17.385	1.00 -0.50
	ATOM	5	CB	LEU S 93	-33.996	16.167	18.941	1.00 0.02
	ATOM	6	CG	LEU S 93	-35.339	15.426	19.042	1.00 0.05
10	ATOM	7	CD1	LEU S 93	-36.286	15.694	17.861	1.00 -0.01
	ATOM	8	CD2	LEU S 93	-35.131	13.920	19.266	1.00 -0.01
	ATOM	9	1H	LEU S 93	-31.777	14.490	17.116	1.00 0.15
	ATOM	10	2H	LEU S 93	-32.810	13.922	18.239	1.00 0.15
	ATOM	11	3H	LEU S 93	-31.641	14.971	18.665	1.00 0.15
15	ATOM	12	N	ARG S 94	-33.510	17.650	16.801	1.00 -0.52
	ATOM	13	CA	ARG S 94	-33.484	19.028	16.320	1.00 0.24
	ATOM	14	C	ARG S 94	-34.175	19.857	17.377	1.00 0.53
	ATOM	15	O	ARG S 94	-33.609	20.841	17.874	1.00 -0.50
	ATOM	16	CB	ARG S 94	-34.128	19.146	14.929	1.00 0.05
20	ATOM	17	CG	ARG S 94	-33.300	18.494	13.811	1.00 0.06
	ATOM	18	CD	ARG S 94	-34.051	18.379	12.475	1.00 0.11
	ATOM	19	NE	ARG S 94	-33.282	17.579	11.523	1.00 -0.49
	ATOM	20	CZ	ARG S 94	-33.792	16.435	11.016	1.00 0.81
	ATOM	21	NH1	ARG S 94	-35.003	15.996	11.360	1.00 -0.63
25	ATOM	22	NH2	ARG S 94	-33.068	15.730	10.153	1.00 -0.63
	ATOM	23	H	ARG S 94	-34.386	17.167	16.817	1.00 0.25
	ATOM	24	HE	ARG S 94	-32.370	17.873	11.238	1.00 0.29
	ATOM	25	1HH1	ARG S 94	-35.352	15.145	10.968	1.00 0.36
	ATOM	26	2HH1	ARG S 94	-35.565	16.510	12.008	1.00 0.36
30	ATOM	27	1HH2	ARG S 94	-33.433	14.882	9.769	1.00 0.36
	ATOM	28	2HH2	ARG S 94	-32.159	16.050	9.887	1.00 0.36
	ATOM	29	N	ASN S 95	-35.397	19.461	17.721	1.00 -0.52
	ATOM	30	CA	ASN S 95	-36.183	20.166	18.729	1.00 0.22
	ATOM	31	C	ASN S 95	-37.332	19.318	19.219	1.00 0.53
35	ATOM	32	O	ASN S 95	-37.969	18.605	18.430	1.00 -0.50
	ATOM	33	CB	ASN S 95	-36.706	21.522	18.229	1.00 0.00

75

	ATOM	34	CG	ASN S	95	-36.363	22.606	19.233	1.00	0.68
	ATOM	35	OD1	ASN S	95	-37.231	23.137	19.913	1.00	-0.47
	ATOM	36	ND2	ASN S	95	-35.056	22.909	19.294	1.00	-0.87
	ATOM	37	H	ASN S	95	-35.797	18.657	17.281	1.00	0.25
5	ATOM	38	1HD2	ASN S	95	-34.725	23.610	19.925	1.00	0.34
	ATOM	39	2HD2	ASN S	95	-34.397	22.435	18.709	1.00	0.34
	ATOM	40	N	LEU S	96	-37.598	19.391	20.520	1.00	-0.52
	ATOM	41	CA	LEU S	96	-38.679	18.626	21.134	1.00	0.20
	ATOM	42	C	LEU S	96	-39.965	19.383	20.901	1.00	0.53
10	ATOM	43	O	LEU S	96	-40.388	20.181	21.751	1.00	-0.50
	ATOM	44	CB	LEU S	96	-38.396	18.419	22.630	1.00	0.02
	ATOM	45	CG	LEU S	96	-37.665	17.107	22.956	1.00	0.05
	ATOM	46	CD1	LEU S	96	-38.413	15.848	22.489	1.00	-0.01
	ATOM	47	CD2	LEU S	96	-36.219	17.129	22.436	1.00	-0.01
15	ATOM	48	H	LEU S	96	-37.044	19.987	21.103	1.00	0.25
	ATOM	49	N	THR S	97	-40.588	19.136	19.753	1.00	-0.52
	ATOM	50	CA	THR S	97	-41.840	19.794	19.394	1.00	0.27
	ATOM	51	C	THR S	97	-42.809	18.826	18.759	1.00	0.53
	ATOM	52	O	THR S	97	-42.400	17.929	18.007	1.00	-0.50
20	ATOM	53	CB	THR S	97	-41.572	20.990	18.466	1.00	0.21
	ATOM	54	OG1	THR S	97	-42.795	21.657	18.160	1.00	-0.55
	ATOM	55	CG2	THR S	97	-40.854	20.578	17.171	1.00	0.01
	ATOM	56	H	THR S	97	-40.193	18.480	19.110	1.00	0.25
	ATOM	57	HG1	THR S	97	-42.562	22.479	17.722	1.00	0.31
25	ATOM	58	N	ILE S	98	-44.093	19.003	19.059	1.00	-0.52
	ATOM	59	CA	ILE S	98	-45.140	18.142	18.518	1.00	0.20
	ATOM	60	C	ILE S	98	-46.361	18.894	18.043	1.00	0.53
	ATOM	61	O	ILE S	98	-46.834	19.818	18.721	1.00	-0.50
	ATOM	62	CB	ILE S	98	-45.444	17.014	19.516	1.00	0.03
30	ATOM	63	CG1	ILE S	98	-46.244	15.862	18.888	1.00	0.02
	ATOM	64	CG2	ILE S	98	-46.123	17.547	20.788	1.00	0.00
	ATOM	65	CD1	ILE S	98	-45.346	14.810	18.219	1.00	0.00
	ATOM	66	H	ILE S	98	-44.356	19.747	19.673	1.00	0.25
	ATOM	67	N	VAL S	99	-46.872	18.500	16.880	1.00	-0.52
35	ATOM	68	CA	VAL S	99	-48.051	19.135	16.298	1.00	0.20
	ATOM	69	C	VAL S	99	-49.253	18.226	16.395	1.00	0.53

SUBSTITUTE SHEET (RULE 26)

	ATOM	70	O	VAL S 99	-49.110	16.994	16.408	1.00	-0.50
	ATOM	71	CB	VAL S 99	-47.698	19.525	14.854	1.00	0.03
	ATOM	72	CG1	VAL S 99	-46.688	20.681	14.780	1.00	0.01
	ATOM	73	CG2	VAL S 99	-47.287	18.331	13.978	1.00	0.01
5	ATOM	74	H	VAL S 99	-46.441	17.747	16.383	1.00	0.25
	ATOM	75	N	ASP S 100	-50.436	18.829	16.461	1.00	-0.52
	ATOM	76	CA	ASP S 100	-51.684	18.077	16.557	1.00	0.25
	ATOM	77	C	ASP S 100	-51.849	17.392	15.222	1.00	0.53
	ATOM	78	O	ASP S 100	-51.673	16.169	15.115	1.00	-0.50
10	ATOM	79	CB	ASP S 100	-52.858	19.041	16.789	1.00	-0.21
	ATOM	80	CG	ASP S 100	-52.508	20.428	16.287	1.00	0.62
	ATOM	81	OD1	ASP S 100	-52.854	20.755	15.156	1.00	-0.71
	ATOM	82	OD2	ASP S 100	-51.889	21.189	17.023	1.00	-0.71
	ATOM	83	H	ASP S 100	-50.481	19.828	16.445	1.00	0.25
15	ATOM	84	N	SER S 101	-52.187	18.177	14.202	1.00	-0.52
	ATOM	85	CA	SER S 101	-52.382	17.652	12.854	1.00	0.29
	ATOM	86	C	SER S 101	-53.017	16.282	12.846	1.00	0.53
	ATOM	87	O	SER S 101	-52.684	15.439	12.000	1.00	-0.50
	ATOM	88	CB	SER S 101	-51.034	17.621	12.116	1.00	0.19
20	ATOM	89	OG	SER S 101	-51.236	17.656	10.705	1.00	-0.55
	ATOM	90	H	SER S 101	-52.314	19.157	14.356	1.00	0.25
	ATOM	91	HG	SER S 101	-50.419	17.987	10.324	1.00	0.31
	ATOM	92	N	GLY S 102	-53.930	16.058	13.786	1.00	-0.52
	ATOM	93	CA	GLY S 102	-54.626	14.779	13.900	1.00	0.25
25	ATOM	94	C	GLY S 102	-53.788	13.536	13.720	1.00	0.53
	ATOM	95	O	GLY S 102	-54.199	12.596	13.024	1.00	-0.50
	ATOM	96	H	GLY S 102	-54.153	16.782	14.439	1.00	0.25
	ATOM	97	N	LEU S 103	-52.615	13.527	14.347	1.00	-0.52
	ATOM	98	CA	LEU S 103	-51.701	12.392	14.263	1.00	0.20
30	ATOM	99	C	LEU S 103	-51.521	11.844	15.658	1.00	0.53
	ATOM	100	O	LEU S 103	-51.586	12.596	16.643	1.00	-0.50
	ATOM	101	CB	LEU S 103	-50.367	12.833	13.641	1.00	0.02
	ATOM	102	CG	LEU S 103	-49.757	14.089	14.284	1.00	0.05
	ATOM	103	CD1	LEU S 103	-48.873	13.793	15.505	1.00	-0.01
35	ATOM	104	CD2	LEU S 103	-49.015	14.944	13.244	1.00	-0.01
	ATOM	105	H	LEU S 103	-52.343	14.319	14.894	1.00	0.25

77

SUBSTITUTE SHEET (RULE 26)

```
        ATOM   106 N   LYS S 104   -51.296 10.536 15.747 1.00 -0.52
        ATOM   107 CA  LYS S 104   -51.102  9.870 17.032 1.00  0.23
        ATOM   108 C   LYS S 104   -49.623  9.824 17.329 1.00  0.53
        ATOM   109 O   LYS S 104   -49.013  8.744 17.326 1.00 -0.50
  5     ATOM   110 CB  LYS S 104   -51.738  8.471 17.005 1.00  0.04
        ATOM   111 CG  LYS S 104   -52.308  8.008 18.355 1.00  0.05
        ATOM   112 CD  LYS S 104   -53.074  6.679 18.249 1.00  0.05
        ATOM   113 CE  LYS S 104   -52.171  5.461 18.503 1.00  0.22
        ATOM   114 NZ  LYS S 104   -52.891  4.233 18.143 1.00 -0.27
 10     ATOM   115 H   LYS S 104   -51.256  9.986 14.913 1.00  0.25
        ATOM   116 1HZ LYS S 104   -53.368  4.364 17.227 1.00  0.31
        ATOM   117 2HZ LYS S 104   -53.600  4.018 18.873 1.00  0.31
        ATOM   118 3HZ LYS S 104   -52.219  3.443 18.071 1.00  0.31
        ATOM   119 N   PHE S 105   -49.043 10.993 17.585 1.00 -0.52
 15     ATOM   120 CA  PHE S 105   -47.619 11.101 17.889 1.00  0.21
        ATOM   121 C   PHE S 105   -46.933 10.882 16.562 1.00  0.53
        ATOM   122 O   PHE S 105   -46.495 11.844 15.914 1.00 -0.50
        ATOM   123 CB  PHE S 105   -47.162 10.024 18.886 1.00  0.04
        ATOM   124 CG  PHE S 105   -45.861 10.412 19.549 1.00  0.01
 20     ATOM   125 CD1 PHE S 105   -44.683  9.692 19.251 1.00 -0.01
        ATOM   126 CD2 PHE S 105   -45.849 11.493 20.457 1.00 -0.01
        ATOM   127 CE1 PHE S 105   -43.474 10.058 19.873 1.00  0.00
        ATOM   128 CE2 PHE S 105   -44.641 11.860 21.078 1.00  0.00
        ATOM   129 CZ  PHE S 105   -43.466 11.139 20.780 1.00  0.00
 25     ATOM   130 H   PHE S 105   -49.592 11.829 17.571 1.00  0.25
        ATOM   131 N   VAL S 106   -46.838  9.619 16.156 1.00 -0.52
        ATOM   132 CA  VAL S 106   -46.200  9.259 14.893 1.00  0.20
        ATOM   133 C   VAL S 106   -44.818  9.859 14.800 1.00  0.53
        ATOM   134 O   VAL S 106   -44.261  9.989 13.699 1.00 -0.50
 30     ATOM   135 CB  VAL S 106   -47.136  9.709 13.760 1.00  0.03
        ATOM   136 CG1 VAL S 106   -46.649  9.261 12.372 1.00  0.01
        ATOM   137 CG2 VAL S 106   -48.612  9.356 14.005 1.00  0.01
        ATOM   138 H   VAL S 106   -47.213  8.889 16.726 1.00  0.25
        ATOM   139 N   ALA S 107   -44.263 10.225 15.951 1.00 -0.52
 35     ATOM   140 CA  ALA S 107   -42.930 10.820 16.013 1.00  0.22
        ATOM   141 C   ALA S 107   -42.034  9.846 16.740 1.00  0.53
```

78

SUBSTITUTE SHEET (RULE 26)

```
        ATOM  142  O   ALA S 107   -41.035 10.247 17.354 1.00 -0.50
        ATOM  143  CB  ALA S 107   -42.939 12.156 16.772 1.00  0.03
        ATOM  144  H   ALA S 107   -44.766 10.093 16.805 1.00  0.25
        ATOM  145  N   TYR S 108   -42.388  8.565 16.671 1.00 -0.52
   5    ATOM  146  CA  TYR S 108   -41.616  7.513 17.325 1.00  0.25
        ATOM  147  C   TYR S 108   -40.181  7.445 16.861 1.00  0.53
        ATOM  148  O   TYR S 108   -39.320  6.888 17.557 1.00 -0.50
        ATOM  149  CB  TYR S 108   -42.269  6.142 17.090 1.00  0.02
        ATOM  150  CG  TYR S 108   -43.761  6.173 17.332 1.00  0.00
  10    ATOM  151  CD1 TYR S 108   -44.625  6.208 16.220 1.00 -0.04
        ATOM  152  CD2 TYR S 108   -44.248  6.166 18.656 1.00 -0.04
        ATOM  153  CE1 TYR S 108   -46.012  6.237 16.436 1.00  0.10
        ATOM  154  CE2 TYR S 108   -45.636  6.196 18.871 1.00  0.10
        ATOM  155  CZ  TYR S 108   -46.500  6.231 17.759 1.00 -0.12
  15    ATOM  156  OH  TYR S 108   -47.863  6.259 17.970 1.00 -0.37
        ATOM  157  H   TYR S 108   -43.207  8.308 16.159 1.00  0.25
        ATOM  158  HH  TYR S 108   -48.199  7.127 17.791 1.00  0.34
        ATOM  159  N   LYS S 109   -39.921  8.011 15.685 1.00 -0.52
        ATOM  160  CA  LYS S 109   -38.579  8.021 15.112 1.00  0.23
  20    ATOM  161  C   LYS S 109   -37.724  8.976 15.910 1.00  0.53
        ATOM  162  O   LYS S 109   -36.497  8.811 15.985 1.00 -0.50
        ATOM  163  CB  LYS S 109   -38.641  8.396 13.622 1.00  0.04
        ATOM  164  CG  LYS S 109   -39.200  9.801 13.345 1.00  0.05
        ATOM  165  CD  LYS S 109   -40.553  9.764 12.617 1.00  0.05
  25    ATOM  166  CE  LYS S 109   -41.148 11.167 12.416 1.00  0.22
        ATOM  167  NZ  LYS S 109   -42.394 11.066 11.645 1.00 -0.27
        ATOM  168  H   LYS S 109   -40.662  8.444 15.173 1.00  0.25
        ATOM  169  1HZ LYS S 109   -42.761 12.020 11.449 1.00  0.31
        ATOM  170  2HZ LYS S 109   -43.099 10.531 12.191 1.00  0.31
  30    ATOM  171  3HZ LYS S 109   -42.209 10.576 10.746 1.00  0.31
        ATOM  172  N   ALA S 110   -38.368  9.974 16.509 1.00 -0.52
        ATOM  173  CA  ALA S 110   -37.671 10.972 17.314 1.00  0.22
        ATOM  174  C   ALA S 110   -37.673 10.482 18.742 1.00  0.53
        ATOM  175  O   ALA S 110   -36.724 10.741 19.497 1.00 -0.50
  35    ATOM  176  CB  ALA S 110   -38.368 12.341 17.251 1.00  0.03
        ATOM  177  H   ALA S 110   -39.360 10.050 16.409 1.00  0.25
```

79

	ATOM	178	N	PHE	S	111	-38.736	9.775	19.114	1.00	-0.52
	ATOM	179	CA	PHE	S	111	-38.873	9.238	20.465	1.00	0.21
	ATOM	180	C	PHE	S	111	-37.731	8.259	20.599	1.00	0.53
	ATOM	181	O	PHE	S	111	-37.123	8.144	21.673	1.00	-0.50
5	ATOM	182	CB	PHE	S	111	-40.207	8.499	20.656	1.00	0.04
	ATOM	183	CG	PHE	S	111	-40.461	8.200	22.115	1.00	0.01
	ATOM	184	CD1	PHE	S	111	-41.035	9.191	22.942	1.00	-0.01
	ATOM	185	CD2	PHE	S	111	-40.116	6.930	22.626	1.00	-0.01
	ATOM	186	CE1	PHE	S	111	-41.269	8.906	24.301	1.00	0.00
10	ATOM	187	CE2	PHE	S	111	-40.349	6.645	23.983	1.00	0.00
	ATOM	188	CZ	PHE	S	111	-40.924	7.636	24.807	1.00	0.00
	ATOM	189	H	PHE	S	111	-39.467	9.602	18.455	1.00	0.25
	ATOM	190	N	LEU	S	112	-37.439	7.552	19.511	1.00	-0.52
	ATOM	191	CA	LEU	S	112	-36.360	6.568	19.494	1.00	0.20
15	ATOM	192	C	LEU	S	112	-35.074	7.293	19.811	1.00	0.53
	ATOM	193	O	LEU	S	112	-34.249	6.798	20.594	1.00	-0.50
	ATOM	194	CB	LEU	S	112	-36.305	5.868	18.127	1.00	0.02
	ATOM	195	CG	LEU	S	112	-35.374	4.646	18.082	1.00	0.05
	ATOM	196	CD1	LEU	S	112	-36.074	3.321	18.421	1.00	-0.01
20	ATOM	197	CD2	LEU	S	112	-34.628	4.563	16.740	1.00	-0.01
	ATOM	198	H	LEU	S	112	-37.970	7.692	18.675	1.00	0.25
	ATOM	199	N	LYS	S	113	-34.900	8.464	19.205	1.00	-0.52
	ATOM	200	CA	LYS	S	113	-33.705	9.275	19.417	1.00	0.23
	ATOM	201	C	LYS	S	113	-33.633	9.650	20.878	1.00	0.53
25	ATOM	202	O	LYS	S	113	-32.578	9.508	21.513	1.00	-0.50
	ATOM	203	CB	LYS	S	113	-33.728	10.505	18.496	1.00	0.04
	ATOM	204	CG	LYS	S	113	-33.318	10.217	17.043	1.00	0.05
	ATOM	205	CD	LYS	S	113	-33.954	11.198	16.045	1.00	0.05
	ATOM	206	CE	LYS	S	113	-33.790	10.739	14.587	1.00	0.22
30	ATOM	207	NZ	LYS	S	113	-34.498	9.467	14.390	1.00	-0.27
	ATOM	208	H	LYS	S	113	-35.605	8.807	18.585	1.00	0.25
	ATOM	209	1HZ	LYS	S	113	-35.239	9.365	15.113	1.00	0.31
	ATOM	210	2HZ	LYS	S	113	-33.826	8.678	14.472	1.00	0.31
	ATOM	211	3HZ	LYS	S	113	-34.933	9.453	13.446	1.00	0.31
35	ATOM	212	N	ASN	S	114	-34.754	10.128	21.412	1.00	-0.52
	ATOM	213	CA	ASN	S	114	-34.832	10.531	22.813	1.00	0.22

SUBSTITUTE SHEET (RULE 26)

	ATOM	214 C	ASN S 114	-34.508 9.379 23.733 1.00 0.53
	ATOM	215 O	ASN S 114	-33.878 9.570 24.784 1.00 -0.50
	ATOM	216 CB	ASN S 114	-36.198 11.131 23.180 1.00 0.00
	ATOM	217 CG	ASN S 114	-36.349 12.495 22.535 1.00 0.68
5	ATOM	218 OD1	ASN S 114	-37.101 12.669 21.585 1.00 -0.47
	ATOM	219 ND2	ASN S 114	-35.597 13.457 23.097 1.00 -0.87
	ATOM	220 H	ASN S 114	-35.572 10.217 20.844 1.00 0.25
	ATOM	221 1HD2	ASN S 114	-35.623 14.393 22.746 1.00 0.34
	ATOM	222 2HD2	ASN S 114	-35.002 13.248 23.873 1.00 0.34
10	ATOM	223 N	SER S 115	-34.937 8.182 23.342 1.00 -0.52
	ATOM	224 CA	SER S 115	-34.696 6.977 24.131 1.00 0.29
	ATOM	225 C	SER S 115	-33.240 6.580 24.160 1.00 0.53
	ATOM	226 O	SER S 115	-32.755 6.037 25.165 1.00 -0.50
	ATOM	227 CB	SER S 115	-35.553 5.825 23.584 1.00 0.19
15	ATOM	228 OG	SER S 115	-36.939 6.156 23.655 1.00 -0.55
	ATOM	229 H	SER S 115	-35.440 8.096 22.482 1.00 0.25
	ATOM	230 HG	SER S 115	-37.081 6.859 23.017 1.00 0.31
	ATOM	231 N	ASN S 116	-32.540 6.850 23.062 1.00 -0.52
	ATOM	232 CA	ASN S 116	-31.121 6.522 22.949 1.00 0.22
20	ATOM	233 C	ASN S 116	-30.264 7.559 23.632 1.00 0.53
	ATOM	234 O	ASN S 116	-29.329 7.216 24.372 1.00 -0.50
	ATOM	235 CB	ASN S 116	-30.671 6.343 21.490 1.00 0.00
	ATOM	236 CG	ASN S 116	-30.988 4.935 21.025 1.00 0.68
	ATOM	237 OD1	ASN S 116	-30.139 4.053 21.046 1.00 -0.47
25	ATOM	238 ND2	ASN S 116	-32.252 4.764 20.603 1.00 -0.87
	ATOM	239 H	ASN S 116	-32.991 7.290 22.286 1.00 0.25
	ATOM	240 1HD2	ASN S 116	-32.564 3.872 20.275 1.00 0.34
	ATOM	241 2HD2	ASN S 116	-32.898 5.528 20.611 1.00 0.34
	ATOM	242 N	LEU S 117	-30.578 8.828 23.387 1.00 -0.52
30	ATOM	243 CA	LEU S 117	-29.835 9.937 23.980 1.00 0.23
	ATOM	244 C	LEU S 117	-30.840 10.862 24.645 1.00 0.50
	ATOM	245 O	LEU S 117	-31.725 11.354 23.951 1.00 -0.25
	ATOM	246 CB	LEU S 117	-29.015 10.660 22.900 1.00 0.02
	ATOM	247 CG	LEU S 117	-27.751 9.905 22.458 1.00 0.05
35	ATOM	248 CD1	LEU S 117	-27.875 9.246 21.075 1.00 -0.01
	ATOM	249 CD2	LEU S 117	-26.506 10.802 22.546 1.00 -0.01

SUBSTITUTE SHEET (RULE 26)

ATOM   250 OXT LEU S 117   -30.723 11.077 25.849 1.00 -0.25

ATOM   251 H LEU S 117   -31.344 9.038 22.780 1.00 0.25

END

*Principal residues are bolded.

SUBSTITUTE SHEET (RULE 26)

Appendix 3. Geometry of the p75^{NTR} binding site for neurotrophins in PDB format.*

REMARK	1 Second CRD of p75^{NTR}, bound to NGF.				
REMARK	2				
ATOM	1 N CYS R 39	-32.488	-11.161	6.915 1.00 0.00	
ATOM	2 CA CYS R 39	-33.024	-9.817	7.111 1.00 0.00	
ATOM	3 C CYS R 39	-33.595	-9.148	5.878 1.00 0.00	
ATOM	4 O CYS R 39	-34.221	-8.095	5.967 1.00 0.00	
ATOM	5 CB CYS R 39	-31.991	-8.907	7.780 1.00 0.00	
ATOM	6 SG CYS R 39	-30.272	-9.354	7.401 1.00 0.00	
ATOM	7 1H CYS R 39	-31.698	-11.178	6.287 1.00 0.00	
ATOM	8 2H CYS R 39	-32.170	-11.586	7.775 1.00 0.00	
ATOM	9 3H CYS R 39	-33.166	-11.799	6.523 1.00 0.00	
ATOM	10 N LEU R 40	-33.398	-9.779	4.707 1.00 0.00	
ATOM	11 CA LEU R 40	-34.095	-9.260	3.530 1.00 0.00	
ATOM	12 C LEU R 40	-35.322	-10.097	3.220 1.00 0.00	
ATOM	13 O LEU R 40	-36.442	-9.632	3.041 1.00 0.00	
ATOM	14 CB LEU R 40	-33.148	-9.230	2.327 1.00 0.00	
ATOM	15 CG LEU R 40	-31.880	-8.404	2.561 1.00 0.00	
ATOM	16 CD1 LEU R 40	-30.862	-8.604	1.438 1.00 0.00	
ATOM	17 CD2 LEU R 40	-32.184	-6.924	2.806 1.00 0.00	
ATOM	18 H LEU R 40	-32.867	-10.625	4.675 1.00 0.00	
ATOM	19 N ASP R 41	-35.034	-11.407	3.188 1.00 0.00	
ATOM	20 CA ASP R 41	-36.070	-12.408	2.947 1.00 0.00	
ATOM	21 C ASP R 41	-35.822	-13.609	3.848 1.00 0.00	
ATOM	22 O ASP R 41	-34.792	-13.673	4.525 1.00 0.00	
ATOM	23 CB ASP R 41	-36.054	-12.772	1.449 1.00 0.00	
ATOM	24 CG ASP R 41	-37.195	-13.703	1.074 1.00 0.00	
ATOM	25 OD1 ASP R 41	-38.299	-13.520	1.568 1.00 0.00	
ATOM	26 OD2 ASP R 41	-36.979	-14.633	0.314 1.00 0.00	
ATOM	27 H ASP R 41	-34.111	-11.739	3.385 1.00 0.00	
ATOM	28 N SER R 42	-36.757	-14.563	3.825 1.00 0.00	
ATOM	29 CA SER R 42	-36.565	-15.812	4.545 1.00 0.00	
ATOM	30 C SER R 42	-35.305	-16.572	4.150 1.00 0.00	
ATOM	31 O SER R 42	-34.755	-17.350	4.918 1.00 0.00	

SUBSTITUTE SHEET (RULE 26)

	ATOM	32	CB	SER	R	42	-37.816	-16.678	4.398	1.00	0.00
	ATOM	33	OG	SER	R	42	-38.988	-15.930	4.780	1.00	0.00
	ATOM	34	H	SER	R	42	-37.497	-14.449	3.168	1.00	0.00
	ATOM	35	HG	SER	R	42	-39.404	-15.604	3.984	1.00	0.00
5	ATOM	36	N	VAL	R	43	-34.794	-16.284	2.940	1.00	0.00
	ATOM	37	CA	VAL	R	43	-33.503	-16.883	2.574	1.00	0.00
	ATOM	38	C	VAL	R	43	-32.270	-16.339	3.305	1.00	0.00
	ATOM	39	O	VAL	R	43	-31.128	-16.743	3.081	1.00	0.00
	ATOM	40	CB	VAL	R	43	-33.300	-16.823	1.054	1.00	0.00
10	ATOM	41	CG1	VAL	R	43	-34.389	-17.623	0.337	1.00	0.00
	ATOM	42	CG2	VAL	R	43	-33.208	-15.383	0.537	1.00	0.00
	ATOM	43	H	VAL	R	43	-35.321	-15.679	2.336	1.00	0.00
	ATOM	44	N	THR	R	44	-32.539	-15.360	4.166	1.00	0.00
	ATOM	45	CA	THR	R	44	-31.443	-14.732	4.879	1.00	0.00
15	ATOM	46	C	THR	R	44	-31.701	-14.680	6.367	1.00	0.00
	ATOM	47	O	THR	R	44	-32.659	-14.063	6.830	1.00	0.00
	ATOM	48	CB	THR	R	44	-31.171	-13.339	4.300	1.00	0.00
	ATOM	49	OG1	THR	R	44	-32.382	-12.578	4.130	1.00	0.00
	ATOM	50	CG2	THR	R	44	-30.430	-13.431	2.962	1.00	0.00
20	ATOM	51	H	THR	R	44	-33.481	-15.090	4.359	1.00	0.00
	ATOM	52	HG1	THR	R	44	-33.031	-12.981	4.718	1.00	0.00
	ATOM	53	N	PHE	R	45	-30.805	-15.368	7.080	1.00	0.00
	ATOM	54	CA	PHE	R	45	-30.829	-15.256	8.526	1.00	0.00
	ATOM	55	C	PHE	R	45	-30.085	-13.996	8.932	1.00	0.00
25	ATOM	56	O	PHE	R	45	-29.293	-13.430	8.175	1.00	0.00
	ATOM	57	CB	PHE	R	45	-30.243	-16.531	9.157	1.00	0.00
	ATOM	58	CG	PHE	R	45	-30.514	-16.587	10.647	1.00	0.00
	ATOM	59	CD1	PHE	R	45	-31.844	-16.581	11.126	1.00	0.00
	ATOM	60	CD2	PHE	R	45	-29.423	-16.628	11.539	1.00	0.00
30	ATOM	61	CE1	PHE	R	45	-32.085	-16.592	12.512	1.00	0.00
	ATOM	62	CE2	PHE	R	45	-29.661	-16.637	12.927	1.00	0.00
	ATOM	63	CZ	PHE	R	45	-30.989	-16.611	13.400	1.00	0.00
	ATOM	64	H	PHE	R	45	-30.025	-15.788	6.623	1.00	0.00
	ATOM	65	N	SER	R	46	-30.382	-13.575	10.161	1.00	0.00
35	ATOM	66	CA	SER	R	46	-29.961	-12.259	10.626	1.00	0.00
	ATOM	67	C	SER	R	46	-28.732	-12.274	11.517	1.00	0.00

84

	ATOM	68	O	SER R	46	-28.497	-11.407	12.346 1.00 0.00
	ATOM	69	CB	SER R	46	-31.156	-11.630	11.337 1.00 0.00
	ATOM	70	OG	SER R	46	-31.890	-12.664	12.026 1.00 0.00
	ATOM	71	H	SER R	46	-31.046	-14.080	10.714 1.00 0.00
5	ATOM	72	HG	SER R	46	-32.811	-12.512	11.820 1.00 0.00
	ATOM	73	N	ASP R	47	-27.906	-13.314	11.317 1.00 0.00
	ATOM	74	CA	ASP R	47	-26.772	-13.543	12.226 1.00 0.00
	ATOM	75	C	ASP R	47	-25.567	-12.610	12.077 1.00 0.00
	ATOM	76	O	ASP R	47	-24.410	-13.027	12.086 1.00 0.00
10	ATOM	77	CB	ASP R	47	-26.337	-15.025	12.168 1.00 0.00
	ATOM	78	CG	ASP R	47	-25.807	-15.429	10.794 1.00 0.00
	ATOM	79	OD1	ASP R	47	-26.456	-15.180	9.790 1.00 0.00
	ATOM	80	OD2	ASP R	47	-24.712	-15.961	10.694 1.00 0.00
	ATOM	81	H	ASP R	47	-28.048	-13.919	10.531 1.00 0.00
15	ATOM	82	N	VAL R	48	-25.857	-11.312	11.875 1.00 0.00
	ATOM	83	CA	VAL R	48	-24.733	-10.395	11.691 1.00 0.00
	ATOM	84	C	VAL R	48	-24.130	-9.906	13.003 1.00 0.00
	ATOM	85	O	VAL R	48	-22.914	-9.763	13.131 1.00 0.00
	ATOM	86	CB	VAL R	48	-25.108	-9.258	10.720 1.00 0.00
20	ATOM	87	CG1	VAL R	48	-26.299	-8.421	11.194 1.00 0.00
	ATOM	88	CG2	VAL R	48	-23.886	-8.416	10.349 1.00 0.00
	ATOM	89	H	VAL R	48	-26.767	-10.954	12.073 1.00 0.00
	ATOM	90	N	VAL R	49	-25.034	-9.713	13.984 1.00 0.00
	ATOM	91	CA	VAL R	49	-24.767	-9.685	15.431 1.00 0.00
25	ATOM	92	C	VAL R	49	-23.506	-9.045	16.022 1.00 0.00
	ATOM	93	O	VAL R	49	-23.103	-9.361	17.142 1.00 0.00
	ATOM	94	CB	VAL R	49	-25.003	-11.080	16.043 1.00 0.00
	ATOM	95	CG1	VAL R	49	-26.440	-11.541	15.783 1.00 0.00
	ATOM	96	CG2	VAL R	49	-23.973	-12.125	15.594 1.00 0.00
30	ATOM	97	H	VAL R	49	-25.987	-9.707	13.681 1.00 0.00
	ATOM	98	N	SER R	50	-22.912	-8.118	15.261 1.00 0.00
	ATOM	99	CA	SER R	50	-21.729	-7.376	15.719 1.00 0.00
	ATOM	100	C	SER R	50	-21.546	-6.123	14.873 1.00 0.00
	ATOM	101	O	SER R	50	-21.505	-4.977	15.336 1.00 0.00
35	ATOM	102	CB	SER R	50	-20.431	-8.205	15.623 1.00 0.00
	ATOM	103	OG	SER R	50	-20.525	-9.489	16.273 1.00 0.00

85

SUBSTITUTE SHEET (RULE 26)

	ATOM	104	H	SER R 50	-23.312	-7.897	14.372	1.00	0.00
	ATOM	105	HG	SER R 50	-21.302	-9.403	16.827	1.00	0.00
	ATOM	106	N	ALA R 51	-21.454	-6.446	13.572	1.00	0.00
	ATOM	107	CA	ALA R 51	-21.546	-5.403	12.562	1.00	0.00
5	ATOM	108	C	ALA R 51	-23.013	-5.196	12.263	1.00	0.00
	ATOM	109	O	ALA R 51	-23.862	-5.866	12.848	1.00	0.00
	ATOM	110	CB	ALA R 51	-20.808	-5.825	11.288	1.00	0.00
	ATOM	111	H	ALA R 51	-21.633	-7.392	13.330	1.00	0.00
	ATOM	112	N	THR R 52	-23.266	-4.259	11.348	1.00	0.00
10	ATOM	113	CA	THR R 52	-24.606	-3.698	11.228	1.00	0.00
	ATOM	114	C	THR R 52	-25.679	-4.557	10.579	1.00	0.00
	ATOM	115	O	THR R 52	-26.564	-5.091	11.239	1.00	0.00
	ATOM	116	CB	THR R 52	-24.481	-2.344	10.532	1.00	0.00
	ATOM	117	OG1	THR R 52	-23.205	-1.766	10.845	1.00	0.00
15	ATOM	118	CG2	THR R 52	-25.624	-1.389	10.891	1.00	0.00
	ATOM	119	H	THR R 52	-22.533	-3.835	10.820	1.00	0.00
	ATOM	120	HG1	THR R 52	-23.136	-0.977	10.314	1.00	0.00
	ATOM	121	N	GLU R 53	-25.602	-4.625	9.241	1.00	0.00
	ATOM	122	CA	GLU R 53	-26.765	-5.151	8.526	1.00	0.00
20	ATOM	123	C	GLU R 53	-26.656	-6.149	7.362	1.00	0.00
	ATOM	124	O	GLU R 53	-27.702	-6.492	6.808	1.00	0.00
	ATOM	125	CB	GLU R 53	-27.678	-3.966	8.146	1.00	0.00
	ATOM	126	CG	GLU R 53	-27.452	-3.289	6.779	1.00	0.00
	ATOM	127	CD	GLU R 53	-25.983	-3.036	6.488	1.00	0.00
25	ATOM	128	OE1	GLU R 53	-25.530	-3.408	5.413	1.00	0.00
	ATOM	129	OE2	GLU R 53	-25.284	-2.484	7.329	1.00	0.00
	ATOM	130	H	GLU R 53	-24.901	-4.146	8.704	1.00	0.00
	ATOM	131	N	PRO R 54	-25.448	-6.634	6.953	1.00	0.00
	ATOM	132	CA	PRO R 54	-25.503	-7.661	5.912	1.00	0.00
30	ATOM	133	C	PRO R 54	-26.227	-8.929	6.351	1.00	0.00
	ATOM	134	O	PRO R 54	-26.254	-9.343	7.509	1.00	0.00
	ATOM	135	CB	PRO R 54	-24.032	-7.892	5.550	1.00	0.00
	ATOM	136	CG	PRO R 54	-23.286	-6.653	6.033	1.00	0.00
	ATOM	137	CD	PRO R 54	-24.070	-6.275	7.278	1.00	0.00
35	ATOM	138	N	CYS R 55	-26.841	-9.564	5.355	1.00	0.00
	ATOM	139	CA	CYS R 55	-27.561	-10.782	5.715	1.00	0.00

86

```
        ATOM   140 C  CYS R 55   -26.758 -12.020  5.403 1.00 0.00
        ATOM   141 O  CYS R 55   -25.722 -11.942  4.747 1.00 0.00
        ATOM   142 CB CYS R 55   -28.884 -10.816  4.980 1.00 0.00
        ATOM   143 SG CYS R 55   -29.966  -9.423  5.373 1.00 0.00
   5    ATOM   144 H  CYS R 55   -26.798  -9.206  4.422 1.00 0.00
        ATOM   145 N  LYS R 56   -27.264 -13.165  5.871 1.00 0.00
        ATOM   146 CA LYS R 56   -26.589 -14.362  5.398 1.00 0.00
        ATOM   147 C  LYS R 56   -27.549 -15.386  4.837 1.00 0.00
        ATOM   148 O  LYS R 56   -28.519 -15.789  5.477 1.00 0.00
  10    ATOM   149 CB LYS R 56   -25.714 -14.916  6.522 1.00 0.00
        ATOM   150 CG LYS R 56   -24.805 -16.085  6.153 1.00 0.00
        ATOM   151 CD LYS R 56   -23.591 -16.147  7.077 1.00 0.00
        ATOM   152 CE LYS R 56   -23.022 -17.552  7.202 1.00 0.00
        ATOM   153 NZ LYS R 56   -23.951 -18.331  8.015 1.00 0.00
  15    ATOM   154 H  LYS R 56   -28.051 -13.262  6.482 1.00 0.00
        ATOM   155 1HZ LYS R 56  -23.881 -18.006  8.995 1.00 0.00
        ATOM   156 2HZ LYS R 56  -23.728 -19.338  7.946 1.00 0.00
        ATOM   157 3HZ LYS R 56  -24.928 -18.196  7.691 1.00 0.00
        ATOM   158 N  PRO R 57   -27.236 -15.830  3.598 1.00 0.00
  20    ATOM   159 CA PRO R 57   -27.952 -16.989  3.057 1.00 0.00
        ATOM   160 C  PRO R 57   -27.718 -18.237  3.898 1.00 0.00
        ATOM   161 O  PRO R 57   -26.590 -18.524  4.312 1.00 0.00
        ATOM   162 CB PRO R 57   -27.397 -17.079  1.631 1.00 0.00
        ATOM   163 CG PRO R 57   -26.018 -16.418  1.682 1.00 0.00
  25    ATOM   164 CD PRO R 57   -26.218 -15.301  2.698 1.00 0.00
        ATOM   165 N  CYS R 58   -28.842 -18.939  4.129 1.00 0.00
        ATOM   166 CA CYS R 58   -28.833 -20.145  4.956 1.00 0.00
        ATOM   167 C  CYS R 58   -28.246 -21.406  4.309 1.00 0.00
        ATOM   168 O  CYS R 58   -27.067 -21.414  3.958 1.00 0.00
  30    ATOM   169 CB CYS R 58   -30.219 -20.336  5.550 1.00 0.00
        ATOM   170 SG CYS R 58   -31.446 -20.570  4.242 1.00 0.00
        ATOM   171 H  CYS R 58   -29.694 -18.544  3.776 1.00 0.00
        ATOM   172 N  THR R 59   -29.040 -22.485  4.171 1.00 0.00
        ATOM   173 CA THR R 59   -28.405 -23.777  3.884 1.00 0.00
  35    ATOM   174 C  THR R 59   -29.331 -24.758  3.170 1.00 0.00
        ATOM   175 O  THR R 59   -30.560 -24.647  3.205 1.00 0.00
```

87

SUBSTITUTE SHEET (RULE 26)

	ATOM	176	CB	THR R 59	-27.872 -24.385 5.190 1.00 0.00
	ATOM	177	OG1	THR R 59	-27.853 -23.393 6.235 1.00 0.00
	ATOM	178	CG2	THR R 59	-26.489 -25.021 5.023 1.00 0.00
	ATOM	179	H	THR R 59	-30.024 -22.480 4.346 1.00 0.00
5	ATOM	180	HG1	THR R 59	-27.610 -23.881 7.025 1.00 0.00
	ATOM	181	N	GLU R 60	-28.701 -25.728 2.496 1.00 0.00
	ATOM	182	CA	GLU R 60	-29.419 -26.674 1.647 1.00 0.00
	ATOM	183	C	GLU R 60	-30.161 -27.753 2.390 1.00 0.00
	ATOM	184	O	GLU R 60	-29.788 -28.927 2.459 1.00 0.00
10	ATOM	185	CB	GLU R 60	-28.473 -27.229 0.578 1.00 0.00
	ATOM	186	CG	GLU R 60	-28.436 -26.362 -0.692 1.00 0.00
	ATOM	187	CD	GLU R 60	-28.332 -24.886 -0.343 1.00 0.00
	ATOM	188	OE1	GLU R 60	-29.269 -24.151 -0.619 1.00 0.00
	ATOM	189	OE2	GLU R 60	-27.340 -24.471 0.243 1.00 0.00
15	ATOM	190	H	GLU R 60	-27.701 -25.728 2.526 1.00 0.00
	ATOM	191	N	CYS R 61	-31.270 -27.273 2.945 1.00 0.00
	ATOM	192	CA	CYS R 61	-32.170 -28.156 3.661 1.00 0.00
	ATOM	193	C	CYS R 61	-33.085 -28.944 2.755 1.00 0.00
	ATOM	194	O	CYS R 61	-34.299 -28.751 2.709 1.00 0.00
20	ATOM	195	CB	CYS R 61	-32.910 -27.347 4.714 1.00 0.00
	ATOM	196	SG	CYS R 61	-31.740 -26.942 6.031 1.00 0.00
	ATOM	197	H	CYS R 61	-31.509 -26.320 2.772 1.00 0.00
	ATOM	198	N	VAL R 62	-32.425 -29.827 1.999 1.00 0.00
	ATOM	199	CA	VAL R 62	-33.134 -30.711 1.091 1.00 0.00
25	ATOM	200	C	VAL R 62	-32.620 -32.122 1.268 1.00 0.00
	ATOM	201	O	VAL R 62	-31.507 -32.351 1.744 1.00 0.00
	ATOM	202	CB	VAL R 62	-32.966 -30.257 -0.371 1.00 0.00
	ATOM	203	CG1	VAL R 62	-33.771 -28.988 -0.662 1.00 0.00
	ATOM	204	CG2	VAL R 62	-31.491 -30.099 -0.762 1.00 0.00
30	ATOM	205	H	VAL R 62	-31.439 -29.935 2.116 1.00 0.00
	ATOM	206	N	GLY R 63	-33.482 -33.057 0.831 1.00 0.00
	ATOM	207	CA	GLY R 63	-33.115 -34.472 0.773 1.00 0.00
	ATOM	208	C	GLY R 63	-32.332 -34.987 1.965 1.00 0.00
	ATOM	209	O	GLY R 63	-32.817 -35.076 3.086 1.00 0.00
35	ATOM	210	H	GLY R 63	-34.346 -32.742 0.449 1.00 0.00
	ATOM	211	N	LEU R 64	-31.064 -35.302 1.662 1.00 0.00

88

SUBSTITUTE SHEET (RULE 26)

```
        ATOM    212 CA  LEU R 64    -30.174 -35.897  2.660 1.00 0.00
        ATOM    213 C   LEU R 64    -29.939 -35.063  3.905 1.00 0.00
        ATOM    214 O   LEU R 64    -29.748 -35.602  4.993 1.00 0.00
        ATOM    215 CB  LEU R 64    -28.818 -36.268  2.047 1.00 0.00
   5    ATOM    216 CG  LEU R 64    -28.759 -37.594  1.273 1.00 0.00
        ATOM    217 CD1 LEU R 64    -29.223 -38.770  2.135 1.00 0.00
        ATOM    218 CD2 LEU R 64    -29.458 -37.548 -0.089 1.00 0.00
        ATOM    219 H   LEU R 64    -30.789 -35.155  0.715 1.00 0.00
        ATOM    220 N   GLN R 65    -29.920 -33.749  3.667 1.00 0.00
  10    ATOM    221 CA  GLN R 65    -29.848 -32.806  4.767 1.00 0.00
        ATOM    222 C   GLN R 65    -31.138 -32.025  4.898 1.00 0.00
        ATOM    223 O   GLN R 65    -31.327 -30.896  4.444 1.00 0.00
        ATOM    224 CB  GLN R 65    -28.607 -31.923  4.628 1.00 0.00
        ATOM    225 CG  GLN R 65    -27.300 -32.698  4.852 1.00 0.00
  15    ATOM    226 CD  GLN R 65    -27.227 -33.242  6.271 1.00 0.00
        ATOM    227 OE1 GLN R 65    -28.016 -32.916  7.148 1.00 0.00
        ATOM    228 NE2 GLN R 65    -26.211 -34.066  6.484 1.00 0.00
        ATOM    229 H   GLN R 65    -30.093 -33.389  2.753 1.00 0.00
        ATOM    230 1HE2 GLN R 65   -26.039 -34.449  7.390 1.00 0.00
  20    ATOM    231 2HE2 GLN R 65   -25.596 -34.408  5.773 1.00 0.00
        ATOM    232 N   SER R 66    -32.061 -32.731  5.554 1.00 0.00
        ATOM    233 CA  SER R 66    -33.390 -32.190  5.816 1.00 0.00
        ATOM    234 C   SER R 66    -33.405 -31.182  6.954 1.00 0.00
        ATOM    235 O   SER R 66    -32.729 -31.340  7.966 1.00 0.00
  25    ATOM    236 CB  SER R 66    -34.355 -33.332  6.140 1.00 0.00
        ATOM    237 OG  SER R 66    -34.545 -34.205  5.013 1.00 0.00
        ATOM    238 H   SER R 66    -31.773 -33.614  5.922 1.00 0.00
        ATOM    239 HG  SER R 66    -33.695 -34.243  4.566 1.00 0.00
        ATOM    240 N   MET R 67    -34.238 -30.147  6.731 1.00 0.00
  30    ATOM    241 CA  MET R 67    -34.452 -29.049  7.683 1.00 0.00
        ATOM    242 C   MET R 67    -34.580 -29.454  9.146 1.00 0.00
        ATOM    243 O   MET R 67    -35.591 -30.030  9.547 1.00 0.00
        ATOM    244 CB  MET R 67    -35.701 -28.290  7.216 1.00 0.00
        ATOM    245 CG  MET R 67    -36.123 -27.081  8.053 1.00 0.00
  35    ATOM    246 SD  MET R 67    -37.648 -26.329  7.454 1.00 0.00
        ATOM    247 CE  MET R 67    -37.010 -25.683  5.898 1.00 0.00
```

89

```
       ATOM   248 H   MET R 67     -34.671 -30.083  5.833 1.00 0.00
       ATOM   249 N   SER R 68     -33.535 -29.137  9.905 1.00 0.00
       ATOM   250 CA  SER R 68     -33.655 -29.183 11.360 1.00 0.00
       ATOM   251 C   SER R 68     -34.023 -27.827 11.919 1.00 0.00
  5    ATOM   252 O   SER R 68     -34.862 -27.691 12.800 1.00 0.00
       ATOM   253 CB  SER R 68     -32.358 -29.637 12.009 1.00 0.00
       ATOM   254 OG  SER R 68     -31.643 -30.509 11.115 1.00 0.00
       ATOM   255 H   SER R 68     -32.761 -28.695  9.455 1.00 0.00
       ATOM   256 HG  SER R 68     -31.558 -30.009 10.294 1.00 0.00
 10    ATOM   257 N   ALA R 69     -33.375 -26.830 11.302 1.00 0.00
       ATOM   258 CA  ALA R 69     -33.917 -25.487 11.420 1.00 0.00
       ATOM   259 C   ALA R 69     -34.131 -24.964 10.022 1.00 0.00
       ATOM   260 O   ALA R 69     -33.406 -25.351  9.101 1.00 0.00
       ATOM   261 CB  ALA R 69     -32.949 -24.567 12.163 1.00 0.00
 15    ATOM   262 H   ALA R 69     -32.643 -27.065 10.660 1.00 0.00
       ATOM   263 N   PRO R 70     -35.166 -24.103  9.901 1.00 0.00
       ATOM   264 CA  PRO R 70     -35.349 -23.341  8.665 1.00 0.00
       ATOM   265 C   PRO R 70     -34.275 -22.271  8.587 1.00 0.00
       ATOM   266 O   PRO R 70     -33.227 -22.350  9.229 1.00 0.00
 20    ATOM   267 CB  PRO R 70     -36.770 -22.793  8.852 1.00 0.00
       ATOM   268 CG  PRO R 70     -36.928 -22.604 10.359 1.00 0.00
       ATOM   269 CD  PRO R 70     -36.166 -23.793 10.921 1.00 0.00
       ATOM   270 N   CYS R 71     -34.550 -21.233  7.785 1.00 0.00
       ATOM   271 CA  CYS R 71     -33.601 -20.119  7.809 1.00 0.00
 25    ATOM   272 C   CYS R 71     -33.970 -19.007  8.772 1.00 0.00
       ATOM   273 O   CYS R 71     -33.266 -18.019  8.957 1.00 0.00
       ATOM   274 CB  CYS R 71     -33.418 -19.571  6.407 1.00 0.00
       ATOM   275 SG  CYS R 71     -33.225 -20.894  5.186 1.00 0.00
       ATOM   276 H   CYS R 71     -35.393 -21.195  7.252 1.00 0.00
 30    ATOM   277 N   VAL R 72     -35.153 -19.212  9.378 1.00 0.00
       ATOM   278 CA  VAL R 72     -35.518 -18.365 10.505 1.00 0.00
       ATOM   279 C   VAL R 72     -35.220 -19.134 11.781 1.00 0.00
       ATOM   280 O   VAL R 72     -34.442 -20.088 11.731 1.00 0.00
       ATOM   281 CB  VAL R 72     -36.968 -17.871 10.369 1.00 0.00
 35    ATOM   282 CG1 VAL R 72     -37.035 -16.768  9.311 1.00 0.00
       ATOM   283 CG2 VAL R 72     -37.963 -18.992 10.064 1.00 0.00
```

90

	ATOM	284	H	VAL R 72	-35.684	-20.042	9.226	1.00 0.00
	ATOM	285	N	GLU R 73	-35.790	-18.668	12.904	1.00 0.00
	ATOM	286	CA	GLU R 73	-35.488	-19.248	14.217	1.00 0.00
	ATOM	287	C	GLU R 73	-34.000	-19.471	14.515	1.00 0.00
5	ATOM	288	O	GLU R 73	-33.279	-18.511	14.794	1.00 0.00
	ATOM	289	CB	GLU R 73	-36.399	-20.461	14.483	1.00 0.00
	ATOM	290	CG	GLU R 73	-37.842	-20.111	14.899	1.00 0.00
	ATOM	291	CD	GLU R 73	-38.628	-19.399	13.805	1.00 0.00
	ATOM	292	OE1	GLU R 73	-39.196	-20.066	12.948	1.00 0.00
10	ATOM	293	OE2	GLU R 73	-38.693	-18.173	13.816	1.00 0.00
	ATOM	294	H	GLU R 73	-36.613	-18.100	12.819	1.00 0.00
	ATOM	295	N	ALA R 74	-33.549	-20.733	14.428	1.00 0.00
	ATOM	296	CA	ALA R 74	-32.139	-20.969	14.723	1.00 0.00
	ATOM	297	C	ALA R 74	-31.209	-20.464	13.628	1.00 0.00
15	ATOM	298	O	ALA R 74	-31.627	-19.858	12.643	1.00 0.00
	ATOM	299	CB	ALA R 74	-31.896	-22.456	14.994	1.00 0.00
	ATOM	300	H	ALA R 74	-34.142	-21.443	14.054	1.00 0.00
	ATOM	301	N	ASP R 75	-29.901	-20.717	13.841	1.00 0.00
	ATOM	302	CA	ASP R 75	-28.988	-20.165	12.838	1.00 0.00
20	ATOM	303	C	ASP R 75	-28.978	-20.946	11.540	1.00 0.00
	ATOM	304	O	ASP R 75	-28.907	-22.175	11.568	1.00 0.00
	ATOM	305	CB	ASP R 75	-27.570	-19.881	13.412	1.00 0.00
	ATOM	306	CG	ASP R 75	-26.502	-20.949	13.148	1.00 0.00
	ATOM	307	OD1	ASP R 75	-25.764	-20.841	12.170	1.00 0.00
25	ATOM	308	OD2	ASP R 75	-26.375	-21.893	13.918	1.00 0.00
	ATOM	309	H	ASP R 75	-29.610	-21.308	14.596	1.00 0.00
	ATOM	310	N	ASP R 76	-29.031	-20.167	10.438	1.00 0.00
	ATOM	311	CA	ASP R 76	-28.563	-20.650	9.133	1.00 0.00
	ATOM	312	C	ASP R 76	-28.887	-22.099	8.799	1.00 0.00
30	ATOM	313	O	ASP R 76	-28.004	-22.960	8.851	1.00 0.00
	ATOM	314	CB	ASP R 76	-27.048	-20.433	9.048	1.00 0.00
	ATOM	315	CG	ASP R 76	-26.651	-19.628	7.832	1.00 0.00
	ATOM	316	OD1	ASP R 76	-26.280	-20.197	6.821	1.00 0.00
	ATOM	317	OD2	ASP R 76	-26.657	-18.412	7.895	1.00 0.00
35	ATOM	318	H	ASP R 76	-29.310	-19.218	10.546	1.00 0.00
	ATOM	319	N	ALA R 77	-30.181	-22.342	8.504	1.00 0.00

91

SUBSTITUTE SHEET (RULE 26)

	ATOM	320	CA	ALA R 77	-30.727	-23.675	8.210	1.00	0.00
	ATOM	321	C	ALA R 77	-29.903	-24.882	8.622	1.00	0.00
	ATOM	322	O	ALA R 77	-28.947	-25.313	7.977	1.00	0.00
	ATOM	323	CB	ALA R 77	-31.146	-23.786	6.745	1.00	0.00
5	ATOM	324	H	ALA R 77	-30.762	-21.532	8.486	1.00	0.00
	ATOM	325	N	VAL R 78	-30.293	-25.370	9.804	1.00	0.00
	ATOM	326	CA	VAL R 78	-29.473	-26.437	10.365	1.00	0.00
	ATOM	327	C	VAL R 78	-29.674	-27.730	9.608	1.00	0.00
	ATOM	328	O	VAL R 78	-30.689	-28.419	9.719	1.00	0.00
10	ATOM	329	CB	VAL R 78	-29.705	-26.621	11.875	1.00	0.00
	ATOM	330	CG1	VAL R 78	-28.824	-27.731	12.461	1.00	0.00
	ATOM	331	CG2	VAL R 78	-29.474	-25.311	12.630	1.00	0.00
	ATOM	332	H	VAL R 78	-31.196	-25.121	10.147	1.00	0.00
	ATOM	333	N	CYS R 79	-28.632	-28.038	8.838	1.00	0.00
15	ATOM	334	CA	CYS R 79	-28.713	-29.247	8.033	1.00	0.00
	ATOM	335	C	CYS R 79	-27.339	-29.828	7.920	1.00	0.00
	ATOM	336	O	CYS R 79	-26.525	-29.376	7.119	1.00	0.00
	ATOM	337	CB	CYS R 79	-29.320	-28.928	6.669	1.00	0.00
	ATOM	338	SG	CYS R 79	-31.114	-28.721	6.825	1.00	0.00
20	ATOM	339	H	CYS R 79	-27.953	-27.324	8.640	1.00	0.00
	ATOM	340	N	ARG R 80	-27.136	-30.778	8.851	1.00	0.00
	ATOM	341	CA	ARG R 80	-25.874	-31.473	9.118	1.00	0.00
	ATOM	342	C	ARG R 80	-26.145	-32.410	10.286	1.00	0.00
	ATOM	343	O	ARG R 80	-27.174	-32.258	10.947	1.00	0.00
25	ATOM	344	CB	ARG R 80	-24.794	-30.457	9.480	1.00	0.00
	ATOM	345	CG	ARG R 80	-23.510	-30.612	8.671	1.00	0.00
	ATOM	346	CD	ARG R 80	-23.609	-30.483	7.144	1.00	0.00
	ATOM	347	NE	ARG R 80	-22.248	-30.464	6.602	1.00	0.00
	ATOM	348	CZ	ARG R 80	-21.752	-29.350	6.025	1.00	0.00
30	ATOM	349	NH1	ARG R 80	-20.446	-29.201	5.899	1.00	0.00
	ATOM	350	NH2	ARG R 80	-22.565	-28.390	5.605	1.00	0.00
	ATOM	351	H	ARG R 80	-27.930	-31.029	9.408	1.00	0.00
	ATOM	352	HE	ARG R 80	-21.632	-31.222	6.850	1.00	0.00
	ATOM	353	1HH1	ARG R 80	-20.066	-28.349	5.510	1.00	0.00
35	ATOM	354	2HH1	ARG R 80	-19.803	-29.904	6.220	1.00	0.00
	ATOM	355	1HH2	ARG R 80	-22.163	-27.510	5.312	1.00	0.00

92

```
         ATOM   356 2HH2 ARG R 80    -23.555 -28.546  5.585 1.00 0.00
         ATOM   357 N  CYS R 81    -25.254 -33.378 10.546 1.00 0.00
         ATOM   358 CA CYS R 81    -25.630 -34.302 11.618 1.00 0.00
         ATOM   359 C  CYS R 81    -24.657 -34.425 12.779 1.00 0.00
    5    ATOM   360 O  CYS R 81    -23.437 -34.482 12.654 1.00 0.00
         ATOM   361 CB CYS R 81    -25.971 -35.691 11.060 1.00 0.00
         ATOM   362 SG CYS R 81    -27.286 -35.685  9.805 1.00 0.00
         ATOM   363 H  CYS R 81    -24.383 -33.437 10.057 1.00 0.00
         ATOM   364 N  ALA R 82    -25.276 -34.521 13.965 1.00 0.00
   10    ATOM   365 CA ALA R 82    -24.515 -34.749 15.194 1.00 0.00
         ATOM   366 C  ALA R 82    -25.304 -35.664 16.121 1.00 0.00
         ATOM   367 O  ALA R 82    -26.298 -36.259 15.706 1.00 0.00
         ATOM   368 CB ALA R 82    -24.220 -33.410 15.880 1.00 0.00
         ATOM   369 H  ALA R 82    -26.275 -34.483 13.959 1.00 0.00
   15    ATOM   370 N  TYR R 83    -24.873 -35.700 17.401 1.00 0.00
         ATOM   371 CA TYR R 83    -25.613 -36.307 18.519 1.00 0.00
         ATOM   372 C  TYR R 83    -25.565 -37.827 18.584 1.00 0.00
         ATOM   373 O  TYR R 83    -24.974 -38.412 19.487 1.00 0.00
         ATOM   374 CB TYR R 83    -27.078 -35.829 18.634 1.00 0.00
   20    ATOM   375 CG TYR R 83    -27.226 -34.328 18.781 1.00 0.00
         ATOM   376 CD1 TYR R 83   -26.962 -33.725 20.028 1.00 0.00
         ATOM   377 CD2 TYR R 83   -27.670 -33.574 17.674 1.00 0.00
         ATOM   378 CE1 TYR R 83   -27.210 -32.351 20.189 1.00 0.00
         ATOM   379 CE2 TYR R 83   -27.914 -32.198 17.834 1.00 0.00
   25    ATOM   380 CZ TYR R 83    -27.710 -31.608 19.099 1.00 0.00
         ATOM   381 OH TYR R 83    -28.024 -30.273 19.294 1.00 0.00
         ATOM   382 H  TYR R 83    -23.940 -35.374 17.555 1.00 0.00
         ATOM   383 HH TYR R 83    -28.217 -29.854 18.456 1.00 0.00
         ATOM   384 N  GLY R 84    -26.236 -38.425 17.591 1.00 0.00
   30    ATOM   385 CA GLY R 84    -26.228 -39.880 17.476 1.00 0.00
         ATOM   386 C  GLY R 84    -25.429 -40.269 16.256 1.00 0.00
         ATOM   387 O  GLY R 84    -24.379 -40.900 16.321 1.00 0.00
         ATOM   388 H  GLY R 84    -26.647 -37.841 16.890 1.00 0.00
         ATOM   389 N  TYR R 85    -25.951 -39.784 15.120 1.00 0.00
   35    ATOM   390 CA TYR R 85    -25.110 -39.752 13.923 1.00 0.00
         ATOM   391 C  TYR R 85    -24.142 -38.590 13.997 1.00 0.00
```

93

```
        ATOM   392 O   TYR R 85    -24.434 -37.463 13.597 1.00  0.00
        ATOM   393 CB  TYR R 85    -25.941 -39.668 12.637 1.00  0.00
        ATOM   394 CG  TYR R 85    -26.885 -40.843 12.509 1.00  0.00
        ATOM   395 CD1 TYR R 85    -26.367 -42.140 12.304 1.00  0.00
     5  ATOM   396 CD2 TYR R 85    -28.271 -40.602 12.591 1.00  0.00
        ATOM   397 CE1 TYR R 85    -27.258 -43.221 12.185 1.00  0.00
        ATOM   398 CE2 TYR R 85    -29.161 -41.681 12.467 1.00  0.00
        ATOM   399 CZ  TYR R 85    -28.645 -42.978 12.269 1.00  0.00
        ATOM   400 OH  TYR R 85    -29.528 -44.039 12.161 1.00  0.00
    10  ATOM   401 H   TYR R 85    -26.801 -39.267 15.189 1.00  0.00
        ATOM   402 HH  TYR R 85    -30.392 -43.682 11.979 1.00  0.00
        ATOM   403 N   TYR R 86    -23.001 -38.941 14.593 1.00  0.00
        ATOM   404 CA  TYR R 86    -21.996 -37.958 14.983 1.00  0.00
        ATOM   405 C   TYR R 86    -21.418 -37.177 13.824 1.00  0.00
    15  ATOM   406 O   TYR R 86    -21.126 -35.992 13.937 1.00  0.00
        ATOM   407 CB  TYR R 86    -20.809 -38.602 15.710 1.00  0.00
        ATOM   408 CG  TYR R 86    -21.207 -39.697 16.673 1.00  0.00
        ATOM   409 CD1 TYR R 86    -20.850 -41.023 16.352 1.00  0.00
        ATOM   410 CD2 TYR R 86    -21.890 -39.374 17.863 1.00  0.00
    20  ATOM   411 CE1 TYR R 86    -21.141 -42.050 17.264 1.00  0.00
        ATOM   412 CE2 TYR R 86    -22.184 -40.403 18.774 1.00  0.00
        ATOM   413 CZ  TYR R 86    -21.785 -41.722 18.473 1.00  0.00
        ATOM   414 OH  TYR R 86    -22.023 -42.711 19.413 1.00  0.00
        ATOM   415 H   TYR R 86    -22.958 -39.890 14.897 1.00  0.00
    25  ATOM   416 HH  TYR R 86    -21.495 -43.480 19.212 1.00  0.00
        ATOM   417 N   GLN R 87    -21.218 -37.946 12.732 1.00  0.00
        ATOM   418 CA  GLN R 87    -20.570 -37.470 11.510 1.00  0.00
        ATOM   419 C   GLN R 87    -19.097 -37.109 11.556 1.00  0.00
        ATOM   420 O   GLN R 87    -18.514 -36.712 12.563 1.00  0.00
    30  ATOM   421 CB  GLN R 87    -21.334 -36.316 10.855 1.00  0.00
        ATOM   422 CG  GLN R 87    -22.628 -36.720 10.170 1.00  0.00
        ATOM   423 CD  GLN R 87    -22.807 -35.859  8.937 1.00  0.00
        ATOM   424 OE1 GLN R 87    -23.553 -34.880  8.908 1.00  0.00
        ATOM   425 NE2 GLN R 87    -22.130 -36.305  7.879 1.00  0.00
    35  ATOM   426 H   GLN R 87    -21.584 -38.879 12.734 1.00  0.00
        ATOM   427 1HE2 GLN R 87   -22.399 -35.962  6.979 1.00  0.00
```

94

```
        ATOM   428 2HE2 GLN R 87    -21.431 -37.016  7.960 1.00 0.00
        ATOM   429 N   ASP R 88     -18.536 -37.210 10.345 1.00 0.00
        ATOM   430 CA  ASP R 88     -17.727 -36.069  9.929 1.00 0.00
        ATOM   431 C   ASP R 88     -18.634 -35.318  8.978 1.00 0.00
    5   ATOM   432 O   ASP R 88     -19.200 -35.901  8.064 1.00 0.00
        ATOM   433 CB  ASP R 88     -16.408 -36.490  9.269 1.00 0.00
        ATOM   434 CG  ASP R 88     -15.384 -35.376  9.431 1.00 0.00
        ATOM   435 OD1 ASP R 88     -14.915 -34.822  8.442 1.00 0.00
        ATOM   436 OD2 ASP R 88     -15.051 -35.032 10.560 1.00 0.00
   10   ATOM   437 H   ASP R 88     -19.040 -37.751  9.666 1.00 0.00
        ATOM   438 N   GLU R 89     -18.883 -34.048  9.301 1.00 0.00
        ATOM   439 CA  GLU R 89     -20.163 -33.427  8.949 1.00 0.00
        ATOM   440 C   GLU R 89     -20.666 -33.353  7.500 1.00 0.00
        ATOM   441 O   GLU R 89     -21.862 -33.159  7.271 1.00 0.00
   15   ATOM   442 CB  GLU R 89     -20.252 -32.098  9.722 1.00 0.00
        ATOM   443 CG  GLU R 89     -19.934 -30.765  9.024 1.00 0.00
        ATOM   444 CD  GLU R 89     -18.588 -30.734  8.336 1.00 0.00
        ATOM   445 OE1 GLU R 89     -18.494 -31.092  7.174 1.00 0.00
        ATOM   446 OE2 GLU R 89     -17.616 -30.321  8.940 1.00 0.00
   20   ATOM   447 H   GLU R 89     -18.289 -33.640  9.988 1.00 0.00
        ATOM   448 N   THR R 90     -19.709 -33.499  6.555 1.00 0.00
        ATOM   449 CA  THR R 90     -19.933 -32.941  5.217 1.00 0.00
        ATOM   450 C   THR R 90     -21.285 -33.118  4.552 1.00 0.00
        ATOM   451 O   THR R 90     -21.938 -34.160  4.600 1.00 0.00
   25   ATOM   452 CB  THR R 90     -18.810 -33.347  4.255 1.00 0.00
        ATOM   453 OG1 THR R 90     -17.674 -33.836  4.984 1.00 0.00
        ATOM   454 CG2 THR R 90     -18.392 -32.204  3.324 1.00 0.00
        ATOM   455 H   THR R 90     -18.784 -33.648  6.889 1.00 0.00
        ATOM   456 HG1 THR R 90     -17.327 -33.064  5.444 1.00 0.00
   30   ATOM   457 N   THR R 91     -21.647 -32.017  3.895 1.00 0.00
        ATOM   458 CA  THR R 91     -22.860 -31.897  3.097 1.00 0.00
        ATOM   459 C   THR R 91     -23.258 -33.149  2.323 1.00 0.00
        ATOM   460 O   THR R 91     -22.484 -33.676  1.526 1.00 0.00
        ATOM   461 CB  THR R 91     -22.647 -30.720  2.141 1.00 0.00
   35   ATOM   462 OG1 THR R 91     -21.666 -29.793  2.666 1.00 0.00
        ATOM   463 CG2 THR R 91     -23.964 -30.007  1.827 1.00 0.00
```

95

ATOM	464	H	THR R	91	-20.984	-31.271	3.860	1.00 0.00
ATOM	465	HG1	THR R	91	-20.894	-29.846	2.096	1.00 0.00
ATOM	466	N	GLY R	92	-24.499	-33.584	2.577	1.00 0.00
ATOM	467	CA	GLY R	92	-24.978	-34.710	1.781	1.00 0.00
ATOM	468	C	GLY R	92	-24.860	-36.093	2.409	1.00 0.00
ATOM	469	O	GLY R	92	-25.335	-37.085	1.850	1.00 0.00
ATOM	470	H	GLY R	92	-25.022	-33.210	3.337	1.00 0.00
ATOM	471	N	ARG R	93	-24.236	-36.138	3.595	1.00 0.00
ATOM	472	CA	ARG R	93	-24.173	-37.427	4.280	1.00 0.00
ATOM	473	C	ARG R	93	-24.418	-37.314	5.777	1.00 0.00
ATOM	474	O	ARG R	93	-24.453	-36.210	6.315	1.00 0.00
ATOM	475	CB	ARG R	93	-22.867	-38.152	3.925	1.00 0.00
ATOM	476	CG	ARG R	93	-21.604	-37.313	4.120	1.00 0.00
ATOM	477	CD	ARG R	93	-20.324	-38.083	3.779	1.00 0.00
ATOM	478	NE	ARG R	93	-19.135	-37.298	4.115	1.00 0.00
ATOM	479	CZ	ARG R	93	-18.683	-37.255	5.391	1.00 0.00
ATOM	480	NH1	ARG R	93	-17.741	-36.386	5.728	1.00 0.00
ATOM	481	NH2	ARG R	93	-19.200	-38.034	6.329	1.00 0.00
ATOM	482	H	ARG R	93	-23.801	-35.328	3.987	1.00 0.00
ATOM	483	HE	ARG R	93	-18.726	-36.705	3.421	1.00 0.00
ATOM	484	1HH1	ARG R	93	-17.400	-36.385	6.666	1.00 0.00
ATOM	485	2HH1	ARG R	93	-17.378	-35.697	5.095	1.00 0.00
ATOM	486	1HH2	ARG R	93	-18.999	-37.871	7.294	1.00 0.00
ATOM	487	2HH2	ARG R	93	-19.832	-38.785	6.135	1.00 0.00
ATOM	488	N	CYS R	94	-24.653	-38.506	6.371	1.00 0.00
ATOM	489	CA	CYS R	94	-24.768	-38.726	7.818	1.00 0.00
ATOM	490	C	CYS R	94	-24.488	-40.182	8.172	1.00 0.00
ATOM	491	O	CYS R	94	-25.041	-41.119	7.594	1.00 0.00
ATOM	492	CB	CYS R	94	-26.138	-38.358	8.397	1.00 0.00
ATOM	493	SG	CYS R	94	-26.692	-36.659	8.083	1.00 0.00
ATOM	494	H	CYS R	94	-24.611	-39.336	5.816	1.00 0.00
ATOM	495	N	GLU R	95	-23.572	-40.320	9.142	1.00 0.00
ATOM	496	CA	GLU R	95	-22.945	-41.588	9.514	1.00 0.00
ATOM	497	C	GLU R	95	-22.224	-41.383	10.836	1.00 0.00
ATOM	498	O	GLU R	95	-22.258	-40.278	11.382	1.00 0.00
ATOM	499	CB	GLU R	95	-21.981	-42.075	8.412	1.00 0.00

SUBSTITUTE SHEET (RULE 26)

```
       ATOM    500  CG  GLU R 95    -20.721 -41.229  8.154  1.00  0.00
       ATOM    501  CD  GLU R 95    -21.085 -39.811  7.761  1.00  0.00
       ATOM    502  OE1 GLU R 95    -21.467 -39.570  6.627  1.00  0.00
       ATOM    503  OE2 GLU R 95    -20.997 -38.922  8.591  1.00  0.00
  5    ATOM    504  H   GLU R 95    -23.203 -39.480  9.540  1.00  0.00
       ATOM    505  N   ALA R 96    -21.599 -42.462 11.332  1.00  0.00
       ATOM    506  CA  ALA R 96    -20.851 -42.305 12.578  1.00  0.00
       ATOM    507  C   ALA R 96    -19.527 -41.574 12.413  1.00  0.00
       ATOM    508  O   ALA R 96    -18.742 -41.952 11.544  1.00  0.00
  10   ATOM    509  CB  ALA R 96    -20.605 -43.668 13.231  1.00  0.00
       ATOM    510  OXT ALA R 96    -19.293 -40.619 13.151  1.00  0.00
       ATOM    511  H   ALA R 96    -21.711 -43.344 10.871  1.00  0.00
       END


  15   REMARK  1 Second CRD of p75$^{NTR}$, bound to BDNF.
       REMARK  2
       ATOM      1  N   CYS R 39    -28.731 -23.425 17.186  1.00  0.00
       ATOM      2  CA  CYS R 39    -29.491 -22.215 17.484  1.00  0.00
       ATOM      3  C   CYS R 39    -30.988 -22.434 17.523  1.00  0.00
  20   ATOM      4  O   CYS R 39    -31.773 -21.495 17.660  1.00  0.00
       ATOM      5  CB  CYS R 39    -29.203 -21.102 16.474  1.00  0.00
       ATOM      6  SG  CYS R 39    -27.698 -21.312 15.471  1.00  0.00
       ATOM      7 1H   CYS R 39    -27.735 -23.264 17.148  1.00  0.00
       ATOM      8 2H   CYS R 39    -28.868 -24.153 17.874  1.00  0.00
  25   ATOM      9 3H   CYS R 39    -28.982 -23.835 16.298  1.00  0.00
       ATOM     10  N   LEU R 40    -31.381 -23.704 17.336  1.00  0.00
       ATOM     11  CA  LEU R 40    -32.802 -24.005 17.397  1.00  0.00
       ATOM     12  C   LEU R 40    -33.098 -24.788 18.662  1.00  0.00
       ATOM     13  O   LEU R 40    -32.371 -24.712 19.645  1.00  0.00
  30   ATOM     14  CB  LEU R 40    -33.224 -24.736 16.114  1.00  0.00
       ATOM     15  CG  LEU R 40    -33.141 -23.868 14.854  1.00  0.00
       ATOM     16  CD1 LEU R 40    -33.498 -24.664 13.599  1.00  0.00
       ATOM     17  CD2 LEU R 40    -33.987 -22.598 14.968  1.00  0.00
       ATOM     18  H   LEU R 40    -30.734 -24.467 17.314  1.00  0.00
  35   ATOM     19  N   ASP R 41    -34.194 -25.545 18.604  1.00  0.00
       ATOM     20  CA  ASP R 41    -34.394 -26.559 19.630  1.00  0.00
```

97

	ATOM	21	C	ASP	R	41	-33.510	-27.762	19.326 1.00 0.00
	ATOM	22	O	ASP	R	41	-32.569	-27.678	18.542 1.00 0.00
	ATOM	23	CB	ASP	R	41	-35.888	-26.923	19.676 1.00 0.00
	ATOM	24	CG	ASP	R	41	-36.282	-27.631	18.391 1.00 0.00
5	ATOM	25	OD1	ASP	R	41	-36.462	-28.842	18.426 1.00 0.00
	ATOM	26	OD2	ASP	R	41	-36.364	-26.975	17.359 1.00 0.00
	ATOM	27	H	ASP	R	41	-34.766	-25.640	17.790 1.00 0.00
	ATOM	28	N	SER	R	42	-33.860	-28.892	19.945 1.00 0.00
	ATOM	29	CA	SER	R	42	-33.192	-30.156	19.648 1.00 0.00
10	ATOM	30	C	SER	R	42	-32.956	-30.499	18.173 1.00 0.00
	ATOM	31	O	SER	R	42	-31.967	-31.144	17.816 1.00 0.00
	ATOM	32	CB	SER	R	42	-33.975	-31.256	20.359 1.00 0.00
	ATOM	33	OG	SER	R	42	-34.507	-30.738	21.597 1.00 0.00
	ATOM	34	H	SER	R	42	-34.638	-28.916	20.568 1.00 0.00
15	ATOM	35	HG	SER	R	42	-35.328	-31.194	21.757 1.00 0.00
	ATOM	36	N	VAL	R	43	-33.884	-30.042	17.310 1.00 0.00
	ATOM	37	CA	VAL	R	43	-33.712	-30.372	15.895 1.00 0.00
	ATOM	38	C	VAL	R	43	-32.454	-29.826	15.235 1.00 0.00
	ATOM	39	O	VAL	R	43	-31.932	-30.402	14.281 1.00 0.00
20	ATOM	40	CB	VAL	R	43	-34.955	-30.058	15.044 1.00 0.00
	ATOM	41	CG1	VAL	R	43	-36.186	-30.773	15.604 1.00 0.00
	ATOM	42	CG2	VAL	R	43	-35.182	-28.560	14.824 1.00 0.00
	ATOM	43	H	VAL	R	43	-34.615	-29.433	17.633 1.00 0.00
	ATOM	44	N	THR	R	44	-31.938	-28.722	15.786 1.00 0.00
25	ATOM	45	CA	THR	R	44	-30.651	-28.248	15.283 1.00 0.00
	ATOM	46	C	THR	R	44	-29.869	-27.538	16.372 1.00 0.00
	ATOM	47	O	THR	R	44	-30.165	-26.391	16.716 1.00 0.00
	ATOM	48	CB	THR	R	44	-30.833	-27.333	14.062 1.00 0.00
	ATOM	49	OG1	THR	R	44	-31.913	-27.770	13.215 1.00 0.00
30	ATOM	50	CG2	THR	R	44	-29.538	-27.231	13.256 1.00 0.00
	ATOM	51	H	THR	R	44	-32.435	-28.226	16.507 1.00 0.00
	ATOM	52	HG1	THR	R	44	-31.927	-28.725	13.271 1.00 0.00
	ATOM	53	N	PHE	R	45	-28.911	-28.291	16.916 1.00 0.00
	ATOM	54	CA	PHE	R	45	-28.186	-27.770	18.069 1.00 0.00
35	ATOM	55	C	PHE	R	45	-26.993	-26.926	17.656 1.00 0.00
	ATOM	56	O	PHE	R	45	-26.806	-26.646	16.478 1.00 0.00

98

	ATOM	57	CB	PHE	R	45	-27.822	-28.924	19.006 1.00 0.00
	ATOM	58	CG	PHE	R	45	-26.899	-29.937	18.362 1.00 0.00
	ATOM	59	CD1	PHE	R	45	-27.449	-31.094	17.770 1.00 0.00
	ATOM	60	CD2	PHE	R	45	-25.503	-29.718	18.376 1.00 0.00
5	ATOM	61	CE1	PHE	R	45	-26.592	-32.040	17.179 1.00 0.00
	ATOM	62	CE2	PHE	R	45	-24.646	-30.663	17.785 1.00 0.00
	ATOM	63	CZ	PHE	R	45	-25.200	-31.813	17.186 1.00 0.00
	ATOM	64	H	PHE	R	45	-28.575	-29.099	16.440 1.00 0.00
	ATOM	65	N	SER	R	46	-26.169	-26.504	18.621 1.00 0.00
10	ATOM	66	CA	SER	R	46	-25.321	-25.406	18.156 1.00 0.00
	ATOM	67	C	SER	R	46	-23.805	-25.596	18.062 1.00 0.00
	ATOM	68	O	SER	R	46	-23.139	-25.015	17.205 1.00 0.00
	ATOM	69	CB	SER	R	46	-25.722	-24.118	18.887 1.00 0.00
	ATOM	70	OG	SER	R	46	-27.050	-24.244	19.441 1.00 0.00
15	ATOM	71	H	SER	R	46	-26.281	-26.700	19.596 1.00 0.00
	ATOM	72	HG	SER	R	46	-26.881	-24.590	20.319 1.00 0.00
	ATOM	73	N	ASP	R	47	-23.284	-26.424	18.982 1.00 0.00
	ATOM	74	CA	ASP	R	47	-21.847	-26.704	19.149 1.00 0.00
	ATOM	75	C	ASP	R	47	-20.914	-25.513	19.394 1.00 0.00
20	ATOM	76	O	ASP	R	47	-19.707	-25.533	19.159 1.00 0.00
	ATOM	77	CB	ASP	R	47	-21.313	-27.830	18.204 1.00 0.00
	ATOM	78	CG	ASP	R	47	-20.687	-27.453	16.853 1.00 0.00
	ATOM	79	OD1	ASP	R	47	-20.787	-28.220	15.898 1.00 0.00
	ATOM	80	OD2	ASP	R	47	-20.046	-26.421	16.716 1.00 0.00
25	ATOM	81	H	ASP	R	47	-23.930	-26.730	19.679 1.00 0.00
	ATOM	82	N	VAL	R	48	-21.525	-24.456	19.953 1.00 0.00
	ATOM	83	CA	VAL	R	48	-20.791	-23.190	20.089 1.00 0.00
	ATOM	84	C	VAL	R	48	-19.752	-23.030	21.212 1.00 0.00
	ATOM	85	O	VAL	R	48	-19.796	-22.163	22.083 1.00 0.00
30	ATOM	86	CB	VAL	R	48	-21.762	-22.000	20.041 1.00 0.00
	ATOM	87	CG1	VAL	R	48	-22.331	-21.847	18.628 1.00 0.00
	ATOM	88	CG2	VAL	R	48	-22.865	-22.095	21.103 1.00 0.00
	ATOM	89	H	VAL	R	48	-22.434	-24.585	20.351 1.00 0.00
	ATOM	90	N	VAL	R	49	-18.722	-23.884	21.116 1.00 0.00
35	ATOM	91	CA	VAL	R	49	-17.548	-23.718	21.974 1.00 0.00
	ATOM	92	C	VAL	R	49	-16.827	-22.386	21.754 1.00 0.00

99

```
        ATOM    93  O   VAL R  49    -16.199 -21.808 22.647 1.00 0.00
        ATOM    94  CB  VAL R  49    -16.621 -24.942 21.815 1.00 0.00
        ATOM    95  CG1 VAL R  49    -16.113 -25.126 20.379 1.00 0.00
        ATOM    96  CG2 VAL R  49    -15.490 -24.948 22.848 1.00 0.00
  5     ATOM    97  H   VAL R  49    -18.738 -24.575 20.398 1.00 0.00
        ATOM    98  N   SER R  50    -16.984 -21.895 20.512 1.00 0.00
        ATOM    99  CA  SER R  50    -16.545 -20.542 20.170 1.00 0.00
        ATOM   100  C   SER R  50    -17.478 -20.015 19.099 1.00 0.00
        ATOM   101  O   SER R  50    -18.142 -20.822 18.450 1.00 0.00
 10     ATOM   102  CB  SER R  50    -15.104 -20.582 19.665 1.00 0.00
        ATOM   103  OG  SER R  50    -14.388 -21.603 20.381 1.00 0.00
        ATOM   104  H   SER R  50    -17.472 -22.447 19.837 1.00 0.00
        ATOM   105  HG  SER R  50    -14.702 -21.503 21.280 1.00 0.00
        ATOM   106  N   ALA R  51    -17.535 -18.689 18.939 1.00 0.00
 15     ATOM   107  CA  ALA R  51    -18.444 -18.111 17.945 1.00 0.00
        ATOM   108  C   ALA R  51    -18.009 -18.327 16.502 1.00 0.00
        ATOM   109  O   ALA R  51    -17.384 -17.480 15.860 1.00 0.00
        ATOM   110  CB  ALA R  51    -18.633 -16.614 18.202 1.00 0.00
        ATOM   111  H   ALA R  51    -16.914 -18.119 19.470 1.00 0.00
 20     ATOM   112  N   THR R  52    -18.362 -19.542 16.034 1.00 0.00
        ATOM   113  CA  THR R  52    -17.855 -20.040 14.756 1.00 0.00
        ATOM   114  C   THR R  52    -18.740 -21.103 14.084 1.00 0.00
        ATOM   115  O   THR R  52    -18.814 -22.264 14.488 1.00 0.00
        ATOM   116  CB  THR R  52    -16.422 -20.581 14.935 1.00 0.00
 25     ATOM   117  OG1 THR R  52    -15.633 -19.712 15.770 1.00 0.00
        ATOM   118  CG2 THR R  52    -15.723 -20.802 13.589 1.00 0.00
        ATOM   119  H   THR R  52    -18.809 -20.200 16.644 1.00 0.00
        ATOM   120  HG1 THR R  52    -15.985 -18.832 15.634 1.00 0.00
        ATOM   121  N   GLU R  53    -19.349 -20.674 12.968 1.00 0.00
 30     ATOM   122  CA  GLU R  53    -20.398 -19.674 13.115 1.00 0.00
        ATOM   123  C   GLU R  53    -21.732 -20.164 13.692 1.00 0.00
        ATOM   124  O   GLU R  53    -22.195 -19.586 14.668 1.00 0.00
        ATOM   125  CB  GLU R  53    -20.639 -18.835 11.840 1.00 0.00
        ATOM   126  CG  GLU R  53    -19.550 -18.814 10.755 1.00 0.00
 35     ATOM   127  CD  GLU R  53    -19.530 -20.110  9.955 1.00 0.00
        ATOM   128  OE1 GLU R  53    -20.581 -20.583  9.522 1.00 0.00
```

100

```
        ATOM    129 OE2 GLU R  53    -18.455 -20.666  9.758  1.00  0.00
        ATOM    130 H   GLU R  53    -19.314 -21.243 12.150  1.00  0.00
        ATOM    131 N   PRO R  54    -22.382 -21.186 13.062  1.00  0.00
        ATOM    132 CA  PRO R  54    -23.801 -21.374 13.363  1.00  0.00
   5    ATOM    133 C   PRO R  54    -24.087 -22.600 14.224  1.00  0.00
        ATOM    134 O   PRO R  54    -23.206 -23.245 14.790  1.00  0.00
        ATOM    135 CB  PRO R  54    -24.322 -21.543 11.933  1.00  0.00
        ATOM    136 CG  PRO R  54    -23.279 -22.449 11.267  1.00  0.00
        ATOM    137 CD  PRO R  54    -21.973 -22.056 11.958  1.00  0.00
  10    ATOM    138 N   CYS R  55    -25.389 -22.945 14.169  1.00  0.00
        ATOM    139 CA  CYS R  55    -25.953 -24.243 14.552  1.00  0.00
        ATOM    140 C   CYS R  55    -25.269 -25.446 13.903  1.00  0.00
        ATOM    141 O   CYS R  55    -24.242 -25.300 13.245  1.00  0.00
        ATOM    142 CB  CYS R  55    -27.451 -24.242 14.222  1.00  0.00
  15    ATOM    143 SG  CYS R  55    -28.150 -22.588 13.922  1.00  0.00
        ATOM    144 H   CYS R  55    -26.029 -22.260 13.834  1.00  0.00
        ATOM    145 N   LYS R  56    -25.873 -26.628 14.098  1.00  0.00
        ATOM    146 CA  LYS R  56    -25.241 -27.917 13.821  1.00  0.00
        ATOM    147 C   LYS R  56    -26.256 -29.045 13.957  1.00  0.00
  20    ATOM    148 O   LYS R  56    -26.703 -29.417 15.037  1.00  0.00
        ATOM    149 CB  LYS R  56    -24.073 -28.150 14.789  1.00  0.00
        ATOM    150 CG  LYS R  56    -23.350 -29.501 14.702  1.00  0.00
        ATOM    151 CD  LYS R  56    -22.658 -29.801 13.373  1.00  0.00
        ATOM    152 CE  LYS R  56    -21.673 -30.966 13.503  1.00  0.00
  25    ATOM    153 NZ  LYS R  56    -20.454 -30.524 14.191  1.00  0.00
        ATOM    154 H   LYS R  56    -26.725 -26.673 14.623  1.00  0.00
        ATOM    155 1HZ LYS R  56    -19.887 -31.370 14.402  1.00  0.00
        ATOM    156 2HZ LYS R  56    -20.632 -30.000 15.073  1.00  0.00
        ATOM    157 3HZ LYS R  56    -19.886 -29.946 13.544  1.00  0.00
  30    ATOM    158 N   PRO R  57    -26.633 -29.599 12.787  1.00  0.00
        ATOM    159 CA  PRO R  57    -27.416 -30.837 12.811  1.00  0.00
        ATOM    160 C   PRO R  57    -26.644 -31.966 13.476  1.00  0.00
        ATOM    161 O   PRO R  57    -25.420 -31.911 13.609  1.00  0.00
        ATOM    162 CB  PRO R  57    -27.665 -31.109 11.323  1.00  0.00
  35    ATOM    163 CG  PRO R  57    -27.447 -29.776 10.607  1.00  0.00
```

101

	ATOM	164	CD	PRO R	57	-26.356	-29.119	11.441	1.00	0.00
	ATOM	165	N	CYS R	58	-27.418	-32.994	13.860	1.00	0.00
	ATOM	166	CA	CYS R	58	-26.761	-34.217	14.319	1.00	0.00
	ATOM	167	C	CYS R	58	-26.309	-35.070	13.141	1.00	0.00
5	ATOM	168	O	CYS R	58	-26.576	-34.743	11.987	1.00	0.00
	ATOM	169	CB	CYS R	58	-27.709	-34.963	15.259	1.00	0.00
	ATOM	170	SG	CYS R	58	-27.015	-36.478	15.973	1.00	0.00
	ATOM	171	H	CYS R	58	-28.408	-32.886	13.776	1.00	0.00
	ATOM	172	N	THR R	59	-25.623	-36.173	13.459	1.00	0.00
10	ATOM	173	CA	THR R	59	-25.066	-37.074	12.445	1.00	0.00
	ATOM	174	C	THR R	59	-26.048	-38.160	11.949	1.00	0.00
	ATOM	175	O	THR R	59	-27.196	-38.234	12.397	1.00	0.00
	ATOM	176	CB	THR R	59	-23.767	-37.636	13.055	1.00	0.00
	ATOM	177	OG1	THR R	59	-23.270	-36.723	14.052	1.00	0.00
15	ATOM	178	CG2	THR R	59	-22.667	-37.924	12.029	1.00	0.00
	ATOM	179	H	THR R	59	-25.398	-36.368	14.415	1.00	0.00
	ATOM	180	HG1	THR R	59	-22.729	-37.252	14.644	1.00	0.00
	ATOM	181	N	GLU R	60	-25.578	-38.985	10.999	1.00	0.00
	ATOM	182	CA	GLU R	60	-26.467	-40.006	10.445	1.00	0.00
20	ATOM	183	C	GLU R	60	-26.899	-41.149	11.355	1.00	0.00
	ATOM	184	O	GLU R	60	-26.152	-42.083	11.672	1.00	0.00
	ATOM	185	CB	GLU R	60	-25.943	-40.541	9.111	1.00	0.00
	ATOM	186	CG	GLU R	60	-27.011	-40.494	8.010	1.00	0.00
	ATOM	187	CD	GLU R	60	-28.263	-41.228	8.450	1.00	0.00
25	ATOM	188	OE1	GLU R	60	-28.349	-42.428	8.253	1.00	0.00
	ATOM	189	OE2	GLU R	60	-29.161	-40.605	9.003	1.00	0.00
	ATOM	190	H	GLU R	60	-24.642	-38.859	10.693	1.00	0.00
	ATOM	191	N	CYS R	61	-28.169	-41.001	11.750	1.00	0.00
	ATOM	192	CA	CYS R	61	-28.775	-41.881	12.742	1.00	0.00
30	ATOM	193	C	CYS R	61	-29.712	-42.937	12.185	1.00	0.00
	ATOM	194	O	CYS R	61	-30.148	-43.845	12.890	1.00	0.00
	ATOM	195	CB	CYS R	61	-29.564	-41.086	13.782	1.00	0.00
	ATOM	196	SG	CYS R	61	-28.791	-39.568	14.416	1.00	0.00
	ATOM	197	H	CYS R	61	-28.690	-40.307	11.255	1.00	0.00
35	ATOM	198	N	VAL R	62	-30.069	-42.806	10.908	1.00	0.00
	ATOM	199	CA	VAL R	62	-31.084	-43.768	10.496	1.00	0.00

102

SUBSTITUTE SHEET (RULE 26)

```
        ATOM  200  C   VAL R 62    -30.571 -44.884  9.598 1.00 0.00
        ATOM  201  O   VAL R 62    -30.480 -46.055  9.964 1.00 0.00
        ATOM  202  CB  VAL R 62    -32.301 -43.050  9.878 1.00 0.00
        ATOM  203  CG1 VAL R 62    -33.489 -44.005  9.713 1.00 0.00
   5    ATOM  204  CG2 VAL R 62    -32.705 -41.812 10.685 1.00 0.00
        ATOM  205  H   VAL R 62    -29.584 -42.202 10.268 1.00 0.00
        ATOM  206  N   GLY R 63    -30.336 -44.466  8.349 1.00 0.00
        ATOM  207  CA  GLY R 63    -30.443 -45.442  7.270 1.00 0.00
        ATOM  208  C   GLY R 63    -29.148 -45.809  6.584 1.00 0.00
   10   ATOM  209  O   GLY R 63    -29.004 -46.882  6.009 1.00 0.00
        ATOM  210  H   GLY R 63    -30.082 -43.508  8.197 1.00 0.00
        ATOM  211  N   LEU R 64    -28.206 -44.867  6.628 1.00 0.00
        ATOM  212  CA  LEU R 64    -26.859 -45.283  6.260 1.00 0.00
        ATOM  213  C   LEU R 64    -26.145 -45.795  7.489 1.00 0.00
   15   ATOM  214  O   LEU R 64    -25.525 -46.855  7.545 1.00 0.00
        ATOM  215  CB  LEU R 64    -26.088 -44.113  5.644 1.00 0.00
        ATOM  216  CG  LEU R 64    -26.754 -43.525  4.397 1.00 0.00
        ATOM  217  CD1 LEU R 64    -26.073 -42.229  3.958 1.00 0.00
        ATOM  218  CD2 LEU R 64    -26.848 -44.540  3.255 1.00 0.00
   20   ATOM  219  H   LEU R 64    -28.391 -43.992  7.076 1.00 0.00
        ATOM  220  N   GLN R 65    -26.262 -44.951  8.515 1.00 0.00
        ATOM  221  CA  GLN R 65    -25.639 -45.245  9.796 1.00 0.00
        ATOM  222  C   GLN R 65    -26.708 -45.080 10.851 1.00 0.00
        ATOM  223  O   GLN R 65    -27.738 -44.460 10.612 1.00 0.00
   25   ATOM  224  CB  GLN R 65    -24.456 -44.300 10.006 1.00 0.00
        ATOM  225  CG  GLN R 65    -23.336 -44.444  8.965 1.00 0.00
        ATOM  226  CD  GLN R 65    -22.421 -45.624  9.253 1.00 0.00
        ATOM  227  OE1 GLN R 65    -21.315 -45.443  9.762 1.00 0.00
        ATOM  228  NE2 GLN R 65    -22.857 -46.816  8.833 1.00 0.00
   30   ATOM  229  H   GLN R 65    -26.850 -44.141  8.449 1.00 0.00
        ATOM  230 1HE2 GLN R 65    -22.292 -47.635  8.846 1.00 0.00
        ATOM  231 2HE2 GLN R 65    -23.800 -46.898  8.500 1.00 0.00
        ATOM  232  N   SER R 66    -26.473 -45.715 12.001 1.00 0.00
        ATOM  233  CA  SER R 66    -27.657 -45.886 12.838 1.00 0.00
   35   ATOM  234  C   SER R 66    -27.604 -45.224 14.204 1.00 0.00
        ATOM  235  O   SER R 66    -26.542 -44.815 14.682 1.00 0.00
```

SUBSTITUTE SHEET (RULE 26)

	ATOM	236	CB	SER R 66	-28.013	-47.373	12.884	1.00	0.00
	ATOM	237	OG	SER R 66	-27.869	-47.927	11.565	1.00	0.00
	ATOM	238	H	SER R 66	-25.586	-46.141	12.173	1.00	0.00
	ATOM	239	HG	SER R 66	-28.474	-47.423	11.013	1.00	0.00
5	ATOM	240	N	MET R 67	-28.808	-45.110	14.779	1.00	0.00
	ATOM	241	CA	MET R 67	-29.048	-44.257	15.939	1.00	0.00
	ATOM	242	C	MET R 67	-28.294	-44.575	17.212	1.00	0.00
	ATOM	243	O	MET R 67	-28.404	-45.649	17.800	1.00	0.00
	ATOM	244	CB	MET R 67	-30.556	-44.203	16.197	1.00	0.00
10	ATOM	245	CG	MET R 67	-31.008	-42.933	16.916	1.00	0.00
	ATOM	246	SD	MET R 67	-32.793	-42.833	17.123	1.00	0.00
	ATOM	247	CE	MET R 67	-33.244	-42.903	15.380	1.00	0.00
	ATOM	248	H	MET R 67	-29.573	-45.360	14.189	1.00	0.00
	ATOM	249	N	SER R 68	-27.557	-43.553	17.633	1.00	0.00
15	ATOM	250	CA	SER R 68	-26.992	-43.620	18.977	1.00	0.00
	ATOM	251	C	SER R 68	-27.868	-42.986	20.035	1.00	0.00
	ATOM	252	O	SER R 68	-27.813	-43.326	21.215	1.00	0.00
	ATOM	253	CB	SER R 68	-25.615	-42.989	18.978	1.00	0.00
	ATOM	254	OG	SER R 68	-25.029	-43.228	17.693	1.00	0.00
20	ATOM	255	H	SER R 68	-27.423	-42.756	17.044	1.00	0.00
	ATOM	256	HG	SER R 68	-24.083	-43.177	17.834	1.00	0.00
	ATOM	257	N	ALA R 69	-28.706	-42.060	19.521	1.00	0.00
	ATOM	258	CA	ALA R 69	-29.837	-41.437	20.214	1.00	0.00
	ATOM	259	C	ALA R 69	-30.311	-40.307	19.312	1.00	0.00
25	ATOM	260	O	ALA R 69	-29.592	-39.924	18.387	1.00	0.00
	ATOM	261	CB	ALA R 69	-29.406	-40.835	21.565	1.00	0.00
	ATOM	262	H	ALA R 69	-28.493	-41.701	18.610	1.00	0.00
	ATOM	263	N	PRO R 70	-31.506	-39.724	19.607	1.00	0.00
	ATOM	264	CA	PRO R 70	-31.722	-38.322	19.207	1.00	0.00
30	ATOM	265	C	PRO R 70	-30.580	-37.436	19.699	1.00	0.00
	ATOM	266	O	PRO R 70	-29.722	-37.895	20.456	1.00	0.00
	ATOM	267	CB	PRO R 70	-33.063	-37.990	19.869	1.00	0.00
	ATOM	268	CG	PRO R 70	-33.779	-39.331	20.022	1.00	0.00
	ATOM	269	CD	PRO R 70	-32.637	-40.289	20.334	1.00	0.00
35	ATOM	270	N	CYS R 71	-30.549	-36.191	19.227	1.00	0.00
	ATOM	271	CA	CYS R 71	-29.381	-35.417	19.642	1.00	0.00

104

```
        ATOM   272 C   CYS R 71    -29.730 -34.124 20.337 1.00 0.00
        ATOM   273 O   CYS R 71    -30.848 -33.618 20.262 1.00 0.00
        ATOM   274 CB  CYS R 71    -28.418 -35.200 18.474 1.00 0.00
        ATOM   275 SG  CYS R 71    -27.801 -36.785 17.835 1.00 0.00
     5  ATOM   276 H   CYS R 71    -31.299 -35.781 18.711 1.00 0.00
        ATOM   277 N   VAL R 72    -28.733 -33.641 21.079 1.00 0.00
        ATOM   278 CA  VAL R 72    -28.793 -32.337 21.739 1.00 0.00
        ATOM   279 C   VAL R 72    -27.441 -31.695 21.515 1.00 0.00
        ATOM   280 O   VAL R 72    -26.587 -32.323 20.897 1.00 0.00
    10  ATOM   281 CB  VAL R 72    -29.087 -32.477 23.244 1.00 0.00
        ATOM   282 CG1 VAL R 72    -30.554 -32.827 23.502 1.00 0.00
        ATOM   283 CG2 VAL R 72    -28.125 -33.455 23.932 1.00 0.00
        ATOM   284 H   VAL R 72    -27.860 -34.132 21.089 1.00 0.00
        ATOM   285 N   GLU R 73    -27.282 -30.465 22.038 1.00 0.00
    15  ATOM   286 CA  GLU R 73    -25.992 -29.787 21.908 1.00 0.00
        ATOM   287 C   GLU R 73    -24.848 -30.522 22.569 1.00 0.00
        ATOM   288 O   GLU R 73    -24.610 -30.447 23.773 1.00 0.00
        ATOM   289 CB  GLU R 73    -26.073 -28.328 22.365 1.00 0.00
        ATOM   290 CG  GLU R 73    -24.825 -27.556 21.923 1.00 0.00
    20  ATOM   291 CD  GLU R 73    -24.974 -26.067 22.159 1.00 0.00
        ATOM   292 OE1 GLU R 73    -25.947 -25.478 21.698 1.00 0.00
        ATOM   293 OE2 GLU R 73    -24.103 -25.484 22.793 1.00 0.00
        ATOM   294 H   GLU R 73    -28.030 -30.065 22.564 1.00 0.00
        ATOM   295 N   ALA R 74    -24.183 -31.276 21.690 1.00 0.00
    25  ATOM   296 CA  ALA R 74    -22.982 -32.030 22.006 1.00 0.00
        ATOM   297 C   ALA R 74    -22.211 -32.099 20.717 1.00 0.00
        ATOM   298 O   ALA R 74    -22.796 -32.213 19.640 1.00 0.00
        ATOM   299 CB  ALA R 74    -23.328 -33.451 22.455 1.00 0.00
        ATOM   300 H   ALA R 74    -24.600 -31.329 20.777 1.00 0.00
    30  ATOM   301 N   ASP R 75    -20.889 -31.945 20.853 1.00 0.00
        ATOM   302 CA  ASP R 75    -20.105 -31.837 19.633 1.00 0.00
        ATOM   303 C   ASP R 75    -20.167 -33.101 18.799 1.00 0.00
        ATOM   304 O   ASP R 75    -20.254 -34.213 19.326 1.00 0.00
        ATOM   305 CB  ASP R 75    -18.676 -31.418 19.976 1.00 0.00
    35  ATOM   306 CG  ASP R 75    -18.194 -30.327 19.038 1.00 0.00
        ATOM   307 OD1 ASP R 75    -17.534 -29.398 19.470 1.00 0.00
```

105

	ATOM	308	OD2	ASP	R	75	-18.410	-30.388	17.841	1.00	0.00
	ATOM	309	H	ASP	R	75	-20.452	-31.968	21.747	1.00	0.00
	ATOM	310	N	ASP	R	76	-20.194	-32.858	17.466	1.00	0.00
	ATOM	311	CA	ASP	R	76	-20.556	-33.842	16.433	1.00	0.00
5	ATOM	312	C	ASP	R	76	-21.294	-35.063	16.965	1.00	0.00
	ATOM	313	O	ASP	R	76	-20.725	-36.140	17.153	1.00	0.00
	ATOM	314	CB	ASP	R	76	-19.324	-34.222	15.591	1.00	0.00
	ATOM	315	CG	ASP	R	76	-18.850	-33.033	14.765	1.00	0.00
	ATOM	316	OD1	ASP	R	76	-18.213	-32.134	15.285	1.00	0.00
10	ATOM	317	OD2	ASP	R	76	-19.132	-32.953	13.580	1.00	0.00
	ATOM	318	H	ASP	R	76	-19.875	-31.943	17.215	1.00	0.00
	ATOM	319	N	ALA	R	77	-22.571	-34.806	17.303	1.00	0.00
	ATOM	320	CA	ALA	R	77	-23.290	-35.694	18.218	1.00	0.00
	ATOM	321	C	ALA	R	77	-23.531	-37.073	17.651	1.00	0.00
15	ATOM	322	O	ALA	R	77	-23.725	-37.259	16.456	1.00	0.00
	ATOM	323	CB	ALA	R	77	-24.619	-35.075	18.644	1.00	0.00
	ATOM	324	H	ALA	R	77	-23.001	-34.012	16.881	1.00	0.00
	ATOM	325	N	VAL	R	78	-23.455	-38.052	18.556	1.00	0.00
	ATOM	326	CA	VAL	R	78	-22.704	-39.281	18.232	1.00	0.00
20	ATOM	327	C	VAL	R	78	-23.295	-40.388	17.344	1.00	0.00
	ATOM	328	O	VAL	R	78	-23.041	-41.583	17.543	1.00	0.00
	ATOM	329	CB	VAL	R	78	-22.160	-39.877	19.542	1.00	0.00
	ATOM	330	CG1	VAL	R	78	-21.189	-38.911	20.224	1.00	0.00
	ATOM	331	CG2	VAL	R	78	-23.287	-40.288	20.497	1.00	0.00
25	ATOM	332	H	VAL	R	78	-23.598	-37.743	19.493	1.00	0.00
	ATOM	333	N	CYS	R	79	-24.111	-40.011	16.349	1.00	0.00
	ATOM	334	CA	CYS	R	79	-24.667	-41.058	15.490	1.00	0.00
	ATOM	335	C	CYS	R	79	-23.639	-41.706	14.569	1.00	0.00
	ATOM	336	O	CYS	R	79	-23.161	-41.097	13.611	1.00	0.00
30	ATOM	337	CB	CYS	R	79	-25.854	-40.535	14.695	1.00	0.00
	ATOM	338	SG	CYS	R	79	-27.265	-40.010	15.706	1.00	0.00
	ATOM	339	H	CYS	R	79	-24.146	-39.049	16.105	1.00	0.00
	ATOM	340	N	ARG	R	80	-23.326	-42.955	14.966	1.00	0.00
	ATOM	341	CA	ARG	R	80	-22.220	-43.688	14.354	1.00	0.00
35	ATOM	342	C	ARG	R	80	-22.617	-45.027	13.739	1.00	0.00
	ATOM	343	O	ARG	R	80	-22.898	-45.120	12.547	1.00	0.00

106

SUBSTITUTE SHEET (RULE 26)

```
        ATOM   344 CB  ARG R  80   -21.047 -43.866  15.333  1.00  0.00
        ATOM   345 CG  ARG R  80   -19.958 -42.787  15.285  1.00  0.00
        ATOM   346 CD  ARG R  80   -19.283 -42.600  13.916  1.00  0.00
        ATOM   347 NE  ARG R  80   -18.739 -43.844  13.361  1.00  0.00
   5    ATOM   348 CZ  ARG R  80   -19.343 -44.423  12.298  1.00  0.00
        ATOM   349 NH1 ARG R  80   -18.915 -45.588  11.814  1.00  0.00
        ATOM   350 NH2 ARG R  80   -20.397 -43.844  11.740  1.00  0.00
        ATOM   351 H   ARG R  80   -23.849 -43.366  15.715  1.00  0.00
        ATOM   352 HE  ARG R  80   -17.952 -44.277  13.804  1.00  0.00
  10    ATOM   353 1HH1 ARG R  80  -19.409 -46.064  11.082  1.00  0.00
        ATOM   354 2HH1 ARG R  80  -18.080 -46.022  12.174  1.00  0.00
        ATOM   355 1HH2 ARG R  80  -20.880 -44.269  10.976  1.00  0.00
        ATOM   356 2HH2 ARG R  80  -20.749 -42.984  12.102  1.00  0.00
        ATOM   357 N   CYS R  81   -22.630 -46.086  14.566  1.00  0.00
  15    ATOM   358 CA  CYS R  81   -22.946 -47.400  14.002  1.00  0.00
        ATOM   359 C   CYS R  81   -23.527 -48.331  15.049  1.00  0.00
        ATOM   360 O   CYS R  81   -22.830 -49.080  15.728  1.00  0.00
        ATOM   361 CB  CYS R  81   -21.732 -48.025  13.284  1.00  0.00
        ATOM   362 SG  CYS R  81   -22.046 -48.494  11.547  1.00  0.00
  20    ATOM   363 H   CYS R  81   -22.342 -45.997  15.517  1.00  0.00
        ATOM   364 N   ALA R  82   -24.869 -48.212  15.160  1.00  0.00
        ATOM   365 CA  ALA R  82   -25.712 -49.047  16.033  1.00  0.00
        ATOM   366 C   ALA R  82   -25.041 -49.677  17.246  1.00  0.00
        ATOM   367 O   ALA R  82   -24.801 -50.881  17.310  1.00  0.00
  25    ATOM   368 CB  ALA R  82   -26.390 -50.148  15.212  1.00  0.00
        ATOM   369 H   ALA R  82   -25.322 -47.577  14.537  1.00  0.00
        ATOM   370 N   TYR R  83   -24.697 -48.786  18.189  1.00  0.00
        ATOM   371 CA  TYR R  83   -23.809 -49.240  19.256  1.00  0.00
        ATOM   372 C   TYR R  83   -24.319 -50.384  20.116  1.00  0.00
  30    ATOM   373 O   TYR R  83   -25.492 -50.522  20.451  1.00  0.00
        ATOM   374 CB  TYR R  83   -23.268 -48.059  20.087  1.00  0.00
        ATOM   375 CG  TYR R  83   -24.247 -47.511  21.108  1.00  0.00
        ATOM   376 CD1 TYR R  83   -25.207 -46.556  20.715  1.00  0.00
        ATOM   377 CD2 TYR R  83   -24.147 -47.951  22.445  1.00  0.00
  35    ATOM   378 CE1 TYR R  83   -26.058 -46.003  21.688  1.00  0.00
        ATOM   379 CE2 TYR R  83   -25.001 -47.400  23.417  1.00  0.00
```

107

```
       ATOM   380 CZ  TYR R 83    -25.937 -46.419 23.031 1.00 0.00
       ATOM   381 OH  TYR R 83    -26.753 -45.849 23.995 1.00 0.00
       ATOM   382 H   TYR R 83    -25.061 -47.858 18.145 1.00 0.00
       ATOM   383 HH  TYR R 83    -27.139 -45.055 23.619 1.00 0.00
   5   ATOM   384 N   GLY R 84    -23.359 -51.236 20.478 1.00 0.00
       ATOM   385 CA  GLY R 84    -23.783 -52.411 21.232 1.00 0.00
       ATOM   386 C   GLY R 84    -23.284 -53.694 20.609 1.00 0.00
       ATOM   387 O   GLY R 84    -23.189 -54.732 21.259 1.00 0.00
       ATOM   388 H   GLY R 84    -22.420 -51.099 20.167 1.00 0.00
  10   ATOM   389 N   TYR R 85    -22.925 -53.551 19.317 1.00 0.00
       ATOM   390 CA  TYR R 85    -21.764 -54.346 18.941 1.00 0.00
       ATOM   391 C   TYR R 85    -20.520 -53.484 19.090 1.00 0.00
       ATOM   392 O   TYR R 85    -20.632 -52.266 19.248 1.00 0.00
       ATOM   393 CB  TYR R 85    -21.930 -54.959 17.539 1.00 0.00
  15   ATOM   394 CG  TYR R 85    -21.890 -53.946 16.413 1.00 0.00
       ATOM   395 CD1 TYR R 85    -23.084 -53.333 15.975 1.00 0.00
       ATOM   396 CD2 TYR R 85    -20.649 -53.671 15.805 1.00 0.00
       ATOM   397 CE1 TYR R 85    -23.042 -52.477 14.860 1.00 0.00
       ATOM   398 CE2 TYR R 85    -20.609 -52.814 14.697 1.00 0.00
  20   ATOM   399 CZ  TYR R 85    -21.808 -52.257 14.215 1.00 0.00
       ATOM   400 OH  TYR R 85    -21.760 -51.493 13.062 1.00 0.00
       ATOM   401 H   TYR R 85    -23.172 -52.734 18.790 1.00 0.00
       ATOM   402 HH  TYR R 85    -20.964 -51.753 12.596 1.00 0.00
       ATOM   403 N   TYR R 86    -19.354 -54.143 19.022 1.00 0.00
  25   ATOM   404 CA  TYR R 86    -18.070 -53.498 19.330 1.00 0.00
       ATOM   405 C   TYR R 86    -17.547 -52.466 18.319 1.00 0.00
       ATOM   406 O   TYR R 86    -16.457 -52.635 17.784 1.00 0.00
       ATOM   407 CB  TYR R 86    -17.072 -54.652 19.552 1.00 0.00
       ATOM   408 CG  TYR R 86    -15.786 -54.368 20.316 1.00 0.00
  30   ATOM   409 CD1 TYR R 86    -15.322 -53.061 20.597 1.00 0.00
       ATOM   410 CD2 TYR R 86    -15.053 -55.502 20.719 1.00 0.00
       ATOM   411 CE1 TYR R 86    -14.087 -52.896 21.255 1.00 0.00
       ATOM   412 CE2 TYR R 86    -13.825 -55.340 21.380 1.00 0.00
       ATOM   413 CZ  TYR R 86    -13.346 -54.040 21.627 1.00 0.00
  35   ATOM   414 OH  TYR R 86    -12.110 -53.911 22.244 1.00 0.00
       ATOM   415 H   TYR R 86    -19.425 -55.102 18.757 1.00 0.00
```

```
        ATOM    416  HH  TYR R  86   -11.829 -53.003  22.149  1.00  0.00
        ATOM    417  N   GLN R  87   -18.334 -51.399  18.081  1.00  0.00
        ATOM    418  CA  GLN R  87   -17.800 -50.310  17.258  1.00  0.00
        ATOM    419  C   GLN R  87   -17.117 -49.255  18.112  1.00  0.00
   5    ATOM    420  O   GLN R  87   -17.704 -48.681  19.022  1.00  0.00
        ATOM    421  CB  GLN R  87   -18.910 -49.706  16.371  1.00  0.00
        ATOM    422  CG  GLN R  87   -18.725 -48.273  15.812  1.00  0.00
        ATOM    423  CD  GLN R  87   -17.729 -48.089  14.663  1.00  0.00
        ATOM    424  OE1 GLN R  87   -17.701 -47.027  14.040  1.00  0.00
  10    ATOM    425  NE2 GLN R  87   -16.936 -49.120  14.374  1.00  0.00
        ATOM    426  H   GLN R  87   -19.143 -51.256  18.647  1.00  0.00
        ATOM    427  1HE2 GLN R  87  -16.239 -49.104  13.659  1.00  0.00
        ATOM    428  2HE2 GLN R  87  -16.869 -50.003  14.846  1.00  0.00
        ATOM    429  N   ASP R  88   -15.845 -49.028  17.759  1.00  0.00
  15    ATOM    430  CA  ASP R  88   -15.041 -48.001  18.429  1.00  0.00
        ATOM    431  C   ASP R  88   -14.442 -47.101  17.361  1.00  0.00
        ATOM    432  O   ASP R  88   -14.123 -47.592  16.276  1.00  0.00
        ATOM    433  CB  ASP R  88   -13.968 -48.725  19.273  1.00  0.00
        ATOM    434  CG  ASP R  88   -12.942 -47.819  19.953  1.00  0.00
  20    ATOM    435  OD1 ASP R  88   -11.758 -48.104  19.876  1.00  0.00
        ATOM    436  OD2 ASP R  88   -13.294 -46.831  20.580  1.00  0.00
        ATOM    437  H   ASP R  88   -15.429 -49.592  17.039  1.00  0.00
        ATOM    438  N   GLU R  89   -14.306 -45.805  17.710  1.00  0.00
        ATOM    439  CA  GLU R  89   -13.680 -44.795  16.839  1.00  0.00
  25    ATOM    440  C   GLU R  89   -14.515 -44.403  15.614  1.00  0.00
        ATOM    441  O   GLU R  89   -15.309 -43.460  15.616  1.00  0.00
        ATOM    442  CB  GLU R  89   -12.257 -45.283  16.493  1.00  0.00
        ATOM    443  CG  GLU R  89   -11.293 -44.524  15.571  1.00  0.00
        ATOM    444  CD  GLU R  89   -10.219 -45.518  15.145  1.00  0.00
  30    ATOM    445  OE1 GLU R  89    -9.962 -45.681  13.957  1.00  0.00
        ATOM    446  OE2 GLU R  89    -9.644 -46.177  15.998  1.00  0.00
        ATOM    447  H   GLU R  89   -14.511 -45.638  18.676  1.00  0.00
        ATOM    448  N   THR R  90   -14.293 -45.184  14.553  1.00  0.00
        ATOM    449  CA  THR R  90   -14.096 -44.591  13.232  1.00  0.00
  35    ATOM    450  C   THR R  90   -15.313 -44.151  12.444  1.00  0.00
        ATOM    451  O   THR R  90   -16.239 -44.933  12.212  1.00  0.00
```

109

SUBSTITUTE SHEET (RULE 26)

	ATOM	452	CB	THR R	90	-13.307	-45.598	12.397	1.00	0.00
	ATOM	453	OG1	THR R	90	-12.719	-46.613	13.229	1.00	0.00
	ATOM	454	CG2	THR R	90	-12.269	-44.936	11.490	1.00	0.00
	ATOM	455	H	THR R	90	-14.031	-46.141	14.672	1.00	0.00
5	ATOM	456	HG1	THR R	90	-11.932	-46.206	13.613	1.00	0.00
	ATOM	457	N	THR R	91	-15.264	-42.906	11.946	1.00	0.00
	ATOM	458	CA	THR R	91	-16.086	-42.598	10.774	1.00	0.00
	ATOM	459	C	THR R	91	-15.551	-43.214	9.474	1.00	0.00
	ATOM	460	O	THR R	91	-15.041	-42.576	8.553	1.00	0.00
10	ATOM	461	CB	THR R	91	-16.263	-41.089	10.611	1.00	0.00
	ATOM	462	OG1	THR R	91	-15.526	-40.320	11.595	1.00	0.00
	ATOM	463	CG2	THR R	91	-17.753	-40.737	10.608	1.00	0.00
	ATOM	464	H	THR R	91	-14.546	-42.271	12.218	1.00	0.00
	ATOM	465	HG1	THR R	91	-16.170	-40.159	12.292	1.00	0.00
15	ATOM	466	N	GLY R	92	-15.638	-44.548	9.437	1.00	0.00
	ATOM	467	CA	GLY R	92	-14.952	-45.240	8.341	1.00	0.00
	ATOM	468	C	GLY R	92	-14.947	-46.747	8.485	1.00	0.00
	ATOM	469	O	GLY R	92	-15.038	-47.506	7.517	1.00	0.00
	ATOM	470	H	GLY R	92	-16.190	-45.008	10.134	1.00	0.00
20	ATOM	471	N	ARG R	93	-14.906	-47.132	9.766	1.00	0.00
	ATOM	472	CA	ARG R	93	-15.165	-48.526	10.101	1.00	0.00
	ATOM	473	C	ARG R	93	-16.597	-48.659	10.561	1.00	0.00
	ATOM	474	O	ARG R	93	-17.179	-47.725	11.108	1.00	0.00
	ATOM	475	CB	ARG R	93	-14.257	-49.027	11.231	1.00	0.00
25	ATOM	476	CG	ARG R	93	-12.866	-49.498	10.801	1.00	0.00
	ATOM	477	CD	ARG R	93	-12.088	-50.205	11.924	1.00	0.00
	ATOM	478	NE	ARG R	93	-11.530	-49.278	12.906	1.00	0.00
	ATOM	479	CZ	ARG R	93	-11.885	-49.270	14.210	1.00	0.00
	ATOM	480	NH1	ARG R	93	-11.321	-48.407	15.046	1.00	0.00
30	ATOM	481	NH2	ARG R	93	-12.806	-50.108	14.666	1.00	0.00
	ATOM	482	H	ARG R	93	-14.866	-46.429	10.469	1.00	0.00
	ATOM	483	HE	ARG R	93	-10.826	-48.644	12.583	1.00	0.00
	ATOM	484	1HH1	ARG R	93	-11.678	-48.273	15.969	1.00	0.00
	ATOM	485	2HH1	ARG R	93	-10.552	-47.825	14.774	1.00	0.00
35	ATOM	486	1HH2	ARG R	93	-13.112	-50.146	15.616	1.00	0.00
	ATOM	487	2HH2	ARG R	93	-13.266	-50.761	14.058	1.00	0.00

SUBSTITUTE SHEET (RULE 26)

	ATOM	488	N	CYS R 94	-17.121	-49.864	10.349	1.00	0.00
	ATOM	489	CA	CYS R 94	-18.327	-50.307	11.053	1.00	0.00
	ATOM	490	C	CYS R 94	-18.187	-51.790	11.280	1.00	0.00
	ATOM	491	O	CYS R 94	-18.340	-52.598	10.361	1.00	0.00
5	ATOM	492	CB	CYS R 94	-19.611	-50.063	10.264	1.00	0.00
	ATOM	493	SG	CYS R 94	-20.314	-48.399	10.429	1.00	0.00
	ATOM	494	H	CYS R 94	-16.640	-50.508	9.754	1.00	0.00
	ATOM	495	N	GLU R 95	-17.798	-52.106	12.524	1.00	0.00
	ATOM	496	CA	GLU R 95	-17.382	-53.477	12.826	1.00	0.00
10	ATOM	497	C	GLU R 95	-18.334	-54.564	12.388	1.00	0.00
	ATOM	498	O	GLU R 95	-19.545	-54.380	12.270	1.00	0.00
	ATOM	499	CB	GLU R 95	-17.063	-53.650	14.313	1.00	0.00
	ATOM	500	CG	GLU R 95	-15.587	-53.436	14.658	1.00	0.00
	ATOM	501	CD	GLU R 95	-15.185	-51.998	14.416	1.00	0.00
15	ATOM	502	OE1	GLU R 95	-14.757	-51.672	13.318	1.00	0.00
	ATOM	503	OE2	GLU R 95	-15.280	-51.193	15.328	1.00	0.00
	ATOM	504	H	GLU R 95	-17.570	-51.381	13.172	1.00	0.00
	ATOM	505	N	ALA R 96	-17.715	-55.723	12.129	1.00	0.00
	ATOM	506	CA	ALA R 96	-18.517	-56.877	11.727	1.00	0.00
20	ATOM	507	C	ALA R 96	-18.962	-57.733	12.900	1.00	0.00
	ATOM	508	O	ALA R 96	-20.158	-57.994	13.010	1.00	0.00
	ATOM	509	CB	ALA R 96	-17.748	-57.740	10.723	1.00	0.00
	ATOM	510	OXT	ALA R 96	-18.116	-58.127	13.704	1.00	0.00
	ATOM	511	H	ALA R 96	-16.728	-55.754	12.290	1.00	0.00
25	END								

*Principal residues are bolded.

111

SUBSTITUTE SHEET (RULE 26)

Appendix 4. The Fortran-77 source code of the VBMC algorithm.*

```
          SUBROUTINE MONTE(XMIN,N,S0)
      C*
 5    C*      Variable Basis Monte Carlo simulated annealing:
      C*      XMIN - initial configurational variables and
      C*          final variables for subsequent local energy
      C*          refinement.
      C*      N - the number of configurational variables.
10    C*      S0 - initial energy.
      C*      FUN - potential energy function.
      C*
          IMPLICIT REAL*8(A-H,O-Z)
          DIMENSION XX(250),X(250),XMIN(1)
15        DIMENSION Y(500,250),C(250,250),E(250),V(250,250)
          IYES=0
          ITEST=0
          READ(5,1)N1,N4,N5,NG1,ITE,IPR1,N33
          IF(N1.EQ.0)RETURN
20        WRITE(6,3000)ITE,S0
          TT=ITE
     3000 FORMAT(/10X,'INITIAL TEMPERATURE',I7,
         1     ' INITIAL ENERGY ',F15.6/)
          PR1=IPR1
25        PR2=PR1*2.D0
          WRITE(6,210)PR1,PR1
      210 FORMAT(' RANDOM TORSIONAL INCREMENT -'
         2     ,F5.2,' TO +',F5.2,' GRAD')
          WRITE(6,302)
30    302 FORMAT(10X,'*VARIABLE BASIS MC SIMULATED ANNEALING*'/)
      C*      Boltzmann factor.
          T=-1./(0.001987*TT)
      C     *** TEMPERATURE T=ITE ***
        1 FORMAT(15I5)
35        N1=N*N1
          N3=N
```

112

```
       K=N
C*        Cooling schedule.
       DT=(ITE-120)/(N5*N3)
       NG=NG1
5      IF(NG.EQ.0)NG=1
C*        Initial set of random number generator.
        CALL SRAND(NG)
        WRITE(6,2)N1,N3,N4,N5,NG
     2  FORMAT(/5X,'MONTE-CARLO PARAMETERS:'/
10      *5X,'BLIND CUT',I10/
        *5X,'BYPASS',I10/
        *5X,'FREQUENCY OF CONTROL OUTPUT',I10/
        *5X,'LENGTH OF ANNEALING REGION',I10/
        *5X,'INITIAL SET OF THE RANDOM GENERATOR ',I10/)
15      IBEGIN=0
        MNCARL=0
        LQ=0
        I7=0
        L1=0
20      EMIN=1.D37
        S3=0.
        S4=0.
C*        Initial set of basis of independent variables.
        DO 88 I=1,N
25      DO 88 J=1,N
        V(I,J)=0.D0
        IF(I.EQ.J)V(I,J)=1.D0
     88 CONTINUE
        DO 2005 I=1,N
30   2005  X(I)=XMIN(I)
      264 S1=0.
        S2=0.
        L=0
C°        Method Monte Carlo.
35      IYES=0
        KG=0
```

113

```
         L2=0
         I=0
      26 I=I+1
C*       Random choice of a variable to move.
 5       H=RAND()
         IK=IDINT(H*N)+1
         RA=RAND()
         D=RA*PR2-PR1
C*       Variable Basis Markov chain: move along basis vectors.
10       DO 513 II=1,N
     513 XX(II)=X(II)+V(II,IK)*D
         CALL FUN(N,XX,SS)
C*       SS - potential energy of the configuration XX.
         S=SS-S0
15       BI=S*T
         IF(BI.GT.50.D0) GOTO 263
C*       CALCULATION OF TRANSITION PROBABILITY
         IF(BI.LT.-50.D0) GOTO 262
         B=DEXP(BI)
20       W7=B/(B+1.D0)
C*       DOES TRANSITION TAKE PLACE ?
         Z=RAND()
         IF(W7-Z)262,263,263
C*       ** NO **
25    262 CONTINUE
         GOTO 274
C*       ** YES ! **
      263 S0=SS
         IYES=IYES+1
30       DO 1314 II=1,N
    1314 X(II)=XX(II)
C*       Blind cut off
      274 IF(IBEGIN.EQ.1) GOTO 266
         MNCARL=MNCARL+1
35       IF(MNCARL-N1)26,1264,265
    1264 WRITE(6,1265)MNCARL,S0
```

114

```
      1265 FORMAT('Initial point has been cut off',I10,1PD17.9)
      C*      Cut off upon criteria.
          GOTO 264
      265 S1=S1+S0
          S2=S2+S0*S0
          L=L+1
          IF(L.NE.20*N) GOTO 26
          L=0
          SR1=S1/I
      DISP1=S2/I-SR1**2
          IF(DABS(SR1-S0)-DSQRT(DISP1))270,270,271
      271 ITEST=0
          GOTO 272
      270 ITEST=ITEST+1
      272 YES=(1.D2*IYES)/I
          WRITE(6,268)I,S0,SR1,DISP1,ITEST,YES
      268 FORMAT('Cut off',I8,3D14.7,I3,2PF7.1)
          IF(I.GE.50000)GOTO 267
          IF(ITEST-3) 26,267,267
      267 IBEGIN=1
          WRITE(6,1265)MNCARL,S0
          WRITE(6,269)
      269 FORMAT(//45X,'Equilibrium has been reached '/)
          GOTO 264
      C*      N3 - parameter of bypassing.
      C*      DT - cooling schedule.
      266 L=L+1
          IF(TT.LE.120.D0)GOTO 3333
      C*      Slow cooling.
          TT=TT-DT
      C*      Boltzmann factor.
          T=-1.D0/(1.987D-3*TT)
          IF(L.LT.N3)GOTO 26
          L=0
          KG=KG+1
      C*      Accumulating N33 sequential points of the Markov chain.
```

115

```
            DO 1992 J=1,N
      1992 Y(KG,J)=X(J)
            L1=L1+1
            L2=L2+1
5           IF(S0.GE.EMIN)GOTO 1957
            EMIN=S0
            DO 1961 IJ=1,N
      1961  XMIN(IJ)=X(IJ)
            LQ=LQ+1
10          WRITE(6,100)LQ,I,EMIN,TT,(XMIN(J),J=1,N)
      100   FORMAT(/' LQ',2I7,D17.9,F7.1/(1X,10F12.3))
      447   FORMAT(/' CR',2I7,D17.9,F7.1/(1X,10F12.3))
      1957 IF(KG.LT.N33)GOTO 45
      C*        Computing covariant matrix of the distribution of
15    C*        the N33 accumulated points in the configurational
      C*        space.
            KG=0
            DO 71 II=1,K
            YYY=0.0
20          DO 82 J=1,N33
        82 YYY=YYY+Y(J,II)
            YYY=YYY/N
            DO 54 J=1,N33
        54 Y(J,II)=Y(J,II)-YYY
25       71 CONTINUE
            DO 710 II=1,K
            DO 710 J=1,K
            S=0.0
            DO 711 LL=1,N33
30       711 S=S+Y(LL,II)*Y(LL,J)
         710 C(II,J)=S
      C*        Covariant matrix is ready.
      C*        Roration of basis V:
            CALL SDIAG2(250,K,C,E,V)
35       45 IF(L2.LT.N4) GOTO 26
```

116

```
            L2=0
            YES=(1.D2*IYES)/I
            WRITE(6,72)I,L1,EMIN,S0,TT,YES
        72  FORMAT(' CO',2I10,2D15.6,F7.1,2PF7.1)
5           IF(L1.LT.N5) GOTO 26
      3333 WRITE(6,1111)
      1111 FORMAT(//10X,'END OF MONTE CARLO STAGE')
            RETURN
            END
10          SUBROUTINE SDIAG2(M,N,A,D,X)
      C*
      C*         Diagonalization of symmetric matrix A (NxN).
      C*         Results: D - eigenvalues; X - eigenvectors.
      C*
15          IMPLICIT REAL*8(A-H,O-Z)
            DIMENSION A(M,M),D(M),X(M,M)
            DIMENSION E(250)
            EPS=1.0D-14
            TOL=1.0D-30
20          IF(N.EQ.1)GOTO 400
            DO 10 I=1,N
            DO 10 J=1,I
        10 X(I,J)=A(I,J)
            DO 150 NI=2,N
25          II=N+2-NI
            DO 150 I=II,II
            L=I-2
            H=.0D0
            G=X(I,I-1)
30          IF(L)140,140,20
        20 DO 30 K=1,L
        30 H=H+X(I,K)**2
            S=H+G*G
            IF(S.GE.TOL)GOTO 50
35          H=.0D0
            GOTO 140
```

117

```
      50 IF(H)140,140,60
      60 L=L+1
         F=G
         G=DSQRT(S)
5        IF(F)75,75,70
      70 G=-G
      75 H=S-F*G
         X(I,I-1)=F-G
         F=.0D0
10       DO 110 J=1,L
         X(J,I)=X(I,J)/H
         S=.0D0
         DO 80 K=1,J
      80 S=S+X(J,K)*X(I,K)
15       J1=J+1
         IF(J1.GT.L)GOTO 100
         DO 90 K=J1,L
      90 S=S+X(K,J)*X(I,K)
     100 E(J)=S/H
20   110 F=F+S*X(J,I)
         F=F/(H+H)
         DO 120 J=1,L
     120 E(J)=E(J)-F*X(I,J)
         DO 130 J=1,L
25       F=X(I,J)
         S=E(J)
         DO 130 K=1,J
     130 X(J,K)=X(J,K)-F*E(K)-X(I,K)*S
     140 D(I)=H
30   150 E(I-1)=G
     160 D(1)=X(1,1)
         X(1,1)=1.D0
         DO 220 I=2,N
         L=I-1
35       IF(D(I))200,200,170
     170 DO 190 J=1,L
```

118

```
              S=.0D0
              DO 180 K=1,L
         180 S=S+X(I,K)*X(K,J)
              DO 190 K=1,L
   5     190 X(K,J)=X(K,J)-S*X(K,I)
         200 D(I)=X(I,I)
              X(I,I)=1.D0
         210 DO 220 J=1,L
              X(I,J)=.0D0
  10     220 X(J,I)=.0D0
              B=.0D0
              F=.0D0
              E(N)=.0D0
              DO 340 L=1,N
  15          H=EPS*(DABS(D(L))+DABS(E(L)))
              IF(H.LE.B)GOTO 235
              B=H
         235 DO 240 J=L,N
              IF(DABS(E(J)).LE.B)GOTO 250
  20     240 CONTINUE
         250 IF(J.EQ.L)GOTO 340
         260 P=(D(L+1)-D(L))*.5D0/E(L)
              R=DSQRT(P*P+1.D0)
              IF(P)270,280,280
  25     270 P=P-R
              GOTO 290
         280 P=P+R
         290 H=D(L)-E(L)/P
              DO 300 I=L,N
  30     300 D(I)=D(I)-H
              F=F+H
              P=D(J)
              C=1.D0
              S=0.D0
  35          J1=J-1
              DO 330 NI=L,J1
```

119

```
        II=L+J1-NI
        DO 330 I=II,II
        G=C*E(I)
        H=C*P
5       IF(DABS(P).LT.DABS(E(I)))GOTO 310
        C=E(I)/P
        R=DSQRT(C*C+1.D0)
        E(I+1)=S*P*R
        S=C/R
10      C=1.D0/R
        GOTO 320
310 C=P/E(I)
        R=DSQRT(C*C+1.D0)
        E(I+1)=S*E(I)*R
15      S=1.D0/R
        C=C/R
320 P=C*D(I)-S*G
        D(I+1)=H+S*(C*G+S*D(I))
        DO 330 K=1,N
20      H=X(K,I+1)
        X(K,I+1)=X(K,I)*S+H*C
330 X(K,I)=X(K,I)*C-H*S
        E(L)=S*P
        D(L)=C*P
25      IF(DABS(E(L)).GT.B)GOTO 260
340 D(L)=D(L)+F
        NI=N-1
350 DO 380 I=1,NI
        K=I
30      P=D(I)
        J1=I+1
        DO 360 J=J1,N
        IF(D(J).GE.P)GOTO 360
        K=J
35      P=D(J)
360 CONTINUE
```

120

```
        IF(K.EQ.I)GOTO 380
        D(K)=D(I)
        D(I)=P
        DO 370 J=1,N
5       P=X(J,I)
        X(J,I)=X(J,K)
370 X(J,K)=P
380 CONTINUE
        RETURN
10  400 D(1)=A(1,1)
        X(1,1)=1.D0
        RETURN
        END
```

15

*The essential places of the VBMC algorithm (different from conventional Monte Carlo technique) are bolded.

20

25

30

35

121

REFERENCES

Allen, M.P., and D.J.Tildesley. 1987. Computer Simulation of Liquids. Claredon Press: Oxford.

Baldwin, A.N., and E.M. Shooter. 1994. *J.Biol.Chem.* 269:11456-11461.

5   Baldwin, A.N., and E.M. Shooter. 1995. *J.Biol.Chem.* 270:4594-4602.

Banner, D.W., A. D'Arcy, W. Janes, R. Gentz, H.-J. Schoenfeld, C. Broger, H. Loetscher, and W. Lesslauer. 1993. *Cell* 73:431-445.

Barbacid, M. 1993. *Oncogene* 8:2033-2042.

Barbacid, M. 1994. *J.Neurobiol.* 25:1386-1403.

10   Barde, Y.-A. 1989. *Neuron* 2:1525-1534.

Barker, P.A., and E.M.Shooter. 1994. *Neuron* 13:203-215.

Baumann, U.; Wu, S.; Flaherty, K.M.; McKay, D.B. 1993. *EMBO J.* 12: 3357-3364.

Ben Ari, Y.; Represa, A. 1990. *TINS* 13: 312-318.

Benedetti, M., A. Levi, and M.V. Chao. 1993. *Proc. Natl. Acad. Sci. U.S.A.* 90:7859-7863.

15   Berkemeier, L., J. Winslow, D. Kaplan, K. Nicolics, D. Goeddel, and A. Rosenthal. 1991. *Neuron* 7:857-866.

Bothwell, M.A. 1991. *Cell* 65:915-918.

Bothwell, M.A., Shooter, E.M. 1977. *J. Biol. Chem.* 23: 8532-8536.

Bradshaw, R.A., J. Murray-Rust, C.F. Ibáñez, N.Q. McDonald, R. Lapatto, and T.L. Blundell.

20   1994. *Protein Science* 3:1901-1913.

Brooks, B.R., R.E. Bruccoleri, B.D. Olason, D.J. States, S. Swaminathan, and M. Karplus. 1983. *J. Comput. Chem.* 4:187-217.

Brooks III, C.L., and D.A. Case, 1993. *Chem. Rev.* 93: 2487-2502.

Brünger, A.T. 1988. *J. Mol. Biol.* 203:803-816.

25   Burton, L.E., C.H. Schmelzer, E. Szönyi, C. Yedinak, and A. Gorrell. 1992. *J. Neurochem.* 59:1937-1945.

Burton, G., C. Schmelzer, M. Sadic, F. Hefti, and J. Treanor. 1995. *Soc. Neurosci. Abs.* 21:1061.

Carter, B.D., C. Kaltschmidt, B. Kaltschmidt, N. Offenhäuser, R. Böhm-Matthaei, P. A.

30   Baeuerle, and Y.-A. Barde. 1996. *Science* 272:542-545.

Cassacia-Bonnefil, P., B.D. Carter, R.T. Dobrowsky, and M.V. Chao. 1996. *Nature* 383:716-719.

Chang, G., W.C. Guida, and W.C. Still. 1989. *J. Am. Chem. Soc.* 111:4379-4386.

Chao, M.V. 1992a. *Cell* 68:995-997.

35   Chao, M.V. 1992b. *Neuron* 9:583-593.

122

Chao, M. 1994. *J. Neurobiol.* 25:1373-1385.

Chao, M.V., and B.L. Hempstead. 1995. *Trends Neurosci.* 18:321-326.

Clackson, T., and J.A. Wells. 1995. *Science* 267:383-386.

Clary, D.O., and L.F. Reichardt. 1994. *Proc. Natl. Acad. Sci. U.S.A.* 91:11133-11137.

5   Davies, A.M. 1994. *J. Neurobiol.* 25:1334-1348.

Dobrowsky, R., M.H. Werner, A.M. Castellino, M.V. Chao, and Y.A. Hannun. 1994. *Science* 265:1596-1599.

Drinkwater, C.C., P.A. Barker, U. Suter, and E.M. Shooter. 1993. *J. Biol. Chem.* 268:23202-23207.

10   Escandon, E., L.E. Burton, E. Szonyi, and K.J. Nikolics. 1993. *Neurosci. Res.* 34:601-613.

Frade, J.M., A. Rodrigues-Tébar, Y.-A. Barde. 1996. *Nature* 383:166-168.

Gibson, K.D., and H.A Scheraga. 1988. In *Structure and Expression: Vol. 1. From Proteins to Ribosomes*; Sarma, M.H., Sarma, R.H., Eds.; Adenine Press: Guilderland, NY, pp. 67-94.

Gidas, B. 1985. *J. Stat. Phys.* 39: 73-131.

15   Glass, D.; Nye, S.; Hantzopoulos, P.; Macchi, M.; Squinto, S.; Goldfarb, M.; Yancopoulos, G. 1991. *Cell* 66: 405-413.

Gotz, R.; Koster, R.; Winkler, C.; Raulf, F.; Lottspeich, F.; Schard, M.; Thoenen, H. 1994. *Nature* 372: 266-269.

Gregory, D.S., A.C.R. Martin, J.C. Cheetham, and A.R. Rees. 1993. *Protein Engineering* 20   6:29-35.

Gunningham, G.W.; Meijer, P.H.E. 1976. *J. Comp. Phys.* 20: 50-63.

Hallböök, F., C.F. Ibáñez, and H. Persson. 1991. *Neuron* 6:845-858.

Hefti, F.H. 1986. *J. Neurosci.* 6:2155-2162.

Hefti, F.H., and Weiner, W.J. 1986. *Annals of Neurology* 20:275-281.

25   Heldin, C.H., A. Ernlund, C. Rorsman, and L. Rönnstrand. 1989. *J. Biol. Chem.* 264:8905-8912.

Hempstead, B.L., D. Martin-Zanca, D.L. Kaplan, L.F. Parada, and M.V. Chao. 1991. *Nature* 350:678-683.

Herrmann, J.L., D.G. Menter, J. Hamada, D. Marchetti, M. Nakajima, and G.L. Nicolson. 30   1993. *Mol. Biol.* 4:1205-1216.

Hobza, P., H.L. Selzle, and E.W. Schlag. 1994. *J. Am. Chem. Soc.* 116:3500-3506.

Hodes, Z.I., G. Nemethy, and H.A. Scheraga. 1979. *Biopolymers* 18:1565-1610.

Hohn, A.; Leibrock, J.; Bailey, K.; Barde, Y.-A. 1990. *Nature* 344: 339-341.

Hopfinger, A.J. 1973. Conformational Properties of Macromolecules. Academic Press, New 35   York-London. pp. 70-85.

123

Hunter, C.A., and J.K.M. Sanders. 1990. *J. Am. Chem. Soc.* 112:5525-5534.

Hunter, C.A., J. Singh, and J.M. Thornton. 1991. *J. Mol. Biol.* 218:837-846.

Ibáñez, C.F., T. Ebendal, and H. Persson. 1991. *EMBO J.* 10:2105-2110.

Ibáñez, C.F., T. Ebendal, G. Barbany, J. Murray-Rust, T.L. Blundell, and H. Persson. 1992. *Cell* 69:329-341.

Ibáñez, C.F., L. Ilag, J. Murray-Rust, and H. Persson. 1993. *EMBO J.* 12:2281-2293.

Ibáñez, C.F. 1994. *J. Neurobiol.* 25:1349-1361.

Ibáñez, C.F. 1995. *Trends Biotech.* 13:217-227.

Ilag, L.L., P. Lönnerberg, H. Persson, and C.F. Ibáñez. 1994. *J. Biol. Chem.* 269:19941-19946.

IUPAC-IUB Commission on Biochemical Nomenclature. 1970. *Biochemistry* 9:3471-3479.

Jing, S.Q., P. Tapley, and M. Barbacid. 1992. *Neuron* 9:1067-1079.

Johnson, D., A. Lanahan, C.R. Buck, A. Sehgal, C. Morgan, E. Mercer, M. Bothwell, and M. Chao. 1986. *Cell* 47:545-554.

Judson, R.S.; Jaeger, E.P.; Treasurywala, A.M. 1994. *J. Mol. Struct. (Theochem)* 308: 191-206.

Kahle, P., L.E. Burton, C.H. Schmelzer, and C. Hertel. 1992. *J. Biol. Chem.* 267:22707-22710.

Kaplan, D.R.; Hempstead, B.L.; Martin-Zanca, D.; Chao, M.V.; Parada, L.F. 1991. *Science* 252: 554-558.

Kaplan, D.R., and R.M. Stephens. 1994. *J. Neurobiol.* 25:1404-1417.

Kincaid, R.H.; Scheraga, H.A. 1982. *J. Comput. Chem.* 3: 525-547.

Kirkpatrick, S., C.D. Gelatt, Jr., and M.P. Vecchi. 1983. *Science* 220:671-680.

Klein, R.; Jing, S.; Nanduri, V.; O'Rourke, E.; Barbacid, M. 1991. *Cell* 65: 189-197.

Klein, R.; Lamballe, F.; Bryant, S.; Barbacid, M. 1992. *Neuron* 8: 947-956.

Kobe, B., and J. Deisenhofer. 1993. *Nature* 366:751-756.

Kobe, B., and J. Deisenhofer. 1994. *Trends Biochem. Sci.* 19:415-421.

Kobe, B., and J. Deisenhofer. 1995. *Nature* 374:183-186.

Korsching, S. 1993. *J. Neurosci.* 13:2739-2748.

Krüttgen, A., J.V. Heymach, P. Kahle, and E.M. Shooter. 1996. *Soc. Neurosci. Abs.* 22:557.

Kullander, K., and T. Ebendal. 1994. *J. Neurosci. Res.* 39:195-210.

Kullander, K., and T. Ebendal. 1996. *Soc. Neurosci. Abs.* 22:557.

Kushner, H.J. 1987. *SIAM J. Appl. Math.* 47: 169-185.

Lai, K.-O., D.J. Glass, D. Geis, G.D. Yancopoulos, and N.Y. Ip. 1996. *J. Neurosci. Res.* 46:618-629.

124

Lamballe, F.; Klein, R.; Barbacid, M. 1991. *Cell* 66: 967-970.

Landreth, G.E., and E.M. Shooter. 1980. *Proc. Natl. Acad. Sci. U.S.A.* 77: 4751-4755.

Large, T.H., G. Weskamp, J.C. Helder, M.J. Radeke, T.P. Misko, E.M. Shooter, and L.F. Reichardt. 1989. *Neuron* 2:1123-1134.

Leibrock, J.; Lottspeich, A.H.; Hohn, A.; Hofer, M.; Hengerer, B.; Masiakowski, P.; Thoenen, H.; Barde, Y.-A. 1989. *Nature* 341: 149-152.

Lelj, F.; Grimaldi, P.; Cristianziano, P.L. 1991. *Biopolymers* 31: 663-670.

Leven, G.R.; Mendel, L.M. 1993. *TINS* 16: 353-359.

Levi-Montalcini, R. 1987. *EMBO J.* 6:1145-1154.

Li, Z.; Scheraga, H.A. 1988. *J. Mol. Struct. (Theochem)* 179: 333-352.

Livnah, O., E.A. Stura, D.L. Johnson, S.A. Middleton, L. S. Mulcahy, N.C. Wrighton, W.J. Dower, L.K. Jolliffe, and I.A. Wilson. 1996. *Science* 273:464-471.

Loeb, D.M.; Maragos, J.; Martin-Zanca, D.; Chao, M.V.; Parada, L.F.; Greene, L.A. 1991. *Cell* 66: 961-966.

Luo, Y., and K.E. Neet. 1992. *J. Biol. Chem.* 267:12275-12283.

MacDonald, J.I.S., and S.O. Meakin. 1996. *Mol. Cell. Neurosci.* 7:371-390.

Mahadeo, D., L. Kaplan, M.V. Chao, and B.L. Hempstead. 1994. *J. Biol. Chem.* 269:6884-6891.

Maisopierre, P.C.; Belluscio, L.S.S.; Squinto, S.; Ip, N.Y.; Furth, M.E.; Lindsay, R.M.; Yancopoulos, G.D. 1990. *Science* 247: 1446-1451.

Maness, L.M., A.J. Kastin, J.T. Weber, W.A. Banks, B.S. Beckman, and J.E. Zadina. 1994. *Neurosci. Biobehav. Rev.* 18:143-159.

Marchetti, D., McQuillan, D.J., W.C. Spohn, D.D. Carson, and G.L. Nicolson. 1996. *Cancer Res.* 56:2856-2863.

Matsumoto, K., R.K. Wada, J.M. Yamashiro, D.R. Kaplan, and C.J. Thiele. 1995. *Cancer Res.* 55:1798-1806.

McDonald, N.Q., R. Lapatto, J. Murray-Rust, J. Gunning, A. Wlodawer, and T.L. Blundell. 1991. *Nature* 354:411-414.

McKee, A.C.; Kosik, K.S.; Kowal, N.W. 1991. *Ann. Neurol.* 30: 156.

McMahon, S.B.; Bennett, D.L.H.; Priestley, J.V.; Shelton, D.L. 1995. *Nature Med.* 1: 774-780.

Meakin, S.O., and E.M. Shooter. 1992. *Trends Neurosci.* 15:323-331.

Merrell, R., M.W. Pulliam, L. Randono, L.F. Boyd, R.A. Bradshaw, and L. Glaser. 1975. *Proc. Natl. Acad. Sci. U.S.A.* 72:4270-4274.

Metropolis, N.; Rosenbluth, A.W.; Rosenbluth, M.N.; Teller, A.H.; Teller, E. 1953. *J. Chem. Phys.* 21: 1087-1092.

125

Moore, J.B., and E.M. Shooter. 1975. *Neurobiology* 5:369-381.

Morgan *et al.* 1989. In Annual Reports in Medicinal Chemistry. Ed.: Vinick, F.J. Academic Press, San Diego, CA, pp. 243-252.

Nayeem. A.; Vila, J.; Scheraga, H.A. 1991. *J. Comput. Chem.* 12: 594-605.

5   Nilges, M., G.M. Clore, and A.M. Gronenborn. 1988. *FEBS Lett.* 229:317-324.

Paine, G.H.; Scheraga, H.A. 1985. *Biopolymers* 24: 1391-1436.

Pérez, P., P.M. Coll, B.L. Hempstead, D. Martin-Zanca, and M.V. Chao. 1995. *Mol. Cell. Neurosci.* 6:97-105.

Persson, H., and C.F. Ibáñez. 1993. *Curr. Opin. Neurol. Neurosurg.* 6:11-18.

10   Piela, L.; Kostrowicki, J.; Scheraga, H.A. 1989. *J. Phys. Chem.* 93: 3339-3346.

Piela, L.; Olszewski, K.A.; Pillardy, J. 1994. *J. Mol. Struct. (Theochem)* 308: 229-239.

Ponnuswamy, P.K., and P. Manavalan. 1976. *J. Theor. Biol.* 60:481-486.

Purves, D. 1988. Body and Brain. A Trophic Theory of Neural Connectors. Cambridge, MA: Harvard University Press, pp. 1-1231.

15   Radeke, M.J., T.P. Misko, C. Hsu, L.A. Herzenberg, and E.M. Shooter. 1987. *Nature* 325:593-597.

Radziejewski, C., and R.C. Robinson. 1993. Biochemistry 32:13350-13356.

Radziejewski, C.; Robinson, R. C.; DiStefano, P.S.; Taylor, J.W. 1992. *Biochemistry* 31: 4431-4436.

20   Raj, N.; Morley, S.D.; Jackson, D.E. 1994. *J. Mol. Struct. (Theochem)* 308: 175-190.

Rao, M.; Pangali, C.; Berne, B.J. 1979. *Mol. Phys.* 37: 1773-1798.

Rashid, K.; van der Zee, C.E.E.M.; Ross, G.M.; Chapman, C.A.; Stanisz, J.; Riopelle. R.J.; Racine, R.J.; Fahnestock, M. 1995. *Proc. Natl. Acad. Sci. U.S.A.* 92: 9495-9499.

Ripoll, D.R.; Scheraga, H.A. 1988. *Biopolymers* 27: 283-1303.

25   Robinson, R.C., C. Radziejewski, D.I. Stuart, and E.Y. Jones. 1995. *Biochemistry* 34:4139-4146.

Rodrigues-Tébar, A., G. Dechant, and Y.-A. Barde. 1990. *Neuron* 4:487-492.

Rodrigues-Tébar, A., G. Dechant, R. Gotz, and Y.-A. Barde. 1992. *EMBO J.* 11:917-922.

Rosenthal, A.; Goeddel, D.V.; Nguyen, T.; Lewis, M.; Shih, A.; Laramee, G.R.; Nikolics, K.;

30   Winslow, J.W. 1990. *Neuron* 4: 767-773.

Ross, A.H., M.-C. Daou, C. A. McKinnon, P.J. Condon, M.B. Lachyankar, R.M. Stephens, D.R. Kaplan, and D.E. Wolf. 1996. *J. Cell Biol.* 132:945-953.

Ross, G.M., I.L. Shamovsky, G. Lawrance, M. Solc, S.M. Dostaler, S.L. Jimmo, D.F. Weaver, and R.J. Riopelle. 1997. *Nature Med.* 3:872-878.

35   Rossky, P. J. ; Doll, J. D. ; Friedman, H. L. 1978. *J. Chem. Phys.* 69: 4628-4633.

126

Rovelli, G.; Heller, R.A.; Canossa, M.; Shooter, E.M. 1993. *Proc. Natl. Acad. Sci. USA* 90: 8717-8721.

Ryckaert, J.-P., Ciccotti, G.; Berendsen, H.J.C. 1977. *J. Comput. Phys.* 23:327-341.

Rydén, M., J. Murray-Rust, D. Glass, L.L. Ilag, M. Trupp, G.D. Yancopoulos, N.Q. McDonald, and C.F. Ibáñez. 1995. *EMBO J.* 14:1979-1990.

Rydén. M., and C.F. Ibáñez, C.F. 1996. *J. Biol. Chem.* 271:5623-5627.

Schauer, M., and E.R. Bernstein. 1985. *J. Chem. Phys.* 82:3722-3727.

Schechter, A.L., and M.A. Bothwell. 1981. *Cell* 24:867-874.

Scheraga, H.A. 1989. *Prog. Clin. Biol. Res.* 289: 3-18.

Scheraga, H.A. 1994. *Pol. J. Chem.* 68: 889-891.

Schmelzer, C.H., L.E. Burton, W.-P. Chan, E. Martin, C. Gorman, E. Canova-Davis, V.T. Ling, M.B. Sliwkowski, G. McCray, J.A. Briggs, T.H. Nguyen, and G. Polastri. 1992. *J. Neurochem.* 59:1675-1683.

Schneider, R., E. Schneider-Scherzer, M. Thurnher, B. Auer, and M. Schweiger. 1988. *EMBO J.* 7:4151-4156.

Schneider, R., and M. Schweiger. 1991. *Oncogene* 6:1807-1811.

Shamovsky, I.L.; Yarovskaya, I.Yu.; Khrapova, N.G.; Burlakova, E.B. 1992. *J. Mol. Struct. (Theochem)* 253: 149-159.

Shamovsky, I.L., G.M. Ross, R.J. Riopelle, and D.F. Weaver. 1996. *J. Am. Chem. Soc.* 118:9743-9749.

Shih, A., G.R. Laramee, C.H. Schmelzer, L.E. Burton, and J.W. Winslow. 1994. *J. Biol. Chem.* 269:27679-27686.

Simon, I.; Nemethy, G.; Scheraga, H.A. 1978. *Macromolecules* 11: 797-804.

Snider, W.D., and E.M. Johnson. 1989. *Ann. Neurol.* 26:489-506.

Snow, M.E. 1992. *J. Comput. Chem.* 13: 579-584.

Soppet, D.; Escandon, E.; Maragos, J.; Middlemas, D.S.; Reid, S.W.; Blair, J.; Burton, L.E.; Stanton, B.; Kaplan, D.R.; Hunter, T.; Nikolics, K.; Parada, L.F. 1991. *Cell* 65: 895-903.

Squinto, S.P.; Stitt, T.N.; Aldrich, T.H.; Davis, S.; Bianco, S.M.; Radziejewski, C.; Glass, D.J.; Masiakowski, P.; Furth, M.E.; Valenzuela, D.M.; DiStefano, P.S.; Yancopoulos, G.D. 1991. *Cell* 65: 885-893.

Suter, U., C. Angst, C.-L. Tien, C.C. Drinkwater, R.M. Lindsay, and E.M. Shooter. 1992. *J. Neurosci.* 12:306-318.

Sutter, A., R.J. Riopelle, R.M. Harris-Warrick, and E.M. Shooter. 1979. *J. Biol. Chem.* 254:5972-5982.

Szentpsly, L.V.; Shamovsky, I.L.; Nefedova, V.V.; Zubkus, V.E. 1994. *J. Mol. Struct.*

127

(Theochem) 308: 125-140.

Taylor, R.A.V., J.F. Kerrigan, F.M. Longo, M. deBoisblanc, and W.C. Mobley. 1991. *Soc. Neurosci. Abs.* 17: 712.

Thoenen, H. 1991. *Trends Neurosci.* 14: 165-170.

5 Treanor, J.J.S., C. Schmelzer, B. Knusel, J.W. Winslow, D.L. Shelton, F. Hefti, K. Nikolics, and L.E. Burton. 1995. *J. Biol. Chem.* 270: 23104-23110.

Ullrich, A., and J. Schlessinger. 1990. *Cell* 61: 203-212.

Urfer, R., P. Tsoulfas, D. Soppet, E. Escandón, L.F. Parada, and L.G. Presta. 1994. *EMBO J.* 13:5896-5909.

10 Urfer, R., P. Tsoulfas, L. O'Connell, D.L. Shelton, L.F. Parada, and L.G. Presta. 1995. *EMBO J.* 14:2795-2805.

Vale, R.D.; Shooter, E.M. 1985. *Methods Enzymol.* 109: 21-39.

Vanderbilt, D., and S.G. Louie. 1984. *J. Comput. Phys.* 56:259-271.

Van der Zee, C.E.E., G.M. Ross, R.J. Riopelle, and T. Hagg. 1996. *Science* 274: 1729-1732.

15 Villani, V.; Tamburro, A.M. 1994. *J. Mol. Struct. (Theochem)* 308: 141-157.

Warme, P.K., and R.S. Morgan. 1978. *J. Mol. Biol.* 118: 289-304.

Washiyama, K., Y. Muragaki, L.B. Rorke, V.M.-Y.Lee, S.C. Feinstein, M.J. Radeke, D. Blumberg, D.R. Kaplan, and J.Q. Trojanowski. 1996. *Amer. J. Path.* 148:929-940.

Weiner, S.J., P.A. Kollman, D.A. Case, U.C. Singh, C. Ghio, G. Alagona, S. Profeta Jr., and

20 P.Weiner. 1984. *J.Am.Chem.Soc.* 106:765-784.

Weskamp, G.; Reichardt, L.F. 1991. *Neuron* 6: 649-663.

Wilson, C., and S. Doniach. 1989. *Proteins* 6:193-209.

Wilson, S.R., W. Cui, J.W. Moscowitz, and K.E. Schmidt. 1988. *Tetrahedron Lett.* 29:4373-4376.

25 Windisch, J.M., B. Auer, R. Marksteiner, M.E. Lang, and R. Schneider. 1995a. *FEBS Lett.* 374:125-129.

Windisch, J.M., R. Marksteiner, and R. Schneider. 1995b. *J. Biol. Chem.* 270: 28133-28138.

Windisch, J.M., R. Marksteiner, M.E. Lang, B. Auer, and R. Schneider. 1995c. *Biochemistry* 34:11256-11263.

30 Wolf, D.E., C.A. McKinnon, M.-C. Daou, R.M. Stephens, D.R. Kaplan, and A.H. Ross. 1995. *J. Biol. Chem.* 270:2133-2138.

Woo, S.B., D.E. Timm, and K.E. Neet. 1995. *J. Biol. Chem.* 270:6278-6285.

Woo, S.B., and K.E. Neet. 1996. *J. Biol. Chem.* 271:24433-24441.

Woolf, C.J.; Doubell, T.A. 1994. *Current Opinions in Neurobiol.* 4: 525-534.

35 Yan, H., and M.V. Chao. 1991. *J. Biol. Chem.* 266:12099-12104.

128

Yoder, M.D.; Keen, N.T.; Jumak, F. 1993. *Science* 260: 1503-1507.

WHAT IS CLAIMED IS:

1.   A variable basis Monte-Carlo (VBMC) simulated annealing method for identifying an optimal structure in a molecular system, comprising:

5   (a)   providing a Markov chain with an initial basis set of N configurational variables which define a structure for said molecular system;

(b)   translating the N configurational variables simultaneously along a basis vector to produce a new structure for the molecular system, wherein magnitude of translation is randomly chosen within a preselected range;

10   (c)   calculating potential energy of the new structure of the molecular system;

(d)   deciding whether to accept or reject the new structure using an effective temperature dependent transition function, and if the new structure is accepted, replacing the current structure with the accepted structure;

(e)   repeating steps (b) to (d), each repetition having a new basis vector, for a

15   preselected first number of repetitions at a preselected upper temperature; then

(f)   decreasing temperature according to a preselected cooling schedule;

(g)   repeating steps (b) to (d) and (f), each repetition having a new basis vector, for a preselected second number of repetitions; then

(h)   storing current structure of the molecular system;

20   (I)   repeating steps (g) and (h) until a preselected number of stored structures have been accumulated; then

(j)   rotating the basis set of configurational variables according to an effective distribution of the accumulated structures so that basis vectors are directed along low-energy valleys of a potential energy hypersurface thereby accelerating conformational motions and

25   structural transitions of the molecular system, and erasing accumulated structures from steps (h) and (I);

(k)   repeating steps (I) and (j) until, after an effective third number of repetitions, a preselected lower temperature limit is reached, thereby producing an unrefined global minimum structure; and

30   (l)   refining the global energy minimum structure so that at least one local minimum on the potential energy hypersurface is identified.

2.   The method of claim 1, wherein the basis vector is chosen randomly within said preselected range.

35

3.   The method of claim 1, wherein the basis vector is chosen deterministically within said

130

preselected range.

4.   The method of claim 1 wherein the preselected second number of repetitions is N or a multiple thereof.

5

5.   The method of claim 1 wherein the preselected second number of repetitions is at least about 2N.

6.   The method of claim 1 wherein the refining step is non-linear minimization.

10

7.   The method of claim 6, wherein the refining step is gradient descent minimization.

8.   The method of claim 6, wherein the refining step is conjugate gradient minimization.

15   9.   The method of claim 6, wherein the refining step is a quasi-Newton minimization method.

10.   The method of claim 9, wherein the quasi-Newton method is Newton -Raphson method.

20

11.   The method of claim 6, wherein the refining step is Marquardt method.

12.   The method of claim 6, wherein the refining step is a variable metric method.

25   13.   The method of claim 6, wherein the refining step is Powell method.

14.   The method of claim 1 wherein said molecular system is at least one peptide domain comprising amino acid residues, each amino acid residue comprising a main chain having α-carbon atoms, carbonyl carbon atoms and nitrogen atoms, said basis set of configurational

30   variables comprising torsional angles (ψ_i) between said α-carbon atoms and neighbouring carbonyl carbon atoms, and torsional angles (ϕ_i) between said α-carbon atoms and neighbouring nitrogen atoms.

15.   The method of claim 14 wherein torsional angles describing planar portions of said

35   peptide domains are held constant.

131

16.   The method of claim 14 wherein said effective temperature dependent transition function for screening a new state x_{i+1} derived from a previous state x_i is given by:

$$W(x_i \to x_{i+1}) = 1/[1 + \exp(\Delta E_i /kT)]$$

where ΔE_i is the difference between conformational energies of the states x_{i+1} and x_i, k is the Boltzmann constant and T is absolute temperature.

17.   The method of claim 14 wherein said effective temperature dependent transition function for screening a new state x_{i+1} derived from a previous state x_i is given by:

$$W(x_i \to x_{i+1}) = 1, \qquad\qquad \text{if } E(x_{i+1}) \le E(W(x_i))$$
$$= \exp(-\Delta E_i /kT), \quad \text{if } E(x_{i+1}) \ge E(W(x_i))$$

where ΔE_i is the difference between conformational energies of the states x_{i+1} and x_i, k is the Boltzmann constant and T is absolute temperature.

18.   The method of claims 14, 15, 16 or 17 wherein said preselected upper temperature is about 1000^0K.

19.   The method of claim 18 wherein said preselected lower temperature is about 120^0K.

20.   A method of identifying structures of a peptide domain of a neurotrophin to bind with a binding site of a receptor, comprising;

a)   providing a plurality of neurotrophin analogues wherein at least one neurotrophin analogue binds said receptor;

b)   identifying an optimal or near-optimal structure for respective peptide domains of the neurotrophin analogues that bind said receptor by applying a preselected number of the variable basis Monte-Carlo (VBMC) annealing simulations according to claim 1 to each of the respective peptide domains to identify minimum or near-minimum energy structures for said peptide domains; and

c)   comparing said minimum or near-minimum energy structures to identify common structural features shared by neurotrophin analogues exhibiting receptor mediated activity.

21.   The method according to claim 20 wherein said common structural features are absent from neurotrophin analogues that do not exhibit receptor-mediated activity.

22.   A method of identifying structures of a domain of a ligand to bind with a binding site of

132

a receptor, comprising;

    a)   providing a plurality of ligand analogues wherein at least one ligand analogue binds said receptor;

    b)   identifying an optimal or near-optimal structure for respective domains of the ligand analogues that bind said receptor by applying a preselected number of the variable basis Monte-Carlo (VBMC) annealing simulations according to claim 1 to each of the respective domains to identify minimum or near-minimum energy structures for said domains; and

    c)   comparing said minimum or near-minimum energy structures to identify common structural features shared by ligands exhibiting receptor mediated activity.

23. The method according to claim 22 wherein said common structural features are absent from ligand analogues that do not exhibit receptor-mediated activity.

24. The method according to claim 20 wherein said neurotrophin is NGF, and said receptor is TrkA.

25. The method according to claim 20 wherein said neurotrophin is brain-derived neurotrophic factor (BDNF), neurotrophin-3 (NT-3), or neurotrophin-4 (NT-4), and said receptor is TrkB.

26. The method according to claim 20 wherein said neurotrophin is neurotrophin-3 (NT-3) and said receptor is TrkC.

27. The method according to claim 20 wherein said receptor is the common neurotrophin receptor $p75^{NTR}$.

28. A ligand for binding with TrkA, wherein TrkA comprises a leucine rich motif (LRM) comprising amino acid residues 93 to 117, wherein coordinates of the residues of said LRM are given in Appendix 1, said LRM having five binding areas, area A comprising amino acid residue Phe^{105tA} capable of hydrophobic interaction, area B comprising amino acid residues Phe^{111tA}, Phe^{113tA}, and Thr^{114tA} capable of hydrophobic interaction, area C comprising amino acid residues Asp^{109tA} and His^{112tA} capable of ionic interaction, area D comprising amino acid residue Lys^{100tA} capable of ionic interaction, and area E comprising Asn^{95tA} to Ile^{98tA} capable of multiple parallel β-strand type hydrogen bonding, the ligand comprising;

at least three moieties each comprising effective atomic elements having spatial

133

occupancy, relative atomic position, bond type and charge to define a three dimensional conformation of said ligand so that a first moiety can bind with a first binding area, a second moiety can bind with a second binding area, and a third moiety can bind with a third binding area.

5

29.   The ligand according to claim 28 wherein the first moiety can hydrophobically bond with binding area A, the second moiety can ionically bind with binding area C, and the third moiety can ionically bind with binding area D.

10   30.   The ligand according to claim 29 comprising a fourth moiety effectively spaced with respect to the other moieties so it can hydrophobically bond with binding area B.

31.   The ligand according to claim 29 comprising a fourth moiety effectively spaced with respect to the other moieties so it can hydrogen bond with binding area E.

15

32.   The ligand according to claim 29 wherein the first moiety is capable of hydrophobic bonding to Phe^{105tA} in binding area A, the second moiety is positively charged and present in an effective position in said ligand to ionically interact with Asp^{109tA} and His^{112tA} in binding area C, and the third moiety is negatively charged and present in an effective position in said

20   ligand to ionically interact with Lys^{100tA} in binding area D.

33.   The ligand according to claim 32 wherein the moiety hydrophobically bonded to Phe^{105tA} in binding area A is Trp, wherein the positively charged moiety which ionically interacts with Asp^{109tA} and His^{112tA} in binding area C is Arg and Lys, and wherein the negatively

25   charged moiety which ionically interacts with Lys^{100tA} in binding area D is Asp.

34.   The ligand according to claim 32 wherein said first, second and third moieties are amino acids or isosteres thereof.

30   35.   The ligand according to claim 30 wherein said fourth moiety is an amino acid or isostere thereof.

36.   The ligand according to claim 31 wherein said fourth moiety is an amino acid or isostere thereof.

35

37.   A method of designing a ligand to bind with a LRM of TrkA, comprising:

134

providing a template of said LRM of TrkA, said LRM comprising amino acid residue sequence 93 to 117 inclusive, said amino acid residues having spatial Cartesian coordinates given in Appendix 1 wherein said binding area A comprises Phe^{105tA} capable of hydrophobic bonding, binding area B comprises Phe^{111tA}, Phe^{113tA}, Thr^{114tA} capable of hydrophobic bonding,

5   binding area C comprises Asp^{109tA} and His^{112tA} capable of ionic interaction, binding area D comprises Lys^{100tA} capable of ionic interaction, and binding area E comprises Asn^{95tA} to Ile^{98tA} capable of hydrogen bonding; and

computationally evolving a ligand using an effective algorithm so that said evolved ligand comprises at least three effective moieties located relative to each other in the ligand

10   so that a first moiety can bind with a first of said five binding areas, a second moiety can bind with a second of said five binding areas, and a third moiety can bind with a third of said binding areas.

38.   The method according to claim 37 including the step of generating said ligand under a

15   constraint that the evolved ligand comprises said first effective moiety spatially located to hydrophobically bind with binding area A, said second moiety spatially located to ionically interact with binding area C, and said third moiety spatially located to ionically interact with· binding area D.

20   39.   The method according to claim 37 including the step of generating said ligand under a constraint that the evolved ligand comprises an effective moiety spatially located to hydrophobically interact with binding area B.

40.   The method according to claim 37 including the step of generating said ligand under a

25   constraint that the evolved ligand comprises an effective moiety spatially located to hydrogen bond with binding area E.

41.   A ligand for binding with TrkB, wherein TrkB comprises a leucine-rich motif (LRM) comprising amino acid residues 93 to 117, the coordinates of the residues of said LRM given

30   in Appendix 2, said LRM having five binding areas, binding area F comprising amino acid residue Asp^{100tB} capable of ionic interaction, binding area G comprising amino acid residue Lys^{109tB} capable of ionic interaction, binding area H comprising amino acid residue Lys^{113tB} capable of ionic interaction, binding area I comprising amino acid residue Arg^{94tB} capable of ionic interaction, and binding area K comprising amino acid residue Lys^{104tB} capable of

35   hydrogen bonding or ionic interaction, the ligand comprising:

at least three moieties each comprising effective atomic elements having spatial

135

occupancy, relative atomic position, bond type and charge to define a three dimensional conformation of said ligand so that a first moiety can bind with a first binding area, a second moiety can bind with a second binding area, and a third moiety can bind with a third binding area.

5

42. The ligand according to claim 41 wherein one of said at least three moieties can ionically bind with binding area F, another of said at least three moieties can ionically bind with binding area G, and another of said at least three moieties can form a hydrogen bond or ionically bind with binding area K.

10

43. The ligand according to claim 42 wherein said ligand includes a fourth moiety effectively spaced relative to said at least three moieties so that it can ionically bind with binding area H.

15 44. The ligand according to claim 42 wherein said ligand includes a fourth moiety effectively spaced relative to said at least three moieties so that it can ionically bind with binding area I.

45. The ligand according to claim 41 wherein the first moiety is positively charged and
20 present in an effective position in said ligand to ionically bind to $Asp^{100\alpha B}$ in binding area F, the second moiety is negatively charged and present in an effective position in said ligand to ionically interact with $Lys^{109\alpha B}$ in binding area G, and the third moiety is neutral or negatively charged and capable of hydrogen bonding or ionically bonding to $Lys^{104\alpha B}$ in binding area K.

25 46. The ligand according to claim 45 wherein a fourth moiety is negatively charged and present in an effective position in said ligand to ionically bind to $Lys^{113\alpha B}$ in binding area H, and wherein a fifth moiety is negatively charged and present in an effective position in said ligand to ionically bind to $Arg^{94\alpha B}$ in binding area I.

30 47. The ligand according to claim 46 wherein the positively charged moiety ionically bonded to $Asp^{100\alpha B}$ in binding area F is Arg, wherein the charged moiety which ionically interacts with $Lys^{109\alpha B}$ in binding area G is Glu and Lys, and wherein the negatively charged moiety ionically bonded with $Lys^{113\alpha B}$ in binding area H is Asp.

35 48. The ligand according to claim 47 wherein the negatively charged amino acid residue ionically bonded to $Arg^{94\alpha B}$ in binding area I is Glu.

136

49.   The ligand according to claim 45 wherein the neutral or negatively charged moiety capable of hydrogen bonding or ionically bonding to Lys^{104tB} in binding area K is Thr.

50.   The ligand according to claim 45 wherein said first, second and third moieties are
5   amino acids or isosteres thereof.

51.   The ligand according to claim 46 wherein said fourth and fifth moieties are amino acids or isosteres thereof.

10   52.   A method of designing a ligand to bind with TrkB, wherein TrkB comprises a leucine-rich motif (LRM) comprising amino acid residues 93 to 117, the coordinates of the residues of said LRM given in Appendix 2, said LRM having five binding areas, binding area F comprising amino acid residue Asp^{100tB} capable of ionic interaction, binding area G comprising amino acid residue Lys^{109tB} capable of ionic interaction, binding area H comprising amino acid residue
15   Lys^{113tB} capable of ionic interaction, binding area I comprising amino acid residue Arg^{94tB} capable of ionic interaction, and binding area K comprising amino acid residue Lys^{104tB} capable of hydrogen bonding or ionic interaction, the method comprising:
        computationally evolving a ligand using an effective algorithm so that said evolved ligand comprises at least three effective moieties located relative to each other in the ligand
20   so that a first moiety can bind with a first of said five binding areas, a second moiety can bind with a second of said five binding areas, and a third moiety can bind with a third of said binding areas.

        53.   A ligand for binding with the common neurotrophin receptor p75^{NTR}, wherein p75^{NTR}
25   comprises a binding site including amino acid residues Cys^{39p} to Cys^{94p} inclusive, said residues of said binding site having spatial coordinates given in Appendix 3, said binding site having three binding areas including binding loop 2A comprising region Cys^{39p} to Cys^{58p} capable of attractive electrostatic interaction, binding loop 2B comprising region Cys^{58p} to Cys^{79p} capable of attractive electrostatic interaction, and binding loop 3A comprising region
30   Cys^{79p} to Cys^{94p} capable of attractive electrostatic interaction, the ligand comprising;
        at least two moieties each comprising effective atomic elements having spatial occupancy, relative atomic position, bond type and charge to define a three dimensional conformation of said ligand so that a first moiety can bind with a first binding area, and a second moiety can bind with a second binding area.
35

        54.   The ligand according to claim 53 wherein said ligand is an agonist, and wherein one

137

of said at least two moieties binds to loop 2B.

55. The ligand according to claim 53 further comprising a third moiety wherein said first moiety can bind to loop 2A, said second moiety can bind to loop 2B and said third moiety can bind to loop 3A.

56. The ligand according to claim 53 wherein said first moiety binds to any two of Asp^{47p}, Lys^{56p} and Glu^{53p}.

57. The ligand according to claim 53 wherein said binding loop 2A includes amino acid residues Asp^{47p} and Lys^{56p} and said first moiety ionically binds to said residues Asp^{47p} and Lys^{56p}.

58. The ligand according to claim 53 wherein said binding loop 2B includes amino acid residues Asp^{75p} and Asp^{76p} and said second moiety ionically binds to said residues Asp^{75p} and Asp^{76p}.

59. The ligand according to claim 55 wherein said binding loop 3A includes amino acid residues Asp^{88p} and Glu^{89p} and said third moiety ionically binds to said residues Asp^{88p} and Glu^{89p}.

60. The ligand according to claim 55 wherein said third moiety binds to any two of Asp^{88p}, Glu^{89p} and Arg^{80p}.

61. A method of designing a ligand for binding with the common neurotrophin receptor $p75^{NTR}$, wherein $p75^{NTR}$ comprises a binding site including amino acid residues Cys^{39p} to Cys^{94p} inclusive, said residues of said binding site having spatial coordinates given in Appendix 3, said binding site having three binding areas including binding loop 2A comprising region Cys^{39p} to Cys^{56p} capable of attractive electrostatic interaction, binding loop 2B comprising region Cys^{58p} to Cys^{79p} capable of attractive electrostatic interaction, and binding loop 3A comprising region Cys^{79p} to Cys^{94p} capable of attractive electrostatic interaction, the method comprising;

computationally evolving a ligand using an effective algorithm so that said evolved ligand comprises at least two effective moieties located relative to each other in the ligand so that a first moiety can bind to a first of said three loops and a second moiety can bind to a second loop of said three loops.

62.   A method of identifying a ligand to bind with a leucine rich motif (LRM) of TrkA, comprising:

providing a three dimensional conformation for said LRM, said LRM comprising amino acid residue sequence 93 to 117 inclusive, said amino acid residues having spatial Cartesian coordinates given in Appendix 1, said LRM having five binding areas, area A comprising amino acid residue Phe^{105tA} capable of hydrophobic interaction, area B comprising amino acid residues Phe^{111tA}, Phe^{113tA}, and Thr^{114tA} capable of hydrophobic interaction, area C comprising amino acid residues Asp^{109tA} and His^{112tA} capable of ionic interaction, area D comprising amino acid residue Lys^{100tA} capable of ionic interaction, and area E comprising Asn^{95tA} to Ile^{98tA} capable of multiple parallel β-strand type hydrogen bonding;

providing a data base containing molecules coded for spatial occupancy, relative atomic position, bond type and/or charge; and

screening said data base to select those molecules comprising moieties having a three dimensional conformation and effective charge that can bind with at least three of said five binding areas.

63.   A method of identifying a ligand to bind with a leucine rich motif (LRM) of TrkB, comprising:

providing a three dimensional conformation for said LRM, said LRM comprising amino acid residues 93 to 117, the coordinates of the residues of said LRM given in Appendix 2, said LRM having five binding areas, binding area F comprising amino acid residue Asp^{100tB} capable of ionic interaction, binding area G comprising amino acid residue Lys^{109tB} capable of ionic interaction, binding area H comprising amino acid residue Lys^{113tB} capable of ionic interaction, binding area I comprising amino acid residue Arg^{94tB} capable of ionic interaction, and binding area K comprising amino acid residue Lys^{104tB} capable of hydrogen bonding or ionic interaction;

providing a data base containing molecules coded for spatial occupancy, relative atomic position, bond type and/or charge; and

screening said data base to select those molecules comprising moieties having a three dimensional conformation and effective charge that can bind with at least three of said five binding areas.

64.   A method of identifying a ligand to bind with common neurotrophin receptor $p75^{NTR}$, comprising:

providing a three dimensional conformation for the common neurotrophin receptor $p75^{NTR}$, wherein $p75^{NTR}$ comprises a binding site including amino acid residues Cys^{39p} to

139

Cys^{94p} inclusive, said residues of said binding site having spatial coordinates given in Appendix 3, said binding site having three binding areas including binding loop 2A comprising region Cys^{39p} to Cys^{58p} capable of attractive electrostatic interaction, binding loop 2B comprising region Cys^{58p} to Cys^{79p} capable of attractive electrostatic interaction, and binding

5   loop 3A comprising region Cys^{79p} to Cys^{94p} capable of attractive electrostatic interaction;

providing a data base containing molecules coded for spatial occupancy, relative atomic position, bond type and/or charge; and

screening said data base to select those molecules comprising moieties that can bind with at least two of said three binding loops.

10

15

SUBSTITUTE SHEET (RULE 26)

First monomer: amino terminus

	1				5					10						15
hNGF	S	S	S	H	P	I	F	H	R	G	E	F	S	V	C	...
mNGF	S	S	T	H	P	V	F	H	M	G	E	F	S	V	C	...
mNGFΔ3-9	-	-	-	-	-	-	-	S	S	G	E	F	S	V	C	...
hNGF-H4D	S	S	S	D	P	I	F	H	R	G	E	F	S	V	C	...
mNGFΔ1-8	-	-	-	-	-	-	-	-	M	G	E	F	S	V	C	...
BDNF	-	-	H	S	D	P	A	R	R	G	E	L	S	V	C	...

Second monomer: carboxyl terminus

				112'					118'		
hNGF	...	C	V	C	V	L	S	R	K	A	V	R
mNGF	...	C	V	C	V	L	S	R	K	A	T	R
mNGFΔ3-9	...	C	V	C	V	L	S	R	K	A	T	R
hNGF-H4D	...	C	V	C	V	L	S	R	K	A	V	R
mNGFΔ1-8	...	C	V	C	V	L	S	R	K	A	T	R
BDNF	...	C	V	C	T	L	T	I	K	R	G	R

Figure 1
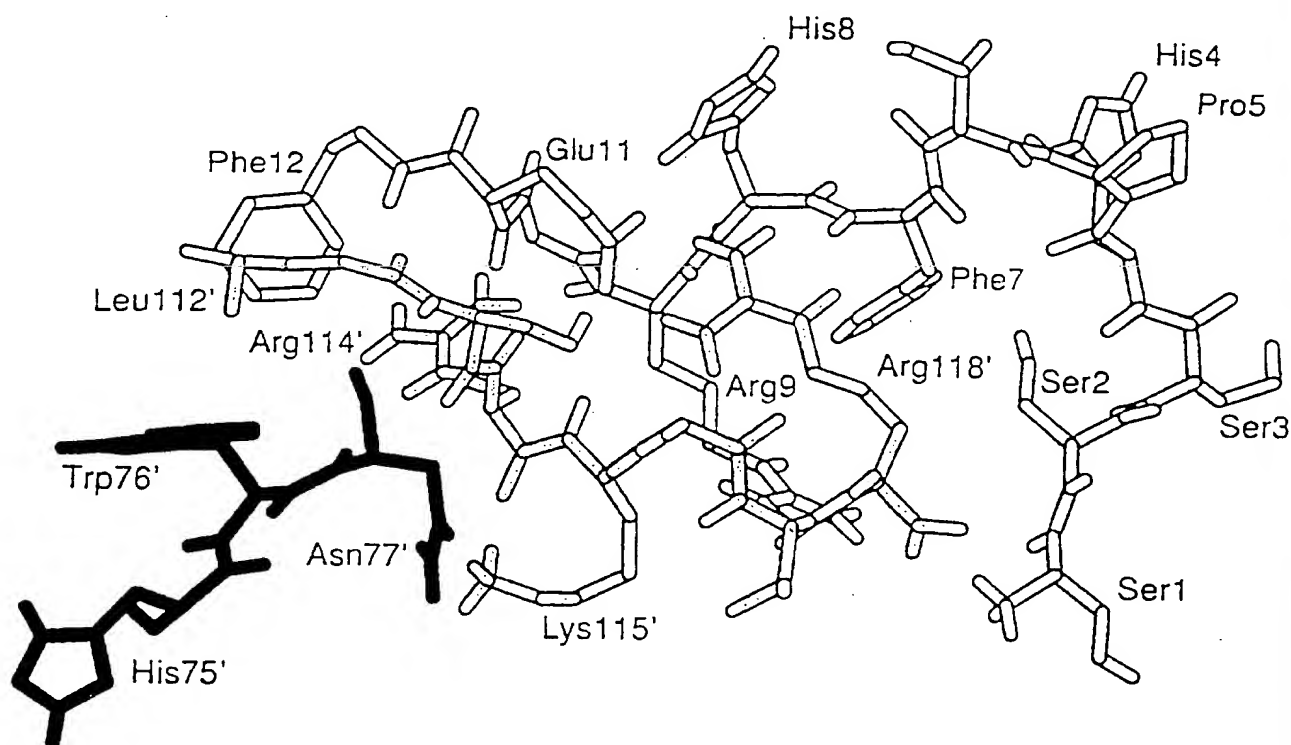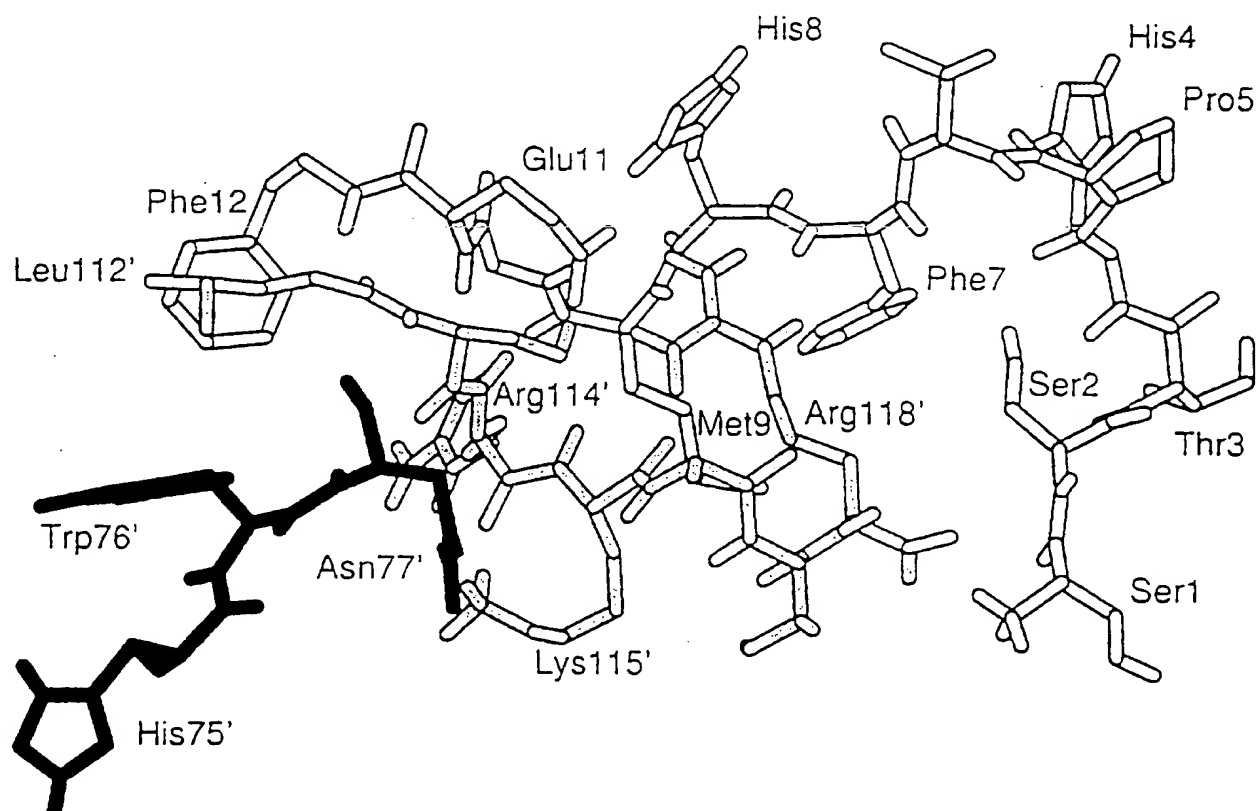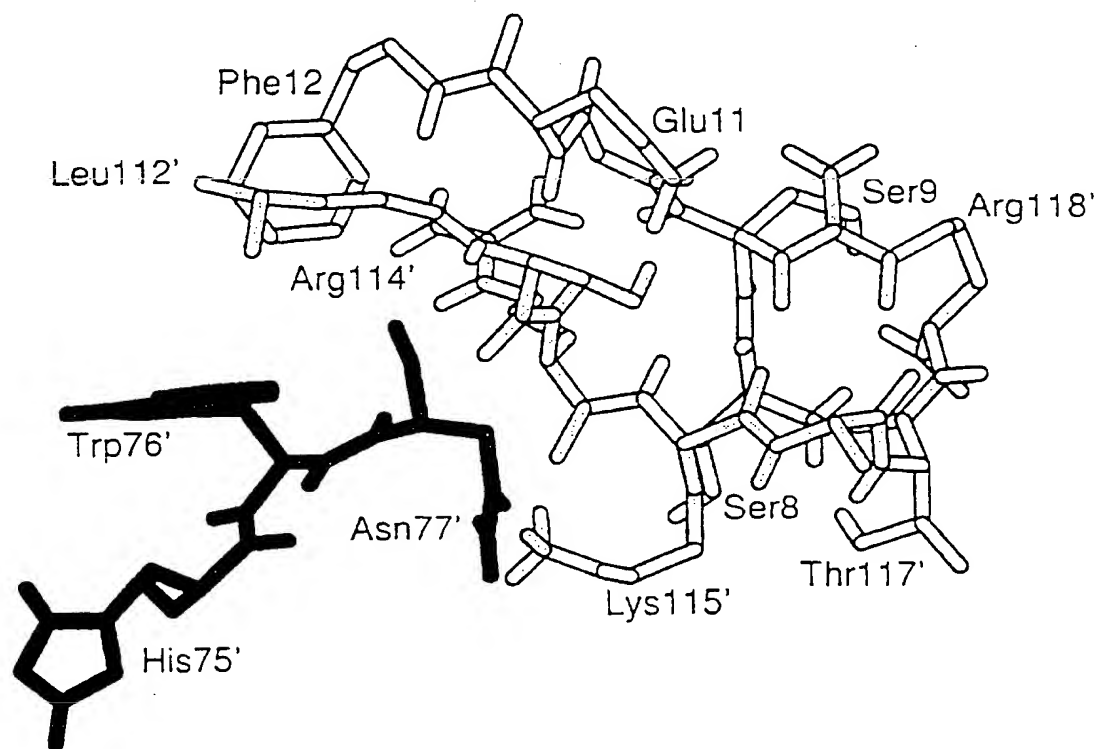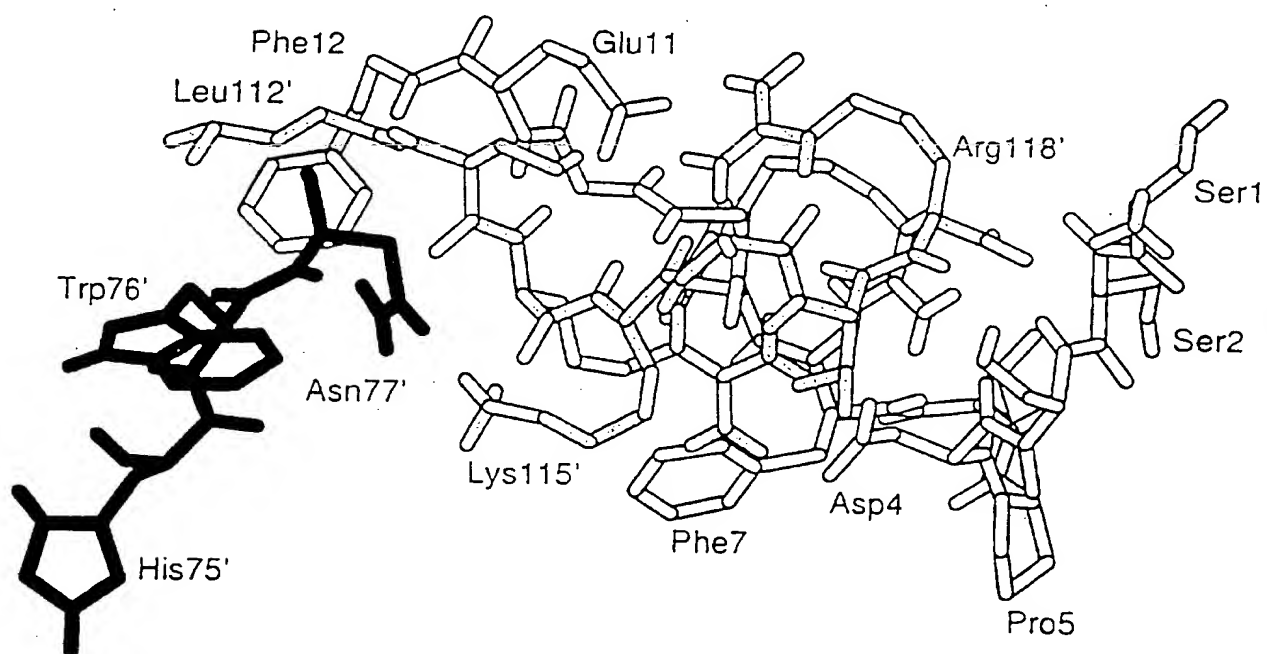
Figure 2

Figure 3
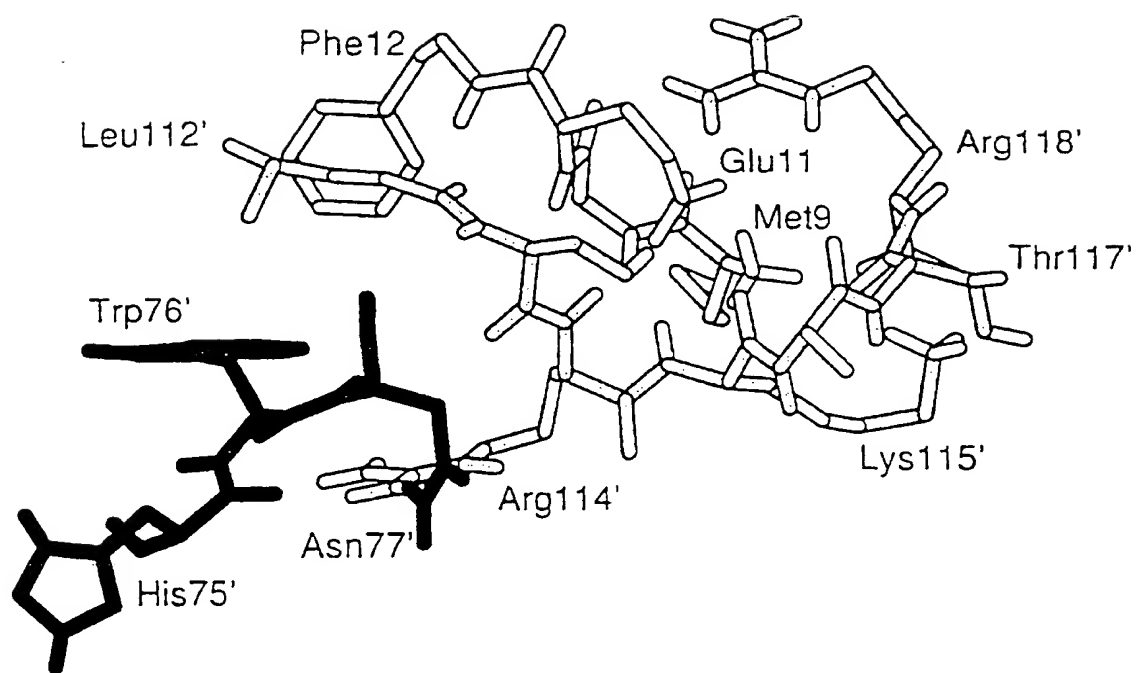
Figure 4
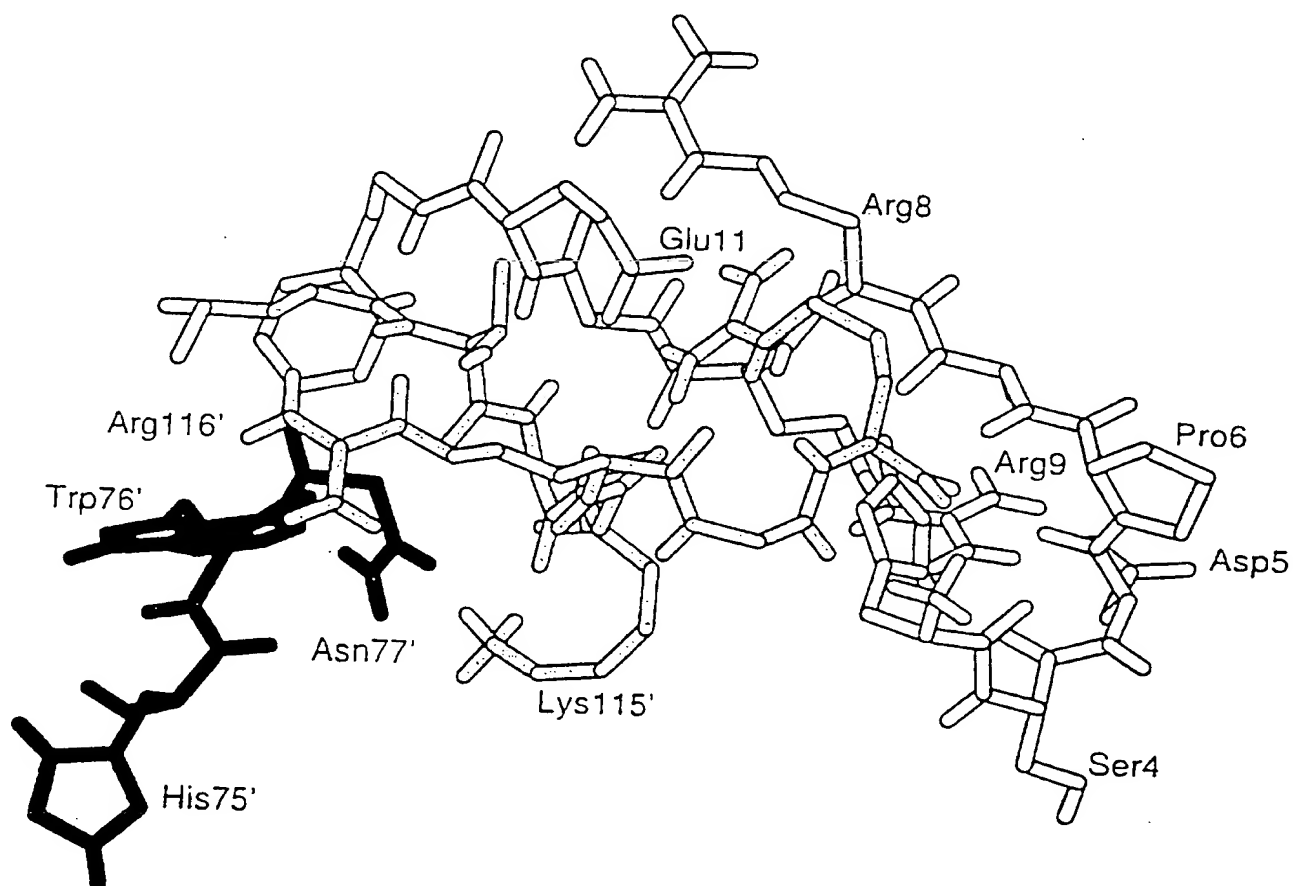
Figure 5

Figure 6

Figure 7

8/29
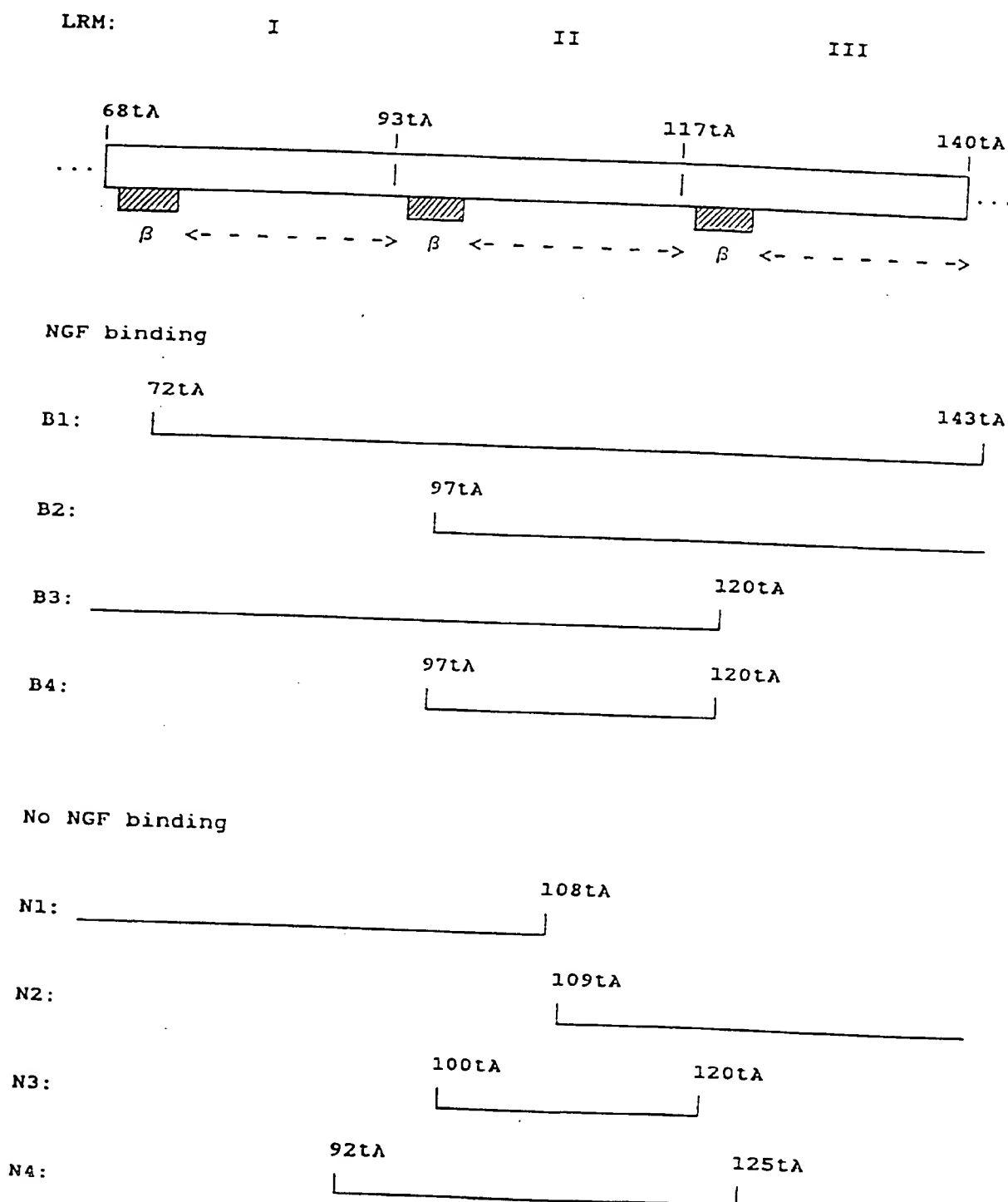
Figure 8

First monomer: amino terminus

	1			5					10					15		
hNGF	S	S	S	H	P	I	F	H	R	G	E	F	S	V	C	D ...
mNGF	S	S	T	H	P	V	F	H	M	G	E	F	S	V	C	D ...
mNGFΔ3-9	-	-	-	-	-	S	S		G	E	F	S	V	C	D ...	
hNGF:NT-4/5	S	S	S	H	P	I	F	H	R	G	E	F	S	V	C	D ...

Second monomer: carboxyl terminus

	75'				110'				115'					118'	
hNGF	... K	H	W	N ...	C	V	C	V	L	S	R	K	A	V	R
mNGF	... K	H	W	N ...	C	V	C	V	L	S	R	K	A	T	R
mNGFΔ3-9	... K	H	W	N ...	C	V	C	V	L	S	R	K	A	T	R
hNGF:NT-4/5	... R	H	W	V ...	C	V	C	T	L	S	R	T	G		R
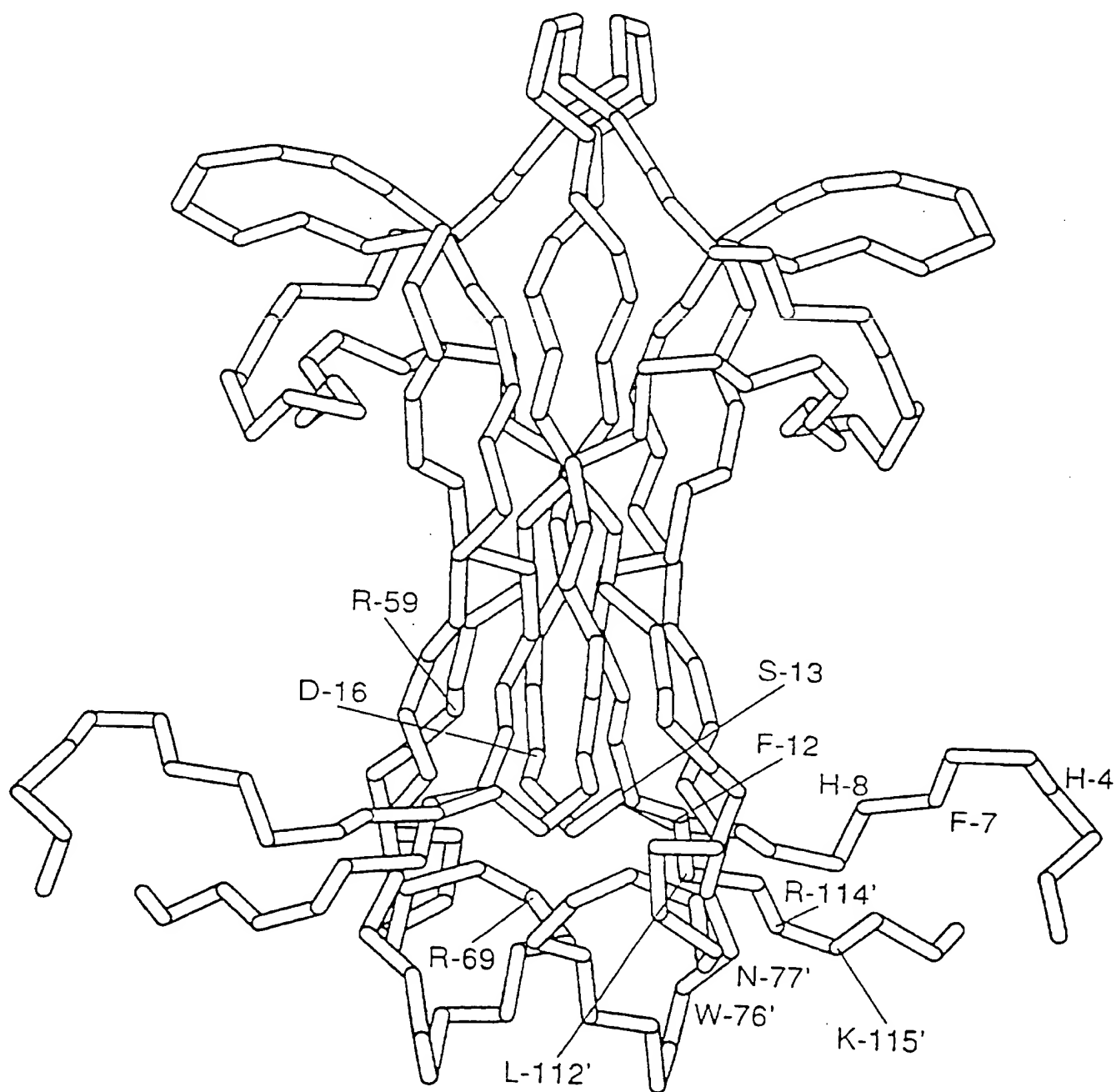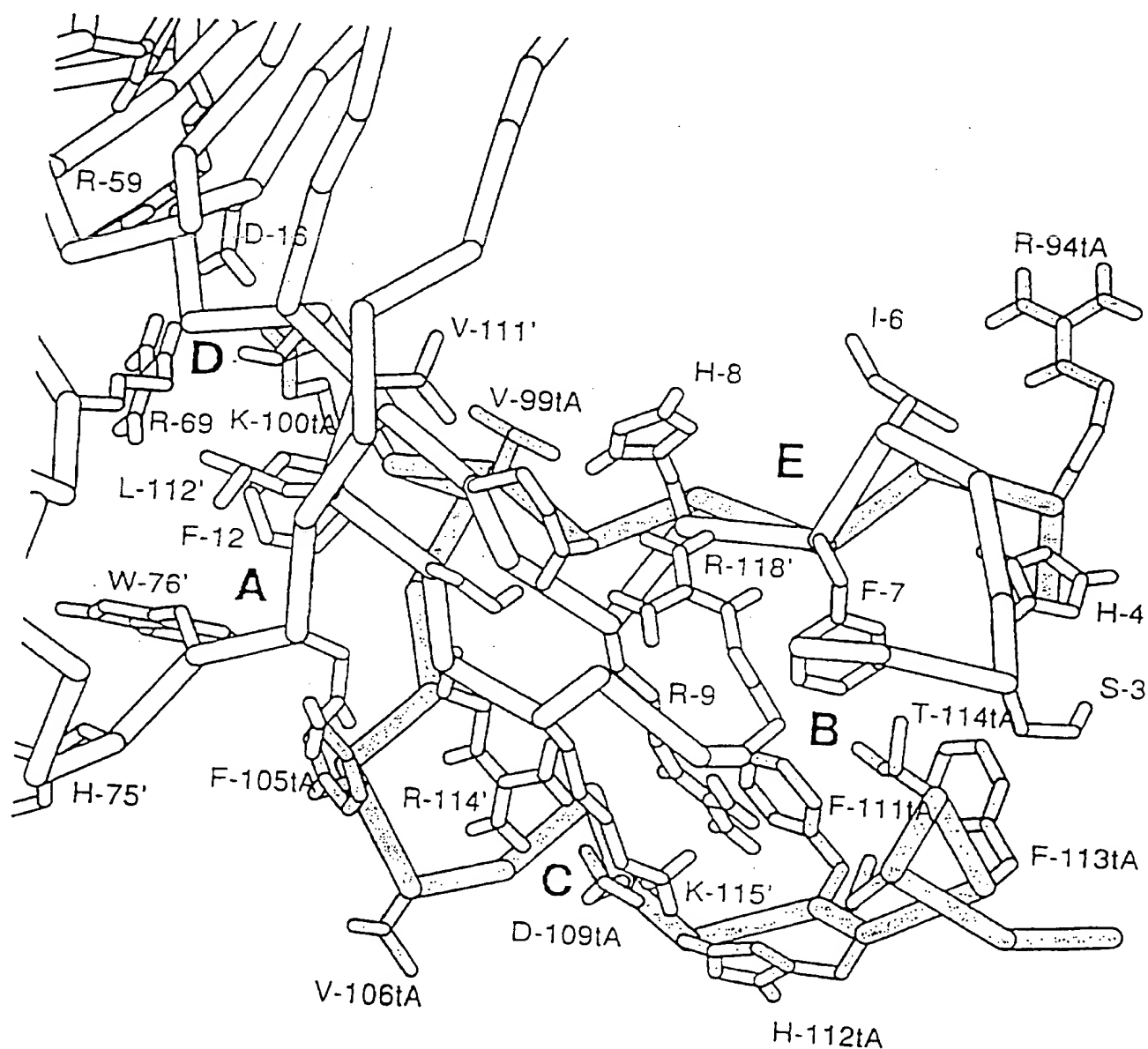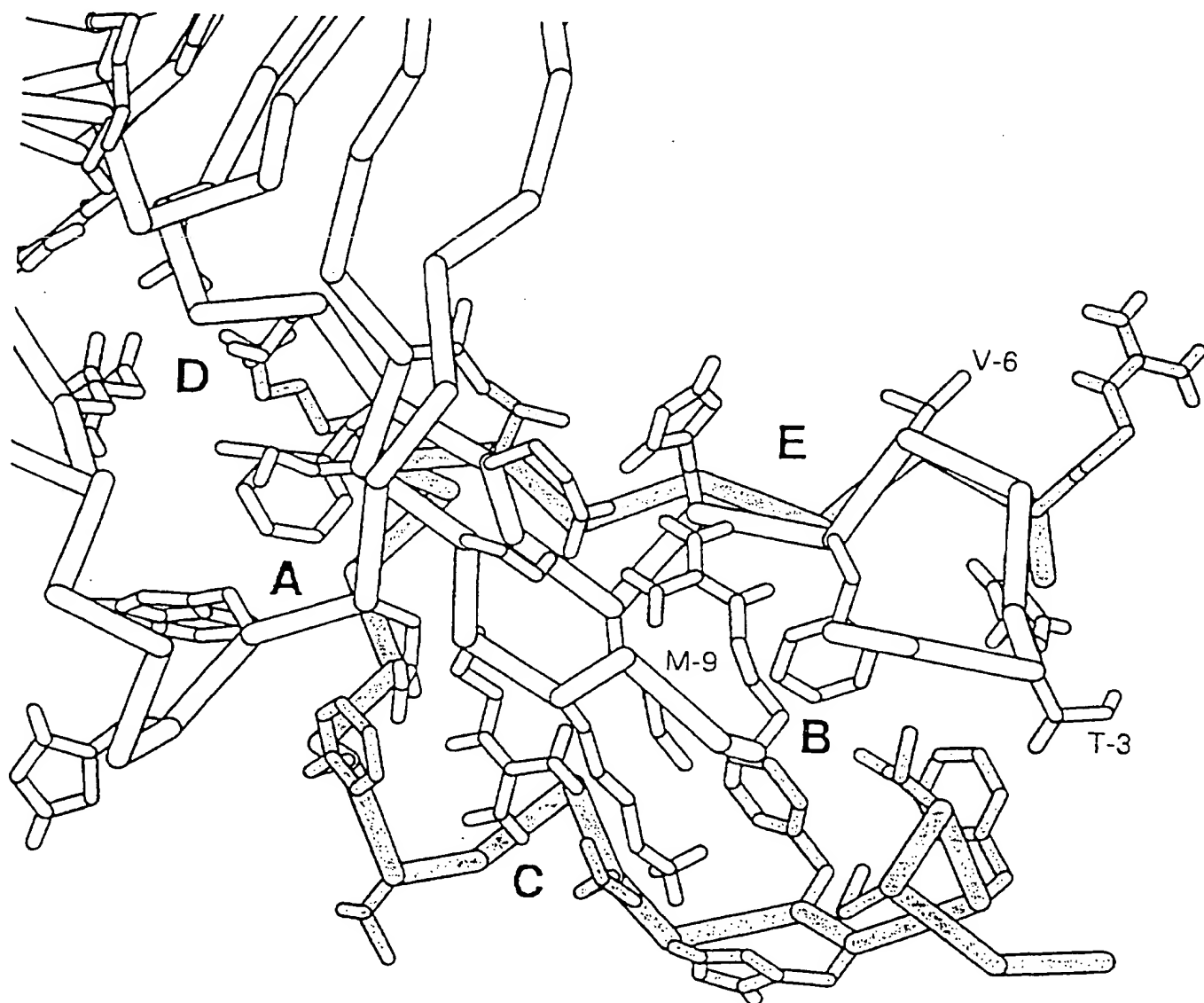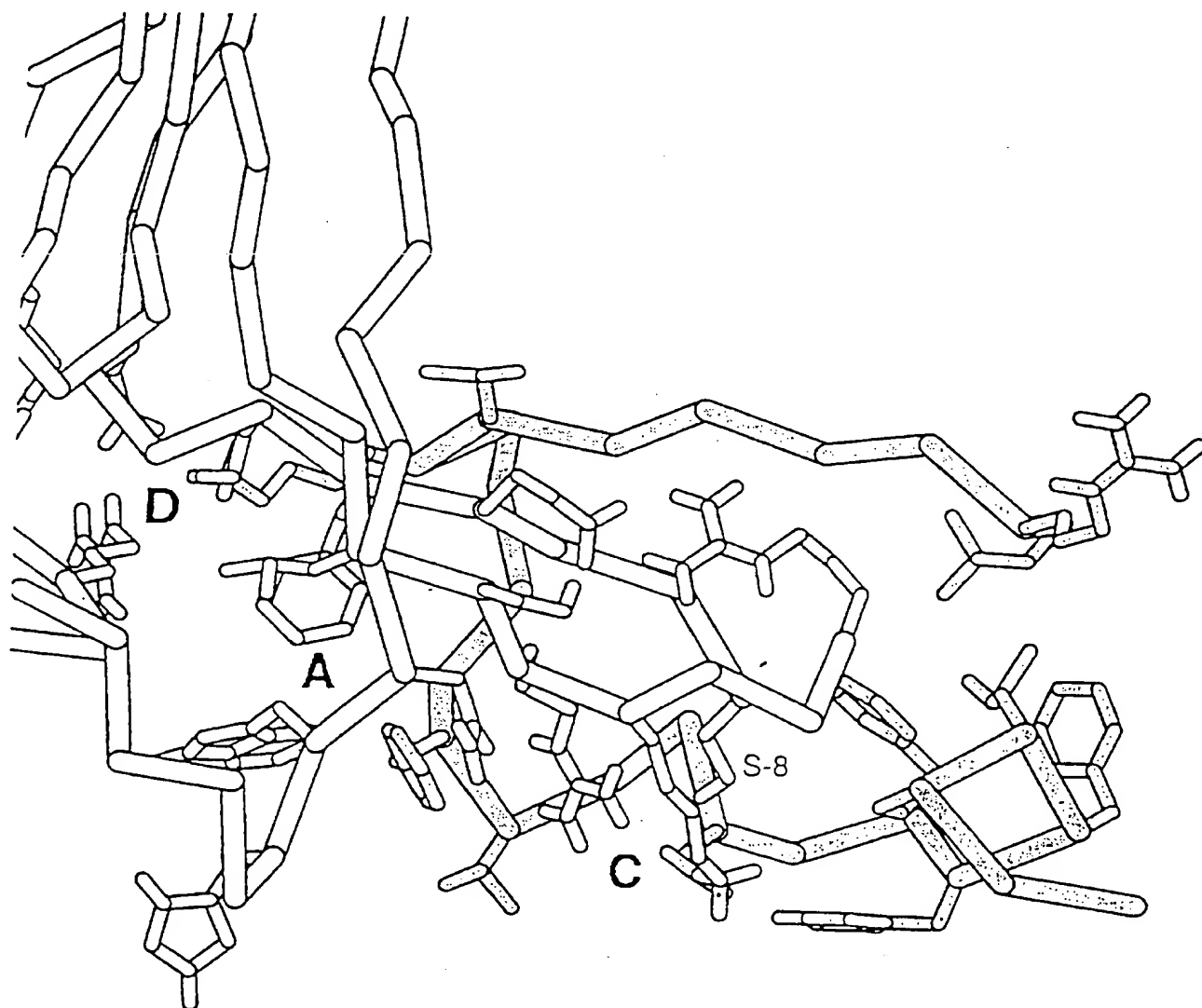
Figure 9
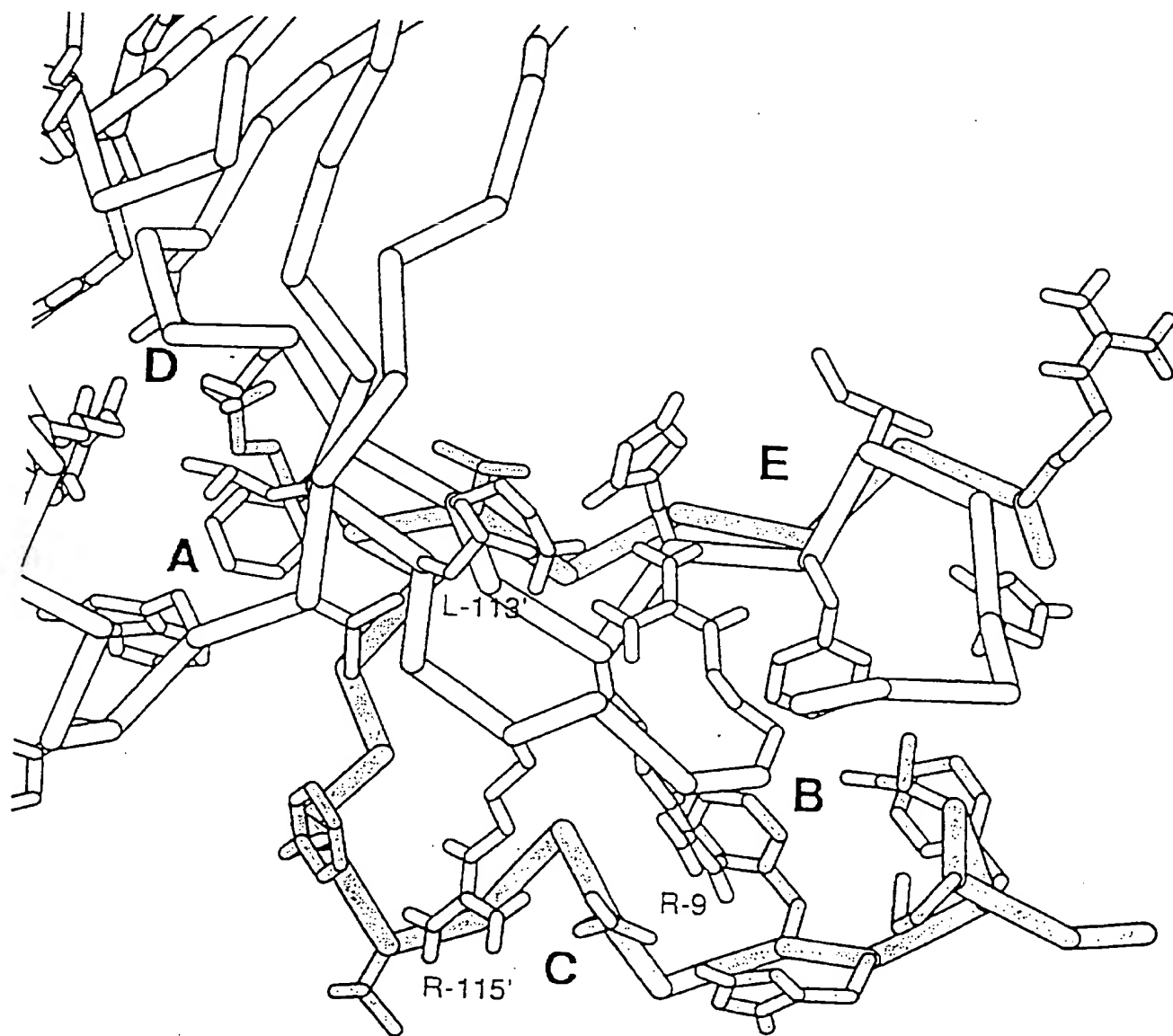
Figure 10a

Figure 10b
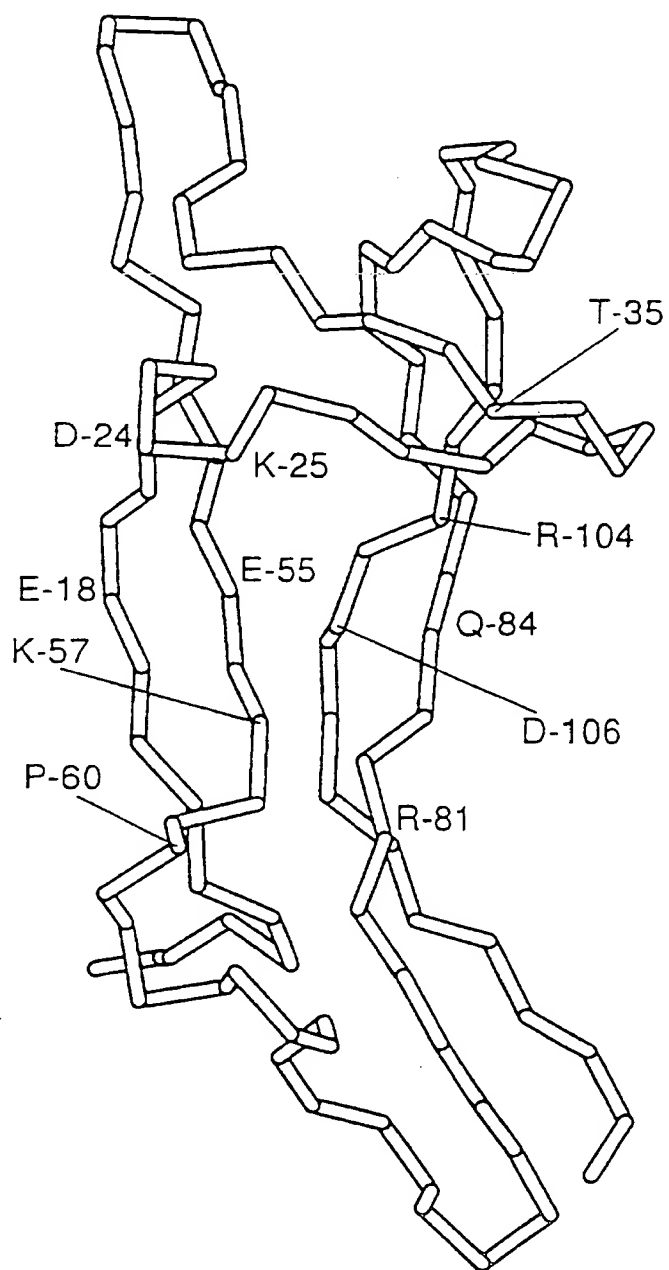
Figure 10c
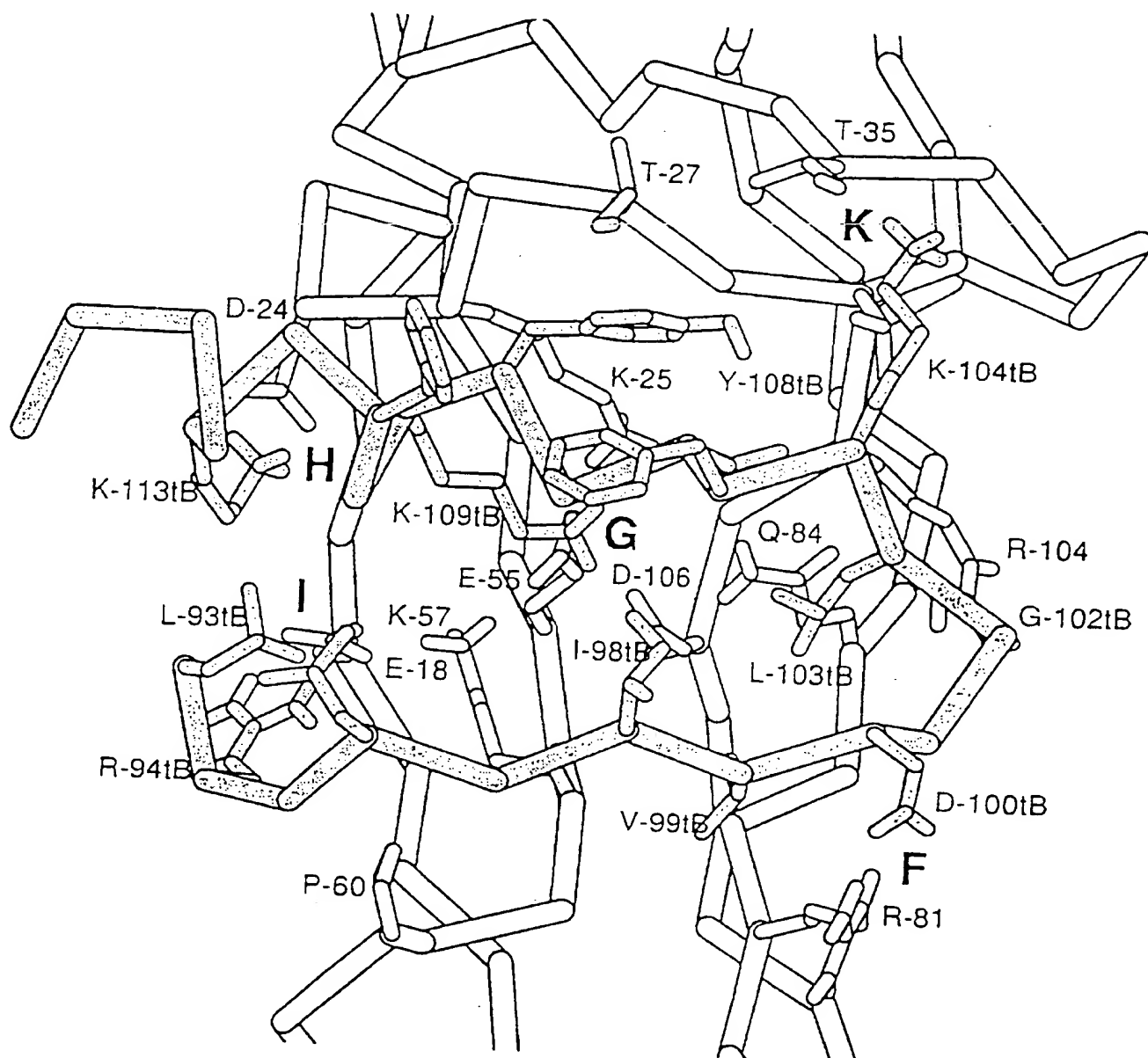
Figure 10d

Figure 10e
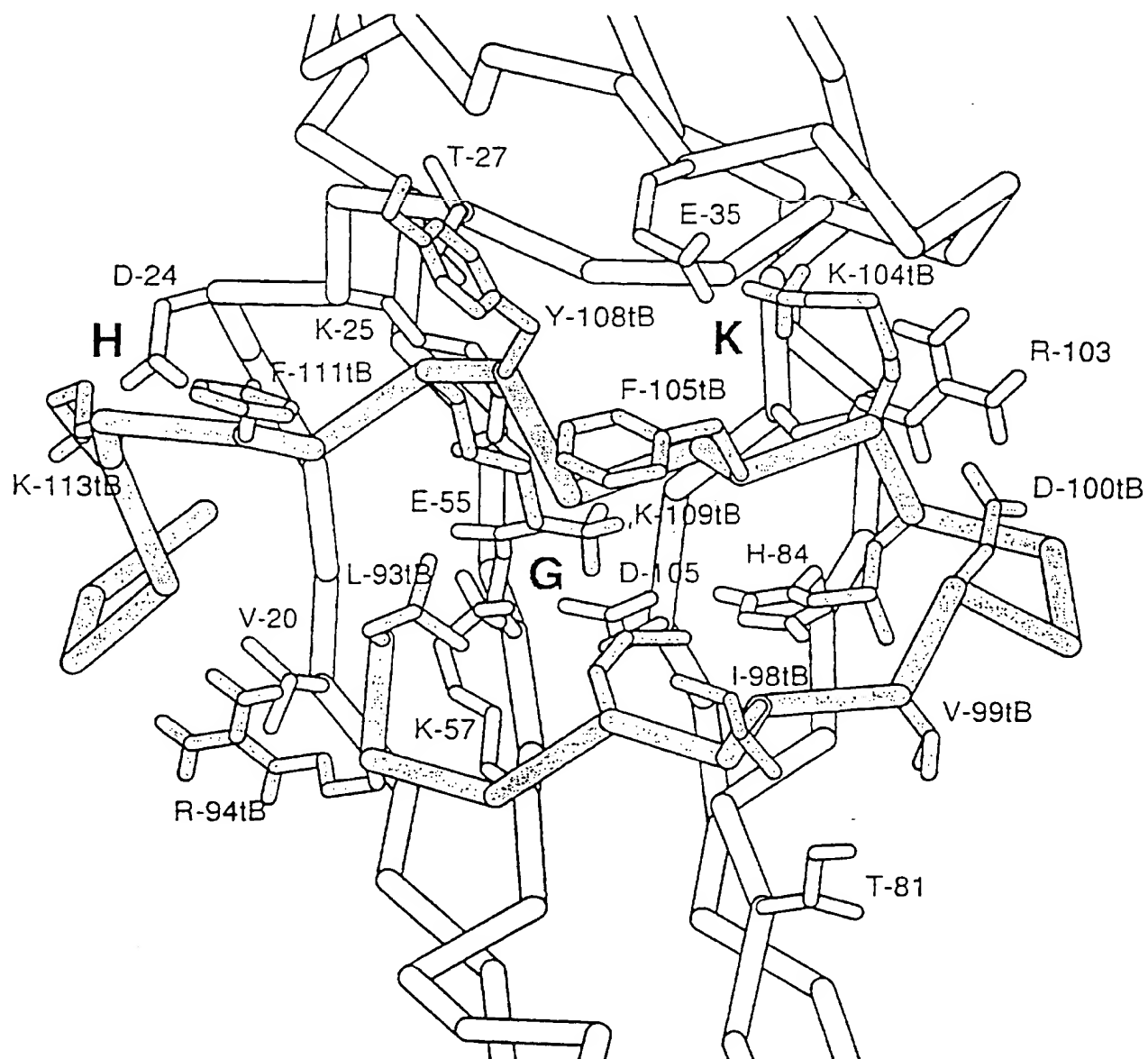
Figure 11a
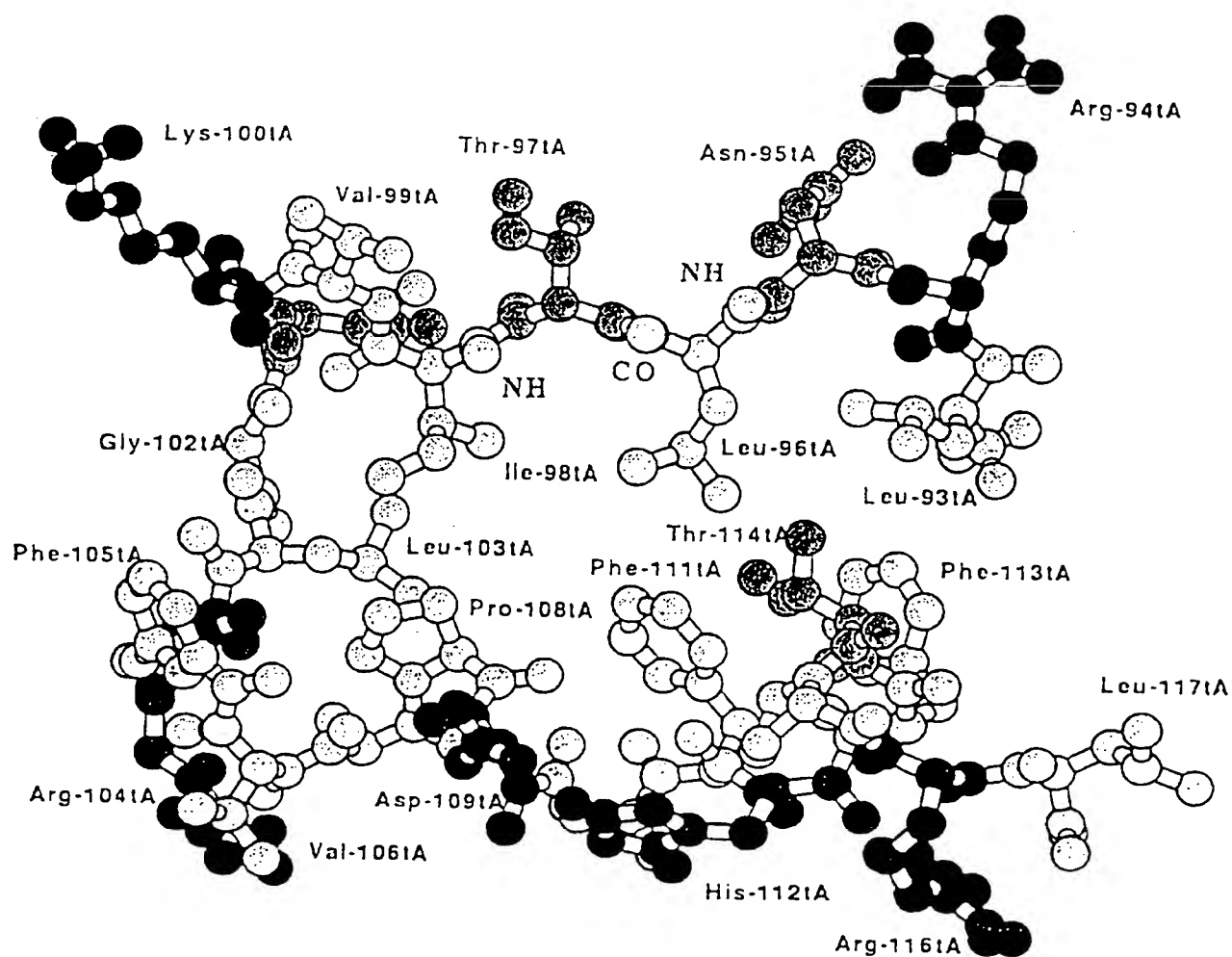
Figure 11b

Figure 11c

Figure 12

Amino terminus

	1				5					10					15	
hNGF sequence	S	S	S	H	P	I	F	H	R	G	E	F	S	V	C	D...
Conserved in NGF	-	-	X	X	X	X	X	-	X	X	X	-	X	X	X	X
Determine structure	-	-	X	X	X	X	X	X	X	-	X	X	X	X	X	X
Interact with LRM	-	-	-	-	X	X	-	X	-	X	-	X	-	X	-	X
LRM binding sites					E	E	E	E	B	D	E	D	D			D

Carboxyl terminus

	75'						110'							115'				
hNGF sequence	...K	H	W	N...	C	V	C	V	L	S	R	K	A	V	R
Conserved in NGF	-	X	X	X	X	X	X	X	X	X	X	X	-	-	X
Determine structure	-	X	X	X	X	X	X	X	X	X	X	-	-	X	X
Interact with LRM	-	X	-	-	-	-	-	-	-	-	X	X	-	-	X
LRM binding sites		A			C	C									

Figure 13

Figure 14

a

b

Figure 15

Figure 16

Second Cysteine-Rich Domain

p75^NTR(h)	39	C L D S V T F S D V V S A T E P C K P C T
p75^NTR(r)	39	C L D N V T F S D V V S A T E P C K P C T
p75^NTR(c)	40	C L D S V T Y S D T V S A T E P C K P C T
p55^TNFR	41	C - E S G S F T A S E N H L R H C L S C S

p75^NTR(h)	60	E C V G L Q S M S A - - P C V E A D D A V C
p75^NTR(r)	60	E C L G L Q S M S A - - P C V E A D D A V C
p75^NTR(c)	61	Q C V G L H S M S A - - P C V E S D D A V C
p55^TNFR	61	K C R K E M G Q V E I S S C T V D R D T V C

Third Cysteine-Rich Domain

p75^NTR(h)	80	R C A Y G Y Y Q D E - - - T T G R C E A
p75^NTR(r)	80	R C A Y G Y Y Q D E - - - E T G H C E A
p75^NTR(c)	81	R C A Y G Y F Q D E - - - L S G S C K E
p55^TNFR	83	G C R K N Q Y R H Y W S E N L F Q C F N

Figure 17

Figure 18a

Figure 18b

Figure 18c

R-107
E-73p
D-47p
K-56p
R-111
D-75p
E-60p
D-76p   R-34
R-98
D-32
R-36
G-35
E-89p
R-114
D-116
Q-83
D-88p

Figure 18d

Figure 19

loop 2A

loop 2B

loop 3A

Figure 20

PCT

INTERNATIONAL APPLICATION PUBLISHED UNDER THE PATENT COOPERATION TREATY (PCT)

(54) Title: MOLECULAR MODELLING OF NEUROTROPHIN-RECEPTOR BINDING

(57) Abstract

The present invention relates to a computational method for identifying the bioactive conformations of peptide domains, in particular, the geometries of complexes of neurotrophins and their receptors. The bioactive conformation of the Nerve Growth Factor (NGF) amino and carboxyl termini (Trk binding domain) was determined. The complex of the NGF termini splits into two distinct regions: a rigid region (residues 9-11 and 112'-118') and a flexible loop (residues 1-8). The geometry of the rigid region, which is maintained by electrostatic interaction between Glu^{11} and $Arg^{118'}$, is conserved in active molecules only. The separation of the flexible loop from the rigid region is necessary in order to eliminate an influence of the loop on the biologically active conformation of the rigid region. The present invention also relates to a method for identifying and theoretically modelling specific receptor binding sites for Nerve Growth Factor (NGF) and Brain-Derived Neurotrophic Factor (BDNF) on their receptors, TrkA and TrkB, respectively. The present invention also relates to a method for identifying and theoretically modelling a receptor binding site for neurotrophins, such as NGF, BDNF, NT-3, and NT-4/5, of the common neurotrophin receptor $p75^{NTR}$. Binding agents for neurotrophin receptors and identification of the binding sites of these.

FOR THE PURPOSES OF INFORMATION ONLY

Codes used to identify States party to the PCT on the front pages of pamphlets publishing international applications under the PCT.

AL	Albania	ES	Spain	LS	Lesotho	SI	Slovenia
AM	Armenia	FI	Finland	LT	Lithuania	SK	Slovakia
AT	Austria	FR	France	LU	Luxembourg	SN	Senegal
AU	Australia	GA	Gabon	LV	Latvia	SZ	Swaziland
AZ	Azerbaijan	GB	United Kingdom	MC	Monaco	TD	Chad
BA	Bosnia and Herzegovina	GE	Georgia	MD	Republic of Moldova	TG	Togo
BB	Barbados	GH	Ghana	MG	Madagascar	TJ	Tajikistan
BE	Belgium	GN	Guinea	MK	The former Yugoslav	TM	Turkmenistan
BF	Burkina Faso	GR	Greece		Republic of Macedonia	TR	Turkey
BG	Bulgaria	HU	Hungary	ML	Mali	TT	Trinidad and Tobago
BJ	Benin	IE	Ireland	MN	Mongolia	UA	Ukraine
BR	Brazil	IL	Israel	MR	Mauritania	UG	Uganda
BY	Belarus	IS	Iceland	MW	Malawi	US	United States of America
CA	Canada	IT	Italy	MX	Mexico	UZ	Uzbekistan
CF	Central African Republic	JP	Japan	NE	Niger	VN	Viet Nam
CG	Congo	KE	Kenya	NL	Netherlands	YU	Yugoslavia
CH	Switzerland	KG	Kyrgyzstan	NO	Norway	ZW	Zimbabwe
CI	Côte d'Ivoire	KP	Democratic People's	NZ	New Zealand		
CM	Cameroon		Republic of Korea	PL	Poland		
CN	China	KR	Republic of Korea	PT	Portugal		
CU	Cuba	KZ	Kazakstan	RO	Romania		
CZ	Czech Republic	LC	Saint Lucia	RU	Russian Federation		
DE	Germany	LI	Liechtenstein	SD	Sudan		
DK	Denmark	LK	Sri Lanka	SE	Sweden		
EE	Estonia	LR	Liberia	SG	Singapore		

INTERNATIONAL SEARCH REPORT

A. CLASSIFICATION OF SUBJECT MATTER
IPC 6   G06F17/50   C07K1/00   C07K14/475   G01N33/68

According to International Patent Classification (IPC) or to both national classification and IPC

B. FIELDS SEARCHED

Minimum documentation searched (classification system followed by classification symbols)
IPC 6   G06F   C07K   G01N

Documentation searched other than minimum documentation to the extent that such documents are included in the fields searched

Electronic data base consulted during the international search (name of data base and, where practical, search terms used)

C. DOCUMENTS CONSIDERED TO BE RELEVANT

Category°	Citation of document, with indication, where appropriate, of the relevant passages	Relevant to claim No.
X	AI SHIH ET AL.: "Mutagenesis identiifies amino-terminal residues of nerve growth factor necessary for Trk receptor binding and biological activity " JOURNAL OF BIOLOGICAL CHEMISTRY., vol. 269, no. 44, 4 November 1994, MD US, pages 27679-27686, XP002062137 see the whole document --- -/--	28-64

[X] Further documents are listed in the continuation of box C.   [X] Patent family members are listed in annex.

° Special categories of cited documents :

"A" document defining the general state of the art which is not considered to be of particular relevance

"E" earlier document but published on or after the international filing date

"L" document which may throw doubts on priority claim(s) or which is cited to establish the publication date of another citation or other special reason (as specified)

"O" document referring to an oral disclosure, use, exhibition or other means

"P" document published prior to the international filing date but later than the priority date claimed

"T" later document published after the international filing date or priority date and not in conflict with the application but cited to understand the principle or theory underlying the invention

"X" document of particular relevance; the claimed invention cannot be considered novel or cannot be considered to involve an inventive step when the document is taken alone

"Y" document of particular relevance; the claimed invention cannot be considered to involve an inventive step when the document is combined with one or more other such documents, such combination being obvious to a person skilled in the art.

"&" document member of the same patent family

2

Date of the actual completion of the international search	Date of mailing of the international search report
15 April 1998	15.05.98

Name and mailing address of the ISA	Authorized officer
European Patent Office, P.B. 5818 Patentlaan 2 NL - 2280 HV Rijswijk Tel. (+31-70) 340-2040, Tx. 31 651 epo nl, Fax: (+31-70) 340-3016	Masturzo, P

C.(Continuation) DOCUMENTS CONSIDERED TO BE RELEVANT		
Category°	Citation of document, with indication, where appropriate, of the relevant passages	Relevant to claim No.
A	J M WINDISCH ET AL.: "Brain-derived neurotrophic factor, neurotrophin-3 and neurotrophin-4 bind to a single leucine-rich motif of TrkB " BIOCHEMISTRY., vol. 34, no. 35, 5 September 1995, EASTON, PA US, pages 11256-11263, XP002062138 see the whole document ---	28-64
P,X	I L SHAMOVSKY ET AL.: "Theoretical studies oon the bioactive conformation of nerve growth factor using VBMC - a novel variable basis Monte Carlo simulated annealing algorithm for peptides " JOURNAL OF THE AMERICAN CHEMICAL SOCIETY, vol. 118, no. 40, 9 October 1996, DC US, pages 9743-9749, XP002062139 see the whole document ---	1-64
X	SZENTPLAY ET AL.: "A "slow-cooling" Monte Carlo conformational space study of 18-crown-6 and its alkali metal cation complexes" JORNAL OF MOLECULAR STRUCTURE (THEOCHEM), vol. 308, 1994, ELSEVIER SCIENCE BV, AMSTERDAM, THE NETHERLANDS, pages 125-140, XP002053425 cited in the application	1-6, 14-19, 22,23
A	see page 127, column 1, line 11 - page 128, column 2, line 31 ---	7-13,20, 21
A	US 5 241 470 A (LEE ET AL.) 31 August 1993 see column 1, line 65 - column 4, line 20 -----	1,14,15

2

INTERNATIONAL SEARCH REPORT

Box I   Observations where certain claims were found unsearchable (Continuation of item 1 of first sheet)

This International Search Report has not been established in respect of certain claims under Article 17(2)(a) for the following reasons:

1. ☐ Claims Nos.:
   because they relate to subject matter not required to be searched by this Authority, namely:

2. ☐ Claims Nos.:
   because they relate to parts of the International Application that do not comply with the prescribed requirements to such an extent that no meaningful International Search can be carried out, specifically:

3. ☐ Claims Nos.:
   because they are dependent claims and are not drafted in accordance with the second and third sentences of Rule 6.4(a).

Box II   Observations where unity of invention is lacking (Continuation of item 2 of first sheet)

This International Searching Authority found multiple inventions in this international application, as follows:

see additional sheet

1. ☒ As all required additional search fees were timely paid by the applicant, this International Search Report covers all searchable claims.

2. ☐ As all searchable claims could be searched without effort justifying an additional fee, this Authority did not invite payment of any additional fee.

3. ☐ As only some of the required additional search fees were timely paid by the applicant, this International Search Report covers only those claims for which fees were paid, specifically claims Nos.:

4. ☐ No required additional search fees were timely paid by the applicant. Consequently, this International Search Report is restricted to the invention first mentioned in the claims; it is covered by claims Nos.:

Remark on Protest

☐ The additional search fees were accompanied by the applicant's protest.

☒ No protest accompanied the payment of additional search fees.

Form PCT/ISA/210 (continuation of first sheet (1)) (July 1992)

1. Claims: 1-27

   A variable basis Monte Carlo (VMBC) simulated annealing
   method for identifying an optimal structure in a molecular
   system.

2. Claims: 28-64

   Binding agents for neurotrophin receptors and identification
   of the binding sites of these.

INTERNATIONAL SEARCH REPORT

Information on patent family members

Patent document cited in search report	Publication date	Patent family member(s)	Publication date
US 5241470 A	31-08-93	NONE	